Fuel, fire and smoke: evolving to meet our climate challenge.

CONFERENCE PROCEEDINGS

APRIL 15-19, 2024

7th International Fire Behavior + Fuels Conference

International Association of Wildland Fire

The 7th International Fire Behaviour and Fuels Conference convened experts from around the world in Boise (USA), Canberra (Australia), and Tralee (Ireland) to discuss the latest developments in wildland fire science, management, and policy.
Key themes included:

- The growing scale and complexity of wildfires due to climate change, changing land use, and fuel accumulation.
- The critical need for global collaboration, knowledge exchange, and adaptive management strategies.
- Indigenous knowledge and cultural fire practices as essential to sustainable fire management, with calls for greater inclusion and respect for Indigenous voices.
- Advances in technology and data, including new fire information and analytics platforms.
- The importance of resilience, mental health, and well-being for fire practitioners and affected communities.
- Challenges such as longer fire seasons, more severe fires, air quality impacts, and the disproportionate effects on Indigenous and vulnerable communities.

Workshops, keynotes, and field trips offered practical insights on topics like prescribed fire, fuel management, climate forecasting, and resilience building.

The conference emphasized the need for ongoing collaboration, more inclusive approaches, and action to address emerging risks, including unexploded ordinance in fire zones and the feedback loops between fire and climate change.

Participants left with a renewed focus on sharing knowledge internationally, strengthening local and Indigenous partnerships, and adapting strategies for a rapidly changing fire landscape.

7th International Fire Behavior + Fuels Conference

Thank you to our Sponsors, Partners, and Exhibitors for their generous support!

Presented by: International Association of Wildland Fire

Partners: USDA Forest Service; NASA

Partner

Boise Sponsors

BURNBOT

esri — THE SCIENCE OF WHERE

technosylva

WATERAX — WE MOVE WATER

servicenow

USGS — science for a changing world

STi | Sonoma Technology

Northern Rockies Fire Science Network

Great Basin Fire Science Exchange

Tralee Sponsors

technosylva

vft vallfirest — the wildfire company

COILLTE

The Emergency Program WILDFIRE

Pau Costa Foundation

EFI

PRECISE

Tralee Chamber Alliance — Advancing business together

The Rose Hotel — Tralee, Co. Kerry

Canberra Sponsors

CSIRO

ACT Government

ACT Parks and Conservation Service

National Parks & Wildlife Service NSW

NSW Government

NSW Rural Fire Service

A.C.T. Rural Fire Service

RFS

UNSW Canberra

afac

Natural Hazards Research Australia

Table of Contents (Title order)

Proceedings for the 7th International Fire Behavior and Fuels Conference April 15-19, 2024, Boise, Idaho, USA – Tralee, Ireland – Canberra, Australia Published by the International Association of Wildland Fire, Missoula, Montana, USA

160-years fire danger from meteorological observations reveal long-term trends, and discrepancies with commonly used reanalysis datasets for the European boreal

Johan Sjöström*
Department of Fire Technology, RISE Research Institutes of Sweden, Box 857, 501 15 Borås, Sweden,

Anders Granström
Department of Forest Ecology and Management, Swedish University of Agricultural Sciences, 901 83 Umeå, Sweden, anders.granstrom@slu.se

**Corresponding Author*

Introduction

Climate change is implicated as a driver of a worsening wildfire situation in certain regions (Barnes *et al*., 2023; Dupuy *et al*., 2020). The European boreal, exemplified here by Sweden, have seen increasing average temperatures, higher annual precipitation and slightly increased geostrophic wind since 1950 (Schimanke *et al*., 2022), but it is not known how these changes have affected forest fire danger.

We extracted 1951-2022 data from nine Swedish weather stations with daily reports on snow cover and noon-observations of temperature (T), 10-m open wind speed (W), relative humidity (RH) as well as 24 hours accumulated precipitation (P). Locations span an 1100 km N-S gradient (Figure 1). From this data we calculated daily indices of the Canadian Forest Fire Weather Index (FWI) System (Van Wagner and Pickett, 1985). We then compared this "observed fire danger" with parallel calculations using the ERA5 atmospheric reanalysis dataset (Hersbach *et al*., 2020).

These weather stations were established in the 1800s and provide daily noon-temperature and 24-h precipitation observations, most of them continuously from the year 1860. The long time series enables us to construct a proxy for the daily Duff Moisture Code (DMC) spanning over 160 years. Here we summarize these datasets and their analyses. Results can be further examined in Sjöström and Granström (2024).

Method

We ran the FWI-algorithm (Van Wagner and Picket, 1985) from 1951 to 2020, starting each season 3 days after snowmelt. Missing data was replaced by last day's observation. Hiatuses longer than 3 days were covered by observations from the nearest weather station. Overall, missing data comprised <0.6 % of the entire data-set.

As an indicator of seasonal severity, we used the season maximum of the running 7-day average FWI, following Van Oldenborgh *et al* (2021) and Barnes *et al* (2023).

Henceforth, we use ‑7x after a specific indicator to denote the season's extreme 7-days average.

To construct RH_{proxy}, a proxy for RH (for periods prior to 1951 lacking RH-observations) we fitted a non-linear multivariable function using day-of-year, temperature, precipitation and latitude to the RH observations from 1951 and onwards. Using RH_{proxy}, we calculated daily DMC-values for the same locations, producing time series up to 160 years long.

Results and discussion

Linear regression show increasing T-7x (max 7-days average of noon-temperature) for all locations, with an average increase of 1.8 °C over the 70-year period, largest in the southeast. Summer precipitation (JJA) also increased among most locations with an average of 20 mm/season, corresponding to roughly a 10% increase. RH-7x decreased for all locations, with an average of -6.5%. As for noon-wind and longest period of drought, there were no clear temporal or geographical trends.

With the exception of the northernmost station, Jokkmokk, the linear FWI-7x-trends increased with an average of 22% over the 70-year-period. Interannual variation was however very large in relation to the trends. For most locations there was a tendency towards multi-year periods of high or low danger, but without any detectable periodicity (Figure 1).

On average, the increase in FWI-7x was, to 79%, caused by increasing ISI, in turn more related to higher FFMC than to increasing wind. Delineating the contribution from weather parameters show RH as contributing most to the increased fire danger. However, since absolute air moisture has increased by approximately 10% during the same period (Schimanke *et al*., 2022) it is the increasing noon-temperatures that causes the decrease in noon RH. Thus, the increasing fire danger in the region is not due to prolonged drought or stronger winds but lower RH (i.e. drier fine fuels), a variable increasing ignition susceptibility and fire rate of spread.

Reanalysis products of weather parameters are spanning progressively longer time series with increasingly better bias correction. However, we found a systematic difference between fire danger indices calculated with observed data as opposed to reanalysis. FWI-calculations using the ERA5 (European Centre for Medium-Range Weather Forecasts (Hersbach *et al*., 2020)), which has a spatial resolution of 31 km, drastically under-predicted high FWI-values and over-predicted the very lowest FWI-values, for all locations. The discrepancy between the two datasets were 5-10 index points for observed FWI-values ranging 20-40 (Figure 2). At the same time, for FWI<2 (48% of the observations), the ERA5 data overestimated the index by 0-1.5 index points. We also tested Mesan, a Swedish reanalysis product with much higher spatial resolution (2.4 km) (Häggmark *et al.,* 2000). It too under-predicted high fire-danger, but with less absolute errors (data not shown).

The systematic discrepancy in FWI-values also greatly impact seasonal indicators, with generally lower FWI-7x as well as changes in trend magnitudes. E.g. FWI-7x calculated from ERA5 at Storuman exhibited a 17% less steep linear trend over 70 years compared to FWI-7x calculated from observation data.

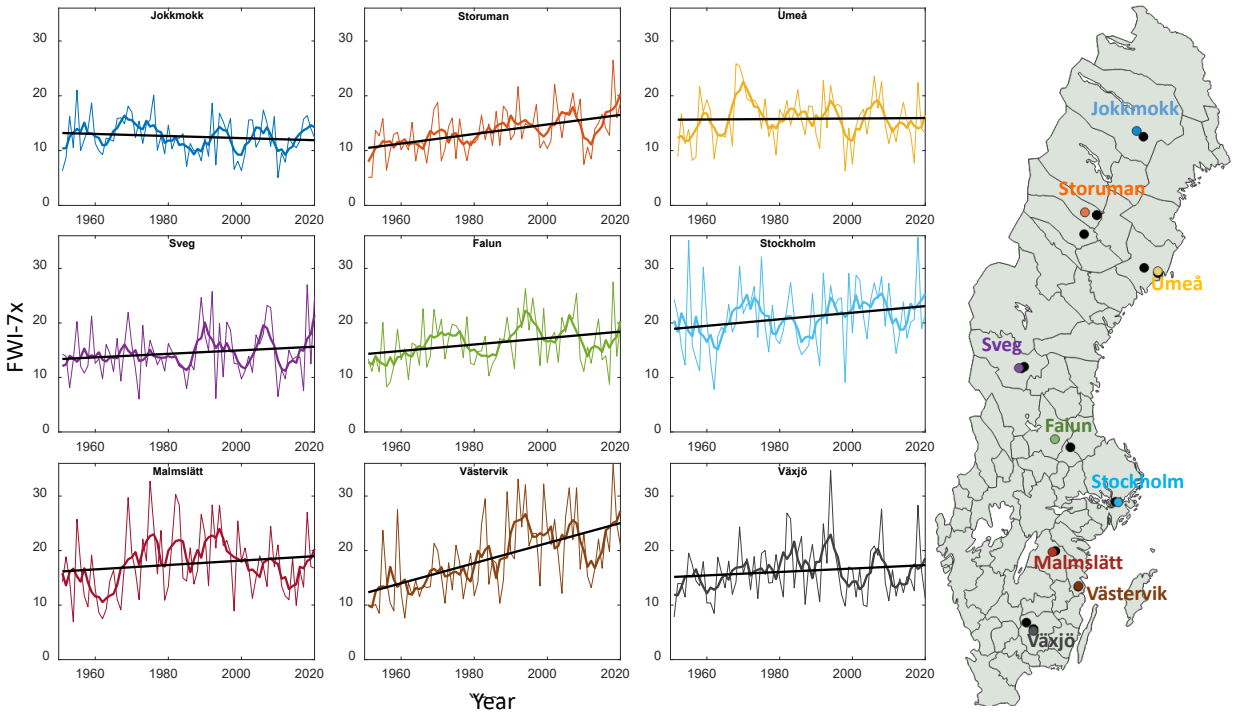

Figure 1: Left: FWI-7x for the nine locations (thin lines), 5 years average (thick lines) and linear trend (black lines). Right: Location of Weather stations (colored) and adjacent stations used for missing data (black).

These discrepancies are to be expected since the reanalysis data represents weather over a whole cell (in the case of ERA5 31×31 km). Thus, it always favors averages over extremes. Additionally, Swedish summer precipitation is predominantly convective, with local showers that will result in more extreme point observations than the reanalysis product.

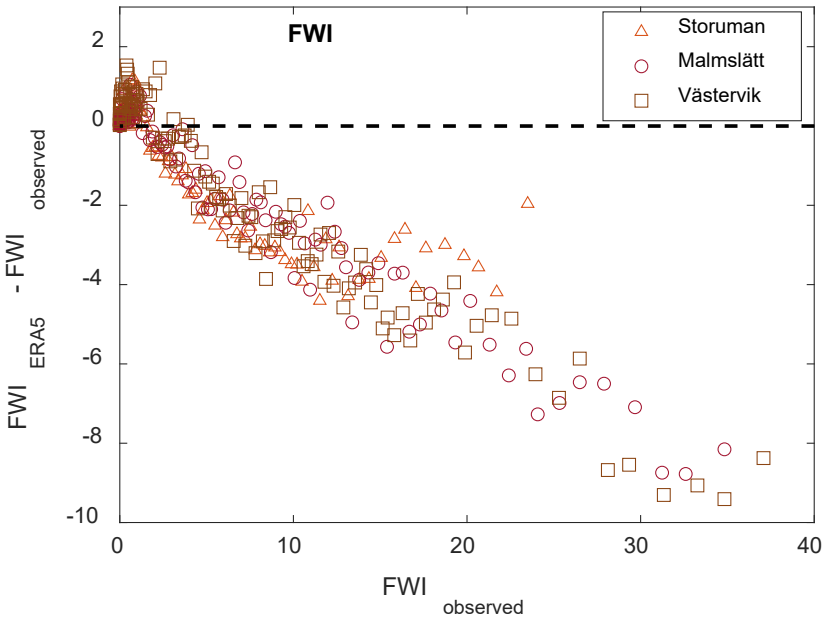

Figure 2: Difference between daily FWI_{ERA5} and $FWI_{observed}$ for Storuman, Malmslätt and Västervik, in relation to $FWI_{observed}$ (binned in groups of 50).

Minimization of a non-linear multivariable regression defined RH_{proxy} as

$$RH_{proxy} = 0.155 \times day - 1.634 \times T + 9.759 \times R^{0.3} - 0.885 \times Lat + 103.9,$$

where day is the ordinal date and Lat is in WGS84.

There was considerable scatter between RH_{proxy} and $RH_{observed}$ (r^2=0.50, Figure 3a), but DMC employing this proxy nevertheless correlated well with "true" DMC (r^2=0.98, Figure 3b). Likewise, the seasonal extreme 7-day period correlated well (r^2=0.93, Figure 3c), without systematic errors over the 70-year period, as exemplified by station Malmslätt (Figure 3d).

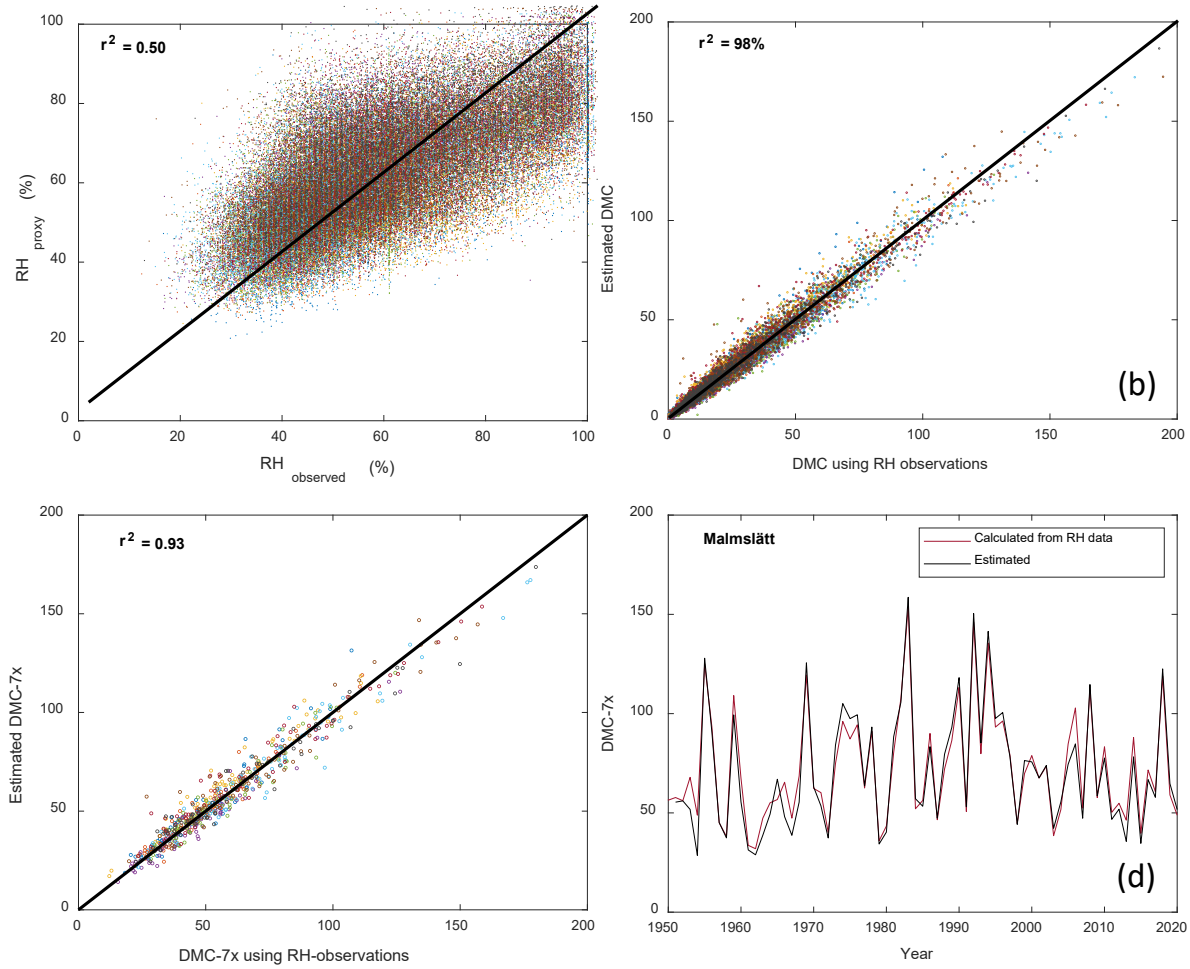

Figure 3: (a) Correlation between RH_{proxy} and $RH_{observation}$. (b) Daily DMC estimated *vs* calculated from observations. (c) Estimated DMC-7x *vs* calculated from observations. (d) The time series for DMC-7x at Malmslätt using $RH_{observation}$ and RH_{proxy}, respectively.

Noon-temperatures increased equally much (1.8°C on average) in the longer dataset from 1860 as in that from 1951. This confer with climate change acceleration in the most recent decades. Summer precipitation increased 33 mm on average. The resulting DMC-7x increased in the eastern locations but decreased for Jokkmokk and Sveg (Figure 4). The interannual standard deviation was 38% with a linear trend (averaged of all locations) of about +12% of the mean. Trend analyses (data not shown) also reveal a minimum of DMC-7x around 1890-1900, followed by a monotonic increase.

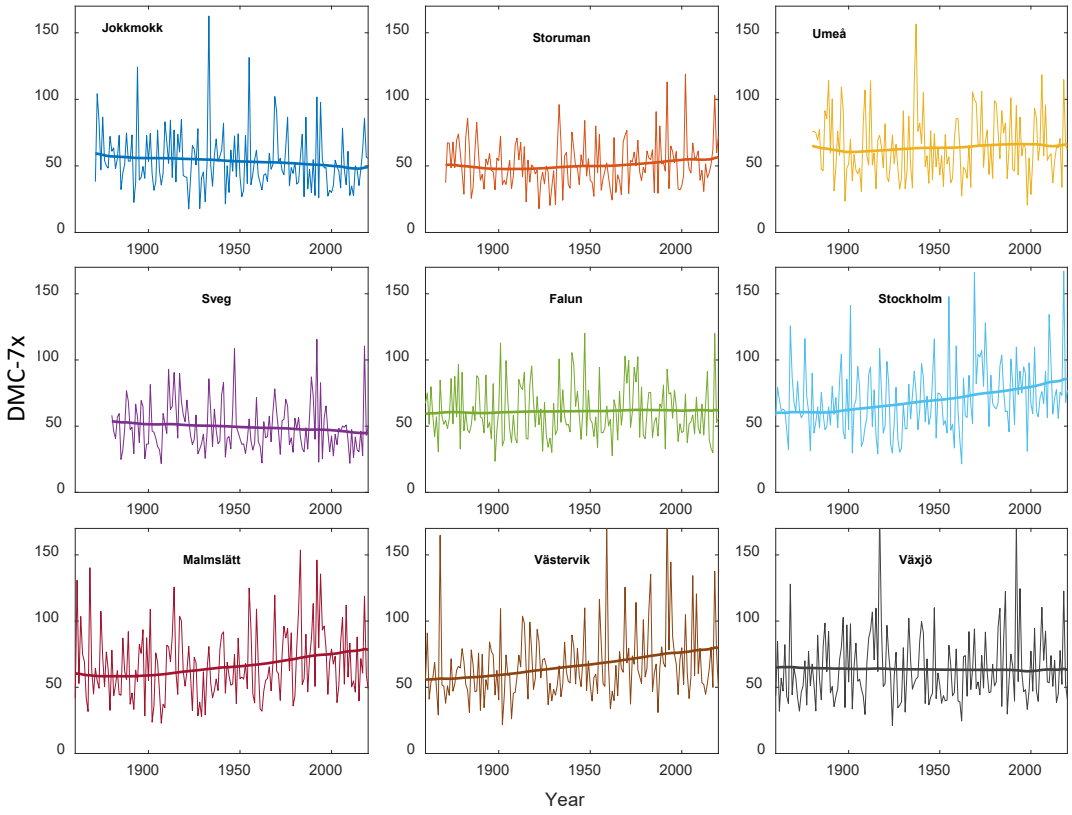

Figure 4: Extended long-term DMC-7x for the nine locations via the RH_{proxy}-data (thin lines), and decomposition of trends using singular spectrum analyses (Golyandina and Zhigljavsky, 2013) (thick lines).

Conclusions

70-year long fire-danger datasets were created for nine Swedish locations using actual meteorological observations. Parallel calculations with the often-used ERA5-reanalysis data reveal that the latter severely underestimates FWI when fire danger is high. Additionally, via a proxy for noon relative humidity, we calculated daily DMC series for the same locations, mostly spanning 160 years (1860-2020). The series reveal very high interannual variations compared to trends. Despite increased summer precipitation in Sweden, fire danger increased, driven mainly by lower RH (implying drier fine fuels) and less so through the duff moisture (DMC) contribution to increasing FWI.

Acknowledgements

This study was funded by MSB - Swedish Civil Contingencies Agency (2332427) and European commission, FirEUrisk project (101003890).

References

Barnes C, *et al*. (2023) Climate change more than doubled the likelihood of extreme fire weather conditions in eastern Canada. Scientific Reports (in review).

Dupuy Jl, *et al*. (2020) Climate change impact on future wildfire danger and activity in southern Europe: a review. Annals of Forest Science 77, 35.

Golyandina N, Zhigljavsky A (2013) Singular Spectrum Analysis for Time Series. SpringerBriefs in Statistics. Berlin, Heidelberg: Springer Berlin Heidelberg. https://doi.org/10.1007/978-3-642-34913-3

Häggmark L, *et al*. (2000). Mesan, an operational mesoscale analysis system. Tellus A, 52, 2-20.

Hersbach H, *et al.* (2020) The ERA5 global reanalysis. Quarterly Journal of the Royal Meteorological Society, 146(730), 1999-2049.

Van Oldenborgh GJ, *et al*. (2020). Attribution of the Australian bushfire risk to anthropogenic climate change. Natural Hazards and Earth System Sciences Discussions, 21, 941–960.

Schimanke S *et al*. (2022) Observerad klimatförändring i Sverige 1860-2021, Klimatologi 69 (SMHI, Norrköping).

Sjöström J, Granström A (2024) Analys av 160 års brandväder i Sverige: Skogsbrandsrisken sedan 1860 för nio lokaler MSB 2300, Swedish Civil Contingencies Agency, ISBN: 978-91-7927-468-9, https://rib.msb.se/filer/pdf/30560.pdf

Van Wagner CE, Picket TL (1985). Equations and FORTRAN program for the Canadian Forest Fire Weather Index System. Can. For. Serv. Ottawa, Ontario. For. Tech. Rep, 33.

Accounting for hardened structures in WUI fire modeling

*Fernando Szasdi-Bardales
University at Buffalo, Department of Civil, Structural and Environmental Engineering, Buffalo, NY, USA, fszasdib@buffalo.edu

Negar Elhami-Khorasani
University at Buffalo, Department of Civil, Structural and Environmental Engineering, Buffalo, NY, USA, negarkho@buffalo.edu

**Corresponding Author*

Introduction

The wildland-urban interface (WUI) is the zone where developed lands transition into the wilderness. In recent years, an increasing trend in the frequency of intense wildfires has inflicted significant damage in WUI communities, resulting in loss of life and severe economic impacts (Schmidt, 2024). Simulation models offer a valuable opportunity to understand the drivers of loss in WUI communities and can be used to conduct wildfire risk assessment and inform mitigation strategies (Schmidt, 2024). Accounting for and characterizing structure fuels is key for WUI fire simulation models. Factors such as exterior materials, defensible space, structure components, and other fire-resistant features affect a structure's vulnerability to ignition, and the intensity of the fire once it is burning (Restaino et al., 2020). This study analyzes the influence of hardened structures on fire spread at the community level. A WUI fire spread model is used to analyze three recent cases of destructive North American WUI fires, as well as a set of idealized community scenarios proposed following uniform grid layouts, to study the influence of hardened structures on fire spread pattern and rate.

Materials and methods

Three historic case studies are analyzed: the 2018 Camp Fire, the 2021 Marshall Fire, and the 2023 Lahaina Fire. A sensitivity analysis of 'idealized' communities, where structures are arranged in grids with controlled separation distances, complements the study. The 'SWUIFT' model (Masoudvaziri et al., 2021) is used for all the community fire spread simulations in this study.

Historical case studies

In all the case studies, buildings are classified following a binary criterion based on the occupancy type and, except for the Marshall Fire, the year of construction. These proxies are used because they provide a general indication of the vulnerability level of the structures (e.g., a modern structure built based on new building codes is more likely to incorporate fire-resistant characteristics, or a non-residential structure is more likely to have better defensible space and in-situ fire suppression capabilities).

Figures 1-3 show the simulation domains used for the Marshall Fire, Camp Fire, and Lahaina Fire respectively, with building hardening categorization indicated in all cases. Details of simulation inputs and transition from wildland to WUI areas for all three cases can be found in (Szasdi-Bardales et al., 2024a and 2024b; Juliano et al., 2024).

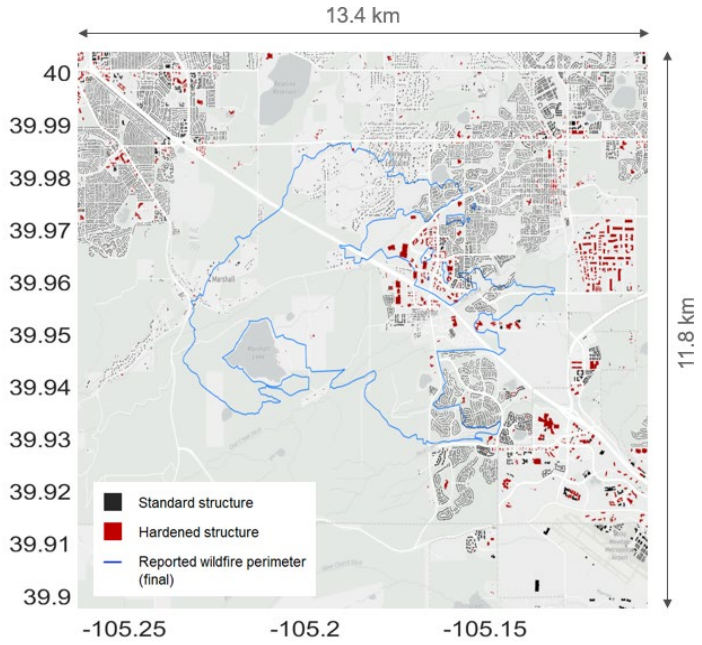

Figure 1: Simulation domain, hardening classification, and final observed fire perimeter for the Marshall Fire

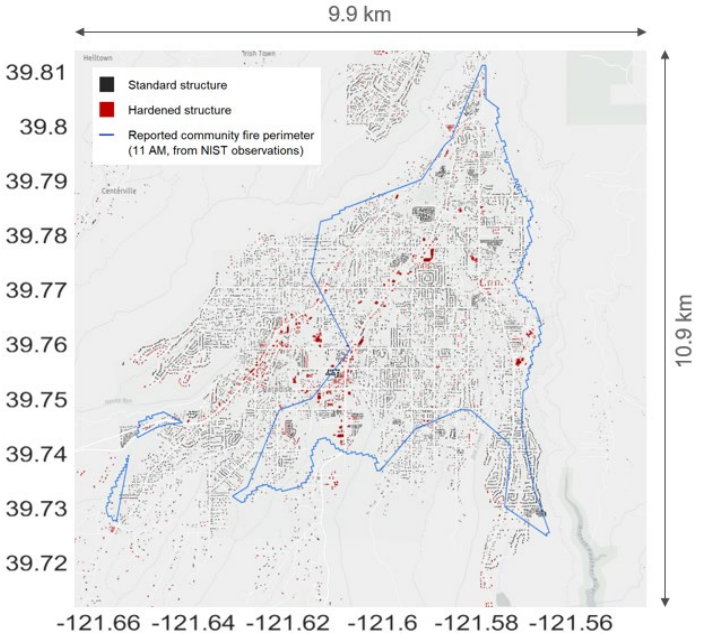

Figure 2: Simulation domain, hardening classification, and final observed fire perimeter for the Camp Fire

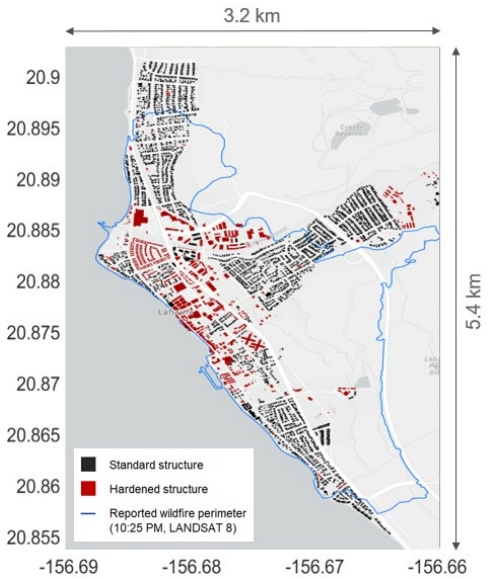

Figure 3: Simulation domain, hardening classification, and final observed fire perimeter for the Lahaina Fire

Idealized community layouts

90 simulations were performed to analyze fire spread inside communities where different parameters could be controlled. The cases include two community layouts with different structure density (Figure 4), two levels of structure hardening (0% and 70%) applied to all structures, five constant wind speeds (5–25 m/s in 5 m/s intervals), and different levels of vegetation coverage (from 0% to 20% for community layout 1 and from 0% to 50% for community layout 2, increased in 10% intervals). The observed rate of spread (ROS) is used to compare the results.

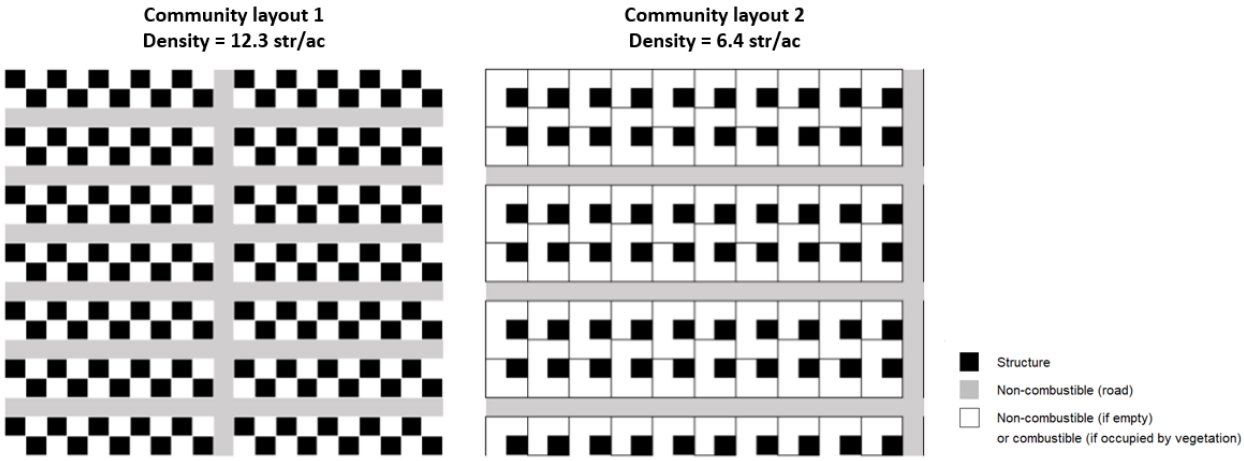

Figure 4: Idealized community layouts with different structure density

Level of hardening

A probabilistic approach is followed to describe the level of hardening of the structures. A non-hardened structure (i.e., 0% hardening) will ignite after any of the conventional ignition thresholds in the SWUIFT model (i.e., thermal radiation, ember accumulation) is exceeded. On the contrary, a fully hardened structure (i.e., 100% hardening) is one that never ignites. For a structure with H% hardening, the likelihood of ignition after exceeding the traditional SWUIFT thresholds is determined by a randomly generated number under uniform distribution in comparison with the associated probability of ignition. Noting that ignitions from different modes of fire spread (radiation and fire spotting) and their associated probabilities are considered independently in SWUIFT.

Results

Historical case studies

Figure 5 shows a set of predicted fire spreads for the Marshall Fire, with the level of hardening for the hardened structures ranging from 0% to 100%. A change in the fire spread pattern that better resembles the progression observed during the incident is observed at about 70% hardening. Thus, this level of hardening is adopted as the 'standard' for hardened structures for the rest of the simulations in this study.

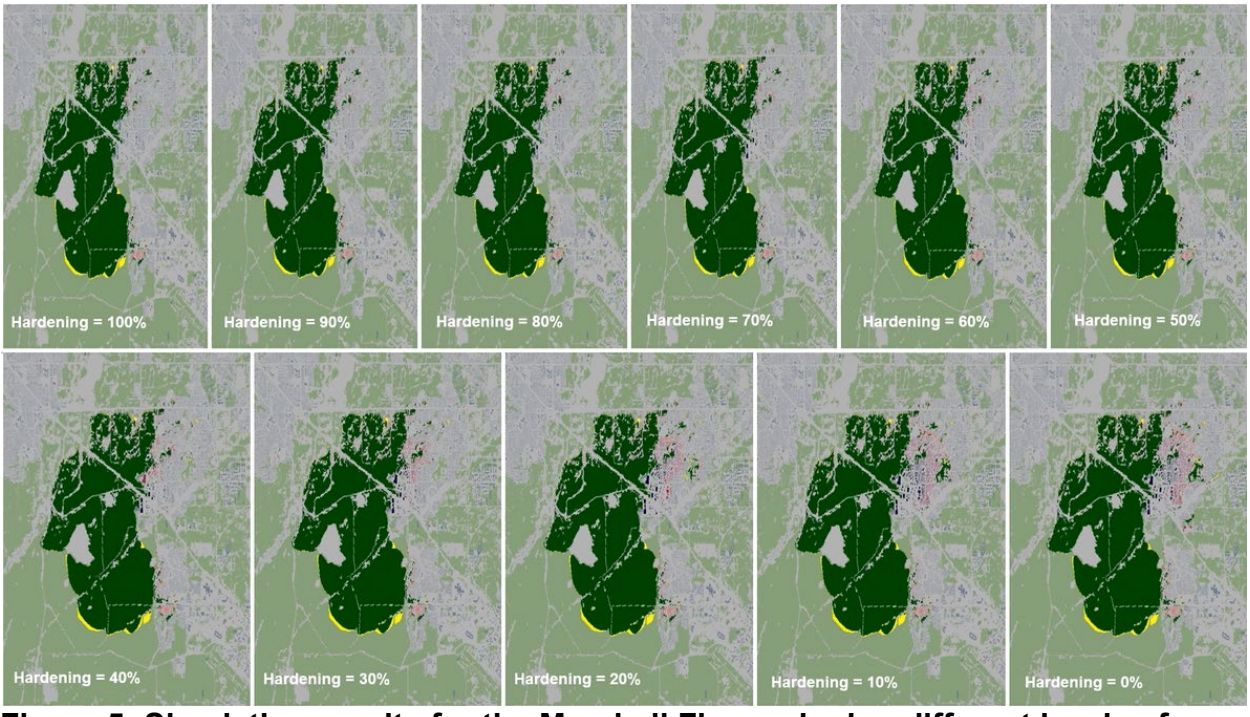

Figure 5: Simulation results for the Marshall Fire assigning different levels of hardening

Figures 6 and 7 show the predicted fire spreads with and without structure hardening for the Camp Fire and the Lahaina Fire respectively.

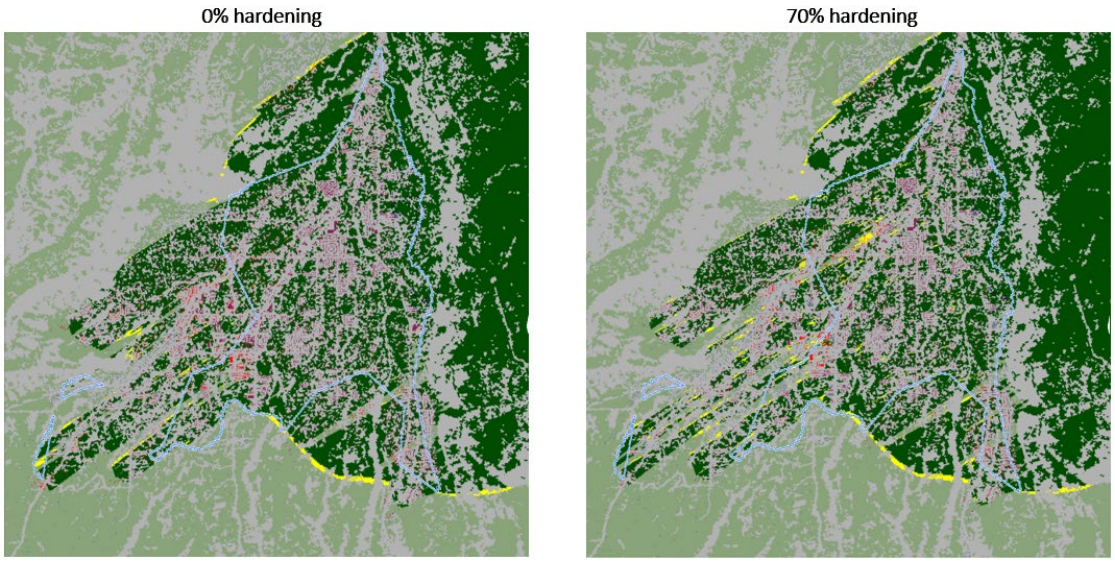

Figure 6: Simulation results for the Camp Fire

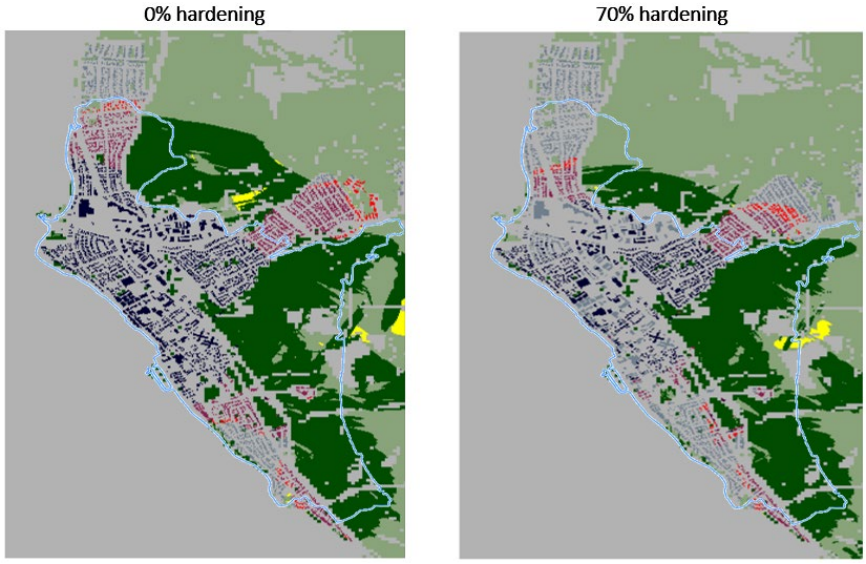

Figure 7: Simulation results for the Lahaina Fire

Sensitivity analysis

Figures 8 and 9 show a summary of the simulation results, in terms of ROS, for the idealized communities.

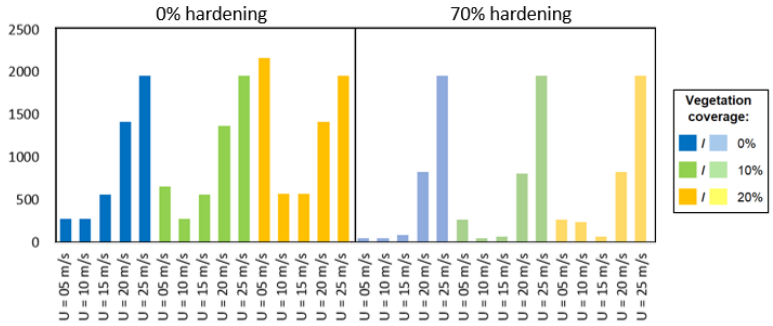

Figure 8: Summary of ROS (in m/h) obtained from the simulations performed for the community layout 1 (12.3 str/acre)

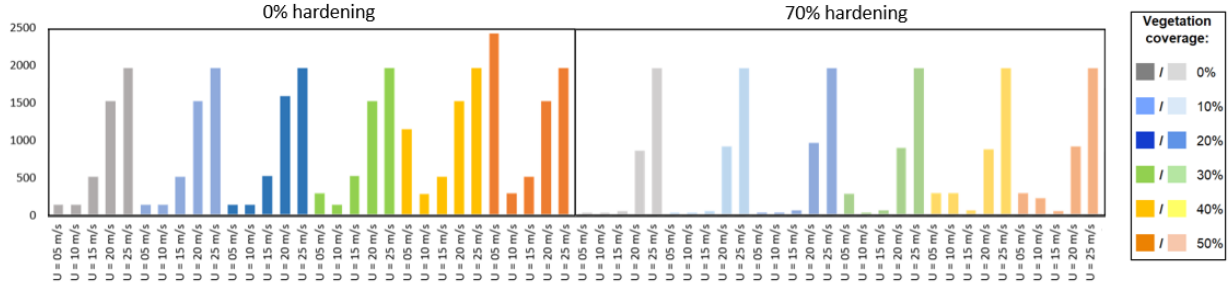

Figure 9: Summary of ROS (in m/h) obtained from the simulations performed for the community layout 2 (6.4 str/acre)

Discussion

The Marshall Fire simulations, where the hardening level of structures varied, show that higher hardening levels change the behavior of the fire spread. Specifically, the fire stops spreading into Louisville from the south despite crossing US-36 early in the simulation. Instead, it enters Louisville from the west several hours later, mirroring the observed fire spread pattern. This suggests that a cluster of commercial buildings that did not ignite likely caused the fire front to stop in this community region. This effect is noticeable at a 60% hardening level, and therefore a value of 70% hardening is conservatively taken to characterize the vulnerability of hardened structures in subsequent simulations. For the Camp Fire, the prediction of damage outcome improves at an individual structure level when hardened structures are included in the simulations. However, at the community level, the change in the fire spread pattern is minimal. This is largely due to the high level of vegetation coverage inside the town of Paradise, which provides an alternative path for fire spread. In the Lahaina Fire, mixed results are observed at the individual structure level. At the community level no improvements are observed. This discrepancy may be explained by a poor correlation between the buildings' vulnerable features (e.g., exterior materials, separation, defensible space, etc.) and their occupancy type.

The study of the idealized communities shows that hardened structures (with characteristics that reduce their ignition probability by about 50%) can result in a drastic reduction in the number of ignited buildings and slow down the ROS. These effects are

more pronounced when both the vegetation coverage inside the community and the wind speed are low.

The findings of this study identify the level of hardening thresholds at which the rate of fire spread inside typical WUI communities can be significantly reduced. The study also highlights that clusters of hardened structures can slow down the rate of spread inside the communities and in some cases completely stop the fire progression. Overall, hardened structures can contribute to bending down the risk curve in WUI communities.

Acknowledgements
This work is supported through the National Science Foundation's Leading Engineering for America's Prosperity, Health, and Infrastructure (LEAP-HI) program by grant no. CMMI-1953333 and by the Insurance Institute for Business & Home Safety (IBHS). We gratefully acknowledge their support. The opinions and perspectives expressed in this study are those of the authors and do not necessarily reflect the views of the sponsors.

References

Juliano TW, Szasdi-Bardales F, Lareau NP, Shamsaei K, Kosovic B, Elhami-Khorasani N, James EP, Ebrahimian H (2024) Brief Communication: the Lahaina Fire disaster: how models can be used to understand and predict wildfires. Natural Hazards and Earth System Sciences **24**, 1, https://doi.org/10.5194/nhess-24-47-2024

Mazoudvaziri N, Szasdi Bardales FJ, Keskin OK, Sarreshtehdari A, Sun K, Elhami-Khorasani N (2021) Streamlined wildland-urban interface fire tracing (SWUIFT): modeling wildfire spread in communities, Environ. Model. Softw. **143**, 105097, https://doi.org/10.1016/jenvsoft.2021.105097

Restaino C, Kocher S, Shaw N, Hawks S, Murphy C, Quarles SL (2020) Wildfire home retrofit guide, University of Nevada, Reno Extension. (Reno, NV)

Schmidt J (2024) 'County Wildfire Risk Ratings in Northern California: FAIR Plan Insurance Policies and Simulation Models vs. Red Flag Warnings and Diablo Winds', Munich Personal RePEc Archive

Szasdi-Bardales F, Elhami-Khorasani N (2024a) An offline coupling of fire spread models to simulate the 2021 Marshall Fire, unpublished data

Szasdi-Bardales F, Shamsaei K, Lareau N, Juliano TW, Kosovic B, Ebrahimian H, Elhami-Khorasani N (2024b) Integrating dynamic wildland fire position input with a community fire spread simulation: a case study of the 2018 Camp Fire, Fire Safety Journal **143**, 104076, https://doi.org/10.1016/j.firesaf.2023.104076

Proceedings for the 7th International Fire Behavior and Fuels Conference April 15-19, 2024, Boise, Idaho, USA – Tralee, Ireland – Canberra, Australia Published by the International Association of Wildland Fire, Missoula, Montana, USA

Accuracy of depicted fire behaviour potential varies with fire-danger rating options

*Paulo M. Fernandes
Center for the Research and Technology of Agro-Environmental and Biological Sciences, UTAD, Quinta de Prados, 5000-801 Vila Real, Portugal, pfern@utad.pt

Akli Benali
Forest Research Center, University of Lisbon, Tapada da Ajuda, 1349-017 Lisboa, Portugal, aklibenali@gmail.com

David Davim
Center for the Research and Technology of Agro-Environmental and Biological Sciences, UTAD, Quinta de Prados, 5000-801 Vila Real, Portugal, david.davim@gmail.com

**Corresponding Author*

Introduction

Fire danger rating is a cornerstone of wildland fire science and management. Fire weather indices are expected to provide realistic and reliable representations of fire behaviour potential, namely when using fire danger rating systems developed elsewhere. Fire researchers increasingly resort to fire danger reanalysis products, namely those pertaining to the Canadian Forest Fire Weather Index System (FWI). Yet, although often used as a proxy for observations, reanalysis data is ultimately the output of a model. For operational purposes, fire danger rating is based on forecasts, informed or not by data from weather stations.

The comparative consistency and accuracy of different fire danger rating options (in terms of data sources) is currently unknown in Portugal and in Europe. Our purpose was to examine how the ability to portray actual fire danger varies with the source of FWI indexes, based on the most objective criterion: observed or reconstructed fire behavior data.

Methods

We assembled a fire behaviour (rate of spread, fuel consumption, fireline intensity) database for Portugal, consisting of data (i) collected in experimental outdoors fires in forest (pine, eucalypt) and in shrubland, extracted from the BONFIRE worldwide database (Fernandes *et al.* 2020), and (ii) data from reconstructed large wildfire spread, mostly from Benali *et al.* (2023). This enabled to cover the entire spectrum of fire weather and fire behavior variation for the more flammable vegetation types in Portugal. In line with fire danger rating processes and goals, we considered fire behavior for daily peak burning conditions only, i.e., around mid-afternoon.

Each fire observation was assigned one fuel complex (experimental fires) or a broad vegetation type (wildfires), the latter based on Portuguese land use and land cover mapping (Caetano *et al.* 2009). Following the Canadian Forest Fire Danger Rating System rationale (Van Wagner 1987), the following indexes were used as proxies for fire behavior characteristics: the Initial Spread Index (ISI) for rate of fire spread, the Build-up Index (BUI) and Duff Moisture Code (DMC) for fuel consumption, and the Fire Weather Index (FWI) for fireline intensity. The FWI index is dependent of the other 5 indexes of the system, including the Fine Fuel Moisture Code (FFMC) and the Drought Code (DC), not mentioned previously. Thus, we compared the six FWI indexes from reanalysis and from weather stations using the Sign text, a non-parametric version of the t-test.

Variability in fire behaviour was examined for three options: (i) daily gridded FWI indexes from the ERA5 reanalysis from the ECMWF (Vitolo *et al.* 2020), (ii) daily FWI indexes interpolated from the nearest IPMA (the Portuguese weather agency) stations; and, for experimental fires only, (iii) hourly FWI indexes calculated from observed local conditions of in-stand wind speed and dead fuel moisture content as per Van Wagner (1987).

Data for 70 experimental-fire days and 63 wildfire runs was retained for analysis. Following theoretical expectations and exploratory analysis, fire-behavior descriptors were log-transformed and modelled from non-transformed (ISI, FWI) or log-transformed (DMC, BUI) indexes, with fuel categorization as a covariate. The fitted models were evaluated by the amount of explained variability (the adjusted R^2) and the mean absolute percentage error (MAPE), for experimental fires. For wildfires, and in face of extreme outliers, we calculated the median absolute percentage error (median APE) and the interquartile APE in lieu of the MAPE.

Results

FWI indexes: reanalysis versus weather stations

FWI indexes differed between reanalysis and weather-station data for the experimental fires (p<0.0001). The reanalysis FWI indexes had lower values than FWI indexes calculated from weather stations observations, with FFMC displaying the greatest difference. No differences between the two FWI sources were found for wildfires. However, reanalysis ISI and FWI were substantially lower for the three highest weather station observations, suggesting underestimation of wind speed.

Fire behavior characteristics depiction by the alternative fire-weather sources

Indexes calculated solely or partially from local data performed better than any other fire-weather source in describing observed experimental fire behaviour (Table 1). FWI indexes calculated from weather stations slightly outperformed the reanalysis for spread rate and fireline intensity, but the opposite was true for fuel consumption.

The regression analyses of combined experimental and wildfire rate of spread modelled from FWI indexes, with vegetation type as co-variate, resulted in better fits than the

analyses of experimental data alone (Table 2). However, no apparent advantage associated to either approach could be discerned.
Rate of fire spread responded exponentially to fire weather and decreased from shrubland to forest for any given FWI, which in part is reflecting the drier and windier conditions of more open environments (Figure 1). Fire danger from weather-stations data can substantially underestimate fire potential when the FWI>30. However, the fastest-spreading fires in forest were severely underestimated by the reanalysis FWI.

Table 1: Adjusted R^2 / mean absolute % error (MAPE) for the models of experimental fire behavior characteristics based on FWI indexes.

Fire characteristic	Index	Reanalysis	Weather station	Local	Local + reanalysis	Local + weather station.
Rate of spread	ISI	0.361 / 72.7	0.383 / 71.0	0.521 / 58.2		
	FWI	0.362 / 72.5	0.378 / 71.4		0.415 / 67.8	0.447 / 64.7
Fuel consumption	DMC	0.507 / 44.6	0.432 / 48.6			
	BUI	0.507 / 44.6	0.401 / 50.1			
Fireline intensity	FWI	0.440 / 117.4	0.463 / 114.7		0.471 / 114.3	0.502 / 107.7

Table 2: Fit statistics for fire-spread rate (experimental fires plus wildfires) of the models based on FWI indexes.

Index	Data source	R^2_{adj}	MAPE, %	Median APE, %	IQR APE, %
ISI	Reanalysis	0.644	95.5	50.7	22.2—90.3
	Weather station	0.626	99.9	50.1	23.8—83.8
FWI	Reanalysis	0.702	84.9	48.0	22.2 — 72.0
	Weather station	0.708	87.7	43.9	22.9 — 70.5

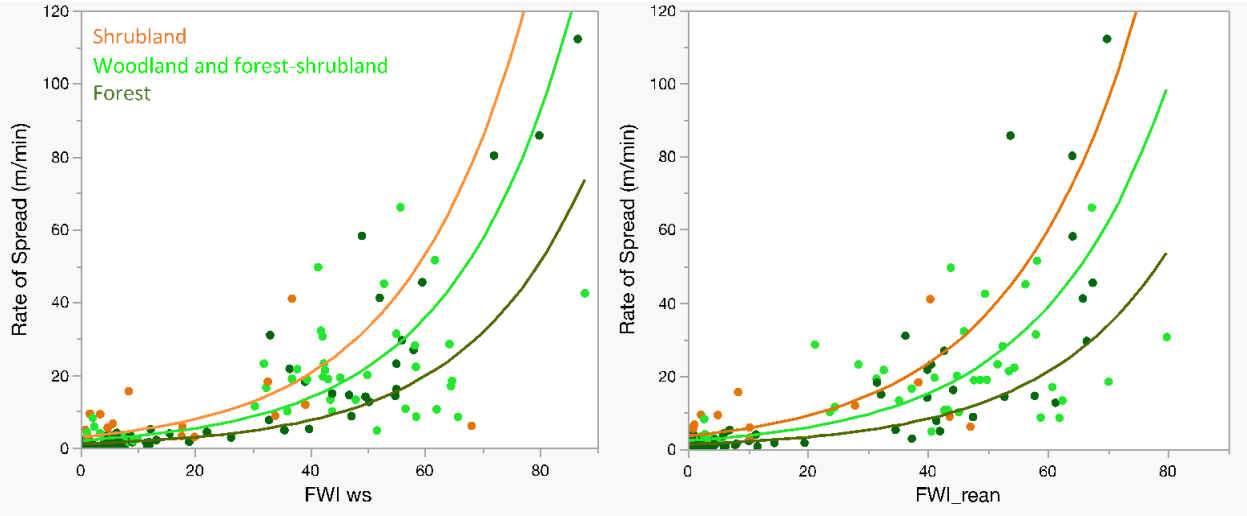

Figure 1: Fire-spread rate relationships with weather-station FWI (left panel) and reanalysis FWI (right panel). The fitted curves respect to the models in Table 2.

Discussion and Conclusion

The explained variability was, surprisingly, substantially higher for the full dataset (experimental fires plus wildfires) than for the experimental fires subset. This may be a natural outcome of the difficulty in capturing fire weather, or components of it, for a point in time and space (a small, possibly non-steady state fire 10 to ~100-m wide) in comparison to a large wildfire. This is valid for all FWI indexes options, given the absence of 10-m wind speed and rainfall measured *in situ*. It is also expected that under mild fire weather the effect of fuel characteristics will be more determinant to fire behavior than under elevated fire danger (Cruz *et al.* 2022) and, additionally, fire spread is responding to specific a fuel complex, whereas a landscape fire integrates the existing substantial variability in fuel types. Description of experimental fire behavior through local FWI indexes would improve by considering fuel characteristics in the analyses and more accurate 10-m windspeed estimation. This in turn would weaken the comparative performance of reanalysis and weather-station FWI indexes.

Higher variability in wind speed and fuel moisture across the landscape under milder fire weather would contribute to explain the difference in performance between reanalysis and weather-station FWI indexes in depicting experimental fire behavior. Results suggest that preference should be given to weather-station FWI indexes over reanalysis or weather models forecasts when fire danger is low to moderate, e.g. for prescribed burning planning. Nonetheless, reanalysis FWI indexes indicate the moisture and consumption of slower-drying fuels better.

No advantages were found for weather-station FWI over reanalysis FWI (hence over ECMWF forecasts) for typical large-fire conditions, but the latter can substantially underestimate the potential for catastrophic fire behavior. Finally, sounder findings and recommendations would presumably result from supplementary higher-intensity experiments and, especially, more wildfire data. Further observation and reconstruction of wildfire runs in the future will be useful for such endeavor.

Acknowledgments

This work was carried out in the frame of COST Action CA22164 (https://nero-network.eu). PMF and DD were supported by national FCT funds (project UIDB/04033/2020.) AB was funded by FCT through a CEEC contract (CEECIND/03799/2018/CP1563/CT0003).

References

Benali A, Guiomar N, Gonçalves H, Mota B, Silva F, Fernandes PM, Mota C, Penha A, Santos J, Pereira JMC, Sá ACL (2023) The Portuguese large wildfire spread database (PT-FireSprd). *Earth System Science Data* **15**, 3791-3818. doi:10.5194/essd-15-3791-2023

Caetano M, Nunes V, Pereira M (2009) Land use and land cover map of continental Portugal for 2007 (COS2007): project presentation and technical specifications development. In '3rd Workshop of the EARSel Special Interest Group on Land Use/Land Cover', Vol. 1.

Cruz MG, Alexander ME, Fernandes PM (2022) Evidence for lack of a fuel effect on forest and shrubland fire rates of spread under elevated fire danger conditions: implications for modelling and management. *International Journal of Wildland Fire* **31**, 471-479. doi:10.1071/WF21171

Fernandes PM, Sil A, Rossa CG, Ascoli D, Cruz MG, Alexander ME (2020) Characterizing fire behavior across the globe. In 'The Fire Continuum—Preparing for the future of wildland fire: Proceedings of the Fire Continuum conference' Rocky Mountain Research Station Proc. RMRS-P-78. (Eds S Hood, S Drury, T Steelman, R Steffens) pp. 258-263. (USDA Forest Service: Fort Collins, CO)

Van Wagner CE (1987) Development and structure of the Canadian Forest Fire Weather Index System. Technical Report 35. (Canadian Forest Service: Ottawa, Canada)

Vitolo C. Di Giuseppe F, Barnard C, Coughlan R, San-Miguel-Ayanz J, Libertá, Krzeminski B (2020) ERA5-based global meteorological wildfire danger maps. Scientific Data **7**, 216. doi:10.1038/s41597-020-0554-z

Airborne LiDAR to Improve Canopy Fuels Mapping for Wildfire Modeling

Troy Saltiel*
Pacific Northwest National Laboratory, Richland, WA, USA troy.saltiel@pnnl.gov
Kyle Larson
Pacific Northwest National Laboratory, Richland, WA, USA kyle.larson@pnnl.gov
Aowabin Rahman
Pacific Northwest National Laboratory, Richland, WA, USA aowabin.rahman@pnnl.gov
André Coleman
Pacific Northwest National Laboratory, Richland, WA, USA andre.coleman@pnnl.gov

**Corresponding author*

Abstract

Increasing conflict between wildfire and the built environment has increased the need for more up-to-date and finer resolution canopy fuels data to improve wildfire modeling and associated risk forecasts. The US Forest Service and US Department of the Interior's LANDFIRE product, which provides 30-m resolution canopy fuels data for the entire US, is one of the most widely used sources of fuels data. However, the last complete mapping effort for LANDFIRE is based on 2016 conditions, and subsequent updates reflect disturbances 1-2 years behind the release year. Airborne systems equipped with Light Detection and Ranging (LiDAR) sensors can be deployed to actively sense canopy structure and estimate canopy fuels data (cover, height, base height, bulk density) at finer resolutions. Canopy base height (CBH) and canopy bulk density (CBD) are difficult to measure both in the field and in LiDAR point clouds. Still, they are important for accurately modeling crown fires, which are often intense and difficult to contain. Additionally, point cloud datasets are large, and calculations require efficient utilization of computational resources. To address these challenges, we are working on an approach that uses openly available National Ecological Observatory Network (NEON) airborne LiDAR data, with calculations processed in the R programming language and parallelized through the *lidR* package. CBH and CBD are often derived from tree height, diameter at breast height, and species-specific allometries using the Fire and Fuels Extension of the Forest Vegetation Simulator (FFE-FVS). We aim to test if airborne LiDAR can estimate CBH and CBD without the use of empirical equations. Reliable estimates of canopy fuels data directly from airborne LiDAR could streamline quick, fine-resolution updates for use in wildfire behavior models.

Keywords: canopy fuels, LiDAR, remote sensing, wildfire behavior modeling, LANDFIRE, canopy bulk density, canopy base height, FFE-FVS

Methods

We used LiDAR data from the National Ecological Observatory Network (NEON). NEON has sites throughout the United States and collects data in a standardized format, openly accessible from data.neonscience.org. We selected the Rocky Mountain National Park (RMNP) site in Colorado, USA for this initial work and have also selected an environmentally diverse set of sites for future work (Figure 1). The RMNP LiDAR dataset was collected in July 2020 and has a point density of 20 points/m^2, covering an area of 20 km^2 (Figure 2) (NEON, 2023).

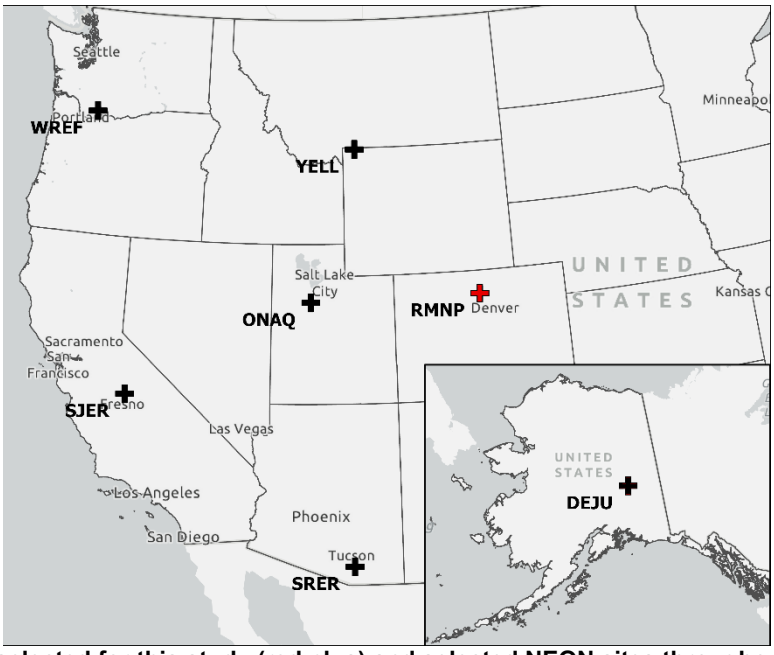

Figure 1: NEON site selected for this study (red plus) and selected NEON sites throughout the western USA for future work (black plus).

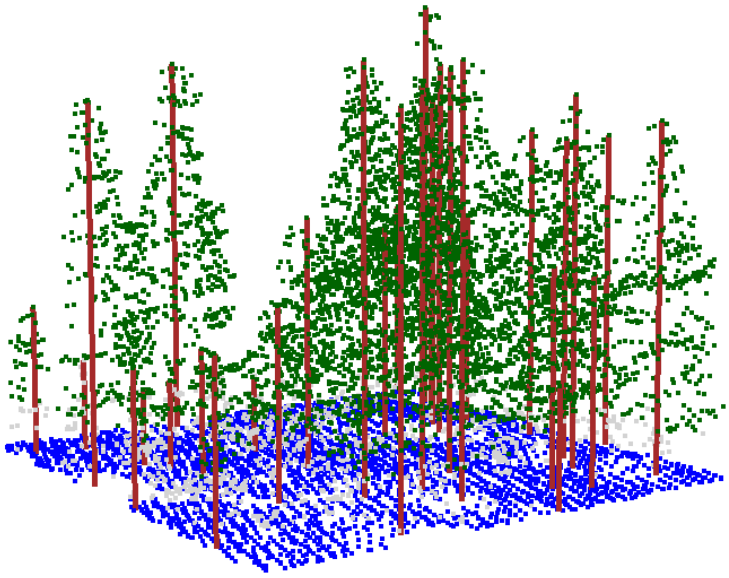

Figure 2: Sample 20×20 m subset of NEON LiDAR data from Rocky Mountain National Park, July 2020, with ground points (blue), vegetation points (green), and individual tree detection (brown).

Outputs were produced using the R programming language (R Core Team, 2023) and the *lidR* package (Roussel et al., 2020). The *lidR* package provides functions for point cloud filtering and normalization, tree detection and segmentation, and user-defined functions. *lidR* can also chunk datasets into smaller tasks and run these tasks in parallel, allowing fast and efficient processing.
Canopy metrics were calculated as follows:

- Canopy Cover (CC)= number of vegetation 1st returns ≥ 1.37 m (breast height) divided by the total number of 1st returns (Campbell et al., 2021)
- Canopy Height (CH) = maximum height of non-ground points
- Canopy Base Height (CBH) = the upper quantile value where the greatest difference in point density exists, applied to segmented tree data; see Figure 3 for an example of an individual segmented tree (Chamberlain et al., 2021)
- Canopy Bulk Density (CBD) = approximated using LANDFIRE by removing values <0.01 kg/m^3, kriging to 1 m resolution, then mapping values where LiDAR CC > 0
    - We also attempted training a Random Forest model on LANDFIRE CC, CH, and CBD data and applied it to NEON-derived CC and CH to predict NEON-derived CBD

Figure 3 shows an example tree and the location in its profile where the canopy metric would be calculated.

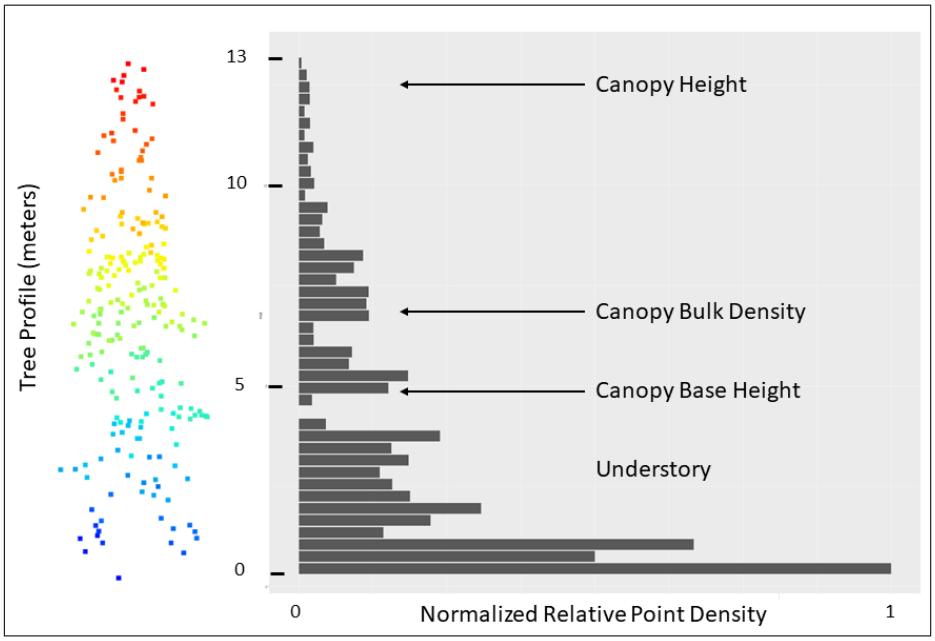

Figure 3: An example tree canopy profile, see Campbell et al. (2018) for an overview of normalized relative point density.

Results and discussion

Our results indicate that airborne LiDAR data can provide enhanced detail and more up-to-date products than existing datasets (Figure 4). Canopy metrics were produced at the individual tree scale, whereas common products, like LANDFIRE, estimate metrics at the forest stand scale. The fine spatial resolution captured tree canopies in places where LANDFIRE showed a lack of tree cover.

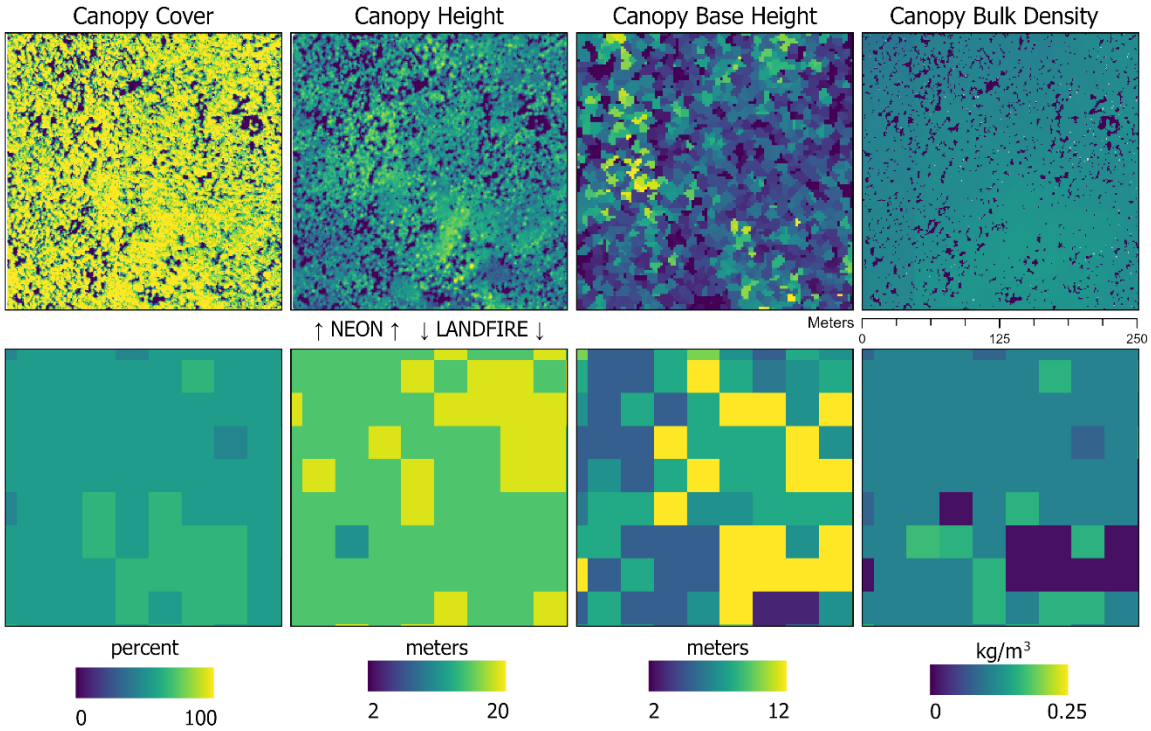

Figure 4: Example outputs for Rocky Mountain National Park, USA, comparing NEON LiDAR to LANDFIRE.

The increase in spatial resolution resulted in a different value distribution for CC. For the LiDAR-derived results at 1-m resolution, the single-pixel area of 1 m^2 often encompassed a single tree canopy, with 100% CC values common. In the 30-m resolution LANDFIRE dataset with 900 m^2 represented by a pixel, no pixel exceeded 85% CC, and 85% CC was uncommon. Taneja et al. (2021) similarly observed a bimodal distribution in CC values at 1-m resolution, with groups at 0 and 100% CC, and the bimodal distribution is not present at 30-m resolution.

Meanwhile, the mean LiDAR-derived CH (12.0 m) was lower than LANDFIRE (15.2 m) by 3.2 m after removing CH values where cover was <50% and reprojecting the LiDAR-derived CH to match LANDFIRE. LiDAR data is known to underestimate CH due to a combination of pulse density, canopy shape, observation scale, and footprint size (Roussel et al., 2017). Resampling with the third quartile value increased agreement, with a mean height of 13.3 m, but if using the LiDAR-derived CH at 1-m resolution, the values may need to be adjusted.

CBH is more difficult to compare to LANDFIRE. LANDFIRE's Existing Vegetation Type product, which is a thematic classification, has a strong effect on the CBH. For example, a Spruce-Fir Forest has canopy near the ground, while an Aspen Forest will have canopy very high up. These trees may mix within one 900 m^2 LANDFIRE pixel but must be assigned to the dominant class, while the LiDAR-derived CBH does not have this limitation.

Due to the nuances associated with the finer resolution of LiDAR-derived canopy metrics, the initial tests with a Random Forest model for LANDFIRE-informed CBD estimation were unsuccessful, essentially producing noise about the distribution of LANDFIRE CBD values. We generated a quick approach to map CBD by matching LANDFIRE values to LiDAR-derived pixels where there is CC.

The lack of reference data prohibited a full quantitative assessment of the results, relying only on physical measurements from the LiDAR data for CC, CH, CBH, and inferences from LANDFIRE for the CBD. Thus, these results require future replication and validation. Additionally, future work could be done to test fine-resolution canopy metrics (<5 m) as inputs to wildfire behavior models. Taneja et al. (2021) indicated that models using such inputs may underestimate wildfire spread because models were developed with coarser resolutions in mind (30 m). Gaps in CC, which are plentiful at 1-m resolution, did not allow fire to propagate. Modeling at a fine scale would better capture fuel breaks, like roads, which could greatly impact fire behavior. This work could also aid in measurements for adjacent work, such as fuel treatments, to quantify the change in canopy structure and potential fire behavior.

References

Campbell, M.J., Dennison, P.E., Kerr, K.L., Brewer, S.C. and Anderegg, W.R. (2021) Scaled biomass estimation in woodland ecosystems: Testing the individual and combined capacities of satellite multispectral and lidar data. *Remote Sensing of Environment*, **262**, 112511.

Campbell, M.J., Dennison, P.E., Hudak, A.T., Parham, L.M. and Butler, B.W. (2018) Quantifying understory vegetation density using small-footprint airborne lidar. *Remote sensing of environment*, **215**, 330-342.

Chamberlain, C.P., Meador, A.J.S. and Thode, A.E. (2021) Airborne lidar provides reliable estimates of canopy base height and canopy bulk density in southwestern ponderosa pine forests. *Forest Ecology and Management*, **481**, 118695.

NEON (National Ecological Observatory Network) (2023) Discrete return LiDAR point cloud (DP1.30003.001), RELEASE-2023. https://doi.org/10.48443/xxby-5a18. Dataset accessed from https://data.neonscience.org/data-products/DP1.30003.001/RELEASE-2023 on August 31, 2023.

Roussel, J.R., Auty, D., Coops, N.C., Tompalski, P., Goodbody, T.R., Meador, A.S., Bourdon, J.F., De Boissieu, F. and Achim, A. (2020) lidR: An R package for analysis of Airborne Laser Scanning (ALS) data. *Remote Sensing of Environment*, **251**, 112061.

Roussel, J.R., Caspersen, J., Béland, M., Thomas, S. and Achim, A. (2017) Removing bias from LiDAR-based estimates of canopy height: Accounting for the effects of pulse density and footprint size. *Remote Sensing of Environment*, **198**, 1-16.

Taneja, R., Hilton, J., Wallace, L., Reinke, K. and Jones, S. (2021) Effect of fuel spatial resolution on predictive wildfire models. *International journal of wildland fire*, **30** (10), 776-789.

R Core Team (2023) R: A language and environment for statistical computing. Vienna, Austria: R Foundation for Statistical Computing.

Proceedings for the 7th International Fire Behavior and Fuels Conference April 15-19, 2024, Boise, Idaho, USA – Tralee, Ireland – Canberra, Australia Published by the International Association of Wildland Fire, Missoula, Montana, USA

A novel method to adjust wind speed to mid-flame in low-intensity fires

*Macarena Ortega
Technosylva, Parque Tecnológico de León, 24009, León, Spain
Forest Fire Laboratory (LABIF), University of Córdoba, Campus de Rabanales, Edificio Leonardo da Vinci, 14071, Córdoba, Spain, mortega@tecnosylva.com

Juan Antonio Navarro
Centre for Technological Risk Studies, Polytechnic University of Catalonia, Campus Diagonal Besòs, Eduard Maristany St., 16 Building I, 08019 Barcelona, Catalonia, Spain, juanan.munoz.navarro@gmail.com

Juan Ramón Molina
Forest Fire Laboratory (LABIF), University of Córdoba, Campus de Rabanales, Edificio Leonardo da Vinci, 14071, Córdoba, Spain, jrmolina@uco.es

**Corresponding Author*

Introduction

Wind speed is a key weather factor driving fire behavior. Minor changes in wind fields can lead to significant variations in rate of spread and flame length. Therefore, accurately characterizing wind fields across the landscape is essential for effective fuel management and reliable fire behavior modeling.

Wind depends on terrain, vegetation, and distance from the ground (Rothermel, 1983). The theoretical logarithmic increase in wind speed with height can be irregular due to vegetation characteristics. Thus, it is important not only to know the wind speed but also to adjust it to the height at which it influences the fire spread. In forested sites, wind speed at 2 m- height (sub-canopy wind speed) affects low-intensity fires, while wind speed at 6 m (20-ft)- height affects high-intensity fires and crown fires. The 10–m wind speed is the standard meteorological height for wind measures of the World Meteorological Organization and the weather forecasts refer to this height.
Midflame wind speed was defined by Albini and Baughman (1979) as the average wind speed from the top of the fuel bed to the height of the flame above the fuel. Fire simulators compute wind speed as the in-stand mid-flame wind. Wind speed at 2-m serves as an approximation for in-stand mid-flame wind speed in the context of low-intensity surface fires. Therefore, wind speed at 2-m has already been used for modeling fire behavior in prescribed burnings (Molina et al., 2022a, 2022b). The in-stand mid-flame wind could be determined by multiplying the open wind speed (10-m wind speed based on the standard height for wind measures of the World Meteorological Organization) by a Wind Adjustment Factor (WAF). To more accurately predict fire behavior, it is necessary to identify WAF from standard weather stations that typically measure wind speed at 10m. WAF is dimensionless, ranging from 0 to 1. Fixed WAF mean values for different fuel

models are widely used to simulate fire spread- However, different forest stand characteristics cause the in-stand mid-flame wind to take on different values for the same fuel model and topographical position. This research aims to identify 1) the vegetation characteristics that influence wind speed; 2) the estimation of a model to adjust the 10-m open wind to in-stand wind speed at 2-m above ground based on the forest characteristics; and 3) the development of a simple and highly operationally applicable way to estimate WAF according to the most influential stand variables.

Our findings demonstrate that WAF varies with vegetation structure and forests stand characteristics. Canopy cover is the most influential variable on WAF, showing differences greater in dense stands than in open woodlands. Stand height and stand density also significantly affect WAF. The non-linear WAF model achieved a coefficient of determination (R^2) of 90% depending on canopy cover, as the variable with the greatest influence on WAF. The proposed model can be used to simulate low-intensity fire behavior such as prescribed burning, as well as simulate the effect of various canopy management alternatives, including fuel treatments and timber harvesting. Additionally, a decision tree analysis identified four decision nodes based on canopy cover, stand height, and stand density.

Materials and methods

This research was conducted in fifty-seven forested sampling sites across Southern Spain covering two regions: Andalucía and Castilla La-Mancha. The areas were dominated by *Pinus* species with and without understory and two wind exposures: sheltered and unsheltered. The variables of the vegetation inventoried in the plots included stand density, stand height, canopy base height (for both live and dead branch), diameter at breast height, crown diameter, and understory height.

The plots were stablished for WAF training and testing from 2014 to 2021 (114 days). Wind speed was measured simultaneously at two locations: one at an open site with no vegetation at 10-meter height, and another within the stand at 2-meter height, ensuring that the distance between the two locations was less than 100 meters. Subsequently, using the results from the field measurements, the WAF was calculated as the ratio between in-stand wind speed at 2-m of height and open wind speed at 10m above ground.

Results

The WAF varied significantly across the study area, ranging from 0.01 to 0.89 at the different sampled sites. Our findings identified canopy cover as the most significant variable in the WAF model, followed by stand density and basal area. Although fuel strata gap had a lower normalized importance, it plays an important role and has considerable implications for certain fuel treatments, such as pruning, brush clearing, and prescribed burnings. Therefore, canopy cover and fuel strata gap were considered the variables that most accurately explain WAF. While canopy cover was negatively correlated with WAF, z^2 was positively related to WAF. Including the fuel strata gap or distance between surface vegetation and the canopy base height (z^2) as an independent variable resulted in a slight

improvement in the model (Table 1). No significant differences were found between sheltered and unsheltered sites.

Table 1: WAF models

Model	Parameter	Estimation (standard deviation)	R^2	F	p	VIF	Training dataset RMSE (%) – MAE	Test dataset RMSE (%)- MAE
$WAF = a + b\ CC$	a	1.04 (0.03)	0.90	340.2	< 0.01	1.01	8 – 0.07	9 – 0.12
	b	−0.01 (0.001)						
$WAF = a + b * CC + c * z_2$	a	1.08 (0.04)	0.904	174.5	< 0.01	1.1	8 – 0.07	9 – 0.12
	b	−0.01 (0.001)						
	c	0.01 (0.009)						

Note: WAF is the Wind Adjustment Factor (0–1), CC is the canopy cover (%), z^2 is the fuel strata gap(m), R^2 is the coefficient of determination, RMSE is the root mean square error and MAE is the mean absolute error.
* RMSE and MAE based on the training and test dataset, respectively.

Cluster analysis identified three main clusters based on canopy cover (CC), with key thresholds at 77.5% and 47.5% CC. In dense forests, WAF was observed to be greater than in open woodlands, underscoring the significant impact of canopy cover on wind adjustment factors. As it is shown in Figure 1, open forests (CC≤47,5%) have a minimal impact on wind reduction (WFA=0,73) while dense forests (CC≥77,5%) had the highest impact reducing wind speed (WFA=0,14).

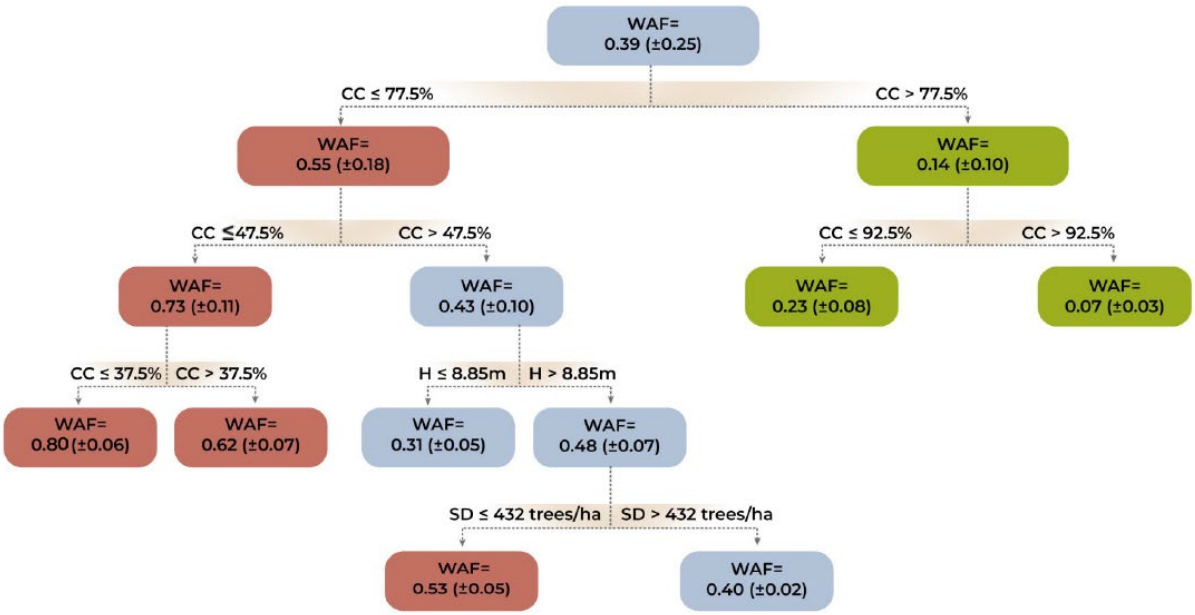

Figure 5: Decision tree for Wind Adjustment Factor (WAF) based on canopy cover, stand height and stand density. Note: CC is the canopy cover (%), H is the stand height (m) and SD is the stand density (trees/ha). Mean WAF value is identified in each node according to the sample.

Discussion

While various authors (Mueller et al., 2014) achieved WAF range in canopies between 0.15 and 0.37, other studies (Moon et al., 2019) showed a wider WAF variation between open woodlands and dense forests. In our study area, WAF ranged from 0.01 to 0.84, revealing significant differences between dense stands and open woodlands.

Significant heterogeneity in vertical wind profiles was observed, consistent with previous research (Cassiani et al., 2008; Dupont and Brunet, 2008). Our results further support earlier studies (Kenney et al., 2008; Pimont et al., 2011), indicating that canopy cover is the most influential variable affecting the WAF. In the same fuel model and topographical position, WAF can be modified by canopy cover (irregular vegetation structure, presence of canopy gaps and fuel treatments), stand height, and stand density. Although the topographical position of the stand (whether sheltered or exposed to the wind) is known to be a significant factor influencing the WAF (Andrews, 2012; Wagenbrenner et al., 2016), our study only detected minor significant differences in canopy cover between 47.5% and 77.5%.

The model proposed in our study assumes a constant WAF based on environmental characteristics, irrespective of changes in wind speed, which is consistent with the approaches used in BehavePlus and FlamMap software (Finney, 2004; Andrews, 2012). This contrasts with the drag coefficient, which continuously adjusts with wind speed due to the alignment of branches with the wind (Rudnicki et al., 2004). Previous research has indicated that WAF tends to be higher under light winds compared to heavy winds, as a result of a greater contact area (Rudnicki et al., 2004; Moon et al., 2019).

Although adding fuel strata gap as independent variable did not improve the accuracy of the model, it would increase the possibility to simulate pruning and/or brush clearing treatments on WAF, and therefore, on potential fire spread. Therefore, forest managers and fire managers could discern the most appropriate forest management to achieve the trade-off between timber harvesting or fuel treatment and fire spread.

Acknowledgements

This research was supported by ENFIRES project (PID2020-116494RR-C44), PDC2021-120845-C54 project (funded by Next Generation EU/PRTR) from the Spanish Ministry of Science and Innovation and the CILIFO project (0753_CILIFO_5_E) (INTERREG VA Spain-Portugal) from European Union. This project has also received funding from the European Union's Horizon 2020 research and innovation programme, FirEUrisk (H2020-LC-417 CLA-2020-101003890) under grant agreement no 101003890.

References

- Albini FA, Baughman RG (1979) Research Paper INT-221. U.S. Department of Agriculture. Forest Service. Intermountain Forest and Range Experiment. Ogden, p. 92.
- Andrews P (2012) General Technical Report RMRS-GTR-266. Department of Agriculture, Forest Service. United States. Rocky Mountain Research Station, 39 p.

- Cassiani M, Katul GG, Albertson JD (2008) The effects of canopy leaf area index on airflow across forest edges: large-eddy simulation and analytical results. *Boundary-Layer Meteorology* 126 (3), 433–460.
- Dupont S, Brunet Y (2008) Influence of foliar density profile on canopy flow: a largeeddy simulation study. *Agricultural and Forest Meteorology* 148, 976–990.
- Finney M (2004). Research Paper RMRS-RP-4. U.S. Department of Agriculture. Forest Service. Rocky Mountain Research Station, Ogden, 47 pp.
- Kenney PM, Keith TG, Ng TT, Linn RR (2008) In-field determination of drag through grass for a forest-fire simulation model. *WIT Transactions on Ecology and the Environment* 119, 23–29.
- Molina JR, Ortega M, Rodríguez y Silva F (2022a) Fire ignition patterns to manage prescribed fire behavior. Application to Mediterranean pine forests. *Journal of Environmental Management* 302, 114052.
- Molina JR, Ortega M, Rodríguez y Silva F (2022b) Scorch height and volume modeling in prescribed fires: effects of canopy gaps in Pinus pinaster stands in Southern Europe. *Forest Ecology and Management* 506, 119979.
- Moon K, Duff TJ, Tolhurst KG (2019) Sub-canopy forest winds: understanding wind profiles for fire behaviour simulation. *Fire Safety Journal* 105, 320–329.
- Mueller E, Mell W, Simeoni A (2014) Large eddy simulation of forest canopy flow for wildland fire modeling. *Canadian Journal of Forest Research* 44, 1534–1544.
- Pimont F, Dupu JL, Linn R, Dupont S (2011) Impacts of tree canopy structure on wind flows and fire propagation simulated with FIRETEC. *Annals of Forest Science* 68, 523–530.
- Rothermel RC (1983) General Technical Report INT-143. U.S. Department of Agriculture, Forest Service. Intermountain Forest and Range Experiment Station, Ogden, 34 pp.
-

- Rudnicki M, Mitchell SJ, Novak MD (2004) Wind tunnel measurements of crown streamlining and drags relationships for three conifer species. *Canadian Journal of Forest Research* 34(3), 666–676.
- Wagenbrenner NS, Forthofer JM, Lamb BK, Shannon KS, Butler BW (2016) Downscaling surface wind predictions from numerical weather prediction models in complex terrain with WindNinja. *Atmospheric Chemistry and Physics* 16, 5229–5241.

Assessing Fire Risk Components At Local Scale in the Wildland Urban Interface

*Eric Maillé, Ondine Le Fur
French National Research Institute for Agriculture, Alimentation and Environment (INRAE), RECOVER joined research unit INRAE-Aix Marseille University, Aix-en-Provence, France. eric.maille@inrae.fr, ondine.le-fur@interieur.gouv.fr

Rémi Savazzi
French National Forest Office (ONF), Forest Defense Against Fires Agency (Agence DFCI), Aix-en-Provence, France. remi.savazzi@onf.fr

**Corresponding Author*

Introduction

Risk assessment is a key activity for land management and planning (Calkin & al., 2019). We specified a model aimed at assessing fire risk at WUI through qualifying the spatial relationship between vegetation fuel and vulnerable anthropogenic values. It is composed of three main modules:

i) a classification of the spatial arrangements of individuated buildings (spatial structures of built up areas, Le Fur & al., 2024)
ii) a fuel land cover classification, including forest, open and semi-open wildlands, and agriculture vegetation. It is derived from a former model WUIMap I (Lampin-Maillet & al. 2010).
iii) The risk module itself (called WUIRisk) that links these spatial arrangements to components of the risk: ignition and spread hazards, and values exposure, defendability and vulnerability.

We implemented a research version in the Python language available to research end-users through a private web service.

Methods

The modules are experts' opinion based models, specified using different levels of formalism. The risk module was specified based on a multicriteria approach, in the INTERMED/MEDSTAR Interreg Project (Maillé & al. 2022) and a statistical analysis of ignition, outbreak, propagation and damages occurrences on anthropogenic values. We collected data on a sample of three main specific case study fires (Savazzi & al., 2024).

Anthropogenic Values Classification: The "Buildings Module"

The Unified INRAE/ONF buildings structures classification (Le Fur & al., 2024)

This model describes the spatial distribution of the scattered buildings areas, in relation to the fire risk. It defines 5 classes of urban and non-urban areas: 3 non-urban (isolated

buildings area, diffuse buildings area, buildings grouped islets) and 2 urban (principal urban area and complex secondary urban area). These three last classes are divided into internal and peripheral ones (first range of buildings, in contact with vegetation). Criteria defining the classes are density, contiguity, shape and proximity indicators, calculated using some simple sequences of spatial analysis operations (buffers, contact length, area/perimeter ratios, etc.). The polygon layer of individuated buildings is the only input. Figure 1 presents the implemented workflow.

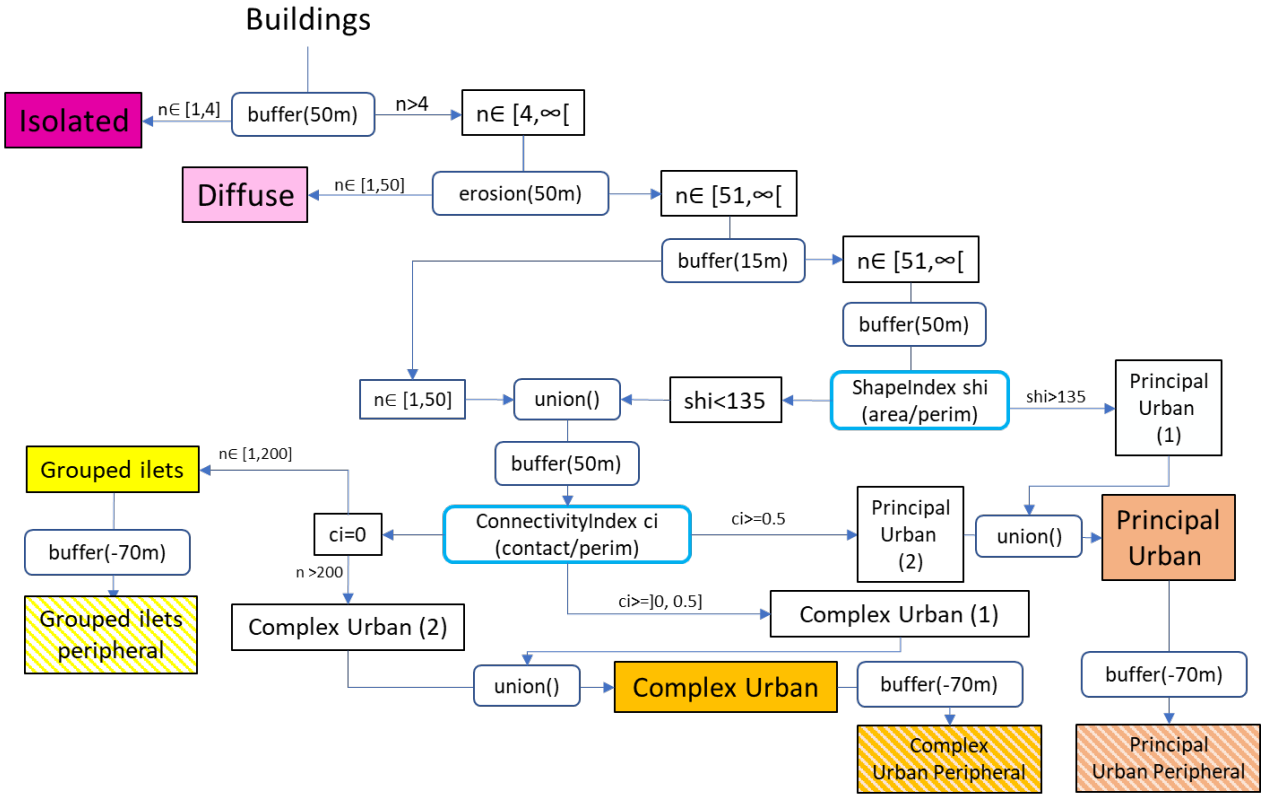

Figure 1: Simplified algorithm workflow of the unified INRAE/ONF model (Le Fur & al. 2024)

The algorithm is endowed with 16 parameters (buffer distances, density thresholds, buildings population thresholds, shape and connectivity indexes, etc.). The operational version, dedicated to French decision makers (land planners) was calibrated for the South Eastern French Mediterranean area context. A research version is also available in order to study the sensibility of the algorithm to the parameters values, and to adapt it to some other contexts.

Defendability indicators

Defendability is defined as the ability of an area to be defended by the firefighting services. In this particular meaning, three main criteria are taken into account: the fuel biomass and structure, and more specifically the clearing state, the accessibility and the hydrants availability. Because the clearing state is cyclical, the only two last criteria are assessed in this module.

Accessibility

For the assessment of the interface accessibility, we distinguish between local and regional accessibility. The regional accessibility is the cumulated route impedance from the closest firefighting station to the interface patch. Only one shortest way is assessed. For the local accessibility of an interface area (polygon), we use two main indicators:

- The route impedance of the different ways that reach the polygon from the closest "base cross" with a two lanes road.
- The average route impedance of the shortest way to the different buildings from their respective closest "base cross" with a two lanes road.

Both prevent routes with one or more bottlenecks (width lower than 3m).

Hydrant availability

Hydrant availability is the assessment of their accessibility from each of the buildings. A scheme of the model of hydrant availability is presented in the next figure 2.

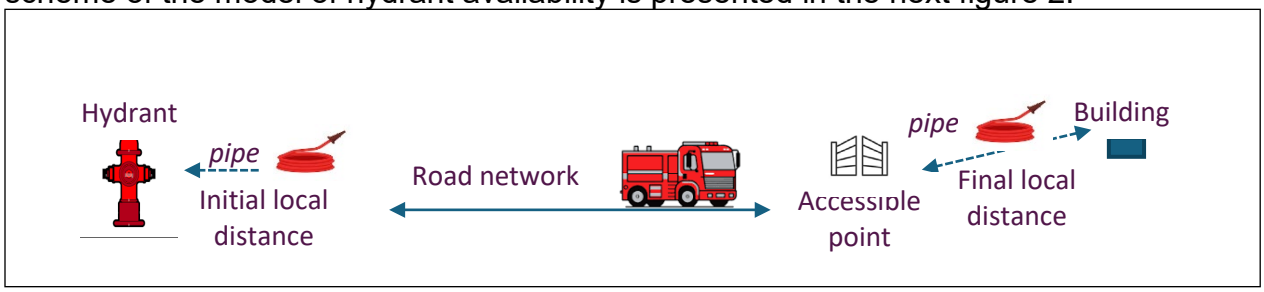

Figure 2. Scheme of hydrant availability assessment

In general, a hydrant allows the firetruck to refill its tank, and to roll up to the closest bottleneck (typically a gate too narrow for the truck to pass through – by default less than 3m). The fire pipe length (20m by default) must be greater or equal to the final local distance.

Exposure to vegetation fuel and contextual hazard

A "fuel model" associating one fuel attribute to each vegetation type was specified based on the particular 'IGN BDForet©' vegetation map. This attribute is a simple coefficient representing the "fuel potential" of each vegetation type, from 0 (no 'fuel potential') to 1 (maximum fuel potential). From this point, two serial of attributes are calculated and assigned to each of the interface polygons:

- A set of "content" fuel attributes characterizing fuel within each of the interface polygon. This local fuel plays the role of transferring energy from the forest massif to the value (building): it is considered as the main factor of exposure.

- A set neighbourhood attributes characterizing fuel in contact with the interface polygon. These indicators are considered as the main hazard factors (contextual hazard).

The Multi-Components Fire Risk Model

The so defined indicators are related to different components of the risk using an expert opinion based multi-criteria analysis. For each component of the risk (hazard, exposure, vulnerability, defendability, etc.) experts first define some relevant classes of each indicator values in relation to the analysed component. Components are then organized into a hierarchy (figure 3), which nodes and classes of indicators values are "weighted" (a weight is assigned to them) using a multi-criteria formalism (Ascendant Hierarchy Process - AHP).

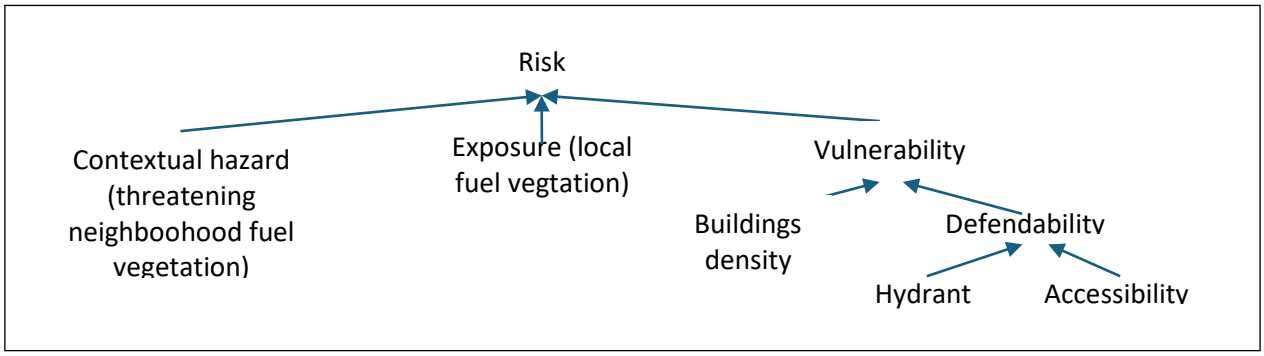

Figure 3. A simple hierarchy for multi-components risk assessment

This experts' opinions based multi-components fire risk model allows to calculate a risk level attribute assigned to each interface polygon in relation to the value of the different indicators. For operational purposes, some generic risk indicators are also assigned to each of the interface classes (figure 4).

	Interface class	Contextual hazard	Unit Buildings vulnerability	Stake density	Cumulated vulnerability	Resulting global risk
500	Isolated buildings, no aggregated fuel	+	++++	+	+++	+
501	Isolated buildings, semi-aggregated fuel	++	++++	+	+++	++++
502	Isolated buildings, aggregated fuel	++++	++++	+	+++	+++++
400	Scattered buildings, no aggregated fuel	+	+++	++	++++	++
401	Scattered buildings, semi-aggregated fuel	++	+++	++	++++	+++
402	Scattered buildings, aggregated fuel	++++	+++	++	++++	++++
300	Clustered internal buildings, no aggregated fuel	+	++	+++	++	+
301	Clustered internal buildings, semi-aggregated fuel	++	++	+++	++	++
302	Clustered internal buildings, aggregated fuel	++++	++	+++	++	+++
310	Clustered peripheral buildings, no aggregated fuel	+	+++	+++	+++	0+
311	Clustered peripheral buildings, semi-aggregated fuel	++	+++	+++	+++	+
312	Clustered peripheral buildings, aggregated fuel	++++	+++	+++	+++	++

	Interface class	Contextual hazard	Unit vulnerability	Stake density	Cumulated vulnerability	Resulting global risk
200	Complex secondary urbanized areas internal buildings, no aggregated fuel	+	++	+++	++	+
201	Complex secondary urbanized areas internal buildings, semi-aggregated fuel	++	++	+++	++	+++
202	Complex secondary urbanized internal buildings, aggregated fuel	++++	++	+++	++	++++
210	Complex secondary urbanized areas peripheral buildings, no aggregated fuel	+	++++	+++	++++	+++
211	Complex secondary urbanized areas peripheral buildings, semi-aggregated fuel	++	++++	+++	++++	+++++
212	Complex secondary urbanized areas peripheral buildings, aggregated fuel	++++	++++	+++	++++	+++++
100	Main urbanized areas internal buildings, no aggregated fuel	+	+	++++	++	0+
101	Main urbanized areas internal buildings, semi-aggregated fuel	++	+	++++	++	+++
102	Main urbanized internal buildings, aggregated fuel	++++	+	++++	++	++++
110	Main urbanized areas peripheral buildings, no aggregated fuel	+	+++	++++	++++	++
111	Main urbanized areas peripheral buildings, semi-aggregated fuel	++	+++	++++	++++	++++
112	Complex secondary urbanized areas peripheral buildings, aggregated fuel	++++	+++	++++	++++	+++++

Figure 4. Example of a rule based model relating interface classes to risk components

Conclusion

We propose a framework implemented as a private web-service aimed at assessing structural wildfire risk of different classes of Wildland Urban Interface. The underlying WUIRisk model is based on the spatial analysis of the relationship between urban structures and spatial distribution of vegetation fuel. Interface classes are endowed with attributes including accessibility, hydrant availability and fuel biomass indicators. Statistical validation of the model is ongoing. Many new indicators (including propagation factors: slope, dominant wind, etc.) should be incorporated in the model in order to refine it. We also developed a dynamic model called WUIDyn in order to simulated risk change at WUI (Maillé & al. 2022).

References

Calkin D, Price O, Salis M (2019) WUI Risk Assessment at the Landscape Level. In 'Encyclopedia of Wildfires and Wildland-Urban Interface (WUI) Fires.' (Eds S Manzello, Samul L), pp. 1-11, (Springer, Cham. https://doi.org/10.1007/978-3-319-51727-8_97-1)

Lampin-Maillet C, Jappiot M, Long M, Morge D, Ferrier JP (2010) Mapping wildland-urban interfaces at large scales integrating housing density and vegetation aggregation for fire prevention in the South of France. Journal of Environmental Management 91.

Lampin-Maillet, C., Bouillon, C., 2010. WUImap© Cemagref 2010 : Tool for mapping wildland-urban interfaces. User's notice 18.

Le Fur O, Savazzi R, Maillé E, Reymond B, Kizirian L (2024) Classification des zones bâties vulnérables aux incendies dans l'interface bâtiments-végétation : démarche, méthodologie et utilisation (rapport technique), p. 55. (INRAE, ONF)

Maillé E, Fablet T, Salis M, Del Giudice L, Arca B, Scarpa C, Pellizzaro G, Duce P, Sirca C, Ribotta C, Costa Saura JM, Bouillon C (2022) Rapport sur la cartographie du risque à l'échelle du paysage et des interfaces urbain-rural. Rapporto sulla zonizzazione del rischio a livello di paesaggio e di interfaccia urbano-rurale. MEDSTAR project, EU Programme Interreg IT-FR MARITTIMO. Product T223.

Maillé E, Ganteaume A, Bouillon C (2022) Anticipation of future fire risk due to land cover change and WUI extend. Application to the Baronnies Provençales Regional Natural Park (France). In 'Advances in Forest Fire Research 2022' . (Eds XD Viegas, LM Ribeiro) pp. 527–532 (ADAI publ. https://doi.org/10.14195/978-989-26-2298-9_82)

Savazzi R, Martin W, Poppi JC, Maillé E (2023) Feu de Gonfaron, Retour d'expérience sur les dégâts aux bâtis en lien avec le débroussaillement, Rapport d'Etude DGPR, ONF, INRAE, DDTM83, SDIS83.

Fundings

This work was partly funded by the "MED-Star" (grant no. E88H19000120007) and "INTERMED" (grant no. G39E18000370007) projects, supported by the European Union under the cross-border Program Italia-France Marittimo 2014–2020, and by the French Ministry of Ecological Transition and Territorial Cohesion.

Assessing Vegetation Flammability According to Different Types of Fuel Treatment

Arthur Boschet*
Aix-Marseille Université – INRAE – UMR RECOVER, 3275 Route de Cézanne, Aix-en-Provence, France, arthur.boschet@inrae.fr

Anne Ganteaume
Aix-Marseille Université – INRAE – UMR RECOVER, 3275 Route de Cézanne, Aix-en-Provence, France, anne.ganteaume@inrae.fr

* *Corresponding Author*

Introduction

Forest fires are a major risk in the Mediterranean area, as in southeastern France, ravaging thousands of hectares every year (www.bdiff.agriculture.gouv.fr). This risk is exacerbated by climate change, e.g. increase in the frequency of extreme weather events, and by changes in land use, e.g. increase in wildland-urban interfaces (WUI) (Chappaz and Ganteaume 2022). In SE France, a regulation has been implemented to prevent as much as possible fires at the WUI, mainly through fuel reduction measures e.g. mechanical or manual bush and grass clearing, prescribed burning (Curt and Fréjaville 2017). However, the effect of the different measures on the fire hazard reduction has a little (Marino et al 2010; Marino et al. 2011; Madrigal et al. 2012) or not been verified yet, especially according to the vegetation type and the treatment return interval, focusing more on the response of the vegetation to the fire (Fernandez et al 2013). The aim of this work is to fill these gaps, focusing on the effect of the treatment on the reduction of the fire ignition and propagation.

Material and methods

Study area and fuel treatments studied

The studied area is the French administrative district Bouches-du-Rhône, a typical mediterranean area in terms of temperature, precipitations and vegetation, and is regularly affected by fires.

Three differents types of fuel treatments have been selected : mechanical bush clearing, prescribed burning and grass-clearing with or without residues left *in situ* (figure 1).

Vegetation was sampled according to two return intervals : T0 – vegetation treated just before the fire season, T1 – vegetation treated the previous year

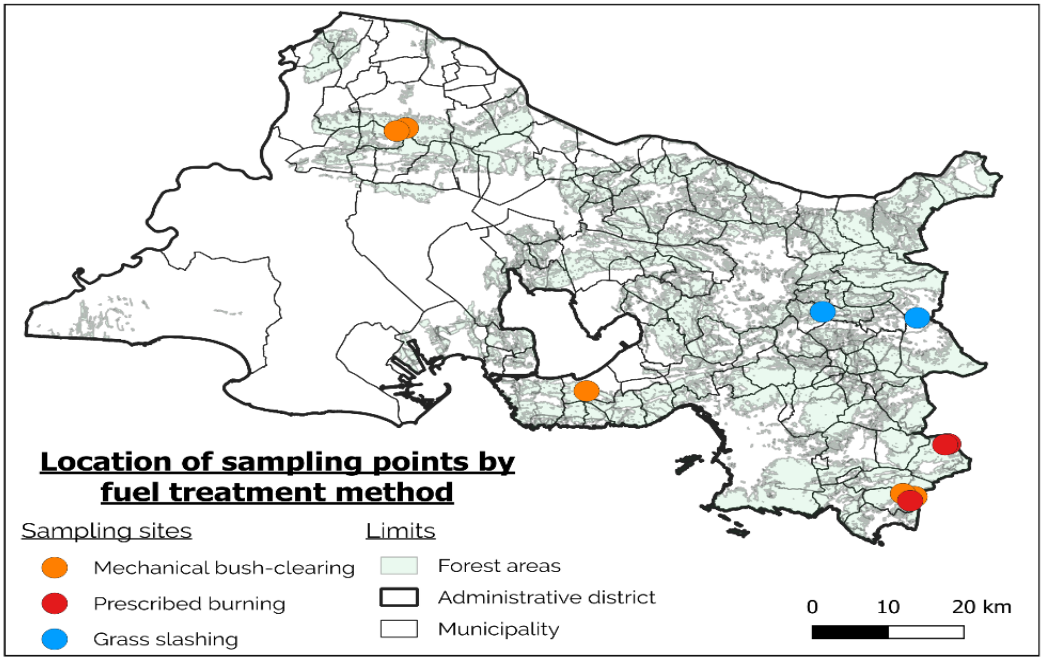

Figure 6 : Location of sampling points for each fuel treatment method in the Bouches du Rhône

Field sampling

The vegetation sampled varied according to the treatment. For mechanical bush clearing and prescribed burning the selected vegetation was the *Quercus coccifera* shrubland growing under a cleared *Pinus halepensis* forest ; and for grass slashing, it was roadside grass (*Bromus* sp.).

Sampling was carried out during the summer 2023 to have a vegetation status corresponding to the fire season (i.e. low moisture content). An aluminium tray (30*25cm) or a metal template (18*20 cm), depending on the type of vegetation, were used to delimit the vegetation samples which were extracted with a large flat shovel or a trowel. The harvested vegetation was cut at ground level (to be reconstructed in the laboratory), then the litterbed was removed with as little disturbance as possible to maintain the fuel microstructure. Samples were kept in a cooler in order to avoid water loss. Some site parameters like exposition, altitude, mean precipitation and temperature over the last 3 months were also recorded.

Burning experiments

Once back in the laboratory, an initial fuel moisture content (FMC) measurement was carried out. The vegetation was replaced in the samples just before the burning experiments and some sample parameters, were also recorded (e.g. FMC, vegetation bulk density, litterbed height, neddle proportion in the litter).

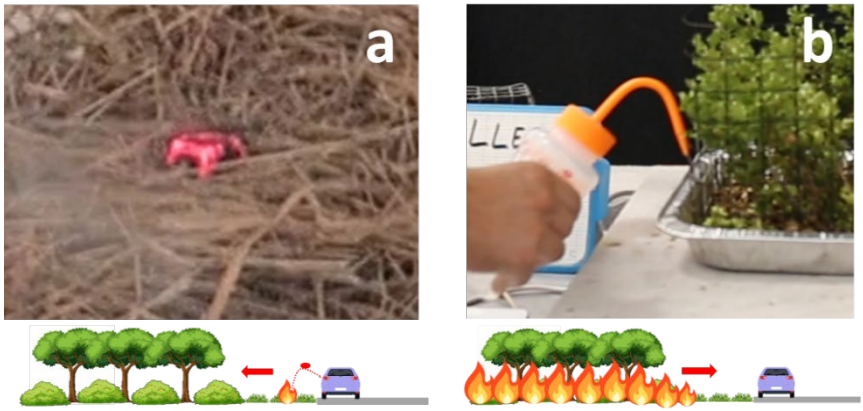

Figure 7 : The 2 ignition protocols : the glowing brand (a), and the alcohol line (b).

Two ignition protocols were implemented to test fire ignition and propagation respectively, successively.

The first ignition source was a glowing firebrand to study fire ignition at the road-forest interface, as already used in previous studies (e.g. AIOLI rapport final 2007, Ganteaume et al. 2009), using a *Pinus sylvestris* cube placed on a 500-W epiradiator and which was then placed in the centre of the sample at the end of the flaming phase (figure 2.a). A 10 km h^{-1} wind was generated using a domestic fan.

The second ignition source was a line of alcohol, drawn across the width of the sample and then lit with a matchstick (figure 2.b).

During the burning experiments, different variables were measured corresponding to the main components of flammability (Anderson. 1970 ; Martin et al. 1993) : ignition frequency (%), ignition delay (in s), flaming duration (in s), fire spread (number of sample side reached by fire), maximum temperature (in °C), total heat flux (in kW), rate of spread (in cm s^{-1}) and flame front intensity (derived from Byram's equation ; in kW m^{-1})) and % of fuel consumed during the burn. The fire bench was inspired by Ganteaume et al. 2009 and Marino et al. 2010 (figure 3).

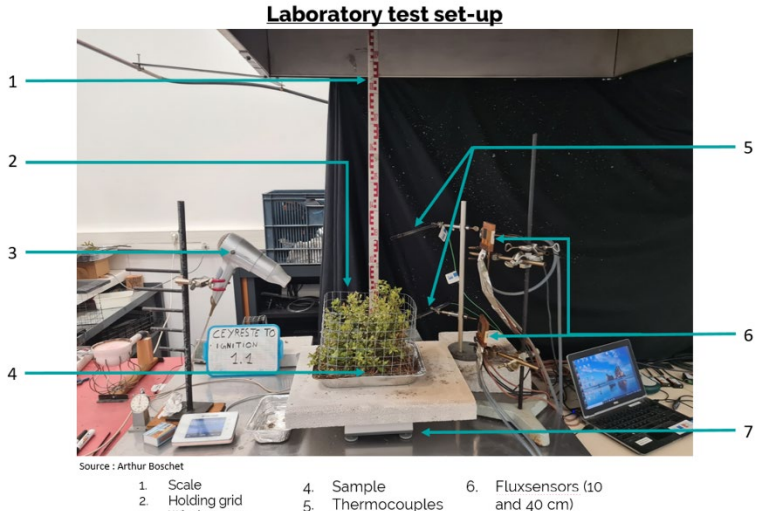

Figure 8 : Fire bench used in laboratory burning experiments

Statistical analyses

Linear Model and/or Global Linear Model analyses were used to show any noticeable influence of site and sample parameters on flammability. So 1-factor ANOVAs were performed on the residuals of these models to only highlight the treatment effect on flammability, free from external effects, comparing flammability in treated vegetation *vs* untreated vegetation.

Results and discussion

Regarding the type of fuel treatment (Table 1), Mechanical brush-clearing and Prescribed burning mostly resulted in a decrease in flammability of the post-treatment vegetation according to other studies (Marino et al 2010, Marino et al 2011, Marino et al 2012, Banerjee 2020), except for spread due to an enhanced effect of wind in the treated vegetation. Lower vegetation bulk density and needle proportion in the litterbed as well as lower litterbed thickness mostly helped to decrease flammability.

Grass slashing presented contrasted effects (Table 1), but mostly increased flammability, regardless of the presence or absence of residues left, mostly because of higher proportion of dead fuel. This result agrees with what had been found in a previous study (AIOLI 2007). Ignition by glowing firebrands was facilitated by higher contact surface with the fuel in the treated samples. Ignition frequency without residues was higher than that of the modality with residues due to higher air flow through the samples.

Regarding the return interval (Table 1), regardless of the treatment, T0 and T1 showed a decrease in flammability compared to the control (except for spread). Comparing T0 and T1, there was no significant effect for prescribed burning but a contrasted effect for mechanical brush-clearing according to the variable considered (but mostly flammability decreased for T1).

Conclusion

Flammability was significantly reduced after prescribed burning and mechanical brush-clearing, regardless of the return interval and the effect of treatment was still effective after one year. Furthermore, very poor ignition by glowing firebrands was highlighted for both types of treatment. Grass slashing mostly increased flammability, with or without vegetation residues left and the ignition by glowing firebrands was facilitated (especially without residues left) which was not the effect intended.

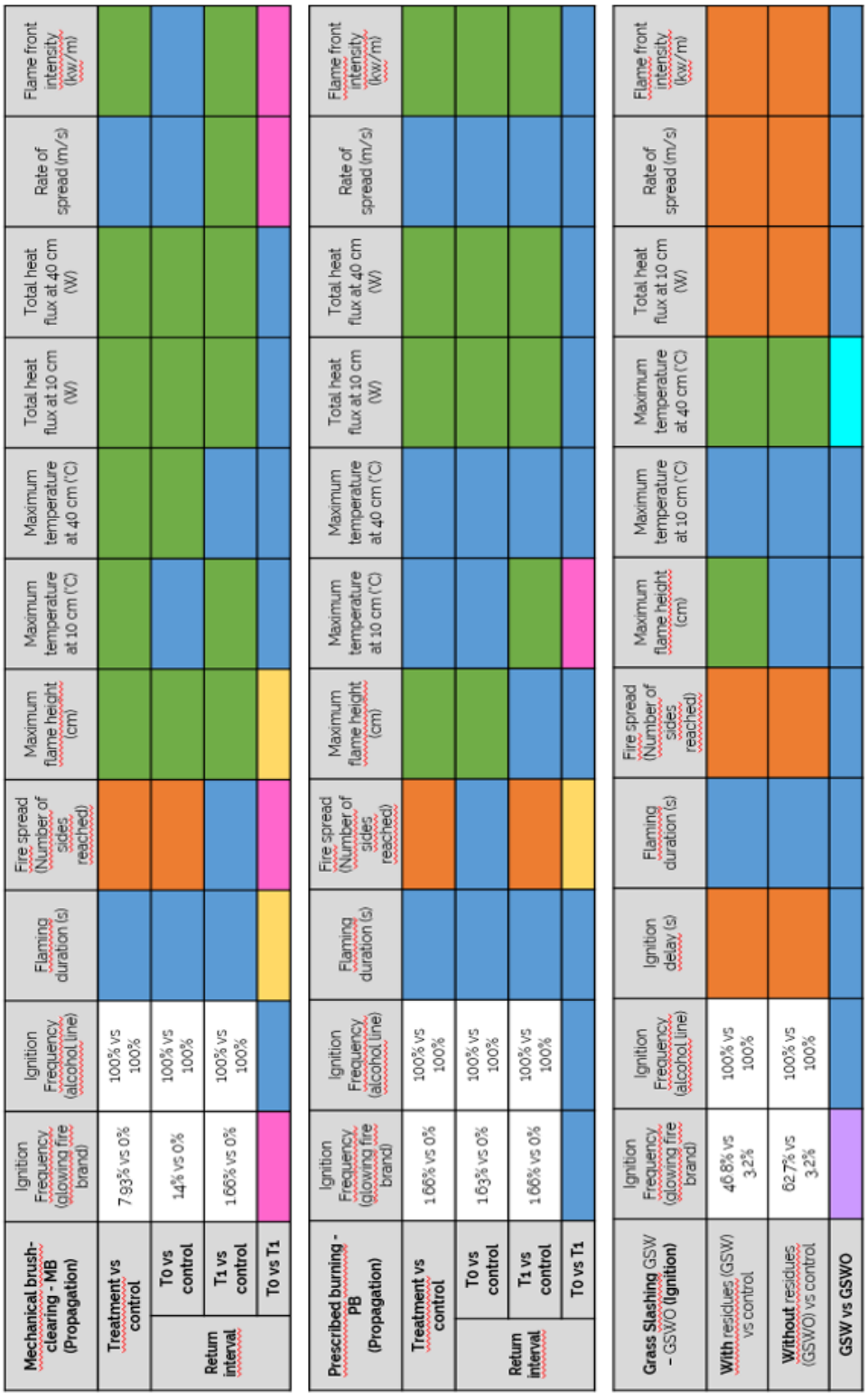

Table 1 : Significant and non-significant effects of fuel treatment methods alone and over time on flammability variables

Acknowledgements
The study was funded by the RMT AFORCE. Special thanks to M Audouard, A Dieudonné, A Dohgmane, J-M Lopez, C Travaglini for their help.

References

- Anderson H E (1970) Forest fuel ignitibility.Fire Technology vol 6, n°4, 312-319.
- Banerjee T (2020) Impact of Forest Thinning on Wildland Fire Behavior. Forests.
- Chappaz F, Ganteaume A (2022) Role of land-cover and WUI types on spatio-temporal dynamics of fires in the French Mediterranean area. Risk Analysis.
- Curt T, Frejaville T (2017) Wildfire Policy in Mediterranean France : How far is it Efficient and Sustainable ?: Wildfire Policy in Mediterranean France. Risk Analysis.
- Fernandez C, Vega JA, Fonturbel T (2013) Shrub resprouting response after fuel reduction treatments: Comparison of prescribed burning, clearing and mastication. ournal of Environmental Management 117 235-241
- Ganteaume A, Lampin-Maillet C, Guijarro M, Hernando C, Jappiot M, Fonturbel T, Perez-Gorostiaga P, Vega JA (2009) Spot fires : fuel bed flammability and capability of firebrands to ignite fuel beds. International Journal of Wildland Fire 18.
- Jappiot M, Lampin C, Curt T, Ganteaume A, Borgniet L, Bouillon C, CHANDIOUX O, Esteve R, Long L, Martin W, Morge D, Alexandrian D, D'Avezac H, Tatoni T, Dumas E, Valette JC, Moro C (2007) Modélisation et cartographie de l'aléa d'éclosion d'incendie de Forêt – Programme AIOLI rapport final
- Madrigal J, Marino E, Guijarro M, Hernando C, Diez C (2012) Evaluation of the flammability of gorse (Ulex europaeus L.) managed by prescribed burning. Annals of Forest Science 69, 387-397.
- Marino E, Madrigal J, Guijarro M, Hernado C, Diez C, Fernandez C (2010) Flammability descriptors of fine dead fuels resluting from two mechanical treatments in shrubland : a comparative laboratory study. International Journal of Wildland Fire 19, 314-324.
- Marino E, Guijarro M, Hernando C, Madrigal J, Diez C (2011) Fire Hazard after prescribed burning in a gorse shrubland : Implications for fuel management. Journal of Environmental Management 92, 1003-1011.
- Marino E, Hernando C, Madrigal J, Dıez C and Guijarro M (2012) Fuel management effetiveness in a mixed heatland : a comparison of the effect of different treatment types on fire initiation risk. International Journal of Wildland Fire 2012, 21, 969–979
- Martin RE, Gordon DA, Gutierrez ME, Lee DS, Molina DM, Schroeder RA, Sapsis DB, Stephens SL, Chambers M (1993) Assessing the flammability of domestic and wildland vegetation. 12 Conference on Fire and Forest Meteorology.

Proceedings for the 7th International Fire Behavior and Fuels Conference April 15-19, 2024, Boise, Idaho, USA – Tralee, Ireland – Canberra, Australia Published by the International Association of Wildland Fire, Missoula, Montana, USA

Best Forest Fuel Treatments to Reduce Emissions from Megafires in the Northern Sierra Nevada, California

Kayla Johnston*
Spatial Informatics Group, 2529 Yolanda Court, Pleasanton, California, USA, kjohnston@sig-gis.com

David Schmidt
Spatial Informatics Group, Pleasanton, California, USA, dschmidt@sig-gis.com

Carrie Levine
Spatial Informatics Group, Pleasanton, California, USA, clevine@sig-gis.com

Thomas Buchholz
Spatial Informatics Group, Pleasanton, California, USA, tbuchholz@sig-gis.com

**Corresponding Author*

Introduction

Across the western United States, wildfire is increasing in intensity, size, and frequency (Westerling et al., 2006). Fuel treatments can reduce wildfire severity and improve wildfire suppression efficiency ultimately resulting in smaller wildfires (Cochrane et al., 2012; Moghaddas and Craggs, 2007). However, the current pace and scale of fuel treatments is inadequate to substantially reduce wildfire and the associated negative impacts on the landscape (Prichard et al., 2021). Many challenges exist to increasing the pace and scale of fuel treatments, including budgetary and personnel limitations. Market-based solutions can help overcome these budgetary and personnel limitations.

In 2023, the Climate Forward program of the Climate Action Reserve, an offset registry for the global carbon market, released the Reduced Emissions from Megafires (REM) Forecast Methodology which quantifies anticipated greenhouse gas (GHG) emission reductions from the implementation of fuel treatments (Ebert et al., 2023). Anticipated GHG emission reductions are quantified over a project duration of 40 years by accounting for carbon in standing live trees, shrubs, and herbaceous understory; standing dead trees; dead surface fuels (woody debris, litter, and duff); harvested wood products; biomass combustion emissions from fires (prescribed and wildfire); mobile combustion emissions; and biological emissions from decomposition of forest products. Carbon estimates are made based on model outputs from the Fire and Fuels Extension to the Forest Vegetation Simulator (FVS-FFE), a wildfire spread simulation model, and the First Order Fire Effects Model. The REM methodology seeks to quantify whether a fuel treatment reduces wildfire carbon emissions enough to overcome the carbon emissions from the treatment and the foregone carbon sequestration of any trees culled in the fuel treatment process. In this context, the performance of a given fuel treatment

to net reduced emissions can vary by forest type and initial forest condition because the outputs will vary with tree species' growth rates and fire resilience and resistance.

We explored the performance of four fuel treatments commonly implemented in California's northern Sierra Nevada for its four most common forest types with varying initial forest conditions. We followed the REM methodology using synthetic landscapes and evaluated all fuel treatments for each forest type-condition.

Materials and methods

Study area

The study area encompasses 19,602 square kilometers in NE California (Figure 1). The area experiences a Mediterranean to montane climate. The dominant forest types were mixed conifer, Douglas-fir (*Pseudotsuga menziesii*), ponderosa pine (*Pinus ponderosa*), and white fir (*Abies concolor*) (Riley et al., 2022).

Synthetic landscapes

Synthetic forested landscapes were created to control for impacts of spatial variability in topography and forest stand conditions. All forest stands within the study area matching each of the four dominant forest types were derived from the TreeMap 2016 dataset (Riley et al., 2022). FVS-FFE was used to simulate wildfire in all stands to determine wildfire hazard based on model-estimated flame length and percent basal area mortality (Figure 2) (Dixon, 2024; Rebain et al., 2022). Twelve synthetic landscapes were created consisting of uniform coverage of either low-, moderate-, or high-wildfire hazard stands for each forest type. Zero slope, elevation, and aspect were used for all synthetic landscapes.

Fuel treatments

Four fuel treatments were independently implemented in each of the 12 synthetic landscapes (Table 1).

Analysis

The REM methodology was implemented as published (Ebert et al., 2023) and the minimum annual burn probability (ABP) required to achieve net GHG emission reductions was iteratively discovered for each forest type-condition-fuel treatment combination. All other inputs being equal, the ABP will drive outcomes. The value of the minimum required ABP and the effectiveness of a given fuel treatment are inversely proportional. We used the following criteria to rate each treatment:

- "best": lowest minimum required ABP
- "alternative": minimum required ABP ≤0.10
- "failed": no reduction in emissions or minimum required ABP > 0.10

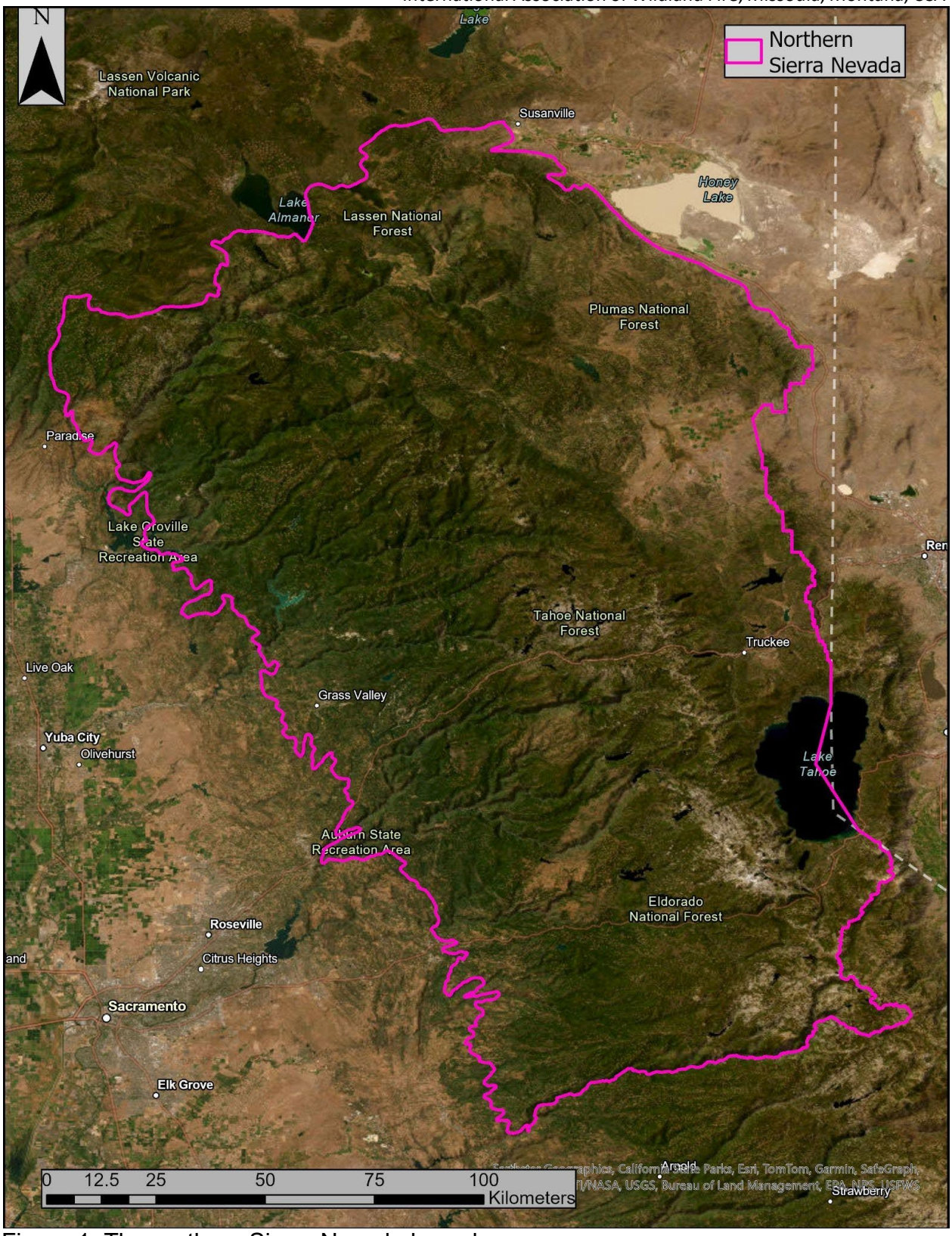

Figure 1. The northern Sierra Nevada boundary.

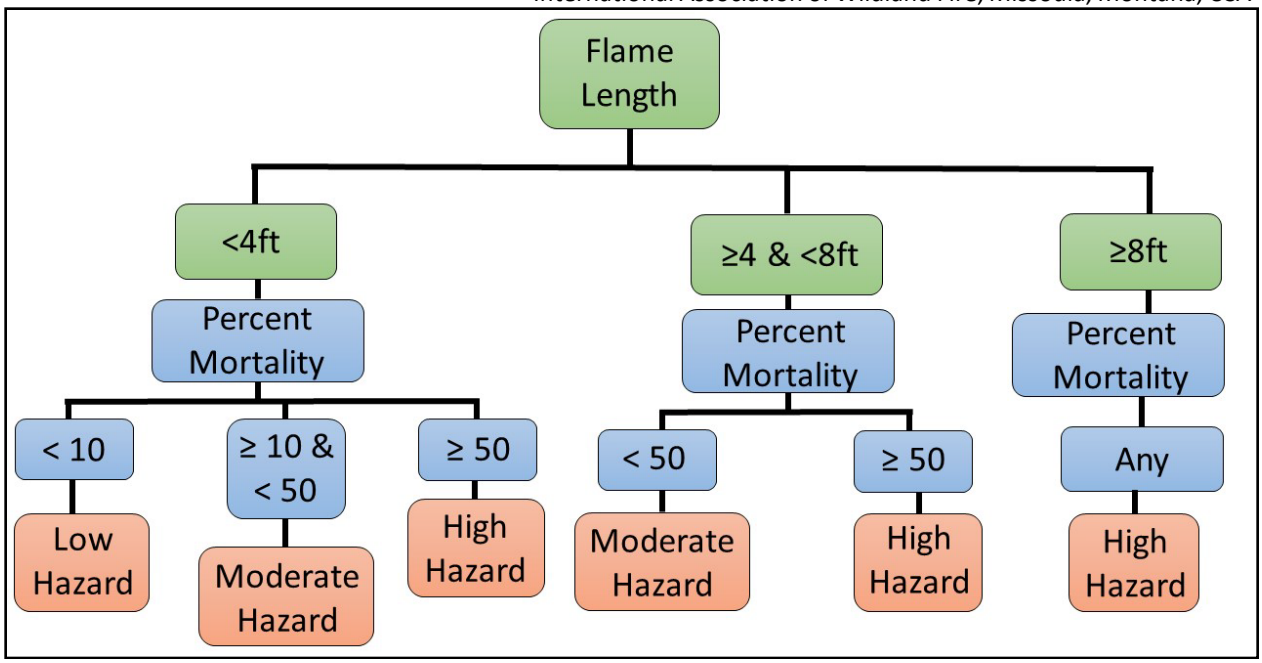

Figure 2. Flowchart showing how each forest stand was assigned a hazard level.

Table 1. The four fuel treatments simulated.

Fuel Treatment	**Thinning Specifications**	**Pile Burn**	**Broadcast Burn**	**Mastication**
Commercial Thin + Broadcast Burn	Thin from below, up to 30” DBH, to a residual 35% of max SDI	—	Yes	—
Hand Thin + Pile Burn	Thin 90% of trees up to 10” DBH	Yes	—	—
Mastication	Thin 90% of trees up to 10” DBH	—	—	Yes
Broadcast Burn Only	—	—	Yes	—

Results

Mixed conifer forest type

In the mixed conifer forest type the “hand thin + pile burn” was the best fuel treatment. The “commercial thin + broadcast burn” and “broadcast burn only” fuel treatments were

alternatives for various hazard levels (Table 2).

Douglas-fir forest type

In the Douglas-fir forest type the "hand thin + pile burn" was the best fuel treatment. The "broadcast burn only", "commercial thin + broadcast burn, and "mastication" fuel treatments were alternatives for various hazard levels (Table 3).

Ponderosa pine forest type

In the ponderosa pine forest, all fuel treatments failed to reduce net GHG emissions in low-hazard conditions. In moderate-hazard conditions, the "hand thin + pile burn" fuel treatment was the best choice with all others as alternatives. In the high-hazard conditions "hand thin + pile burn" was also the best fuel treatment but all others failed (Table 4).

White fir forest type

In the white fir forest, the "hand thin + pile burn" was the best fuel treatment while all other fuel treatments failed (Table 5).

Table 2. Mixed conifer forest type results.

Fuel Treatment	**Low Hazard**	**Moderate Hazard**	**High Hazard**
Commercial Thin + Broadcast Burn	Alternative (ABP >0.043)	Alternative (ABP >0.045)	Alternative (ABP >0.025)
Hand Thin + Pile Burn	Best (ABP >0.010)	Best (ABP >0.010)	Best (ABP >0.005)
Mastication	Failed	Failed	Failed
Broadcast Burn Only	Failed	Failed	Alternative (ABP >0.020)

Table 3. Douglas-fir forest type results.

Fuel Treatment	**Low Hazard**	**Moderate Hazard**	**High Hazard**
Commercial Thin + Broadcast Burn	Alternative (ABP >0.025)	Alternative (ABP >0.017)	Failed
Hand Thin + Pile Burn	Best (ABP >0.005)	Best (ABP >0.004)	Best (ABP >0.005)
Mastication	Alternative (ABP >0.030)	Failed	Failed
Broadcast Burn Only	Alternative (ABP >0.010)	Alternative (ABP >0.013)	Alternative (ABP >0.050)

Table 4. Ponderosa pine forest type results.

Fuel Treatment	Low Hazard	Moderate Hazard	High Hazard
Commercial Thin + Broadcast Burn	Failed	Alternative (ABP >0.100)	Failed
Hand Thin + Pile Burn	Failed	Best (ABP >0.004)	Best (ABP >0.010)
Mastication	Failed	Alternative (ABP >0.020)	Failed
Broadcast Burn Only	Failed	Alternative (ABP >0.018)	Failed

Table 5. White fir forest type results.

Fuel Treatment	Low Hazard	Moderate Hazard	High Hazard
Commercial Thin + Broadcast Burn	Failed	Failed	Failed
Hand Thin + Pile Burn	Best (ABP >0.020)	Best (ABP >0.018)	Best (ABP >0.005)
Mastication	Failed	Failed	Failed
Broadcast Burn Only	Failed	Failed	Failed

Discussion

Land managers can use these findings when selecting fuel treatments for the REM methodology. Forest type, hazard level, and ABP for the project area can all be easily assessed. That information combined with any other social or economic considerations can allow the manager to make an informed decision about where and which fuel treatments are most likely to reduce net GHG emissions from megafires.

Acknowledgments

Jason Moghaddas provided expertise on Sierra Nevada fuel treatments.

References

Cochrane, M.A., Moran, C.J., Wimberly, M.C., Baer, A.D., Finney, M.A., Beckendorf, K.L., Eidenshink, J., Zhu, Z., (2012). Estimation of wildfire size and risk changes due to fuels treatments. Int. J. Wildland Fire 21, 357-367. https://doi.org/10.1071/WF11079

Dixon, G.E., (2024). A User's Guide to the Forest Vegetation Simulator. USDA For. Serv.

Ebert, C., Gorguinpour, K., Mao, J., Remucal, J., Spence, M., Baruch, S., Buchholz, T., Nickerson, J., Ravage, J., Saah, D., Schmidt, D., (2023). Reduced Emissions from Megafires Forecast Methodology v.1.0.

Moghaddas, J.J., Craggs, L., (2007). A fuel treatment reduces fire severity and increases suppression efficiency in a mixed conifer forest. Int. J. Wildland Fire 16, 673-678. https://doi.org/10.1071/WF06066

Prichard, S.J., Hessburg, P.F., Hagmann, R.K., Povak, N.A., Dobrowski, S.Z., Hurteau, M.D., Kane, V.R., Keane, R.E., Kobziar, L.N., Kolden, C.A., North, M., Parks, S.A., Safford, H.D., Stevens, J.T., Yocom, L.L., Churchill, D.J., Gray, R.W., Huffman, D.W., Lake, F.K., Khatri-Chhetri, P., (2021). Adapting western North American forests to climate change and wildfires: 10 common questions. Ecol. Appl. 31, e02433. https://doi.org/10.1002/eap.2433

Rebain, S.A., Reinhardt, E.D., Crookston, N.L., Beukema, S.J., Kurz, W.A., Greenough, J.A., Robinson, D.C.E., Lutes, D.C., (2022). The Fire and Fuels Extension to the Forest Vegetation Simulator: Updated Model Documentation. USDA For. Serv.

Riley, K.L., Grenfell, I.C., Shaw, J.D., Finney, M.A., (2022). TreeMap 2016 Dataset Generates CONUS-Wide Maps of Forest Characteristics Including Live Basal Area, Aboveground Carbon, and Number of Trees per Acre. J. For. 120, 607–632. https://doi.org/10.1093/jofore/fvac022

Westerling, A.L., Hidalgo, H.G., Cayan, D.R., Swetnam, T.W., (2006). Warming and Earlier Spring Increase Western U.S. Forest Wildfire Activity. Science 313, 940–943. https://doi.org/10.1126/science.1128834

Burning with Friends; Collaborating in the Blackfoot Valley

Valentijn Hoff*
National Center for Landscape Fire Analysis, University of Montana, 32 Campus Drive, Missoula, Montana 59812, USA, valentijn.hoff@firecenter.umt.edu

**Corresponding Author*

Introduction

In Western Montana, a few small land management organizations are counting on each other when implementing prescribed fire. We discuss some of the obstacles these smaller burners face and the solutions they found to overcome them, when building a prescribed fire program. From utilizing university students to writing formal agreements, nothing is off the table when it comes to increasing the pace and scale of prescribed fire implementation in the Blackfoot watershed. Building relationships is the key to success because burning with friends is more efficient, more effective, and more fun.

Methods

Strong collaborations provide many benefits for resource-challenged organizations that want to meet prescribed fire objectives. The coalition of landowners, natural resource managers, and fire professionals in the Blackfoot valley in western Montana put a lot of effort into creating an environment that allows for the exploitation of each other's strengths, creates efficiencies, and maximizes the use of short burn windows. And for some, these collaborations make prescribed fire implementation a reality! This takes a lot of time and energy. During the burn season the Prescribed Fire Working Group starts each week with a video conference, discussing fuel and weather conditions, burns on the docket, and resource availability. They prioritize burns based on these factors as well as the location on the landscape (aspect, elevation, potential smoke impacts), the time since a unit has been prepped, and the persuasive capacity of the person representing that unit on the call. These calls are invaluable to the burners, not only for providing clarity on big picture of burning in the Blackfoot watershed, but also to hear about the conditions and fire effects of burns that happened during the previous week.

While these in-the moment calls, where the rubber meets the road, are important, a lot of work happens during the year leading up to the burn season. During the long Montana winter a few folks are still thinking about burning, so the Prescribed Fire Working Group organizes an all-hands meeting during which the plans for the spring and fall burn seasons are discussed. This time is also used to think about strategies to meet landscape level, cross-boundary, interagency, objectives. The cliché that fire does not know ownership is often true, especially in a more fragmented landscape (except of course when previous treatments, such as prescribed fire, follow the property lines). Using existing fire breaks, some that might cross property lines, reduces costs, makes

implementation easier, and causes less disturbance to the resource. This means that landowners on both sides of the fence need to agree on objectives, be aware of each other's needs, and know what each can contribute to all phases of a prescribed fire.

The partners who burn together in the Blackfoot watershed often meet at a burn unit long before a drip torch is ignited. Seeing, feeling, and discussing the fuel load and its condition, laying out the fire breaks in the optimal location, walking up the steep slopes together, all augment the cooperation, which also happens through analysis, modeling, and sharing of spatial data between the partners. Seeing and discussing potential problems long before a burn day aids in the writing of better burn plans. And those partners who are better at making maps and running fire behavior models are lending others a hand with those more technical tasks.

When a good burn window finally opens, everyone with a burn plan will want to apply for a permit. Without the weekly meetings and open discussions, everyone would apply, and once approved not have enough resources to pull off a burn. The informal prioritization that happens each week allows for better resource allocation, a more efficient approval process where fewer people apply, but they are all in a position to actually implement a burn once the permit has been approved.

On a burn day, with resources from usually 3-4 but sometimes 7-8 different organizations, a lot of the time consuming *get-to-know your partner* has already happened. People know the capabilities of each other and the equipment they bring. Everyone has their radios programmed with at least a few common channels, so that communications are seamless. Usually each partner brings hand tools, drip torches and a few gallons of torch-mix to share. Contractors also provide invaluable services to small organizations with limited resources. And while the burn unit host certainly benefits from the extra peoplepower and equipment, the spring burn season is also a good time for the contractors to fine-tune their crews and get ready for the wildfire season ahead.

The collaboration in the Blackfoot valley goes beyond the resources needed to implement prescribed fires. The University of Montana (UM) often hosts researchers on burns. These include both university and visiting scientists. While collecting pre-fire, during fire, or post-fire data is their main objective, they often return the favor by dragging a torch, doing the weather, or leaning on a shovel while holding a line. Students at UM also benefit greatly from being in these partnerships. They are exposed to a greater number of burns, have a chance to network with a variety of natural resource professionals, and help with both those technical pre-burn tasks and the physical preparation of burn units.

Results

The benefits of burning with friends are many. It has led to stronger partnerships, it has built more trust, more acres were burned, and more landowners were happy with the results. Without collaboration most smaller organizations would not be able to implement much prescribed fire. It has provided great experiences for students, including networking, leadership opportunities, in-the-field fire ecology experience, and insights into the logistics of implementing a burn. Prescribed fires where the researchers are also on the burn crew makes data collection easier. And when the burn boss is a primary investigator on a research project, controlling one's destiny for how to burn a plot is greatly increased.

Discussion

Prescribed burning involves large amounts of hard labor. It is always easy to find a reason not to burn. Having many friends count on you to burn, makes it easier to pull the trigger and actually implement a burn. Especially when they are as excited about prescribed fire as you are.

These local partnerships are important. But we have learned a lot of valuable lessons from our partners in other areas of the country. For example, during annual trips to Georgia where we have helped the Nature Conservancy (TNC) with prescribed fire over the past 17 years, we saw the importance of working together on prescribed fires firsthand, especially when resources are in short supply.

The Blackfoot Prescribed Fire Work Group acts like a Prescribed Burn Association (PBA) in many ways. It is a pool of knowledge, equipment, time, and resources, and maybe one day it will become an official PBA, if only to make easier for others to understand how the group functions.

While the partners in the Blackfoot watershed have been successful in increasing the pace and scale of prescribed burning, there are still some obstacles to overcome. The usually small burn windows in the Northern Rockies will still exist, but at least they can take advantage of them more often, due to effective resource sharing and planning.

One topic that comes up frequently is whether all partners should be following the National Wildfire Coordinating Group (NWCG) standards. In the Blackfoot valley all agencies and NGOs do follow NWCG standards, but this not feasible for all private landowners. Having the flexibility to allow non-red carded personnel on a burn creates opportunities to expand the group of partners. But these opportunities are limited to a few occasions each season, only when the hosting unit is able and willing to provide an organizational structure that allows for a safe integration of non-red carded personnel.

One area where progress is still to be made is the formalization of the partnerships. Formal agreements are currently in place between many of the partners. These agreements are negotiated individually every few years. A multi-party, multi-year agreement is under development, which hopefully will preclude the need for many of the two-party agreements and make collaboration even easier.

Acknowledgements
None of this work would have been possible with the help of the friends and partners who plan and execute burns together in the Blackfoot valley in Western Montana. These include the FireCenter at the University of Montana, the Montana Chapter of the Nature Conservancy, the Blackfoot Challenge, the Montana Department of Natural Resources and Conservation, the Montana Department of Fish Wildlife and Parks, the Bureau of Land Management, the Forest Service, the Fish and Wildlife Service, Rob Dillon Tree Service, Grayback Forestry, and many private landowners. A special thanks to Carl Seielstad, Mike Schaedel, and Cindy Super for putting a lot of energy into deepening these partnerships, collaborations, and friendships.

Calculation and validation of new high resolution FirEUrisk fuel maps for Croatia

*Marin Bugarić, Darko Stipaničev, Ljiljana Šerić, Damir Krstinić
Faculty of Electrical Engineering, Mechanical Engineering and Naval Architecture, University of Split, Croatia, marin.bugaric@fesb.hr

**Corresponding Author*

Introduction

Wildfires represent a significant threat to ecosystems and communities across Europe, with fuel mapping being a critical component of fire risk assessment and management. The FirEUrisk project has contributed to this endeavor by developing a comprehensive fuel classification system consisting of 24 fuel types categorized into six main groups: forest, shrubland, grassland, cropland, wet and peat/semi-peat land and urban type, along with a non-fuel category (Aragoneses et al., 2023). Figure 1 shows all FirEUrisk categories, while Figure 2 shows a fuel map for the entire European territory that was created with a resolution of 1 square kilometer. This European-wide map was a significant step forward in wildfire management, providing a comprehensive overview that is crucial for macro-level planning and decision-making.

Fuel Code	Fuel Description	Crosswalk A*	Crosswalk H*
1111	Open broadleaf ev. forest	SH7	**SH8**
1112	Closed broadleaf ev. forest	TU1	**TU2**
1121	Open broadleaf dec. forest	SH5	**SH9**
1122	Closed broadleaf dec. forest	TU5	**TU3**
1211	Open needleleaf ev. forest	SH7	**SH8**
1212	Closed needleleaf ev. forest	TU1	**TU2**
1221	Open needleleaf dec. forest	SH5	**SH9**
1222	Closed needleleaf dec. forest	TU5	**TL3**
1301	Open mixed forest	SH7	**SH8**
1302	Closed mixed forest	TU5	**TL3**
21	Low shrubland	SH2	**SH3**
22	Medium shrubland	SH7	**SH8**
23	High shrubland	SH5	**SH9**
31	Low grassland	GR2	**GR6**
32	Medium grassland	GR4	**GR8**
33	High grassland	GR7	**GR9**
41	Herbaceous cropland	GR4	**GR6**
42	Woody cropland	GR2	**GR6**
51	Tree wet & peatland	SH7	**SH8**
52	Shrubland wet & peatland	SH5	**SH9**
53	Grassland wet & peatland	GR7	**GR9**
61	Urban continuous fabric	NB	**NB**
62	Urban discontinuous fabric	SH2	**SH3**
7	Nonfuel	NB	**NB**

Figure 1: FirEUrisk fuel categories and codes (Aragoneses et al., 2023)

However, for local and regional applications, such as in Croatia, a higher resolution map is necessary to accurately capture the diversity of fuel types and their spatial distribution. Building upon the groundwork laid by the FirEUrisk project, this paper presents the calculation and validation of new high-resolution fuel maps for Croatia with an improved spatial resolution of 100 square meters. This higher resolution offers a more detailed view of fuel distribution across the landscape, enhancing the accuracy of fire risk assessment and management.

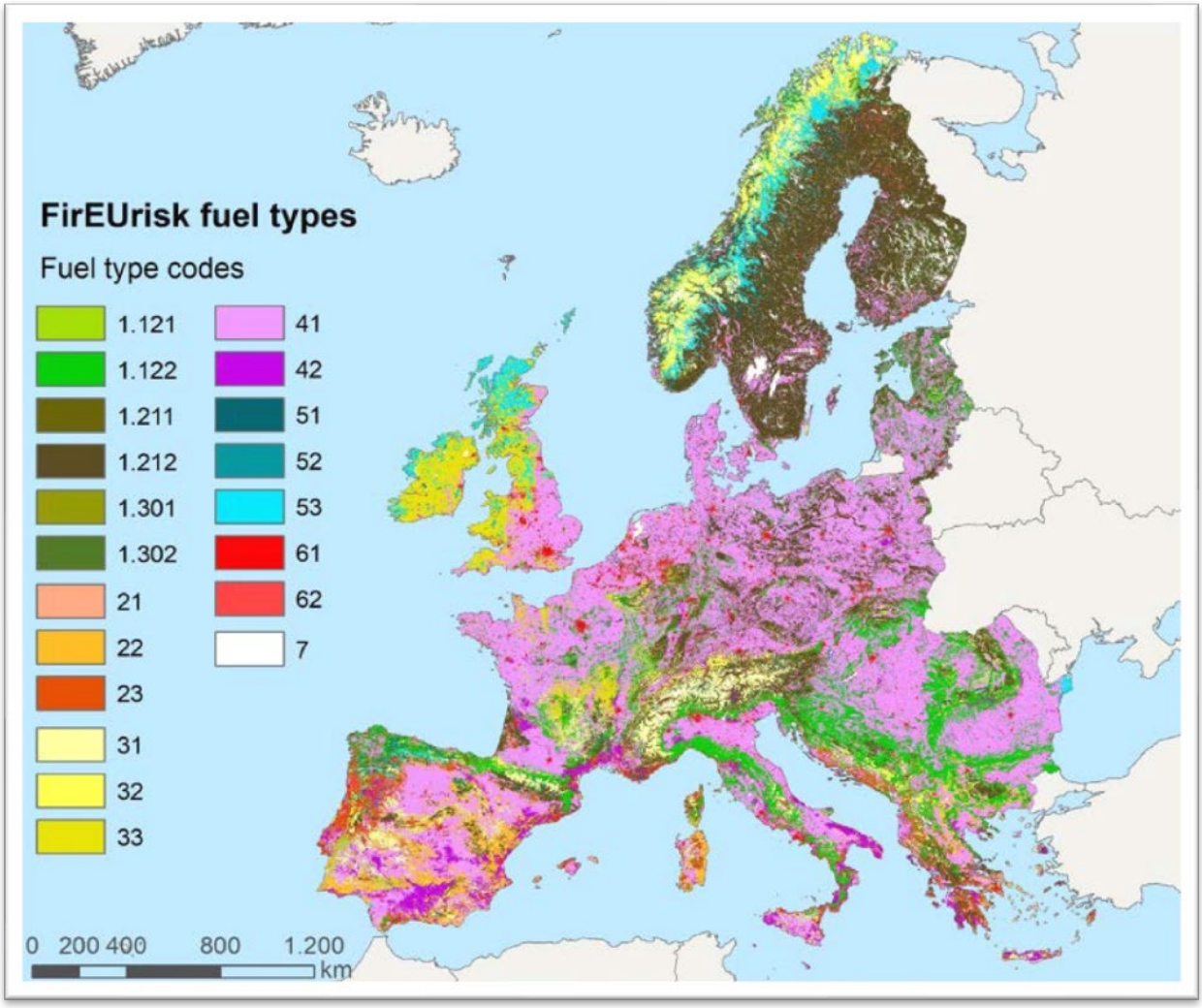

Figure 2: European territory FirEUrisk fuel map in 1 km resolution (Aragoneses et al., 2023)

Motivation

High-precision fuel maps are foundational to effective wildfire risk assessment, serving as a crucial tool for planning and decision-making. The accuracy of fire-spread and behavior simulations is directly tied to the level of detail in fuel maps. The granularity of a fuel map greatly influences the reliability of risk assessments and the quality of fire spread models. The FirEUrisk project contributed significantly to both fuel modeling and mapping, emphasizing the importance of accurate, high-resolution data for effective fire management.

In Croatia, the need for high-resolution fuel maps is particularly acute due to the country's diverse landscapes and the varying fire risk across different regions. The coastal areas, characterized by Mediterranean vegetation, are prone to frequent wildfires, whereas the continental regions with different vegetation types face different challenges. Accurate fuel maps are essential for both regions to ensure effective fire management strategies.

The European territory fuel map created by FirEUrisk has a resolution of 1 square kilometer and was validated using LUCAS points and other resources, achieving an accuracy of 88.4% at the European level and 90% within Croatia. Unfortunately, only 70 LUCAS points were used to validate the accuracy of this maps for Croatia (Aragoneses, 2024). This limited validation raised concerns about the map's reliability for local applications, necessitating a more comprehensive approach. Figure 3 shows LUCAS 2018 points used for FirEUrisk map validation, as well as all LUCAS 2018 (4240 points) and 2022 (5816 points) points available on Croatian territory.

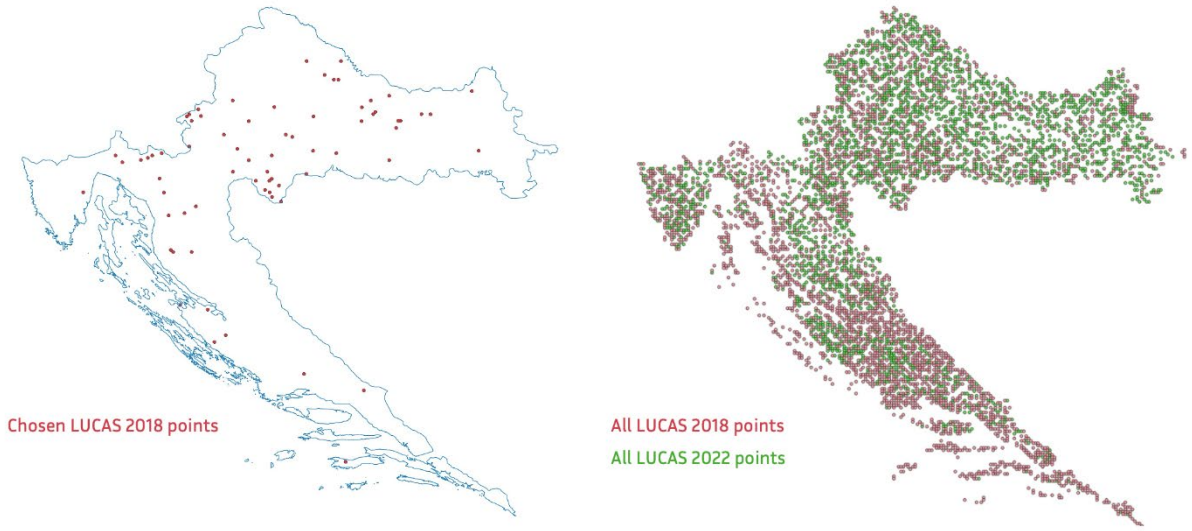

Figure 3: LUCAS 2018 points used for FirEUrisk fuel maps validation (left) and all LUCAS 2018 and 2022 points (right)

When validating the original 1km FirEUrisk map using all 5816 LUCAS points from 2022, the accuracy was only 29.54%. Confusion matrix for this analysis is shown in Figure 4. In contrast, using all 4240 LUCAS points from 2018 resulted in an accuracy of 43.79%. This demonstrates that the initial validation, based on a limited number of points, was overly optimistic and highlights the necessity for higher-resolution maps and a more comprehensive validation process.

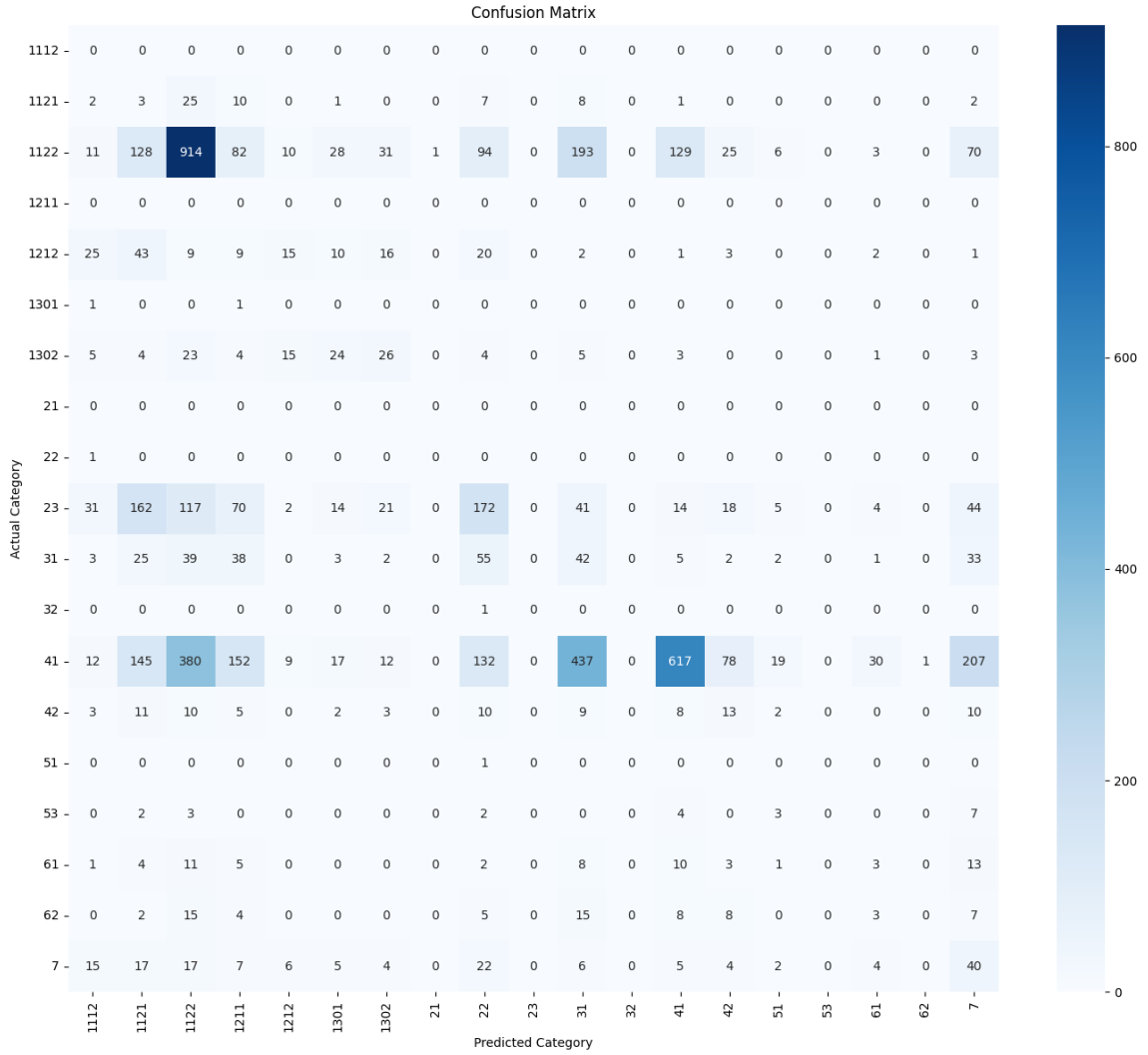

Figure 4: Confusion matrix for original FirEUrisk map and 2022 LUCAS points

High-Resolution Fuel Maps Calculation Methodology

To generate new high-resolution fuel maps for Croatia, a revised set of input data sources was used:

- Copernicus Tree Cover Density (2018) (Copernicus, 2018),
- Global Forest Canopy Height (2019) (Potapov et al.),
- CLC+ backbone (Copernicus CLC+, 2021)
- The De Martonne aridity index (De Martonne, 1926), and
- other climate data and a burned area database.

Each of these data sources contributes unique information that, offers a comprehensive picture of the fuel distribution across Croatia.

The initial procedure for the 100m map of Croatia was based on the method developed by the University of Lleida and used for the FirEUrisk Barcelona PS (FirEUrisk Del.1.1.,

2023). Additional tuning was performed by comparing with 5816 points of 2022 LUCAS using an optimized conversion table, shown in Figure 5.

LUCAS	LUCAS description	firEUrisk	firEUrisk description
A11	Buildings with one to three floors	61	Urban continuous fabric
A12	Buildings with more than three floors	61	Urban continuous fabric
A13	Greenhouses	62	Urban discontinuous fabric
A21	Non built-up area features	7	Nonfuel
A22	Non built-up linear features	7	Nonfuel
B11	Common wheat	41	Herbaceous cropland
B12	Durum wheat	41	Herbaceous cropland
B13	Barley	41	Herbaceous cropland
B14	Rye	41	Herbaceous cropland
B15	Oats	41	Herbaceous cropland
B16	Maize	41	Herbaceous cropland
B18	Triticale	41	Herbaceous cropland
B19	Other cereals	41	Herbaceous cropland
B21	Potatoes	41	Herbaceous cropland
B22	Sugar beet	41	Herbaceous cropland
B31	Other root crops	41	Herbaceous cropland
B32	Rape and turnip rape	41	Herbaceous cropland
B33	Sova	41	Herbaceous cropland
B36	Tobacco	41	Herbaceous cropland
B37	Other non-permanent industrial crops	41	Herbaceous cropland
B41	Dry pulses	41	Herbaceous cropland
B43	Other fresh vegetables	41	Herbaceous cropland
B51	Clovers	41	Herbaceous cropland
B52	Lucerne	41	Herbaceous cropland
B53	Other leguminous and mixtures for fodder	41	Herbaceous cropland
B55	Temporary grasslands	41	Herbaceous cropland
B71	Apple fruit	42	Woody cropland
B72	Pear fruit	42	Woody cropland
B73	Cherry fruit	42	Woody cropland
B74	Nuts trees	42	Woody cropland
B75	Other fruit trees and berries	42	Woody cropland
B77	Other citrus fruit	42	Woody cropland
B81	Olive groves	42	Woody cropland
B82	Vineyards	42	Woody cropland
B83	Nurseries	42	Woody cropland
B84	Permanent industrial crops	42	Woody cropland
C10	BROADLEAVED WOODLAND	1122	Closed broadleaf dec. forest
C2	CONIFEROUS WOODLAND	1212	Closed needleleaf ev. forest
C21	Spruce dominated coniferous woodland	1212	Closed needleleaf ev. forest
C22	Pine dominated coniferous woodland	1112	Closed broadleaf ev. forest
C23	Other coniferous woodland	1112	Closed broadleaf ev. forest
C3	MIXED WOODLAND	1302	Closed mixed forest
C31	Spruce dominated mixed woodland	1302	Closed mixed forest
C32	Pine dominated mixed woodland	1302	Closed mixed forest
C33	Other mixed woodland	1301	Open mixed forest
D	SHRUBLAND	21	Low shrubland
D10	SHRUBLAND WITH SPARSE TREE COVER	1121	Open broadleaf dec. forest
D20	SHRUBLAND WITHOUT TREE COVER	22	Medium shrubland
E10	GRASSLAND WITH SPARSE TREE/SHRUB COVER	1211	Open needleleaf ev. forest
E20	GRASSLAND WITHOUT TREE/SHRUB COVER	31	Low grassland
E30	SPONTANEOUSLY RE-VEGETATED SURFACES	41	Herbaceous cropland
F10	ROCKS AND STONES	7	Nonfuel
F20	SAND	7	Nonfuel
F40	OTHER BARE SOI	7	Nonfuel
G11	Inland fresh water bodies	7	Nonfuel
G21	Inland fresh running water	7	Nonfuel
G30	TRANSITIONAL WATER BODIES	7	Nonfuel
G40	SEA AND OCEAN	7	Nonfuel
H11	Inland marshes	51	Tree wet & peatland
H21	Salt marshes	51	Tree wet & peatland
H22	Salines and other chemical deposits	51	Tree wet & peatland

Figure 5: Optimized conversion table between LUCAS categories and FirEUrisk categories

As a final result, three maps were created:

1. A 100m Croatia fuel map with original FirEUrisk categories.
2. A 100m Croatia fuel map where vegetation categories in arid areas have a minus sign.
3. A 100m Croatia fuel map where FirEUrisk categories were converted to Scott-Burgan categories using a conversion table from Figure 1 based on arid (A) and humid (H) zones (Figure 5).

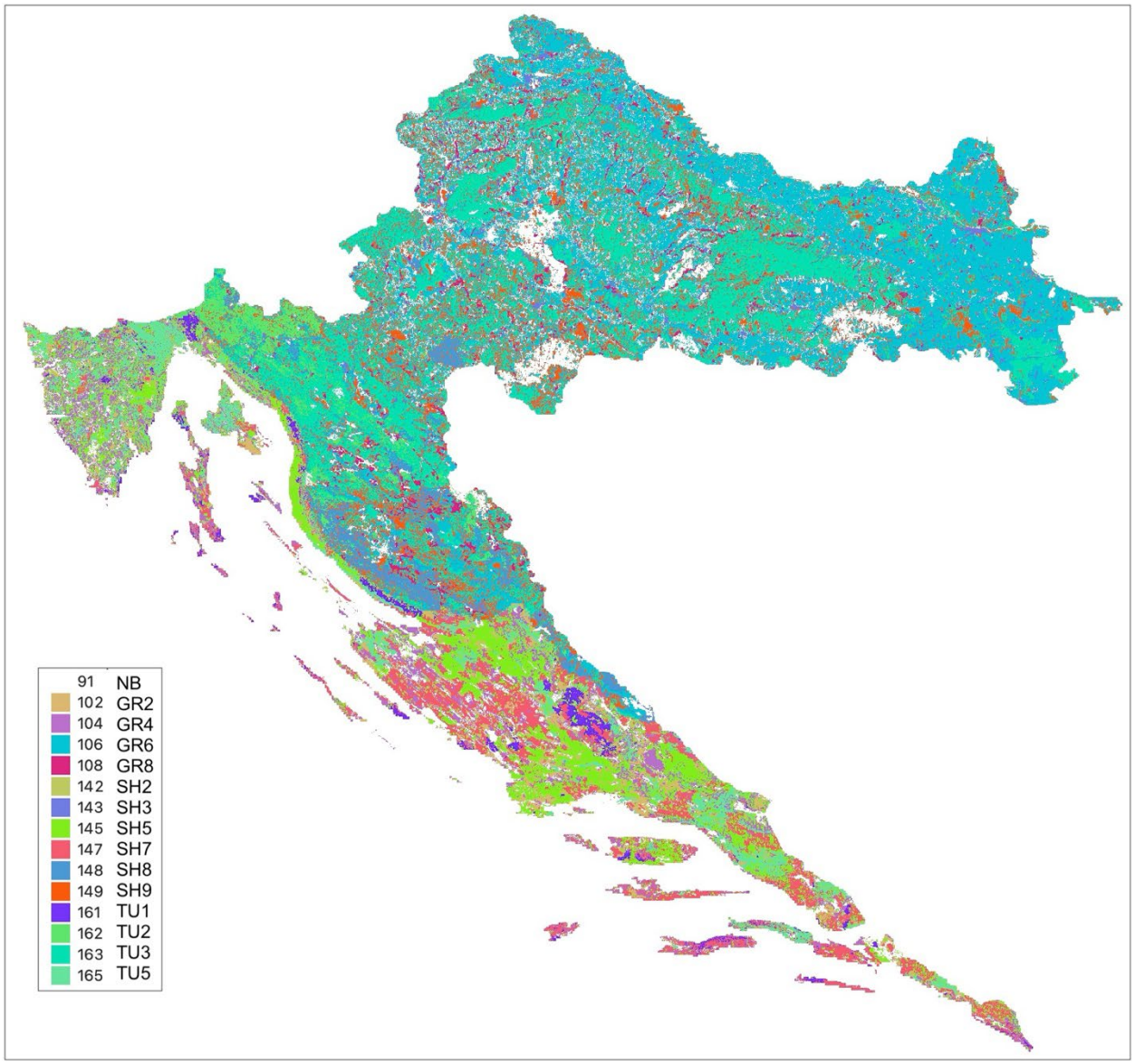

Figure 5: Newly developed fuel map for Croatia with Scott-Burgan categories

High-Resolution Fuel Maps Validation

The validation process included region-specific data to ensure that the new high-resolution fuel maps accurately represent local conditions and variations in vegetation and land cover. Validation was conducted using the latest available data sources, with newer LUCAS points from 2022 providing a current reference dataset for comparison. A two-step validation was conducted, first to validate the six main fuel types, and then to assess all fuel types.

The new high-resolution maps provide a finer detail of fuel distribution, leading to more accurate fire risk assessment and management. Using all 5816 LUCAS points from 2022, the accuracy of the new maps was found to be 74.68%. This significant

improvement in accuracy demonstrates the value of higher-resolution maps and comprehensive validation.

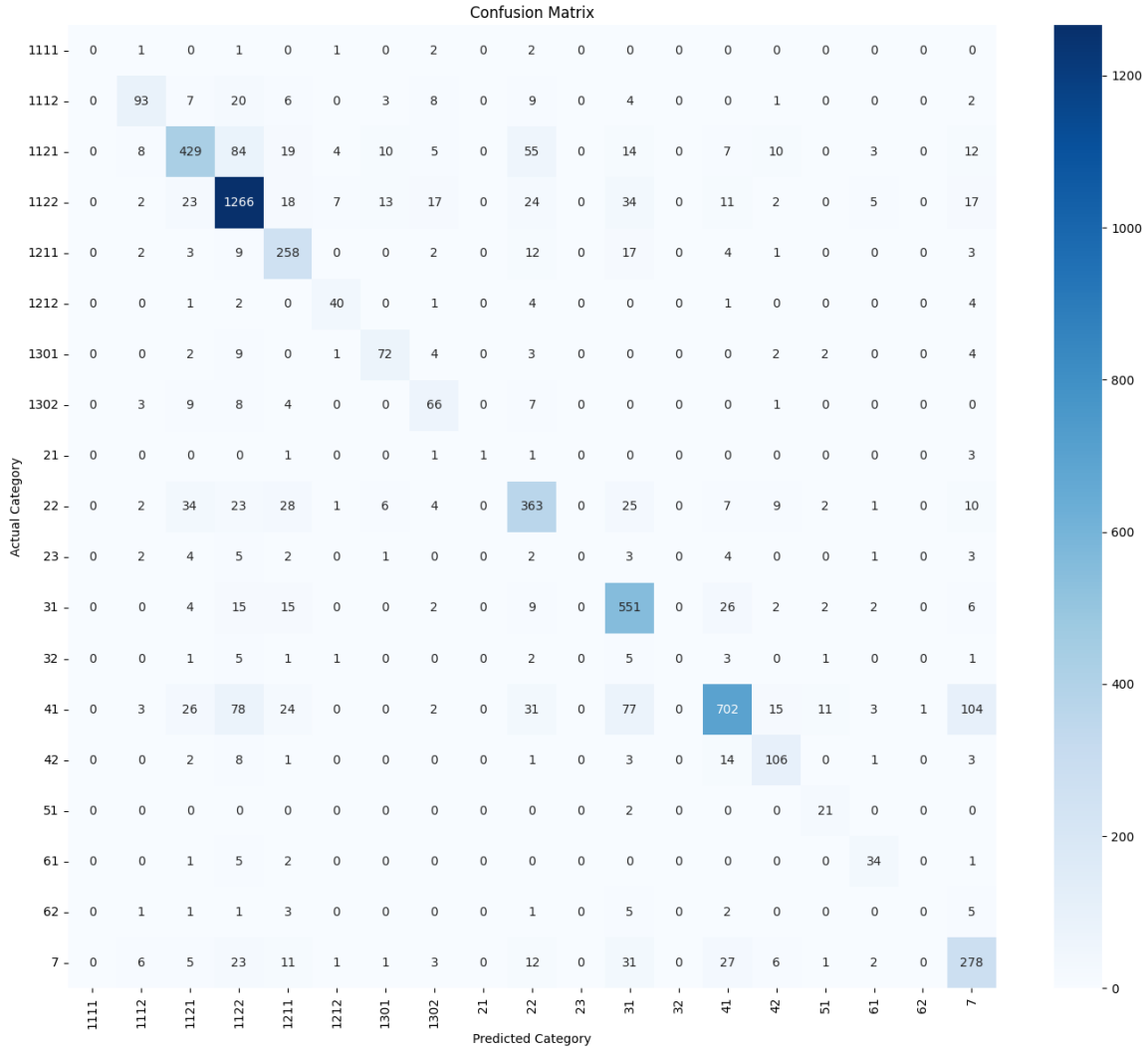

Figure 6: Confusion matrix for newly developed Scott-Burgan map and 2022 LUCAS points

The improved accuracy of the high-resolution maps has several practical implications:

- Firstly, it allows for more precise allocation of firefighting resources, ensuring that high-risk areas receive the necessary attention.
- Secondly, it enhances the accuracy of fire spread simulations, which are critical for both real-time response and long-term planning.
- Lastly, it provides a more reliable basis for environmental planning and conservation efforts, ensuring that fire management strategies are aligned with broader environmental goals.

Additionally, manual validation was carried out using Google Street View, where random points were chosen and manually validated. An example is shown in Figure 7.

Figure 7: Manual validation using Google Street view for new Scott-Burgan map and 2022 LUCAS points

The validation process also highlighted some areas for improvement. While the overall accuracy was significantly improved, certain fuel types and regions still exhibited lower accuracy. This suggests the need for ongoing refinement of the models and continuous updating of the data sources. Future work will focus on integrating additional data, such as high-resolution satellite imagery and ground-based observations, to further enhance the accuracy and reliability of the maps.

Conclusions

Figure 8 illustrates the difference between original FirEUrisk map in 1 km resolution and new 100m map for part of Split-Dalmatia County. The new high-resolution fuel maps represent a significant improvement in the precision and applicability of fire risk assessment and management strategies in Croatia. These efforts contribute to a more sustainable and safer coexistence with the ever-present threat of wildfires.

The new higher resolution FirEUrisk fuel map of Croatia will be freely available with this paper, providing a valuable resource for researchers, policymakers, and fire management professionals (CIPOP – HR Fuel Maps, 2024). By providing a more detailed and accurate picture of fuel distribution, they enhance the ability to assess and manage fire risk, ultimately contributing to a safer and more sustainable coexistence with wildfires.

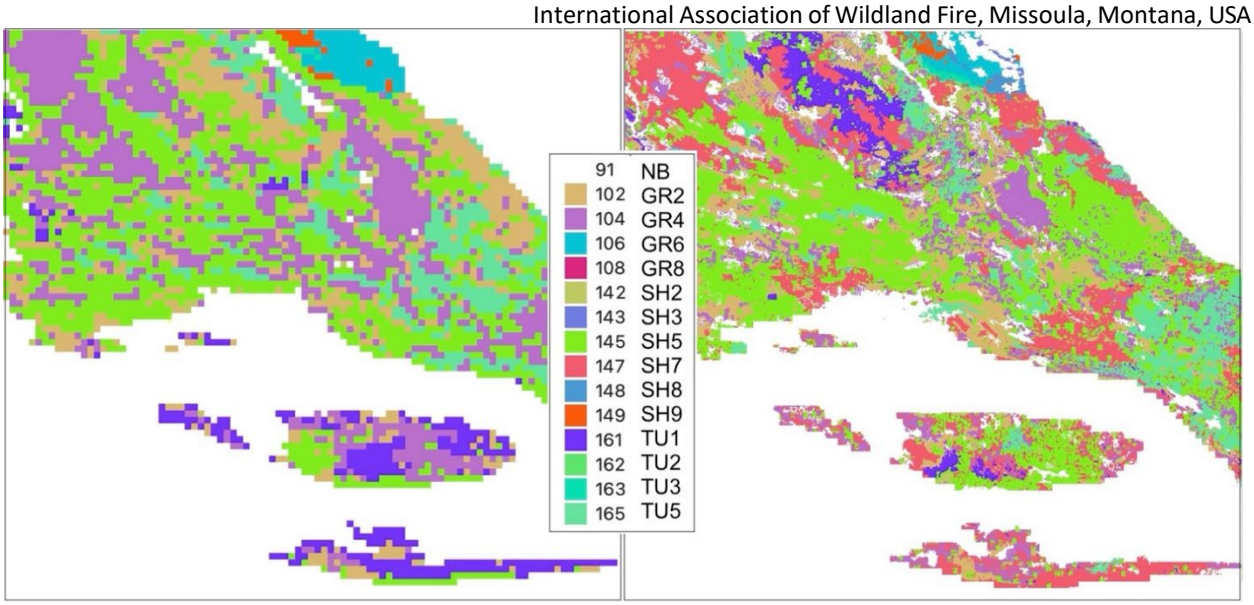

Figure 7: Comparison of original 1km FirEUrisk fuel map and new 100m map for part of Split-Dalmatia County

Acknowledgement

Research in this paper has received funding from the European Union's Horizon 2020 research and innovation programme under grant agreement No 101003890 – project firEUrisk. Special thanks goes to Fermín Alcasena and Pere Joan Gelabert Vadillo for their help with fuel maps generation.

References

(Aragoneses et al., 2023) Aragoneses, E., García, M., Salis, M., Ribeiro, L. M., and Chuvieco, E. (2023) Classification and mapping of European fuels using a hierarchical, multipurpose fuel classification system, Earth Syst. Sci. Data, 15, 1287–1315, https://doi.org/10.5194/essd-15-1287-2023

(Aragoneses, 2024) Aragoneses, E., (2024) Personal communication about validation of FirEUrisk new fuel maps.

(CIPOP – HR Fuel Maps, 2024) High Resolution FirEUrisk Fuel Maps for Croatia (in Croatian), https://cipop.fesb.hr

(Copernicus, 2018) Copernicus Tree Cover Density 2018 – 100m resolution (2018) https://doi.org/10.2909/c7bf34ea-755c-4dbd-85b6-4efc5fd302a2

(Copernicus CLC+, 2021) Copernicus CLC+ Backbone 2021 (raster 10 m), Europe, https://doi.org/10.2909/71fc9d1b-479f-4da1-aa66-662a2fff2cf7

(De Martonne, 1926) De Martonne, E. (1926). Aerisme, et índices d'aridite. *Comptesrendus de L'Academie des Sciences* , *182* , 1395–1398.

(Eurostat, 2024) Eurostat: LUCAS Data Base (2006-2022), https://ec.europa.eu/eurostat/web/lucas

(FirEUrisk Del.1.1., 2023) FireEUrisk Del.1.1.- Report on methodological frameworks for each danger modelling process (2023) – internal report

(Potapov et al.) Potapov, P. et al. (2020) Mapping and monitoring global forest canopy height through integration of GEDI and Landsat data. *Remote Sensing of Environment,* 112165. https://doi.org/10.1016/j.rse.2020.112165

Can we estimate the probability of Initial Attack success?

Joaquín Ramírez*, Adrián Cardil, Adrián Jiménez-Ruano, Santiago Monedero, Macarena Ortega, Raúl Quílez, Scott Purdy
Technosylva Inc., La Jolla, California, USA,
jramirez@tecnosylva.com, acardil@tecnosylva.com, ajimenez@tecnosylva.com, smonedero@tecnosylva.com, mortega@tecnosylva.com, rquilez@tecnosylva.com, spurdy@tecnosylva.com

Phillip SeLegue, Jeff Fuentes, Geoff Marshall, Tim Chavez
CAL FIRE, Sacramento Headquarters Intel, Sacramento, California, USA,
phillip.selegue@fire.ca.gov, geoff.Marshall@fire.ca.gov, tim.chavez@fire.ca.gov

Kristen Allison
USDA Forest Service, Pacific Southwest Region, Operations Southern California, USA,
kristen.allison@usda.gov

**Corresponding Author*

Introduction

The first and most crucial phase in operational fire risk is the initial attack or response, which is the first extinction effort taken to control the wildfire spread by the suppression resources. We proposed the Initial Attack Index (IAA) as a dynamic risk indicator easily comprehensible by the operational end-users. It synthesizes the risk modeling implemented in Technosylva Inc.'s Wildfire Analyst (WFA) app. Since its inception in 2019, fire agencies, electrical utilities and the insurance sector have employed the IAA index (in both America and Europe).

The IAA is the result of a collaboration between the California Department of Forestry and Fire Protection (CAL FIRE) and Technosylva aiming to address California's challenging wildfires. It is based on expert criteria from small and medium-sized enterprises, trying to obtain a synthetic index that could be valuable for preparedness, dispatching and response. Specifically, it aims to evaluate the difficulties anticipated by the response teams during the first 1 to 2 hours after ignition time, being used by CAL FIRE to prepare resources for deployment. After more than three years of implementation, we evaluated its performance in terms of fire containment likelihood and, in those cases where the initial attack fails, whether the index can highlight the potential for problematic fire behavior affecting suppression operations.

The main objectives of this study are: a) assess the probability of initial attack success employing the proposed IAA index; b) estimate the wildfire potential when initial attack fails, especially in the early containment phase; c) evaluate the contribution of

suppression resources in the prediction of initial attack success or fail; and d) validate the IAA with recent incidents, fire-related predictors and other machine learning algorithms in California and other areas.

Materials and methods

Wildfire and suppression resources data

We employed wildfire records (26,907) retrieved from the IRWIN database from the whole state of California for the period 2020-2023 (Figure 1).

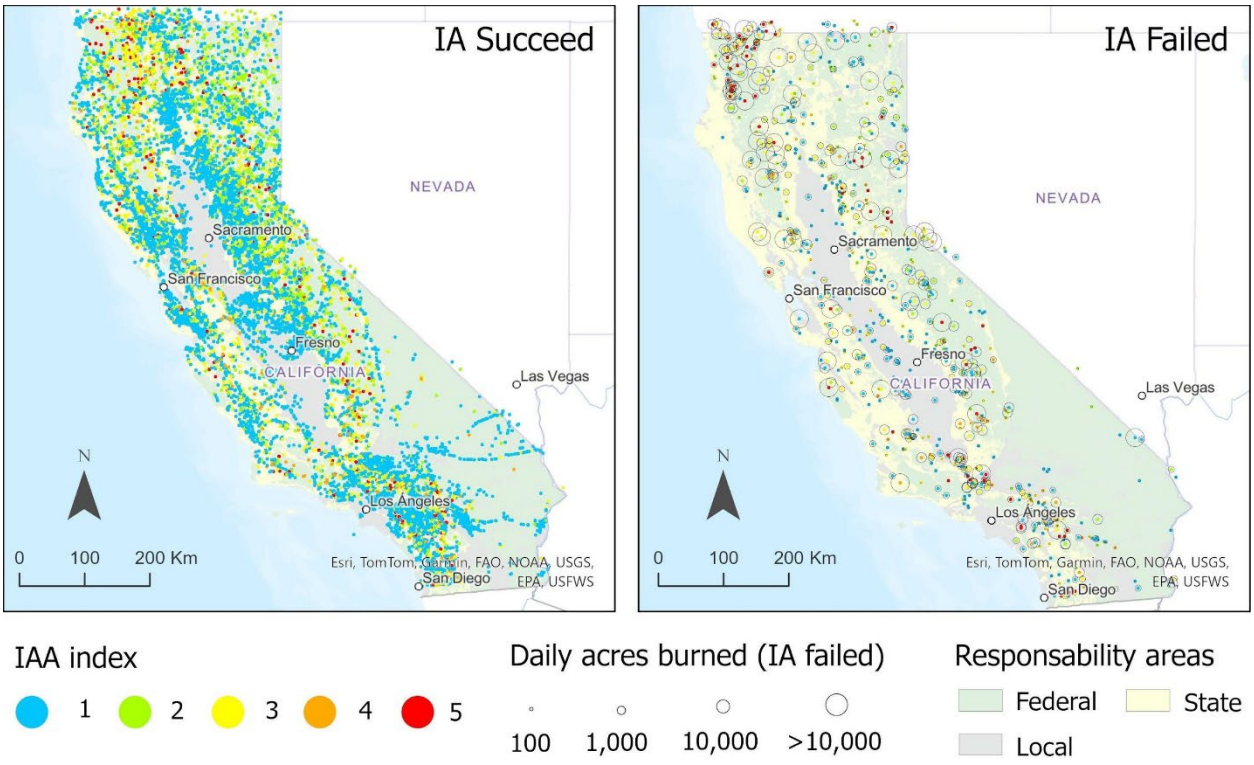

Figure 1: Initial Attack Assessment Index for Californian fires considering the success (left: fire size < 10 ac) and failure (right: fire size > 10 ac). Graduated circles represent final fire size.

The role of initial response was evaluated with CAL FIRE data from 9,886 incidents. We computed three variables: response time, containment time and density of resources during containment time, in addition to means of extinction.

WFA automated simulations

We automatically simulated fire incidents with weather forecasts and diverse semi-empirical fire spread models implemented in WFA. We employed Rothermel's (1972) surface fuel models (30m) updated yearly by Technosylva using Scott and Burgan (2005) methodology including new timber fuels models (Cardil *et al*. 2023). We used hourly weather data (2km) and mean wind speed-direction (at 10-m height). Finally, we employed dead fuel moisture using weather data (Nelson 2000) and live fuel moisture by Technosylva's machine learning models with US Fuel Moisture National Database (WFAS 2022, Cardil *et al*. 2023).

Initial Attack Assessment Index computation

The IAA was computed using two different indices: Fire Behavior Index (FBI) and Terrain Difficulty Index (TDI). All are represented by five categories (from 1 to 5), where the higher the value, the more active fire behavior, the more complex the terrain, and thus the more likely it is to escape the initial attack, ending in a potential threat (Figure 2).

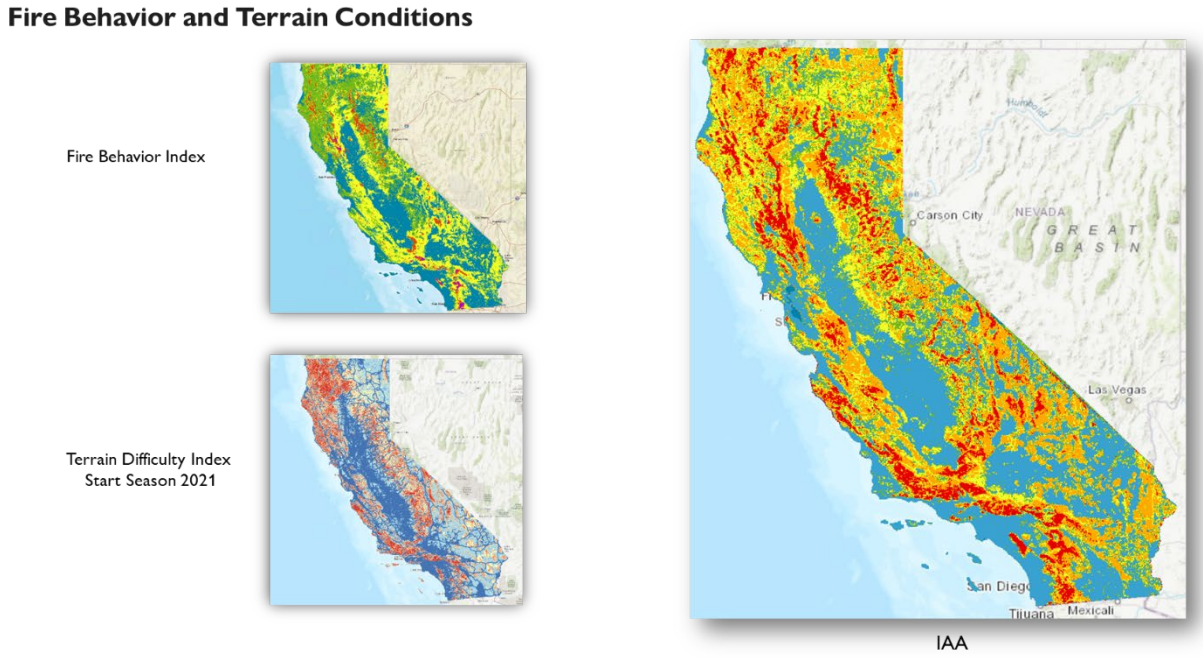

Figure 2: Fire Behavior Index and Terrain Difficulty Index employed to calculate the IAA for California State (start season 2021).

Results and validation

IAA index performance

The probability of Initial Attack success for different fire size thresholds decreases while the level of IAA increases (Figure 3). Generalized Linear Model (GLM) fitted with CAL FIRE incidents showed that IA success increases >89% in all classes, especially 4 and 5 (Table 1).

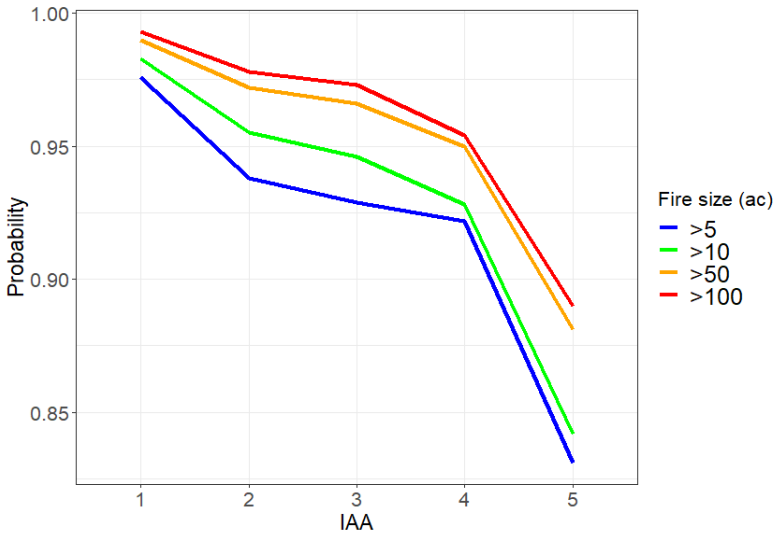

Figure 3: Comparison of the modeled probability of Initial Attack success based on the IAA classes for different fire size objectives (acres).

Table 1: Comparison between probability of Initial Attack success and the wildfire data source (all agencies, CAL FIRE incidents and without CAL FIRE incidents.

Success threshold (10 acres)		IAA				
	N	1	2	3	4	5
All agencies	26,907	98.3%	95.5%	94.5%	92.8%	84.2%
CAL FIRE	**18,697**	**97.9%**	**96%**	**94.4%**	**94.8%**	**89.5%**
No CAL FIRE	8,210	97.2%	93.2%	92.8%	89%	81.1%

What happens when Initial Attack is not successful?

When fires escape initial attack, the index explains that the average final fire size is larger as the index grows (Figure 4), especially for the highest IAA values (4 and 5).

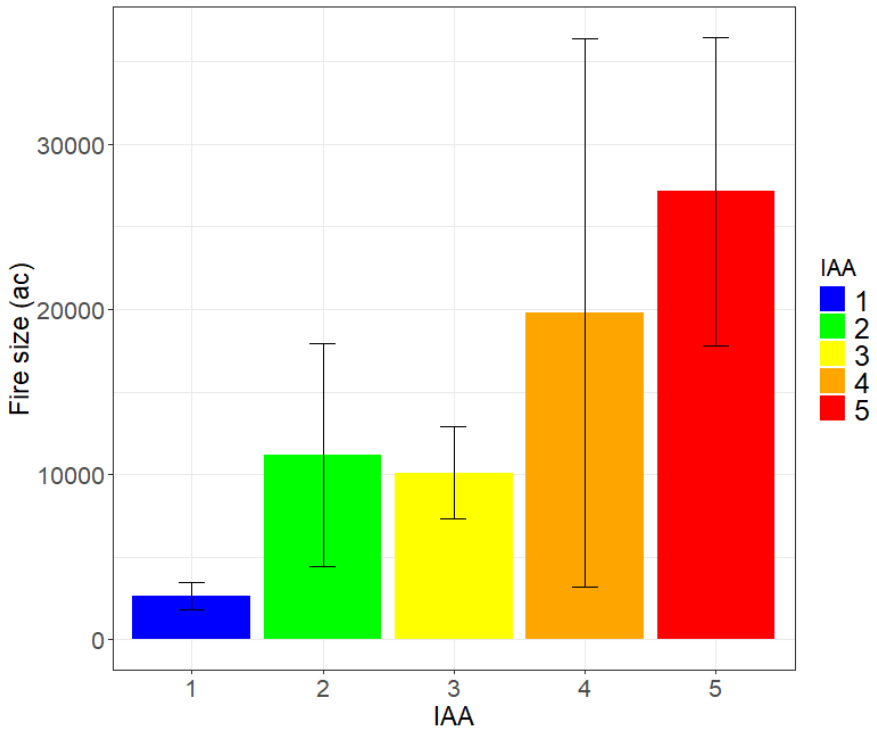

Figure 4: Comparison of average fire size in acres when the Initial Attack fails for each IAA class.

Contribution of fire-related variables, suppression factors and ML algorithms

Fire size at 1 hour, rate of spread (ROS) and flame length are the most significant fire-related variables. Containment time, density of resources and engines are the most relevant suppression factors. Random Forest and Artificial Neural Networks improved the discrimination for successful IA. However, they showed reduced accuracy when IA fails.

WFA simulations outside California

We individually simulated eight incidents with different fire conditions, terrain difficulties or impacts observed (Figure 5, upper panels). We could find from very devastating wildfires (high ROS, such Archie Creek fire), natural-caused triggered by worsening wind-moisture conditions (Lionshead fire) or convective propagation affecting WUI in the first hour (Spain). Generally, simulations spatially match with VIIRS satellite hotspots as well as, with date time of fire ignition and subsequent days (Figure 5, lower panels).

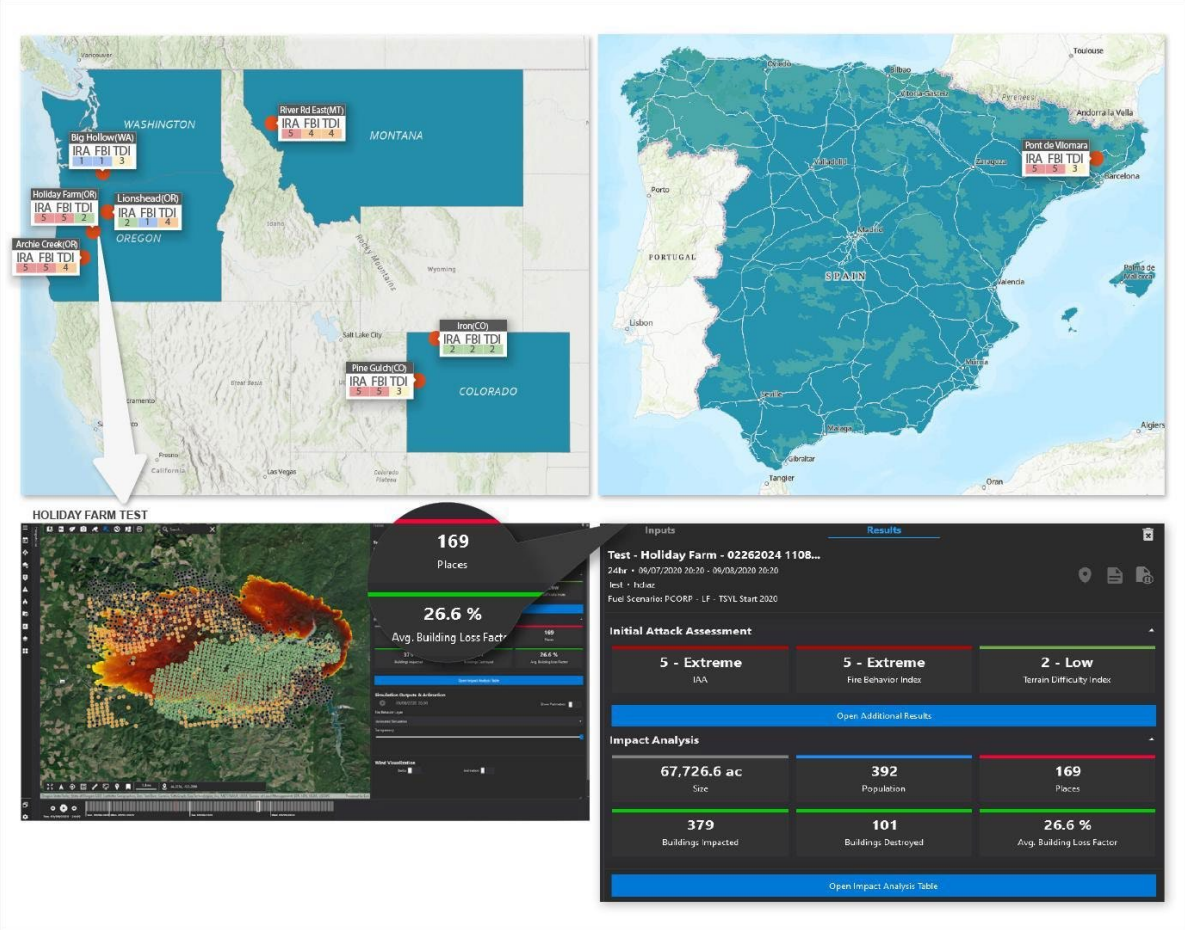

Figure 5: Locations and IAA-IRA, FBI and TDI values of the wildfires simulated outside California (upper panels). 24-h simulation example of Holiday Farm fire in Oregon conducted in WFA (lower panels).

Implementation

CAL FIRE wildfires management

The main value of the IAA index was its contracted implementation from 2020 in the CAL FIRE wildfire management statement. Daily IAA metrics are evaluated and summarized per unit by CAL FIRE. At the same time, each alert is automatically simulated and associated with an IAA value to provide information from the detection time to units on the field. Additionally, units get a report as soon as the incident gets into the Computer-Aided Design (CAD) through the Tactical Analyst mobile app.
WFA's integration with complementary technologies and data sources facilitates verification of predictions and on-going calibration of simulations for even more accurate results. Currently, WFA seamlessly integrates with the CAL FIRE dispatch system to provide automatic spread predictions within seconds of receiving incident notifications for every incident. In turn, FireGuard data for active incidents updates the automatic simulations with the current ignition location.

Conclusions

We choose the proposed IAA for its simplicity and robustness above the rest of models. In fact, machine learning failed to improve escaped wildfire detection. The IAA has been built with expert criteria and successfully implemented during initial attack on most fires in California. It is ideal for operations due to its ease of communication. Regarding the contribution of suppression factors, containment time, density of resources and the number of engines delivered were key drivers that contributed to suppression success. Finally, we demonstrated the potential of exploiting the index outside California and internationally, by evaluating IAA with fire growth as detected by satellite hotspots. Therefore, both can be directly extrapolated to other environments and fire conditions.

Acknowledgments

This research received funding from the Spanish Ministry of Science and Innovation and the State Investigation Agency (MCIN-AEI institution code: 10.13039/501100011033) by means of the 'Torres Quevedo' grant (PTQ2022-012740).

References

Cardil A, Monedero S, Selegue P, Navarrete MÁ, De-Miguel S, Purdy S, Marshall G, Chavez T, Allison K, Quilez R, Ortega M, Silva CA, Ramirez J (2023) Performance of operational fire spread models in California. *International Journal of Wildland Fire*.

Nelson RM (2000) Prediction of diurnal change in 10-h fuel stick moisture content. *Canadian Journal of Forest Research* **30**, 1071–1087.

Rothermel RC (1972) ´A mathematical model for predicting fire spread in wildland fuels.´ USDA Forest Service, Intermountain Forest and Range Experiment Station, Research Paper INT-115. (Ogden, UT)

Scott JH, Burgan RE (2005) ´Standard fire behavior fuel models: a comprehensive set for use with Rothermel's surface fire spread model.´ USDA Forest Service, Rocky Mountain Research Station General Technical Report RMRS-GTR-153. (Fort Collins, CO)

Wildland Fire Assessment System (2022) National Fuel Moisture Database. Available at https://www.wfas.net/index.php/national-fuel-moisture-database-moisture-drought-103 [Verified 12 March 2024].

Proceedings for the 7th International Fire Behavior and Fuels Conference April 15-19, 2024, Boise, Idaho, USA – Tralee, Ireland – Canberra, Australia Published by the International Association of Wildland Fire, Missoula, Montana, USA

Classification and mapping of custom fuel models and their associated fire behaviour in a Mediterranean region

Stéfano Arellano-Pérez*, Eva Marino, José Luis Tomé, Santiago Martín-Alcón
AGRESTA Sociedad Cooperativa. Madrid, Spain
sarellano@agresta.org; emarino@agresta.org; jltome@agresta.org; smartin@agresta.org

Juan Ramón Molina-Martínez, Francisco Rodríguez y Silva
Laboratorio de Incendios Forestales (LABIF). Universidad de Córdoba, Spain
092momaj@uco.es; ir1rosif@uco.es

Francisco Senra, Francisco Javier Castelló
Agencia de Medio Ambiente y Agua. Junta de Andalucía, Sevilla, Spain
francisco.senra.rivero@juntadeandalucia.es; franciscoj.castello@juntadeandalucia.es

**Corresponding Author*

Introduction

Forest fuels classification is essential for the improvement of fire behaviour prediction (Keane, 2015). Hence, the availability of custom fuel models with their associated fire behaviour information offers advantages from the point of view of fuel management, fire suppression and restoration at regional level (Arellano et al., 2017). In Andalusia (Southern Spain), the University of Cordoba established custom fuel models called UCO40 based on the methodology defined by the American system proposed by Scott and Burgan (2005), adapting these fuel models and their descriptive parameters to the particularities of the vegetation present in this Mediterranean region (Rodríguez y Silva and Molina-Martínez, 2012). In recent years, the need to obtain high resolution fuel model maps has increased. Remote sensing technologies provide a major opportunity for this purpose, despite certain adaptations being required to overcome sensors limitations.

Therefore, the present study was carried out with the aim of: (i) adapting the UCO40 models to a new field version called UCO30 to improve the field identification criteria; (ii) adapting the UCO30 models to a new version called UCO20 for map generation from airborne laser scanning and field inventories previously described; (iii) adapting the UCO30 models to standard fuel models developed by the Northern Forest Fire Laboratory by direct assignment, called NFFL9 version; (iv) updating fuel model parameters; and (v) incorporating potential surface and crown fire behaviour for each fuel model defined.

Materials and methods

Study area and field inventories

The study area of the current work was the entire Mediterranean region of Andalusia (Figure 1), in southern Spain, with a total area of 87,597 km^2. Of this area, 65% is forested, of which 32% is tree cover, 19% grassland and 14% shrubland. The most abundant tree species are *Pinus halepensis*, *Pinus pinea*, *Quercus ilex*, *Quercus suber* and the shrub species belong to the genus: *Cistus* sp., *Cytisus*, *Erica* sp., *Ulex* sp.

Three different types of field inventory were carried out according to their purposes:

- Surface fuel inventory: more than 3,400 plots, whose data made it possible to establish the new field identification key of the fuel models of with their respective criteria and to have good photographic archive to prepare the sheets. Some of the measurements carried out were vegetation cover and height, litter and mulch depth, canopy cover and vertical continuity.
- Tree inventory: More than 800 plots, with a detailed characterization of the canopy fuels included in the data sheets. In these plots, all species were identified and diameters at breast height, dead and live crown base height, total height, bark thickness and crown diameter were measured.
- Fuel destructive inventory: More than 200 plots, whose information served as the basis for the parameterization included in the field guide sheets. In this inventory, the material was cut and extracted, to be moved to the laboratory and to determine the loads.

The field plots location of these three inventory types is shown in Figure 1.

LiDAR data

The LiDAR data used correspond to the PNOA flights (National Aerial Orthophotography Plan) of the 2nd coverage over Andalusia. The flight dates range from July 2020 to May 2021. The density of these LiDAR data was 1.5 pulses/m^2 with a horizontal sweep accuracy of 0.3 m and a vertical accuracy of 0.15 m.

The LiDAR data were processed with Agresta's own software developments using the free R software (lidR package). The data processing workflow is as follows: (1) the point cloud was filtered and interpolated to generate a digital terrain model (DTM) and a digital surface model (DSM), from which the normalized height of the vegetation returns on the ground were calculated; (2) processing of the metrics from the vegetation returns of the LiDAR point cloud on the plots. Metrics of the vertical distribution of heights, the number and percentages of laser returns were calculated for different height cut-off thresholds: 0.2 m, 2 m, and 4 m.

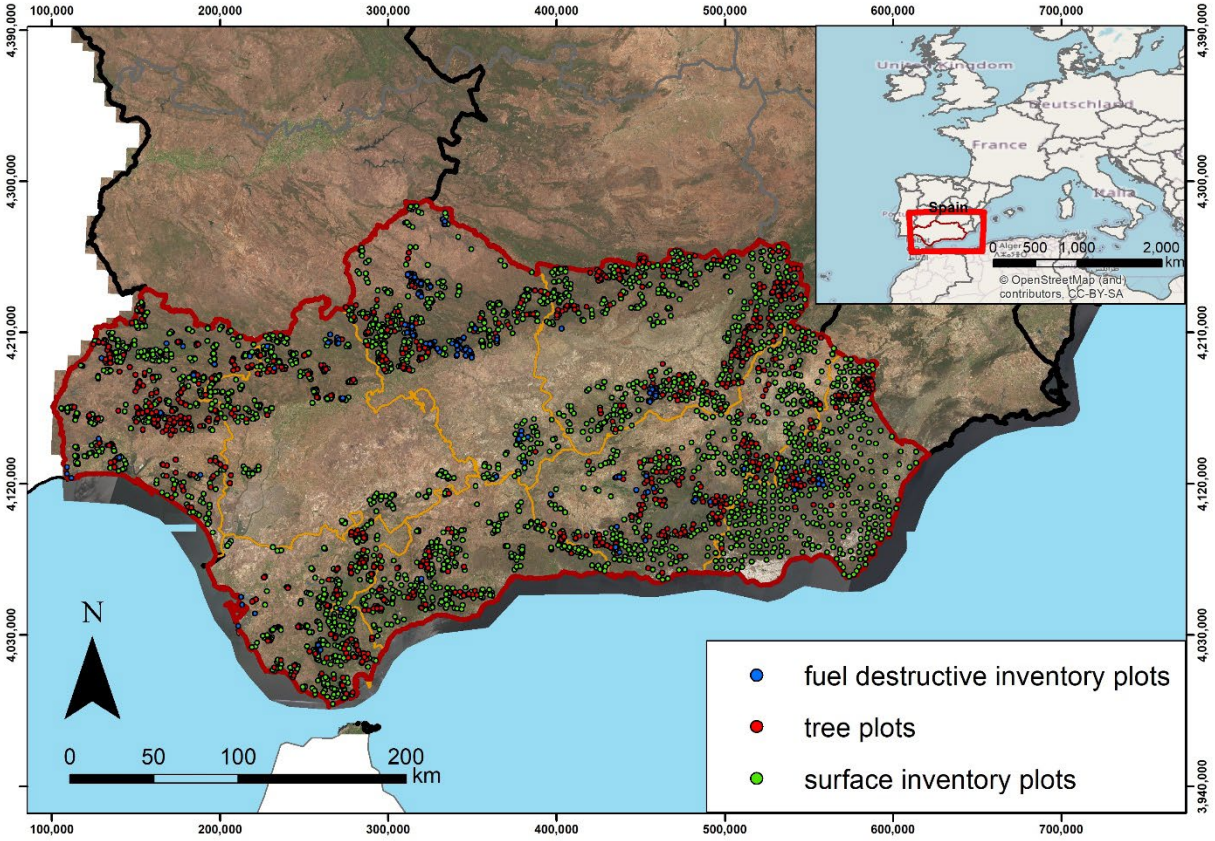

Figure 9: Field plots location of the three inventory types in Andalusia region (southern Spain)

Fuel Models adaptations

Before conducting the surface inventory field work, it was necessary to carry out a revision of the original UCO40 fuel models with the main objective of facilitating their identification in the field. The main reasons for this adaptation were the following:

- Incorporation of objective and quantifiable identification criteria with fuel structural variables that are easy to estimate and/or measure.
- Enhance or simplify field identification to make it objective and easy to apply.
- Removal of criteria or subjective assessments affected by variables that are difficult to estimate and/or measure with uncertain threshold values.

The result of this revision is the UCO30 fuel models included in this manual and field guide.

After finishing the field work and once the LiDAR metrics were generated, we explored obtaining the mapping of the UCO30 fuel models (field version) with LiDAR technology, but it was not possible to differentiate all of them due to the following technological limitations:

- Impossibility to differentiate between shrub or grass species, and/or a mixture of both.
- Impossibility to estimate the litter and duff depth.
- Challenges in estimating grass height, exacerbated by significant temporal variations in herbaceous plants throughout the year.

The result of the models that showed differentiation was the classification called UCO20 (LIDAR map version).

Furthermore, to generate the mapping of the NFFL9 mapping version, a direct assignment was made from UCO20 version by establishing equivalences according to the similarities between the values of these parameters in both classifications.

Finally, the flow chart of the different adaptations and fuel model systems established is shown in Figure 2.

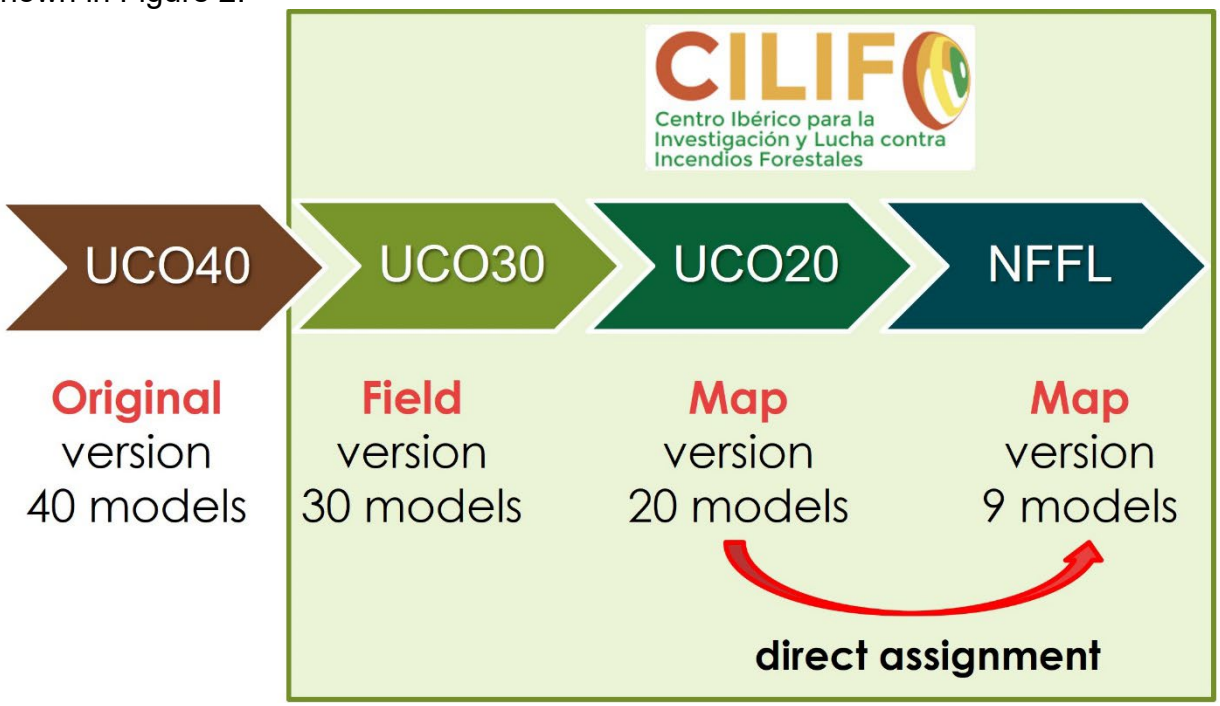

Figure 2: Flow chart of the different fuel model classification systems obtained from the UCO40 system

Results

The final results were compiled in a fuel model manual that includes the 3 new versions (UCO30, UCO20 and NFFL9) adapted from the original UCO40 classification system. This manual incorporates the guide with the key (Figure 3) and field sheets for the identification and characterisation of the fuel models. The sheets include a general photo, surface and canopy fuel parameters and fire behaviour graphs (Figure 4).

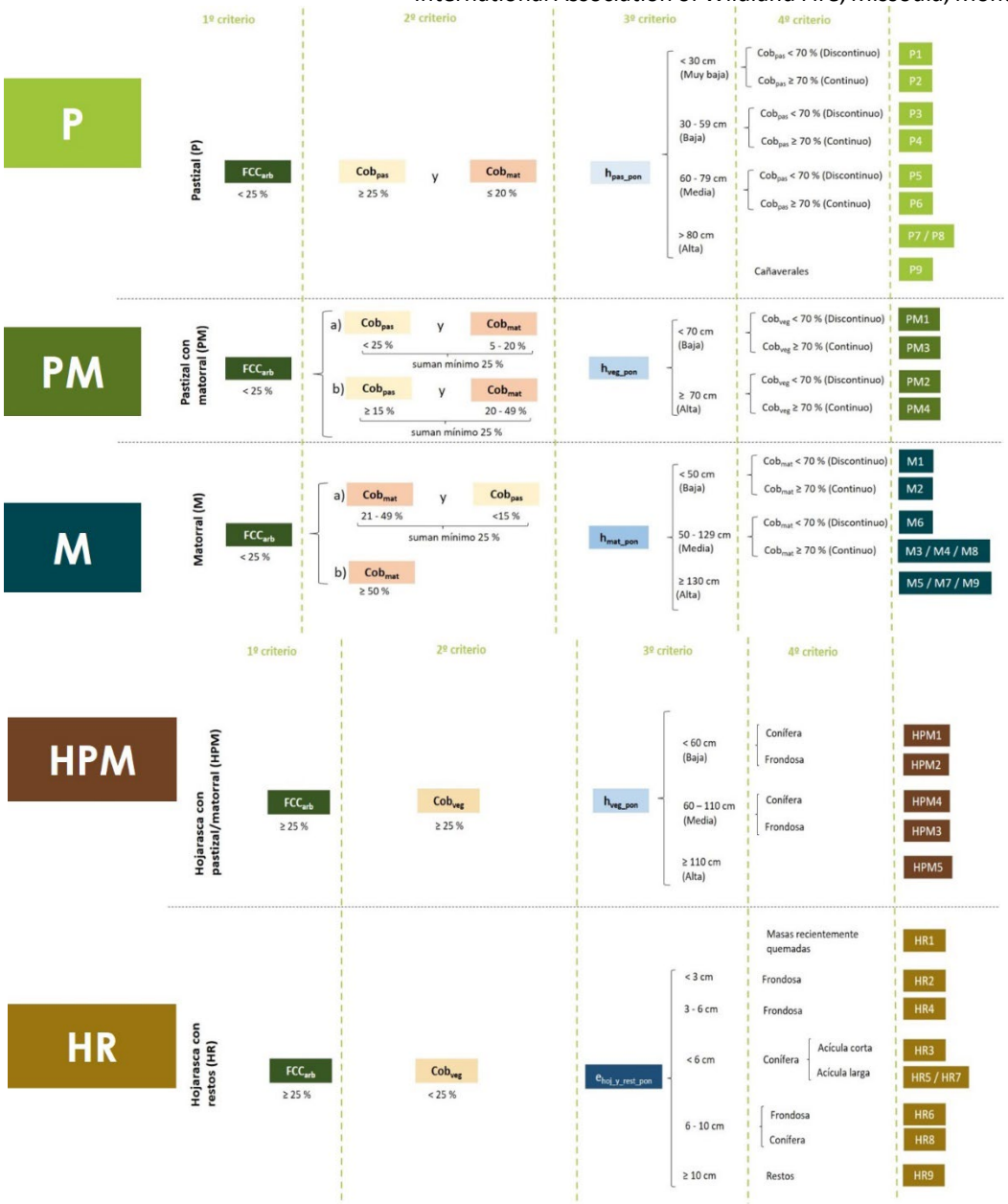

Figure 3: Identification key for UCO30 surface fuel models. Fuel types: P = Grass, PM = Grass-Shrub, M = Shrub, HPM = Timber-Understory and HR = Timber-Litter. Variables: FCC = Canopy Cover, Cob = vegetation cover, h = vegetation height.

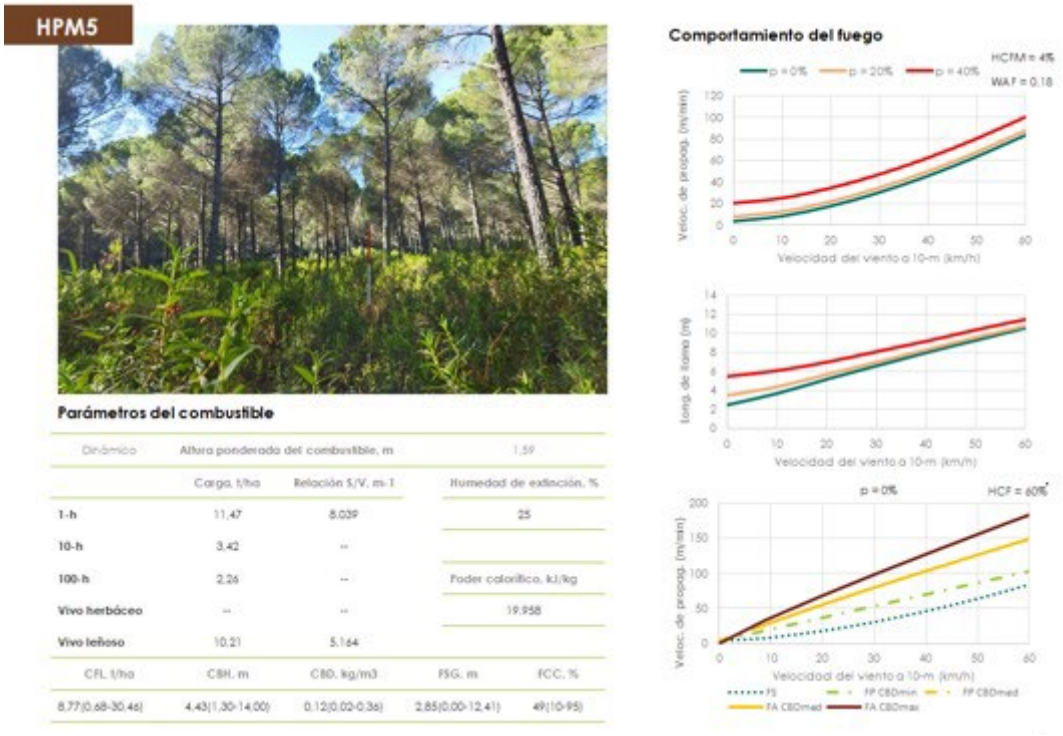

Figure 4: Feetsheet example of HPM5 fuel model. HPM = Timber understory

Conclusions

These new fuel classification systems enable the generation of high-resolution fuel maps at landscape-scale with their associated updated parameters, which can enhance fire behaviour predictions in wildfire simulation software. However, the performance of these new fuel parameters in the fire behaviour models currently included in operational wildfire simulators remains a challenge, with these new fuel parameters in real wildfire being critical.

Acknowledgements

This study is framed within the NET872330 contract - Forest fuel modelling within the framework of the EU project CILIFO (Iberian Centre for Research and Forest Firefighting). Co-financed by Andalusia regional government and European Regional Development Fund (ERDF) within the Cooperation Programme INTERREG VA Spain-Portugal (POCTEP) 2014-2020

The work of first author: Stéfano Arellano-Pérez in this study was supported by grant PTQ 2021- 012150 awarded by the MCIN/AEI/10.13039/501100011033.

References

- Anderson HE (1982) Aids to determining fuel models for estimating fire behavior. Gen. Tech. Rep. INT-122. Ogden, Utah: U.S. Department of Agriculture, Forest Service, Intermountain Forest and Range Experiment Station, 22 p. https://doi.org/10.2737/INT-GTR-122

- Arellano S, Vega JA, Ruíz AD, Arellano A, Álvarez, JG, Vega D, Pérez E (2017) Foto-guía de combustibles forestales de Galicia y comportamiento del fuego asociado. Andavira Editora S. L.

- Keane RE (2015) Wildland fuel fundamentals and applications. New York, US: Springer International Publishing. https://doi.org/10.1007/978-3-319-09015-3

- Rodríguez y Silva F, Molina-Martínez JR (2012). Modeling Mediterranean Forest fuels by integrating field data and mapping tools. *European Journal of Forest Research*, 131(3), 571–582. https://doi.org/10.1007/s10342-011-0532-2

- Scott JH, Burgan RE (2005) Standard fire behavior fuel models: A comprehensive set for use with Rothermel's surface fire spread model. Gen. Tech. Rep. RMRS-GTR-153. Fort Collins, CO: U.S. Department of Agriculture, Forest Service, Rocky Mountain Research Station. 72 p. https://doi.org/10.2737/RMRS-GTR-153

Proceedings for the 7th International Fire Behavior and Fuels Conference April 15-19, 2024, Boise, Idaho, USA – Tralee, Ireland – Canberra, Australia Published by the International Association of Wildland Fire, Missoula, Montana, USA

Combustion of cylindrical wooden firebrands under forced convection

Weidong Yan
State Key Laboratory of Fire Science, University of Science and Technology of China, Hefei, Anhui 230026, P.R. China, yanwd@mail.ustc.edu.cn

Naian Liu*
State Key Laboratory of Fire Science, University of Science and Technology of China, Hefei, Anhui 230026, P.R. China, liunai@ustc.edu.cn

Hong Zhu*
State Key Laboratory of Fire Science, University of Science and Technology of China, Hefei, Anhui 230026, P.R. China, zhuh15@ustc.edu.cn

**Corresponding Authors*

Introduction

Spot fire is one of the most significant mechanisms of rapid fire spread in wildland and wildland-urban interface (WUI) fires (Suzuki *et al.* 2015). Over the past several decades, there has been a focus on firebrand generation, transport, and ignition (Manzello *et al*. 2020). In terms of firebrand transport, most firebrand combustion under forced convection studies are based on empirical modelling or experimental analysis (Tarifa *et al.* 1965; Almeida *et al.* 2011). The firebrand combustion characteristics (burning rate and projected area) are essential for predicting the flight trajectory for firebrand transport. The firebrands under forced convection may exhibit a flaming or smouldering combustion pattern. However, the combustion patterns have rarely been distinguished in studies of firebrand burning rate and projected area. Tse and Fernandez-Pello (1998) proposed that the reduction of projected area could be attributed to the char oxidation on the firebrand surface. Lattimer *et al.* (2022) used analytical equations to evaluate burning rate, char diameter, and combustion duration based on char oxidation. However, wood pyrolysis was not taken into consideration.

With the above problem in mind, this work studies the combustion characteristics of flaming and smouldering cylindrical wooden firebrands under forced convection. The firebrand burning rate and projected area are analyzed using experimental and modelling approaches.

Materials and methods

In terms of the firebrand shape and size observed in WUI fires (Manzello *et al*. 2020), cylindrical wooden firebrands with different firebrand sizes (diameter D = 10, 12, and 15 mm, length L = 30, 36, and 45 mm) were used as the samples in this work. The cylinder is one of the typical shapes of firebrands (cylinder, sphere, and disk). The experimental samples were dried in a drying oven (Jinghong, XMTD-8222) at 100-120 °C for 24 hours (Mukunda *et al*. 1985) before the experiments.

The experimental setup for firebrand combustion under forced convection is illustrated in Fig. 1. A jet fan (SDS4.0-2.2kw-2p), equipped with damping nets and honeycomb inside the outlet end, was used to provide a stable airflow. The wind speed was controlled by a frequency converter. The wind speeds ranged from 0 m s^{-1} to 8 m s^{-1}. A digital video camera (Sony FDR-AX60, 50 frames per second, 1920×1080 pixels) recorded the firebrand combustion from the front view. Firebrands were ignited using a propane igniter, and the igniter was immediately turned off once the firebrands reached self-sustaining combustion. We quenched the firebrand at about 20 instants in each experimental condition and then measured the firebrand mass and projected area. The firebrand image captured by a digital video camera was transformed into a grayscale image and subsequently converted into a binary image using a cutoff threshold. The firebrand projected area was calculated using pixels and a reference scale.

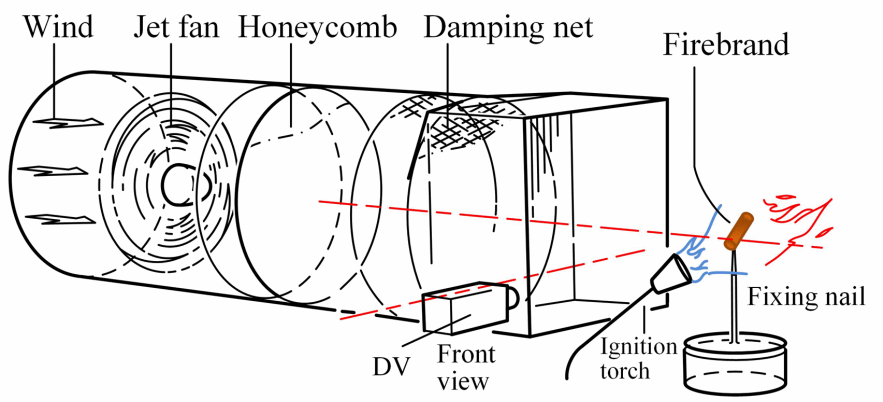

Fig. 1. Experimental setup for firebrand combustion under forced convection.

Results and discussion

Projected area

The variation in the projected area of the firebrand is primarily due to char oxidation (Tse and Fernandez-Pello 1998; Porteiro *et al*. 2007). The char oxidation rate of a firebrand is

$$\frac{dm_{char}}{dt} = -m'_{char} \tag{1}$$

where m_{char} is char mass (kg), t the burning time (s), and m'_{char} the char oxidation rate (kg s^{-1}).

The char mass is

$$m_{char} = \rho_{char}\Omega = \frac{\rho_{char}\pi D^2 L}{4} \tag{2}$$

where ρ_{char} is the char density (kg m^{-3}), Ω the firebrand volume (m^3), and *L* the firebrand length (m). The cylindrical-shaped firebrands are assumed to have a constant aspect ratio L_0/D_0 (Lattimer *et al*. 2022), where *0* means the initial value.

The char oxidation rate of spherical wooden firebrands under forced convection (Yan *et al*. 2024) is

$$m'_{char} = 2\pi D \rho_g D_m \ln(1+B)\left[1+\frac{fbRe^{1/2}Pr^{1/3}}{2}\right] \quad (3)$$

where the air density $\rho_g = 1.1614$ kg m^{-3} at 300 K (Yan *et al*. 2024), the gas diffusion constant $D_m = 1.84\times10^{-5}$ m^2 s^{-1} (Lattimer et al. 2022). The mass transfer number *B* for flaming and smouldering stages is 0.175 and 0.942 (Yan *et al*. 2024). The correction factor *fb* for flaming and smouldering stages is 0.28 and 0.42 (Yan *et al*. 2024). $Re = D_0\rho_g U/\mu$ (Lattimer *et al*. 2022), where *U* is the wind speed (m s^{-1}), D_0 is the initial firebrand diameter (m), and the dynamic viscosity $\mu = 1.846\times10^{-5}$ (N s m^{-2}) (Yan *et al*. 2024). The Prandtl number *Pr* = 0.707 (Lattimer *et al*. 2022; Yan *et al*. 2024).

Based on the char oxidation rate of spherical wooden firebrands under forced convection. The combustion model for spherical firebrands can be extended for cylinder firebrands by geometric transformation. The char oxidation rate of cylindrical firebrands under forced convection is formulated as

$$m'_{char} = \pi D \rho_g D_m \ln(1+B)\left[1+\frac{fbRe^{1/2}Pr^{1/3}}{2}\right] L_0/D_0 \quad (4)$$

Based on the Eq. 1, Eq. 2, and Eq. 4, the reduction rate of the firebrand projected area *S* is

$$\frac{dS}{dt} = -\frac{8\rho_g D_m}{\rho_{char}}\ln(1+B)*\left[1+\frac{fbRe^{1/2}Pr^{1/3}}{2}\right] \quad (5)$$

The theoretical *dS* / *dt* values for flaming and smouldering combustion are shown in Fig. 2, and agree with the experimental data. Based on Eq. 5, the *dS* / *dt* is

$$\frac{dS}{dt} = -f\left(\rho_{char}{}^{-1}, \ln(1+B), \left[1+\frac{fbD_0^{1/2}\rho_g{}^{1/2}Pr^{1/3}}{2\mu^{1/2}}U^{1/2}\right]\right) \quad (6)$$

The higher *dS* / *dt* value corresponds to the higher char density, lower ln(1+*B*), lower firebrand diameter, and lower wind speed. The ln(1+*B*) value in smouldering is

lower than in flaming. Thus, the dS/dt in flaming is slightly lower than in smouldering under 2 m s^{-1} and 4 m s^{-1} in Fig. 2.

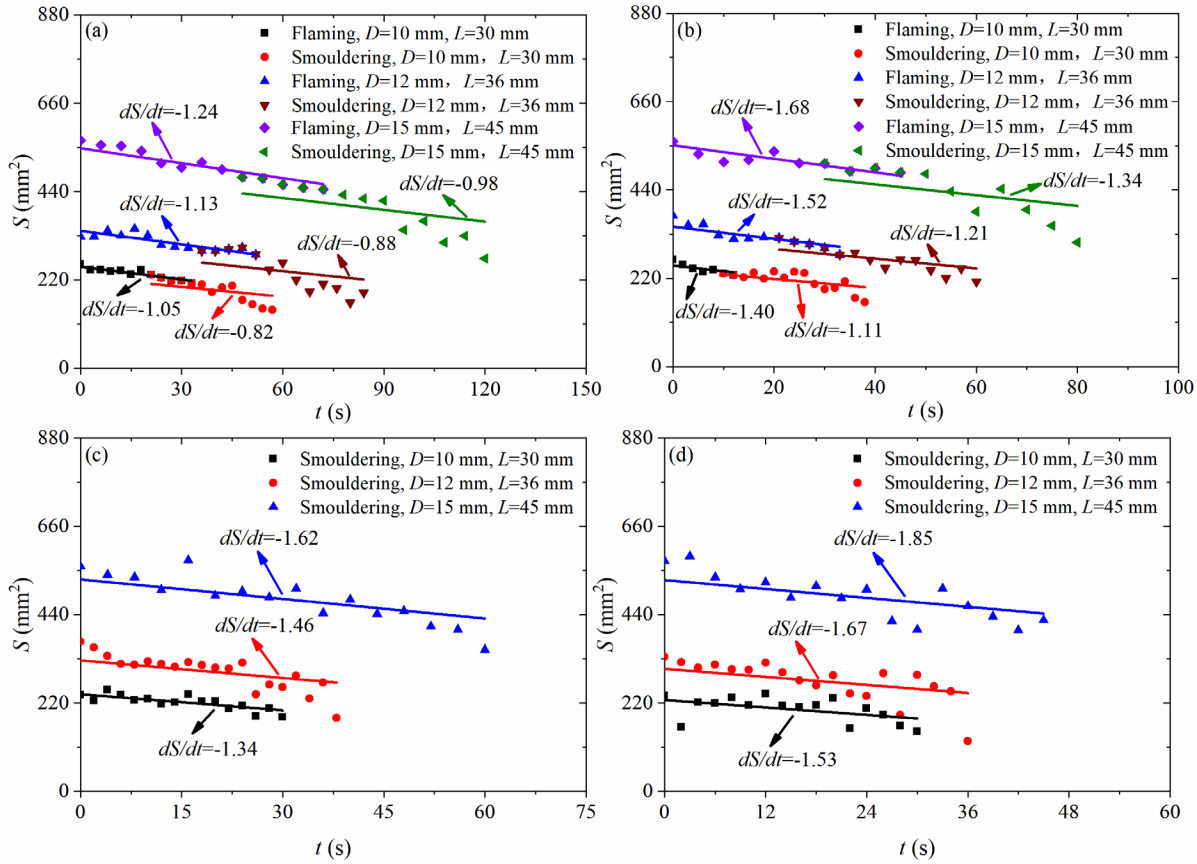

Fig. 2. Theoretical and experimental *dS/dt* values at wind speeds of (a) 2 m s^{-1}, (b) 4 m s^{-1}, (c) 6 m s^{-1}, and (d) 8 m s^{-1}.

Burning rate

The burning rate of a firebrand is

$$\frac{dm_{fb}}{dt} = -\left(1+\varphi_{pyr}\right)m'_{char} \tag{7}$$

where m_{fb} is the firebrand mass (g), and φ_{pyr} is the ratio of wood pyrolysis rate to char oxidation rate. The subscript *fb* and *pyr* denote firebrand and wood pyrolysis, respectively. Based on the Eq. 4 and Eq. 7, the burning rate of cylindrical firebrands m'_{fb} is

$$m'_{fb} = \pi D \rho_g D_m \ln\left(1+B\right)\left(1+\overline{\varphi_{pyr}}\right) * \left[1+\frac{fbRe^{1/2}Pr^{1/3}}{2}\right] L_0/D_0 \tag{8}$$

where the $\overline{\varphi_{pyr}}$ value is 4.51 (Yan *et al*. 2024). Then, based on Eq. 8, the m'_{fb} satisfies

$$m'_{fb} = m'_{fb,nc}\left(1+K*U^{1/2}\right) \tag{9}$$

where the subscript *nc* denotes the natural convection, and *K* is the function coefficient. The firebrand mass is expressed as

$$m_{fb} = m_0 - \int_0^t m'_{fb}dt \tag{10}$$

Then, based on Eq. 10, the m_{fb} satisfies

$$m_{fb} = m_0 - \frac{6\pi\rho_g D_m \ln\left(1+B\right)\left(1+\overline{\varphi_{pyr}}\right)*\left[1+fbRe^{1/2}Pr^{1/3}/2\right]}{K}\left[D_0^3 - \left(D_0^2 - \frac{Kt}{3}\right)^{1.5}\right] \tag{11}$$

The theoretical m_{fb} for flaming and smouldering combustion is shown in Fig. 3, which agrees with the experimental data. The larger the firebrand diameter and wind speed, the faster the firebrand burning rate. The firebrand burning rate significantly depends on the wind speed, and the burning rate is proportional to $U^{1/2}$.

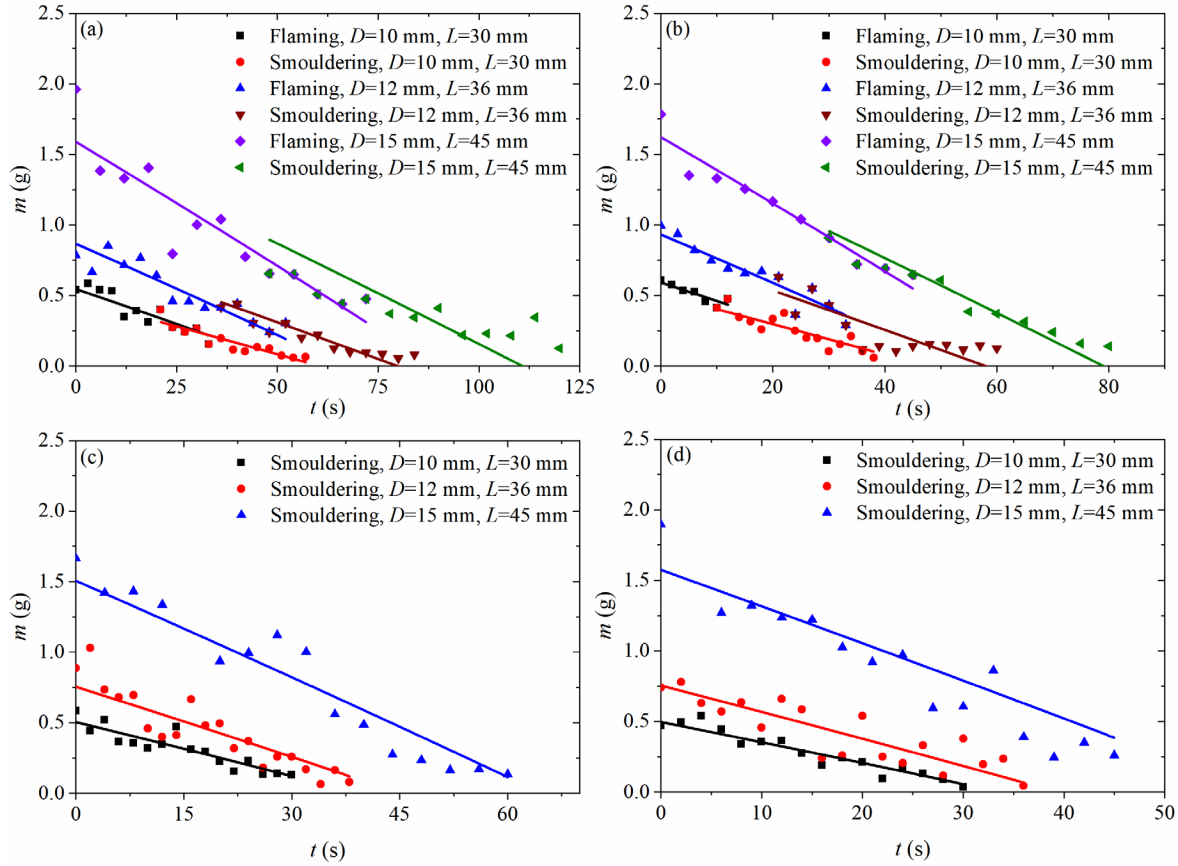

Fig. 3. Firebrand mass under (a) 2 m s^{-1}, (b) 4 m s^{-1}, (c) 6 m s^{-1}, and (d) 8 m s^{-1}.

Conclusions

In this work, cylindrical wooden firebrand combustion was conducted under forced convection. The projected area and burning rate of firebrands are estimated in self-sustaining combustion. The reduction rate of the firebrand projected area depends on char density, flaming or smouldering combustion, firebrand diameter, and wind speed. The projected area of firebrands in flaming combustion decreases more rapidly than those in smouldering combustion. The burning rate is correlated to firebrand size (length and diameter), flaming or smouldering combustion, and wind speed. The burning rate of a firebrand is proportional to $U^{1/2}$ (U is wind speed).

Acknowledgements

This research is sponsored by the National Key Research and Development Plan (No. 2022YFC3003000), the National Natural Science Foundation of China (No. 52321003), the China Postdoctoral Science Foundation (2021M703083), and the Foundation of State Key Laboratory of Laser Interaction with Matter (SKLLIM2001).

References

Almeida M, Viegas DX, Miranda AI, Reva V (2011) Effect of particle orientation and of flow velocity on the combustibility of Pinus pinaster and Eucalyptus globulus firebrand material. *International Journal of Wildland Fire* **20**, 946-962. doi:10.1071/WF09080

Lattimer BY, Bearinger E, Wong S, Hodges JL (2022) Evaluation of models and

important parameters for firebrand burning. *Combustion and Flame* **235**, 111619. doi:10.1016/j.combustflame.2021.111619

Manzello SL, Suzuki S, Gollner MJ, Fernandez-Pello AC (2020) Role of firebrand combustion in large outdoor fire spread. *Progress in Energy and Combustion Science* **76**, 100801. doi:10.1016/j.pecs.2019.100801

Mukunda HS, Paul PJ, Srinivasa U, Rajan NKS (1985) Combustion of wooden spheres - Experiments and model analysis. *Proceedings of the Combustion Institute* **20**, 1619-1628. doi:10.1016/S0082-0784(85)80657-3

Porteiro J, Granada E, Collazo J, Patiño D, Morán JC (2007) A model for the combustion of large particles of densified wood. *Energy & Fuels* **21**, 3151-3159. doi:10.1021/ef0701891

Suzuki S, Manzello SL, Kagiya K, Suzuki J, Hayashi Y (2015) Ignition of mulch beds exposed to continuous wind-driven firebrand showers. *Fire Technology* **51**, 905-922. doi:10.1007/s10694-014-0425-2

Tarifa CS, Notario PPD, Moreno FG (1965) On the flight paths and lifetimes of burning particles of wood. *Proceedings of the Combustion Institute* **10**, 1021-1037. doi:10.1016/s0082-0784(65)80244-2

Tse SD, Fernandez-Pello AC (1998) On the flight paths of metal particles and embers generated by power lines in high winds - a potential source of wildland fires. *Fire Safety Journal* **30**, 333-356. doi:10.1016/S0379-7112(97)00050-7

Yan W, Liu N, Zhu H (2024) Firebrand burning under wind: an experimental study. *International Journal of Wildland Fire* **33**, WF23151. doi:10.1071/WF23151

Proceedings for the 7th International Fire Behavior and Fuels Conference April 15-19, 2024, Boise, Idaho, USA – Tralee, Ireland – Canberra, Australia Published by the International Association of Wildland Fire, Missoula, Montana, USA

Comparing Fire Spread Predictions from the Fire Dynamics Simulator & QUIC-Fire to Observations

*William Mell, Anthony Bova
Pacific Wildland Fire Sciences Lab, Seattle, WA, USA
william.mell@usda.gov, anthony.bova@usda.gov

Derek McNamara
Geospatial Measurement Solutions, Hood River, OR, USA
dmgeo@gmsgis.com

Eric Mueller
National Institute of Standards and Technology, Gaithersburg, MD, USA
eric.mueller@nist.gov

Xareni Sanchez-Monroy
Insurance Institute of Building and Home Safety, Richburg, SC, USA
xmonroy@ibhs.org

**Corresponding Author*

Introduction

The promise of 3D models, such as the models used here, lies mainly in their higher physical fidelity accounting of: 1) the influence of spatially variable vegetation and terrain on fire behavior and 2) the interaction of the fire and the atmosphere. Evaluating how well 3D models capture these two important aspects of fire behavior requires appropriately designed experiments (to get the desired fire behavior) and appropriate measurements and supporting geospatial data science practices (McNamara and Mell, 2021) in order to produce usable and useful observational data.

The use of observations of the evolution of an evolving fire's footprint (Figure 10) supports the evaluation of a model's ability to capture (indirectly or directly) the net heat transfer environment, which varies along the fire's perimeter and results in a faster spreading, larger depth, head fire and slower, smaller depth, spreading flank fire. A model that adequately predicts the fire depth, spread rate, and mass consumption throughout the fire's footprint is also likely to well-predict the local and global heat release rate. These heat release rates are, respectively, relevant to local fire effects and overall smoke plume rise.

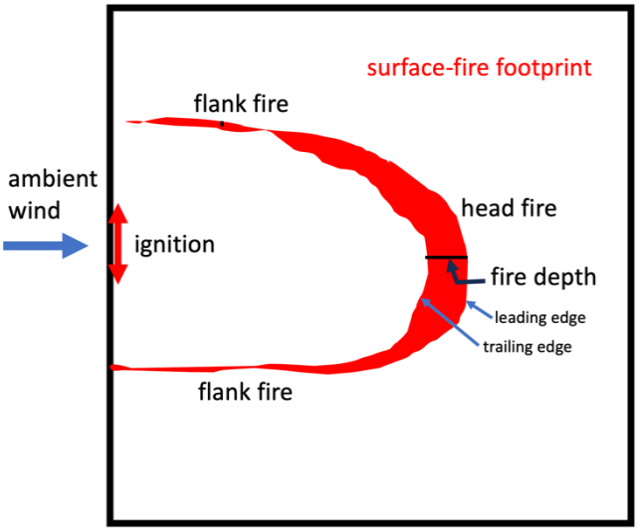

Figure 10: Schematic of a footprint of a freely evolving surface fire originating from a line ignition. A backfire cannot occur because vegetation is removed upwind of the burn block.

Below, models are compared to field observations of the fire footprint. It's worth noting that, currently, such observational data sets are rare.

Methods

The observational data

Observations from field experiments of surface fire are used as a basis for model evaluation. Surface fires are fundamental in prescribing burning and, in general, drive fire in raised vegetation. Thus, a basic requirement of a generally applicable fire behavior model is that it is adequately proven to model surface fire behavior.

The following two research burns provide the observational data for model evaluation:

1) 1986 Annaburro Experimental Grassland Fire Data (Gould et al., 2023). Observations from experiment C064 are used here (Figure 11, left side)
2) 2014 Camp Swift Experiment (McNamara and Mell, 2018). There are three dominant surface vegetation types (bluestem, camphorweed, and threeawn). Observations from burn block 1 are used here (Figure 11, right side).

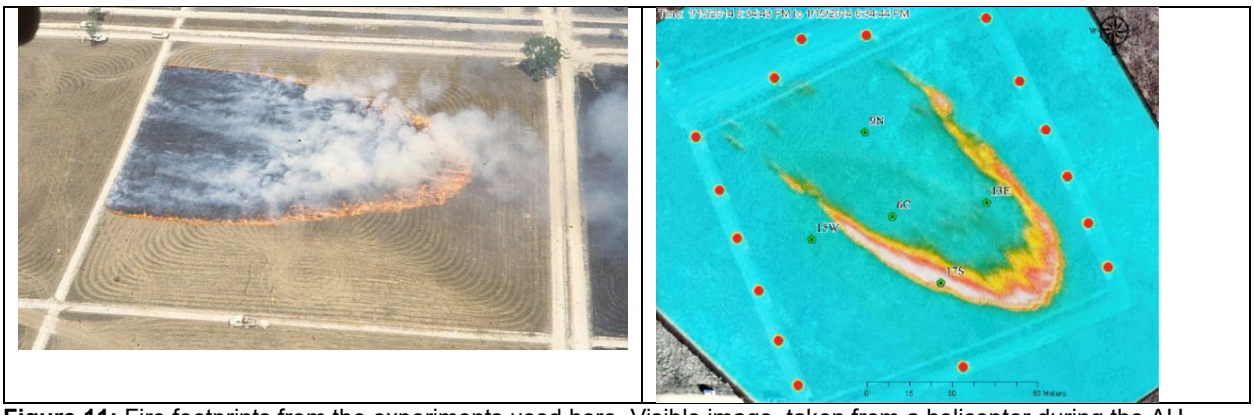

Figure 11: Fire footprints from the experiments used here. Visible image, taken from a helicopter during the AU grassland fire experiment C064, on the left. Infrared image taken from a fixed wind UAV during the Camp Swift burn block 1 experiment, on the right.

Vegetation characteristics are given in Table 1. Both experimental campaigns ignited the vegetation along the upwind edge of the burn block via drip torches. Two people started at the center of the ignition line and walked (walking speed is given in Table 1) in opposite directions for the appropriate distance.

Table 1: Information on plot size, ignition, vegetation, and wind for each experiment (cyl = cylindrical shaped vegetation element)

	AU C064	Camp Swift
plot size, m^2	100 x 100	100 x 100
Ignition line length, m	50	50
ignitor walk speed, m s^{-1}	1.0	1.0
fuel moisture, %	6.3	26, bluestem 11, camphorweed 7, threeawn
fuel height, m	0.21	0.30, bluestem lower 0.30-0.80 bluestem upper 0.45, camphorweed 0.41, threeawn
fuel loading, kg m^{-2}	0.283	0.1 cylinder, 0.2 blade, bluestem lower 0.04 large cylinder, 0.04 small cyl, 0.02 blade bluestem upper 0.55 camphorweed 0.09 cylinder and blade, threeawn
surface-to-volume, m^{-1}	9770	1850 cylinder, 8439 blade, bluestem upper 2438 large cylinder, 6768 small cylinder, 9147 blade bluestem upper 3896 camphorweed 5910 cylinder, 12280 blade, threeawn
wind speed, m s^{-1}	4.6 @ 2m AGL	4.6 @ 3.3 m AGL

The models

Word count limitations on this abstract prevent a full description of the models used here. In brief, the models are:

1) FDS (version 6.8.0, from the National Institute of Standards and Technology) has two main modeling approaches (FDS, 2024; Vanella et al., 2021):
    a. Full physics based (FDS-PB), explicitly models the processes driving fire behavior
    b. Reduced physics (FDS-LS), simplified model for the burning of surface vegetation

2) QF (QUIC-fire, version 6.0.0, from the Los Alamos National Laboratory), reduced physics approach for both the burning of vegetation and atmospheric flow (Linn et al., 2020)

Results

Australian Grassland Experiment C064 Simulations

The observed and FDS-predicted fire footprints for experiment C064 are shown in Figure 12. Both FDS-PB and FDS-LS underpredict the average head fire rate of spread

by 28% (~ 0.72 m/s FDS; ~ 1 m/s observed). FDS-PB underpredicts head fire depth (~ 10 m observed; ~ 5 m FDS-PB); FDS-LS well-predicts the head fire depth.

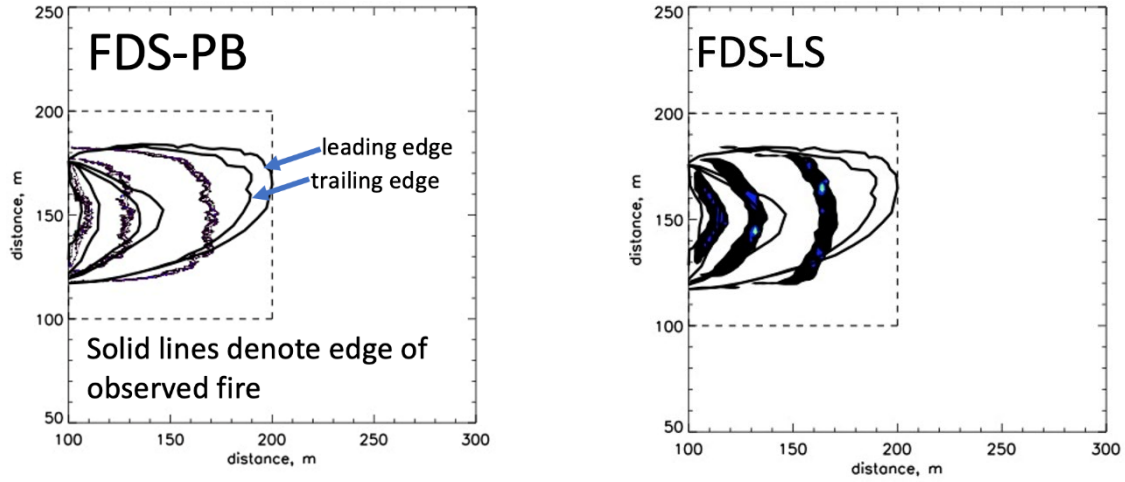

Figure 12: Australian grassfire experiment C064 fire footprint at 27 s, 53 s, 100 s after ignition start from observations and FDS simulations. Solid lines denote the leading and trailing edges of the observed fire. FDS predictions of flaming location are the shaded regions.

Figure 13 shows the observed and QF predicted fire footprints for experiment C064. The fire has an initial "spin-up" period in which it burns more like an area fire and then spreads with a more delineated footprint at later times (not shown). QF underpredicts the head fire rate of spread by 53% (~ 0.47 m/s QF; ~ 1 m/s observed). The fire depth in QF is larger than the observations.

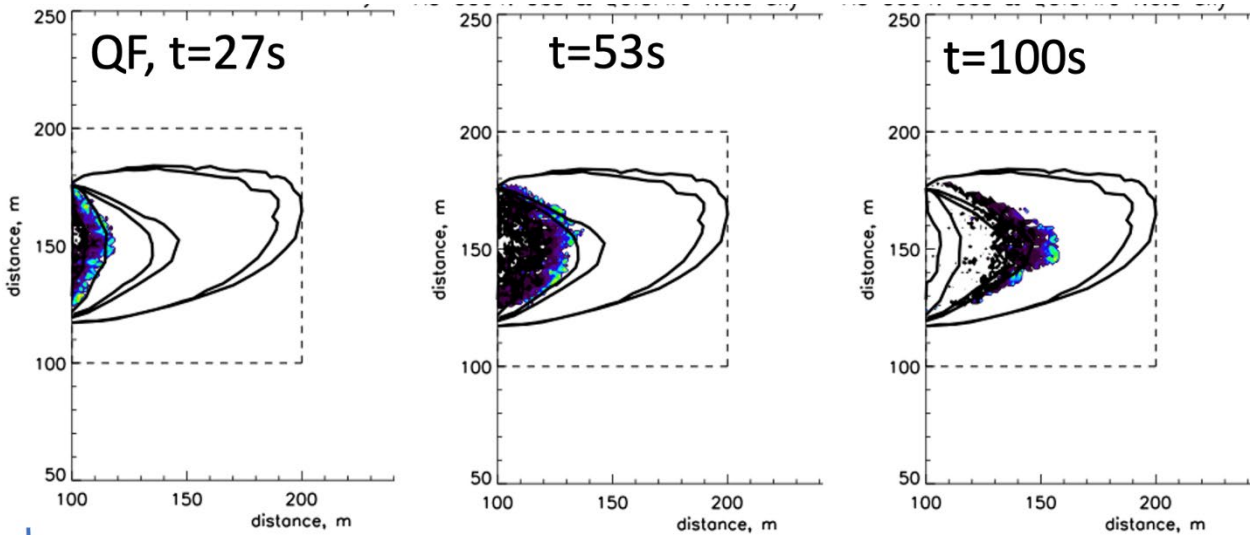

Figure 13 Australian grassland experiment C064 fire footprint from observations (solid lines) and QF (shaded regions correspond to active burning) at the same times shown in Figure 12.

Camp Swift Experiment Burn Block 1 Simulations

Figure 14: Photo taken during the Camp Swift experiments exhibiting the three major vegetation types used the models: bluestem, threeawn, and camphorweed.

Vegetation present at the Camp Swift experiments is shown in Figure 14 and Figure 15. The influence of vegetation on flank fire behavior in burn block 1 is displayed in Figure 16.

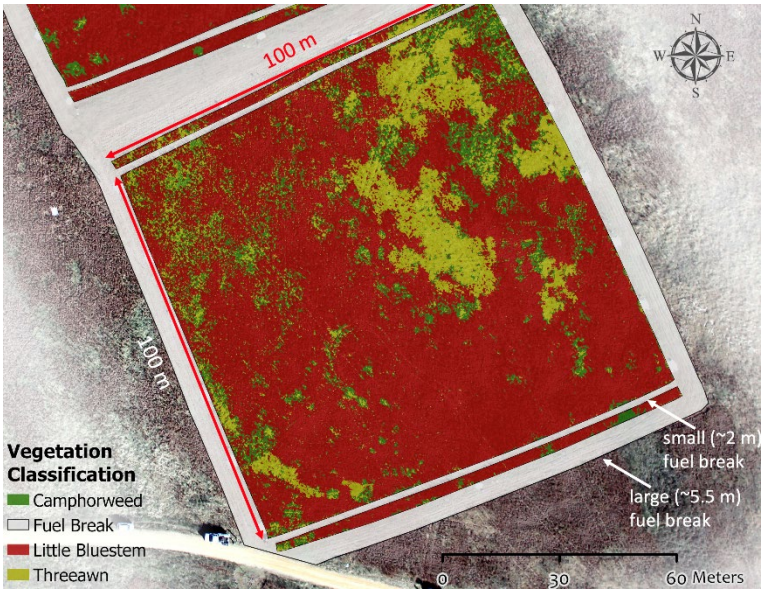

Figure 15: Distribution of vegetation in Camp Swift burn block 1 based on overhead imagery and ground sampling (McNamara and Mell, 2018).

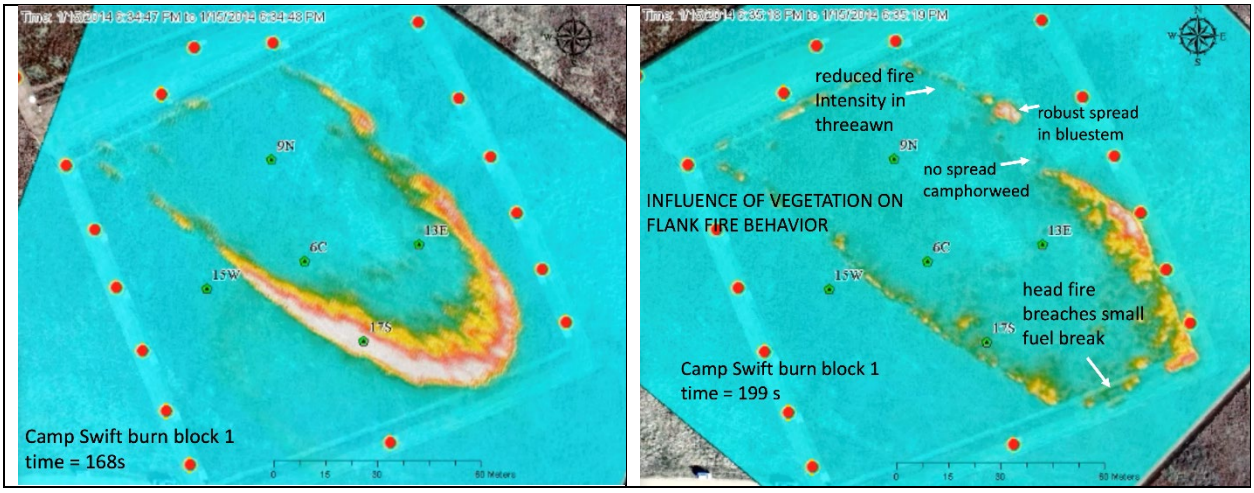

Figure 16: Infrared images of fire overlying vegetation map for Camp Swift burn block 1. On left: head fire reaches end of burn block at 168 s. On right: influence of vegetation on flank fire behavior.

In the FDS-PB (Figure 17, left side) and FDS-LS (Figure 18, left side) simulations, the fire reached the end of the burn block 140 s (28 s sooner than the observed fire in Figure 16) and did breach the small fire break for FDS-PB (Figure 17, right side). Extended flank fires did not survive in FDS-PB; head fire depth ~4 m FDS-PB and 2.9 m +/- 0.5 m observations. In FDS-LS, flank fires survive, head fire depth ~ 6 m, flank fire depth ~1m FDS (2.25 m +/- 1.1 m observation). FDS-LS does not yet handle fire crossing a fuel break. QUIC-fire simulations are shown in Figure 19. The QF simulated fire spreads significantly slower than observations, reaching the end of the burn block (Figure 19, right side) at 1085 s (917 s later than the observed fire).

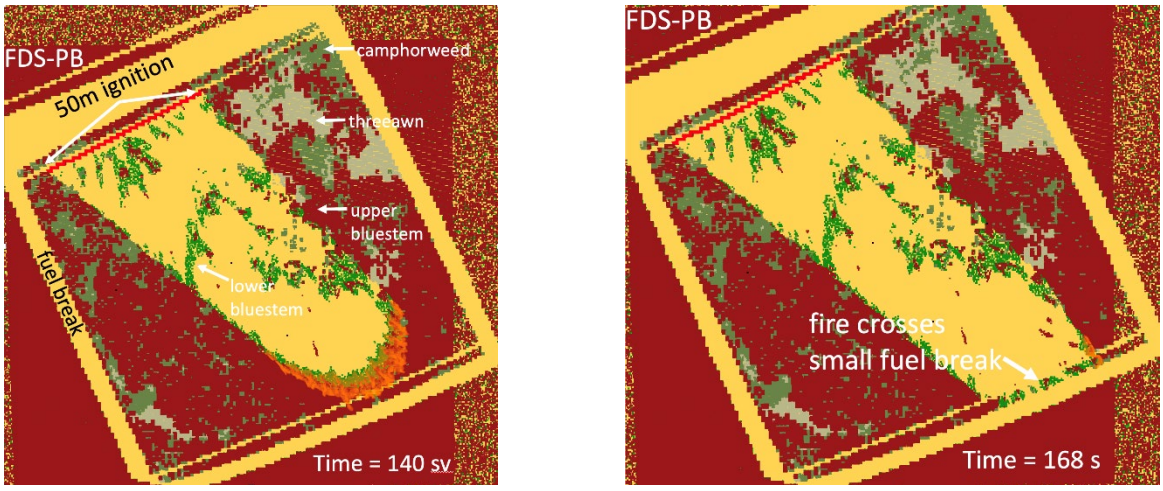

Figure 17: FDS-PB Camp Swift simulation (gas phase heat release rate isosurface is shown) when head fire reaches end of burn block (on left) and after breaching the fuel break (on right).

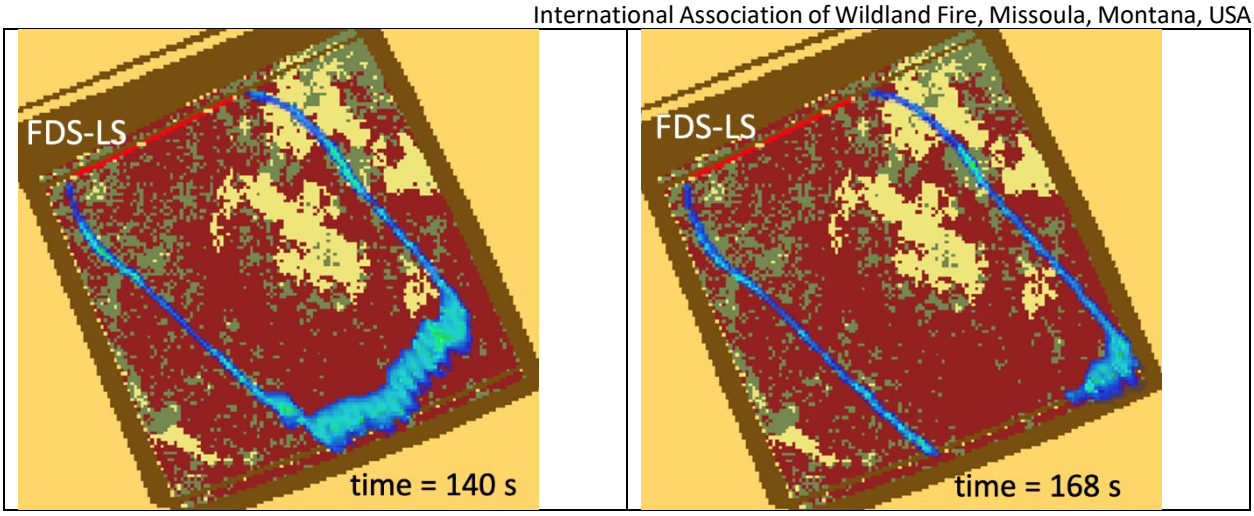

Figure 18: FDS-LS Camp Swift simulation (mass burning rate is shown) at the same two times as Figure 17. Bluestem is reddish-brown; camphorweed is green; threeawn is yellow. Unlike Figure 17, consumption of the vegetation is not shown.

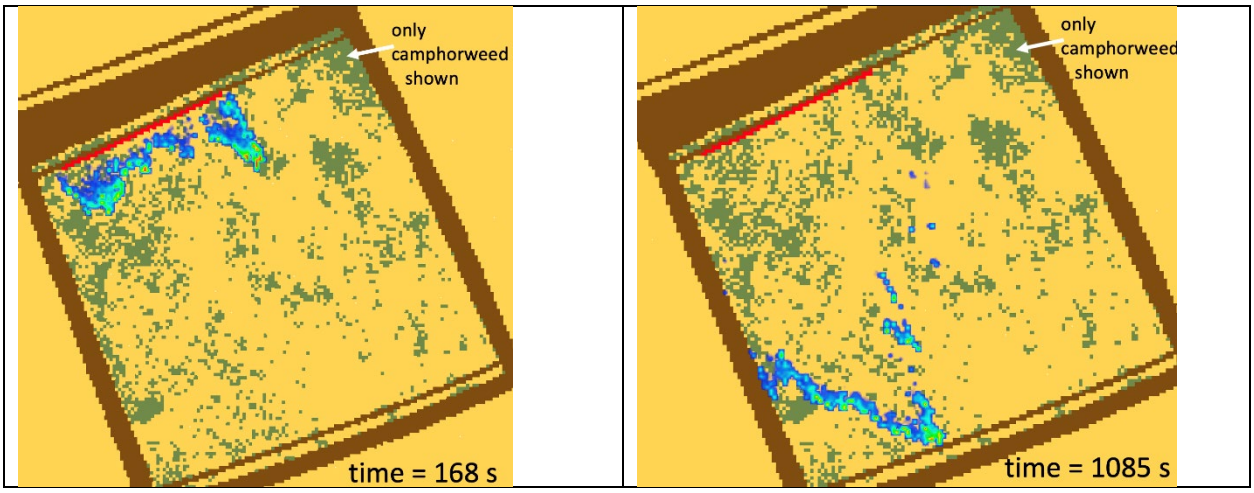

Figure 19: QF Camp Swift simulation (surface energy is shown) at two different times.

Discussion

All the models considered here require further evaluation and development (word limits restrict discussion here). All models performed better for the relatively dry, uniform, Australian grassland fuel. In Camp Swift's more complex vegetation environment Camp, flank fires did not survive in FDS-PB and the rate of spread was significantly underpredicted in QF.

References

- FDS program suite (2024). https://pages.nist.gov/fds-smv/downloads.html
- FDS validation suite (2024). https://github.com/firemodels/fds/tree/master
- Gould, James; Gomes Da Cruz, Miguel; Sullivan, Andrew (2023): 1986 Annaburroo Experimental Grassland Fire Data. v2. CSIRO. Data Collection. https://doi.org/10.25919/24fg-2q32

- Linn RR, Goodrick SL, Brambilla S, Brown MJ, Middleton RS, O'Brien JJ, Hiers JK (2020) QUIC-fire: A Fast-Running Simulation Tool for Prescribed Fire Planning, *Environmental Modelling and Software*, **125**. https://doi.org/10.1016/j.envsoft.2019.104616
- McNamara DJ, Mell WE (2018) Camp Swift Fire Experiment 2014: Integrated Data Quality Assessment. https://www.arcgis.com/home/item.html?id=aa3726577d9549a2a26b7d000fb98512
- McNamara DJ, Mell WE (2021) An Approach to Integrated Data Management for Three-Dimensional, Time-Dependent Fire Behavior Model Evaluation, *International Journal Wildland Fire*, **30**(12), 911-920. https://doi.org/10.1071/WF2102
- Vanella M, McGrattan K, McDermott R, Forney G, Mell W, Gissi E, Fiorucci P (2021) A Multi-Fidelity Framework for Wildland Fire Behavior Simulations over Complex Terrain, *Atmosphere*, **12**, 273 https://doi.org/10.3390/atmos12020273

Conflicts In Fire-prone Degraded Forests: Case Of Afrensu Brohuma Forest, Ghana

Anin Bismark
Resource Management Support Centre of Forestry Commission, Ghana
Box 1457 Adum, Kumasi Ghana-West Africa
bismakanin2020@yahoo.com

Abstract

People worldwide constantly compete for vital natural resources like land, water and forest products to sustain their livelihoods. As demand for natural resources grows, there is significant potential for conflicts over such resources. This study sought to identify conflict types, their causes and actors' interest in managing Afrensu Brohuma Forest Reserve. It also sought to evaluate the strategies employed to manage wildfire-associated conflicts and their effects on conflict dynamics. Both primary and secondary data sources were used for the study. The study identified four types of conflicts in the study area namely, wildfire conflict, land-use conflict, resource utilisation and illegal activities conflicts. Wildfire conflict situation was predominant in the study area. The major cause of the conflict was the setting of fire in the forest by farmers, group hunters and migrants in a bid to dispose of degraded forestlands for farming and the collection of Non-Timber Forest Products (NTFPs) by community members living in and around the forest reserve. The use of community fire prevention and suppression strategies were employed to curb the devastating effects of fire on forests, farmlands and settlements in the study area. The study recommends revamping of local fire volunteer squads to support wildfire management in fire-prone degraded forest areas.

Keywords: Conflict, Wildfire, Forest, Degraded

Introduction

In recent times, fire has become a major threat to the forest resources in Ghana (Nsiah-Gyabaah, 1996). The extent and use of anthropogenic fires have become prevalent and are considered a major threat to forests in Ghana (Kalame *et al.,* 2009). Even though forests in the transition parts of the forest zone are known to have a long association with fires, the fires shape the forest vegetation in terms of structure and species composition (Hall and Swaine, 1981).

Presently wildfire is considered the most serious threat to the long-term productivity, genetic wealth and the general health of the semi-deciduous forest in Ghana having significantly altered the composition and structure of more than 30% of the forest (Hawthorne, 1994).

According to Appiah *et al.*, (2010) forest households lose an average of about US$231 in terms of agriculture and forest produce to fire annually but the impact of fires on agriculture may extend beyond simple stock damage.

Uncontrolled wildfire by forest managers, Illicit Forest activities, especially illegal timber exploitation and chainsaw milling, as well as the excessive exploitation of Non-Timber Forest Products (NTFPs) and illegal farming have led to the degradation of the Afrensu Brohuma Forest Reserve (ABFR) in the Offinso North District of the Ashanti Region of Ghana (Derkyi, 2012).

Materials and Methods

Afrensu Brohuma Forest Reserve is located in the Offinso North District of the Ashanti Region in Ghana. The communities were selected based on a report of long-standing conflicts between indigenous farmer groups and between migrants and FSD over degraded lands as well as a recommendation from the FSD office at Offinso. The communities surveyed are Mantukwa, Meta and Amponsah-Krom. Both primary and secondary data sources were used for the study. Semi-structured interviews, key informant interviews, focus group discussions and questionnaires were employed as data collection methods. Informal conversational discussions were also conducted in the forest fringe communities to obtain their perspectives on wildfire conflict issues in the study area. Qualitative data obtained was analysed based on transcribed interviews. Quantitative data was also analysed using the Statistical Package for Social Sciences (SPSS) version 21.

Results

Types of conflicts, actors and causes of natural resource conflicts

The study identified four types of conflicts in the study area namely, wildfire conflict, land-use conflict, resource utilisation and conflicts arising out of illegal activities. Wildfire conflict situation was predominant in the study area. Among the four types of conflict that were identified 47% of the respondents disclosed that the wildfire conflict is the type of conflict that has the highest level of conflict escalation followed by illegal activities 29%, land use 14% and resources utilisation 9% respectively. The study revealed that wildfire conflicts escalated from one stage to another due to the scarcity of fertile lands for farming by community members. Table 1.1 indicates the conflict types, causes, main actors and their interests in the conflict within the selected communities.

Table 1:1 Conflict types, causes, actors involved and interests

Types of Conflict	Causes of conflicts	Actors involved	Actors Interest
Wildfire conflict	The setting of fire into the forest by farmers and hunters	Farmers, group hunters and Resource managers	Acquisition of degraded forest land for farming Setting fire for games/bush meat
land-use conflict,	Land scarcity on the part of fringe communities	Resources managers Community members	Land for farming activities
Illegal activities	Illegal harvesting of economic trees by chainsaw operators	Chain saw operators, resource managers	Availability of wood for sale

Resource Utilizations	Excessive hunting at ABFR by group hunters	Hunters, Community members/farmers	Game for commercial purposes

Source: Field survey, 2022

Strategies employed to manage the conflicts and effects on the conflict dynamics.
The findings from the study demonstrate different strategies employed by resource managers and actors to address conflicts in fire-prone degraded forest areas. Table 2 indicates

Table 2: Distribution of actors, conflict types, management strategies and effects on conflict dynamics

Types of Conflict	**Actors involved**	**Conflict coping strategies used**	**Conflict dynamics**
Wildfire Conflict	Hunters, Farmers, Resource managers, Migrants	Formation of local Fire Volunteer Squads (FVS) (participatory approach)	De-escalation
Land-use conflict	Admitted farm owners/ Migrants, Resource managers	Extended farms were destroyed by forest guards (Coercion)	Escalation
		Allocated degraded forestland for farming and tree planting(negotiation)	De-escalating
Illegal activities	Chainsaw operators, Community members, Farmers, Migrants	Community members were educated to stay away from illegal forest activities and setting fire to the reserve (Avoidance)	De-escalation
Resource Utilizations	Community members, chain saw operators, hunters	Resource managers engaged communities to sustain forest resources and the ecosystem (participatory approach)	De-escalation

Source: Field survey, 2022

Discussion
Four types of conflict were identified with different actors, causes and interests as it indicated in Table 1. These types of conflicts have existed over time due to environmental change in the study area. Among the four types of conflict that were identified in the study area, conflicts associated with the wildfire were the ones that escalated. This is in line with the Systemic theory of conflict which indicates that environmental degradation (forest

degradation) is the root cause of natural resource conflict and has led to changes (Harper and Snowden 2017).

The actors have different interests and perceptions in the management of the forest reserve. The interest of the resource managers is to conserve and protect the forest for future generations while resource users, however, have an interest in acquiring the forest lands for farming and game for commercial use. This is in line with Oduro-Ofori et al. (2015) who confirmed that actors' interests and differences in the management of natural resources are always associated with conflicts.

Conclusion

Four types of conflicts were identified in the study area and wildfire conflicts were predominant in the study area. The main causes of the wildfire conflicts are the setting of fire to the degraded forest by farmers and hunters to dispose of the land for farming or enhance the early sprouting of fresh grass for game animals. The study recommends revamping local fire volunteer squads to support wildfire management in fire-prone degraded forest areas

Acknowledgements

I am also grateful to all the RMSC and Offinso FSD Staff, who supported me in the field during data gathering in diverse ways. Special gratitude also goes to the Mantukwa, Amponsahkrom and Meta communities for their cooperation and invaluable input.

References

Appiah, M., Damnyag, L., Blay, D. and Pappinen, A. (2010). Forest and agroecosystem fire management in Ghana. Mitig Adapt Strateg Glob Change (2010) 15:551–570. DOI 10.1007/s11027-010-9236-z

Beevers, M. D. (2019). Natural Resources: A Catalyst for Conflict and Peace? In *Peacebuilding and Natural Resource Governance After Armed Conflict* (pp. 39-61). Palgrave Macmillan, Cham

Derkyi, M. A. A. (2012). *Fighting over forest: interactive governance of conflicts over forest and tree resources in Ghana's high forest zone* (No. 41). African Studies Centre.

Hall, J. B. and Swaine, M. D. (1981). Distribution and Ecology of Vascular Plants in a Tropical Rain Forest: Forest Vegetation in Ghana. W. Junk, The Hague. http://dx.doi.org/10.1007/978-94-009-8650-3

Harper, C. L., and Snowden, M. (2017). *Environment, Human System and Socia Science:* Book Environment and Society, *Human perspectives on environmental issues*. Routledge. Pages43, eBook ISBN9781315463254

Hawthorne, D.W. (1994). Fire Damage and Forest Regeneration in Ghana. ODA forestry series number 4. Natural Resource Institute, Chatam Maritime, Kent, UK

Kalame, F. B, Nkem, J., Idinoba, M. Kanninen, M (2009). Matching national forest policies and management practices for climate change adaptat.ion in Burkina Faso and Ghana. Mitig Adapt Strateg Glob Change 14:135–151

Oduro-Ofori, E., Ocloo, K. A., Peprah, C., & Effah, G. (2015). Assessing natural resource use conflicts in the Kogyae Strict Nature Reserve, Ghana. *Environment and Natural Resources Research*, *5*(3), 56.

Proceedings for the 7th International Fire Behavior and Fuels Conference April 15-19, 2024, Boise, Idaho, USA – Tralee, Ireland – Canberra, Australia Published by the International Association of Wildland Fire, Missoula, Montana, USA

Cross-border wildfires in the Pacific Northwest- the example of British Columbia, Canada

Clara Aubonnet
IFG Lab', Institut Français de Géopolitique, Université Paris 8, Saint-Denis, France
clara.aubonnet@etud.univ-paris8.fr

Introduction

Every year in the Pacific Northwest, hitherto exceptional climatic events occur, and records are broken for the area burned by wildfires. These wildfires, which cover thousands of hectares, spread beyond the jurisdictional boundaries of the affected territories. They also cross international, regional, administrative, ecological, cultural, and traditional boundaries. Today, the "coexistence with fire" (Copes-Gerbitz *et al*., 2022) era calls into question sovereign fire governance policies, land-use planning, and the power rivalries that hamper the necessary cooperation between the many stakeholders involved. In the western province of British Columbia, Canada, we observe multidimensional issues at stake and the plurality of actors and their points of view. This invites a geopolitical analysis of three complementary research dimensions: environmental, political, and socio-cultural.

Method and reflexivity

The method used in this research work corresponds to the field of geopolitics as a study of "the geographical analysis of concrete socio-political situations that are localized, and the everyday perceptions that describe them" (Rosière, 2007). In British Columbia, when we talk about cross-border wildfires, this method can be applied to the study of rivalries provoked by the disruption of space, which then becomes a political object of confrontation. So, there are power relationships between the people involved. By power, we mean "not only that of a State but also that of other forms of political organization or group of people that exercise or seek to exercise power over a territory that other powers may contest" (Lacoste, 2014). Geopolitical analysis thus provides an epistemological basis for this study.

In addition to this predominantly qualitative approach (with research fieldwork, semi-structured interviews, and observation), I mobilize tools from other social science fields such as sociology, anthropology, and geography. I also refer to methodologies specific to research with Indigenous Peoples (Christianson, 2014) as a foreigner to step back from my own interpretative biases.

This work concerns human beings and is part of a desire to understand and improve the complex situations we are currently experiencing. Respect and acknowledgment of people, their way of life and the context in which they develop is therefore essential. Research was (and still is) a powerful tool of domination, and geography was a

discipline whose tools, notably through the production of maps, were used as a means of oppressing Indigenous Peoples. The borders we know today are colonial and do not correspond to the traditional territories of Indigenous Nations. So, I am constantly questioning the simple division of space in this subject, how settlers appropriated it, and the claims to sovereign rights over these same lands by Indigenous Peoples today.

Thus, I do not wish this research work to be extractive and lead to harmful consequences for Indigenous communities, by reproducing neo-colonial mechanisms of domination without considering the needs and interests of the people concerned. In other words, I want everyone to be able to benefit from this study and make it their own.

Maps have power

What led me to do this study is also the question of borders, territory, and therefore wildfire cartography and its social stakes.

In which context is a wildfire shown on a map? What elements do we choose to present? What data takes priority? And what kind of borders are we talking about?

So, the question is, how are these boundaries represented in wildfire response strategies so that people know they exist? Sometimes they exist only through oral transmission, and sometimes they're put down on paper. Depending on the map used, and the boundaries they represent, wildfire response strategies will not be the same, because the areas to be protected will not be the same either.

In the example of British Columbia, these cross-border wildfires are redistributing the roles of the many governmental and non-governmental organizations involved in forest fire management on both sides of the Canada-U.S. international border. To prevent harm, they must learn to communicate, cooperate, and delegate at international, national, and local levels. This risk management challenge adds complexity to the balance of power between people. Indeed, the elements that need to be protected in the event of a fire are not the same for a forestry company, a federal agency, or an Indigenous volunteer fire department. The question is: Whose maps have the most power in the decision-making process?

In British Columbia, these are the maps of BC Wildfire Service, the provincial agency over which lobbying by the forestry industry still has a major influence. And this is despite the agency's stated wish to take power away from the industry and give more to the locals, and Indigenous communities.

Research dimensions

In this study of cross-border wildfires, particularly in British Columbia, I have identified three complementary dimensions: environmental, political, and socio-cultural.

Firstly, the environmental dynamics need to consider the characteristics of the forest ecosystem being studied and the type of fires affecting it. In this way, we can better understand the interdependencies between environmental dynamics and human actions and examine the impact of political actions on the wider picture.

There are also political issues at stake, with long-standing and structural conflicts. For example, the intensification of wildfires accentuates intra- and inter-organizational tensions in the response to cross-border fires and modifies the balance of power. I, therefore, question the fragmentation of this management, with conflicting decisions made by different actors, which could complicate the response to wildfire by excluding local knowledge, or even render it ineffective in emergencies.

Lastly, the socio-cultural dimension concerns the different relationships of stakeholders to nature and their know-how in terms of fire practices and forest governance. In terms of response to fire, Gifford Pinchot considered "the father of forestry" (Struzik, 2022) and the first head of the USFS (US Forest Service) from 1905 to 1910, imposed fire as a new enemy throughout the North American continent, with firefighters using military tactics when responding. He was a good friend of Elihu Stewart, the first person at the Canadian Forest Service (formerly named Dominion Forest Service). The population was (and still is) educated to fear fire which was considered dangerous both for them and for the forest. Smokey the Bear, the mascot of colonial propaganda, is a perfect example (Minor and Boyce, 2018)

Thus, the plurality of people involved and their points of view concerning the problem of cross-border forest fires are on several scales, with multidimensional issues such as fire risk response and forest governance.

References

Copes-Gerbitz K, Hagerman SM, Daniels LD (2022) Transforming Fire Governance in British Columbia, Canada: An Emerging Vision for Coexisting with Fire. *Regional Environmental Change* **22**(2):48. DOI: 10.1007/s10113 022-01895-2.

Christianson A (2014) ‘Social Science Research on Indigenous Wildfire Management in the 21st Century and Future Research Needs. *International Journal of Wildland Fire* **24**(2) 190-200. DOI: 10.1071/WF13048.

Lacoste Y (2014) ‘La géographie, ça sert, d'abord, à faire la guerre.’ (La Découverte) DOI : 10.3917/dec.lacos.2014.01.
Minor J, Boyce GA (2018) Smokey Bear and the Pyropolitics of United States Forest Governance. *Political Geography* **62**, 79-93. DOI : 10.1016/j.polgeo.2017.10.005.

Rosiere S (2007) ‘Géographie politique et Géopolitique.’ (Ellipses).

Struzik E (2022) ‘Dark days at noon, the future of fire.’ (McGill-Queen’s University Press).

Proceedings for the 7th International Fire Behavior and Fuels Conference April 15-19, 2024, Boise, Idaho, USA – Tralee, Ireland – Canberra, Australia Published by the International Association of Wildland Fire, Missoula, Montana, USA

Data and Tools for Quantifying Post-Fire Erosion in a Semi-Arid Watershed

*Tao Huang
Boise State University, 1910 W University Dr, Boise, ID 83725, USA,
taohuang@u.boisestate.edu

**Corresponding Author*

Introduction

The composition of plant communities control rates of soil erosion by water in dryland regions (Li et al. 2022). Fire could shift ecohydrological function from vegetation-controlled soil retention to runoff driven soil loss (Williams et al. 2020). Fire can also alter soil-hydraulic properties, often resulting in an increased prevalence of infiltration-excess overland flow and the potential connectivity of runoff (Wilson et al. 2021). Soils in burned areas could become water repellent after a fire, leading to increased erosion when it rains.

Soil erodibility is influenced by soil properties and vegetation condition (Han et al. 2023). Bare areas are more susceptible to water erosion than vegetated areas. Spatial arrangement of bare and vegetated patches played very different roles in terms of water and sediment generation, movement and storage on a hillslope in rangelands (Bartley et al. 2006).

Although empirical models such as the Universal Soil Loss Equation are easy to implement, they usually do not represent time varying soil moisture and infiltration (Kampf et al. 2020). Moreover, empirical methods have limited extrapolation capacity to simulate hydrological processes outside of the domain of input data used, which can be critical for analysis of previously unobserved scenarios (Neumann et al. 2021). A physically-based model that simulates runoff and sediment yield could more accurately represent the hydrologic responses to disturbance.

High spatial resolution unoccupied aircraft systems (UAS) can be highly effective in vegetation cover mapping. UAS technologies offer practical methods to create landcover maps for monitoring of areas affected by natural disasters (Furukawa et al. 2021).

Dryland post-fire hydrology and erosion modeling is less studied than forest ecosystems (Lopes et al. 2021). Our goals were to (1) quantify pre-fire and post-fire vegetation cover and (2) model post-fire hillslope event-based soil erosion.

Materials and methods

The study was conducted within Johnston Draw, a small catchment (1.83 km^2). The Bureau of Land Management (BLM) implemented the Johnston Draw Prescribed Burn in October 2023.

The processing workflow is shown in Figure 1. The effect of input data resolution on hydrological model performance was not considered in many studies (Ait M'Barek et al. 2023). We used two images with different resolutions (UAS, 4 cm and WorldView, 50

cm) to quantify hillslope vegetation cover. Each UAS image dataset was processed using Agisoft Metashape.

To compare the fire effects on the overland flow and sediment yield, we simulated pre- and post-fire runoff and erosion using the Rangeland Hydrology and Erosion Model (RHEM). The RHEM consists of overland flow and soil erosion equations. The RHEM model relies on four key inputs: topography, soil properties, vegetation cover, and weather data (Williams et al. 2022).

Water infiltrates soil mainly due to a negative pressure gradient or suction (matrix suction) into the soil matrix. Infiltration is significantly influenced by the saturated hydraulic conductivity of the soil profile. Saturated hydraulic conductivity is used in the model to determine the rate of vertical water percolation through soil layers. To quantify the impact of burn scars on runoff, information on changes in hydraulic conductivity is essential. We collected field data on soil hydraulic properties through in-situ measurements to determine the field-saturated hydraulic conductivity.

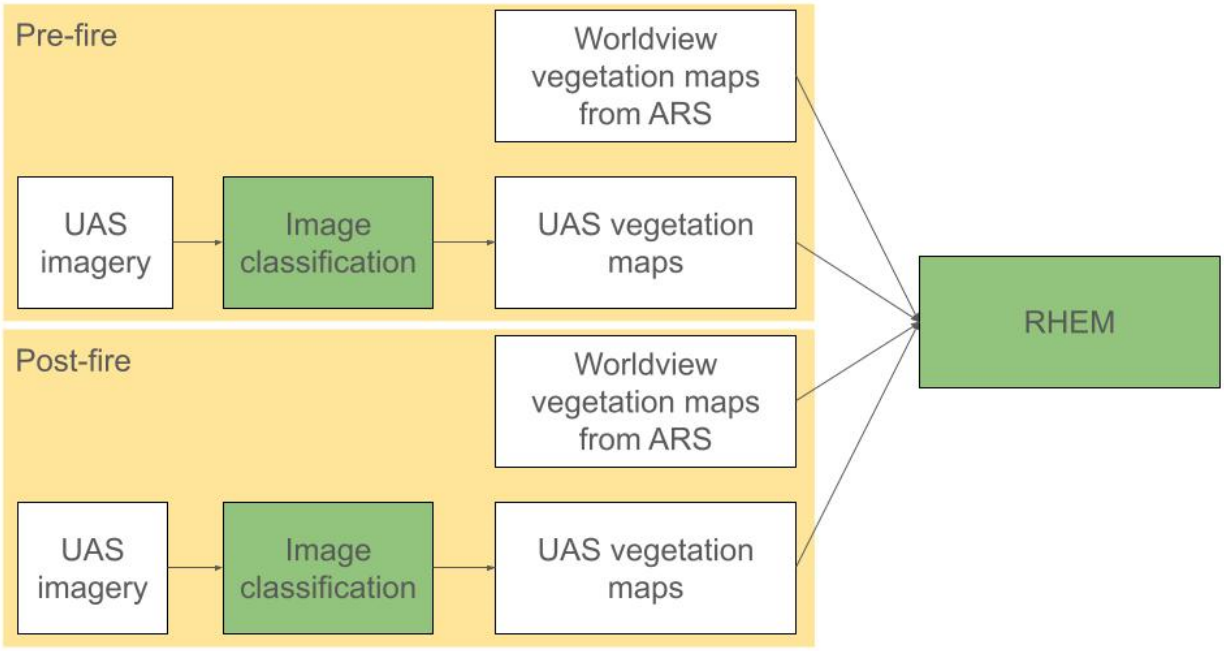

Figure 1. Workflow of this study.

Results

Pre-fire and post-fire orthomosaics were shown in Figure 2 and Figure 3. Vegetation cover at the south facing slope reduced after the fire. UAS imagery (Figure 4) provides higher spatial resolution compared to Worldview imagery (Figure 5).

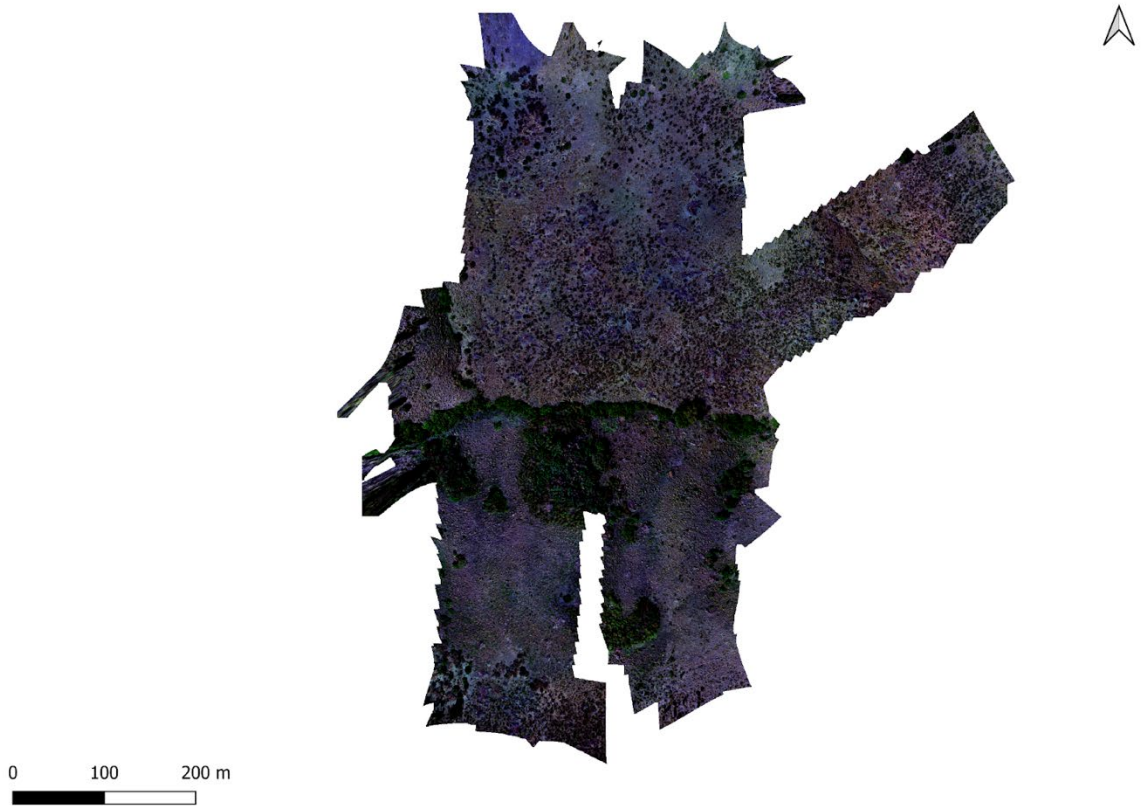

Figure 2. Pre-fire orthomosaic (Aug 2023).

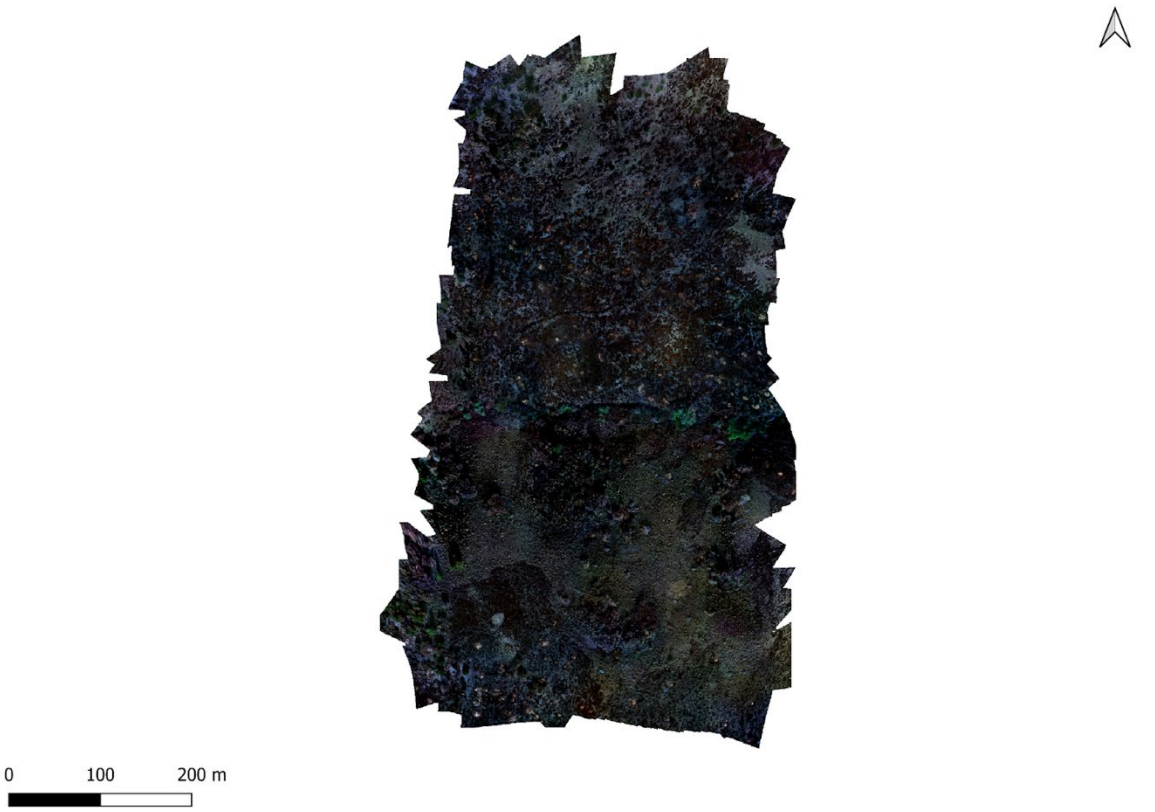

Figure 3. Post-fire orthomosaic (Oct 2023).

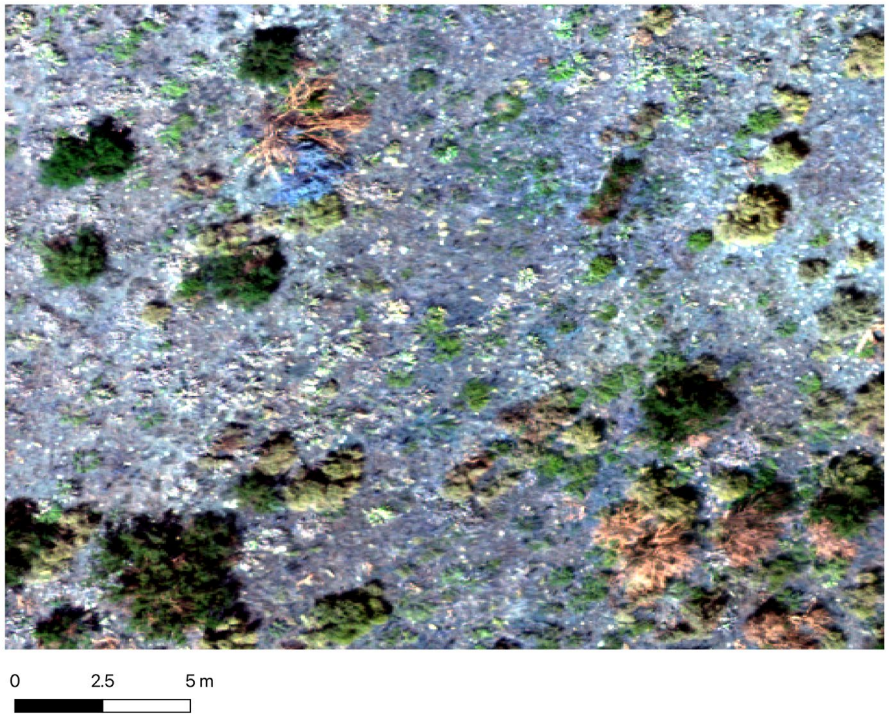

Figure 4. Zoom-in view of the UAS imagery.

Figure 5: Zoom-in view of the WorldView imagery.

Acknowledgements
We would like to thank the USDA Agricultural Research Service under Cooperative Agreement 59-2052-8-002 and 59-2052-1-002 for funding this research. This research was a contribution from the Long-Term Agroecosystem Research (LTAR) network. LTAR is supported by the United States Department of Agriculture. Any use of trade, firm, or product names is for descriptive purposes only and does not imply endorsement by the U.S. Government.

References
Ait M'Barek S, Bouslihim Y, Rochdi A, Miftah A (2023) Effect of LULC data resolution on hydrological and erosion modeling using SWAT model. *Modeling Earth Systems and Environment* ***9***(1), 831-846.
Bartley, R., Roth, C.H., Ludwig, J., McJannet, D., Liedloff, A., Corfield, J., Hawdon, A. and Abbott, B., 2006. Runoff and erosion from Australia's tropical semi-arid rangelands: Influence of ground cover for differing space and time scales. *Hydrological Processes: An International Journal* ***20***(15), pp.3317-3333.
Kampf SK, Gannon BM, Wilson C, Saavedra F, Miller ME, Heldmyer A, Livneh B, Nelson P, MacDonald L (2020) PEMIP: Post-fire erosion model inter-comparison project. *Journal of Environmental Management* **268**, 110704.

Lopes AR, Girona-García A, Corticeiro S, Martins R, Keizer JJ, Vieira DC (2021) What is wrong with post-fire soil erosion modelling? A meta-analysis on current approaches, research gaps, and future directions. *Earth Surface Processes and Landforms* **46**(1):205-19.

Neumann, A., Dong, F., Shimoda, Y., Arnillas, C. A., Javed, A., Yang, C., ... & Arhonditsis, G. B. (2021). A review of the current state of process-based and data-driven modelling: guidelines for Lake Erie managers and watershed modellers. *Environmental Reviews*, ***29*****(4)**, 443-490.

Williams CJ, Pierson FB, Al-Hamdan OZ, Nouwakpo SK, Johnson JC, Polyakov VO, Kormos PR, Shaff SE, Spaeth KE (2022) Assessing runoff and erosion on woodland-encroached sagebrush steppe using the Rangeland Hydrology and Erosion Model. *Ecosphere* **13**, 4145.

Proceedings for the 7th International Fire Behavior and Fuels Conference April 15-19, 2024, Boise, Idaho, USA – Tralee, Ireland – Canberra, Australia Published by the International Association of Wildland Fire, Missoula, Montana, USA

Developing Fine-Scale Fuel Model Classifications and Wildfire Risk Maps in California

*Carol L. Rice
Wildland Res Mgt, Reno, NV, USA
carollricewildlandresilience@gmail.com

Petronila E. Mandeno
Digital Mapping Solutions, Cotati, CA, USA
mandeno@digitalmappingsolutions.com

Mark Tukman
Tukman Geospatial LLC, Forestville, CA, USA
mark@tukmangeospatial.net

Kass Green
Kass Green and Associates, Berkeley, CA, USA
kassgreen@earthlink.net

**Corresponding Author*

Introduction

We describe the methods and benefits of using fine-scale fuel maps in the wildland-urban interface (WUI) where values at risk from wildfire are high.

Scott and Burgan 2005 surface fuel models, a Wildfire Risk to Structures map and a Wildfire Hazard 20m raster were developed in collaborative partnership. Tukman Geospatial served as the technical lead and was responsible for implementing the model design, python coding, and geospatial data analysis. Tukman Geospatial partners Digital Mapping Solutions (Esther Mandeno) and Wildland Res Mgt (Carol Rice) provided guidance on the risk model design, its data inputs, and the weights used for the inputs. Drafts of the risk map were reviewed by all team members, who balanced internal input with community input from more than 100 different stakeholders.

Scott and Burgan 2005 surface fuel models were assigned to 5m pixels covering eight counties in the greater San Francisco Bay Area, California. Classification of fuels was based on Enhanced Vegetation Lifeform primarily derived from LiDAR and eCognition and informed by field calibration. Where fires burned recently, burn severity was determined and used to inform crosswalk decisions from lifeform to fuel types. Fuels formed the foundation of a risk map that displays the hazard and risk posed to structures.

While existing coarser fuel data sets are appropriate for planning for large areas, the WUI requires finer-scale resolution. The coarser fuel data sets depict much of the built environment as non-burnable. The 5m resolution fuel model improves the mapping of vegetative fuels in the built environment, extending mapping of fuels into creeks and yards.

In the future, as structures are contemplated as part of the fuelbed, fine-scale resolution of vegetative fuels will be needed. Luckily, the widespread interpretation of LiDAR data has made fine-scale fuels mapping more common.

This effort included several innovations. The most heavily-relied-upon innovation is the development of a ladder fuel index, which describes the proportion of vegetation in the lowest 4 meters, compared to the volume of canopy fuels. Ladder fuels was one factor considered when determining fuel model classification and can also be used to suggest the most effective type of treatment, especially in hardwoods where torching potential can be reduced by removing ladder fuels while simultaneously keeping a desirable closed canopy.

Other innovations included the use of Google Earth Engine to create Differenced Normalized Burn Ratio (dNBR) for areas burned recently, created from pre- and post-fire Sentinel imagery. Another innovation was the integration of impervious surfaces, accurately mapping a true no-fuel condition for all paved locations based on semi-automated Object-based Image Analysis. Building footprints were included in this layer, though we recognize buildings contribute to fire spread.

The risk model combined several variables at different weights, including fire behavior, terrain, extreme weather potential, ignition history, powerline proximity, and a “halo” buffer around the WUI, while providing a nuanced depiction of hazards and risks in the WUI.

Project overview

In the San Francisco Bay Area in Northern California, wildfire hazard and wildfire risk fine-scale datasets were designed for land managers and fire responders who are interested in relative rankings of wildfire hazard and risk to structures. These datasets were assembled for eight counties including Napa, Sonoma, Marin, San Mateo, Santa Cruz, Santa Clara, Alameda, and Contra Costa, as depicted in the map below.

The risk and hazard map products are modeled outputs based on the best available data which varies in date of collection, scale, and detail. They provide an interpretation of risk and hazard that is based on a set of weighted input variables and decision rules. Though we are using the best available input data, there are many approaches to modeling wildfire risk and hazard, all of which are both complex and imperfect.
The nature of the fine-scale datasets allowed interpretation of potential fire impacts within and surrounding communities based on vegetation data.

Figure 1: The Nine counties in the mapping project.

Definitions

Hazard combines fuel characteristics combined with physical landscape characteristics such as weather, topography, and the distribution of ignitions across the landscape.

Risk is the potential for realization of adverse consequences to valued resources or assets. Wildfire risk considers not only the potential for hazardous wildfire, but also the values exposed to hazard. For the purposes of this project, the “risk” aspect of the model applies to one value: structures.

Methods

Surface Fuel Model

Surface fuel models are a means to convey numeric values more easily for various fuel parameters that drive Rothermel's (1972) fire spread equation, which is the foundation of fire behavior modeling in the United States. Thus, instead of users having to know the specific fuel loadings for each size class of dead and down fuels in a dense, closed canopy oak stand, they can instead simply designate the fuel configuration as a "TL6" fuel model (Moderate Load Broadleaf Litter).

The 5m wildland fuel model is foundational to the hazard and risk mapping. Below is a conceptual diagram of how the 5m Scott and Burgan fuel model crosswalk works. The Scott and Burgan 40 fuel models are nationally accepted for use with fire spread models.[1] The 5m fuel model is created from the enhanced lifeform (vegetation) map, LiDAR-derived forest structure, recent burn severity, and in some places, a layer that depicts grazed versus ungrazed lands.

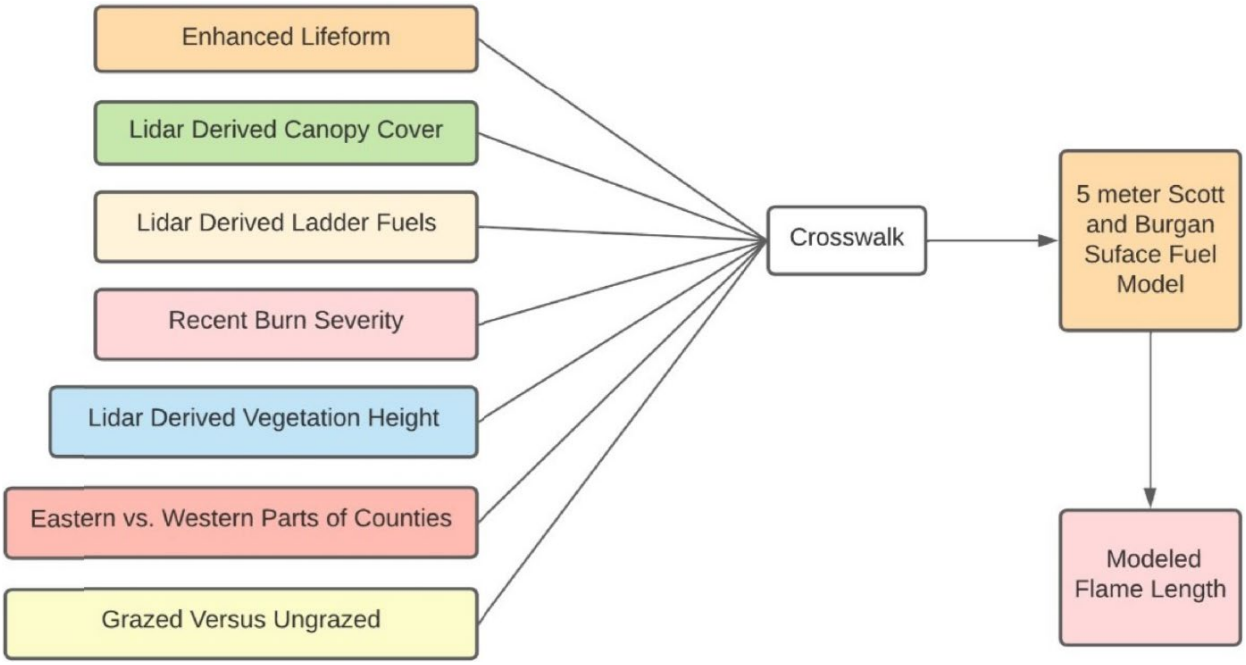

Figure 2: Decision crosswalk to determine 5m Scott and Burgan surface fuel models.

Surface fuel models were assigned based on enhanced lifeform classes, which were mapped at a 5m resolution following the collection of LiDAR data and high-resolution imagery in all counties. Classes included vegetation types such as Evergreen Hardwoods, Herbaceous, Redwood/Douglas Fir, Shrub, Deciduous Hardwood, Pine and/or Cypress, Riparian Shrub, Riparian Forest, Agriculture, Developed, and others

[1] See https://gacc.nifc.gov/docs/40-Standard%20Fire%20Behavior%20Fuel%20Models.pdf.

Some enhanced lifeforms were easily classified into surface fuel models. Enhanced lifeforms that do not normally ignite were classified as either NB8 (Open Water) or NB9 (Bare Ground), dependent on the specific nature of the enhanced lifeform class.

Agricultural vegetation classes were classified as NB3, since Agriculture is designated a non-burnable fuel model.

All other lifeform classes were assigned based on the following principles:

1) Canopy height superseded enhanced lifeform designations;
2) A higher ladder fuel index led to a fuel model assignment with higher volumes of live woody fuels;
3) In some cases, lower absolute cover led to a fuel model assignment with a lower fuel load; and
4) Deciduous hardwoods were evaluated for application of a grass fuel model.

We designated fuel models for each enhanced lifeform class based on lifeform (i.e., Herbaceous was assigned a GR [grass] model), then differentiated the fuel types into specific surface fuel models (i.e., GR1, SH5, TL6, etc.) based upon vegetation characteristics such as absolute cover, canopy height, or ladder fuel index, all of which were measured during the 2020 LiDAR data collection for Santa Cruz and Santa Clara Counties.

A given enhanced lifeform class does not necessarily address the surface fuels that would burn underneath them. Thus, we assigned a fuel model that reflected the surface fuels that would carry the fire. These are determined from field observations and our expert knowledge about fire behavior within the enhanced lifeforms we were assigning.

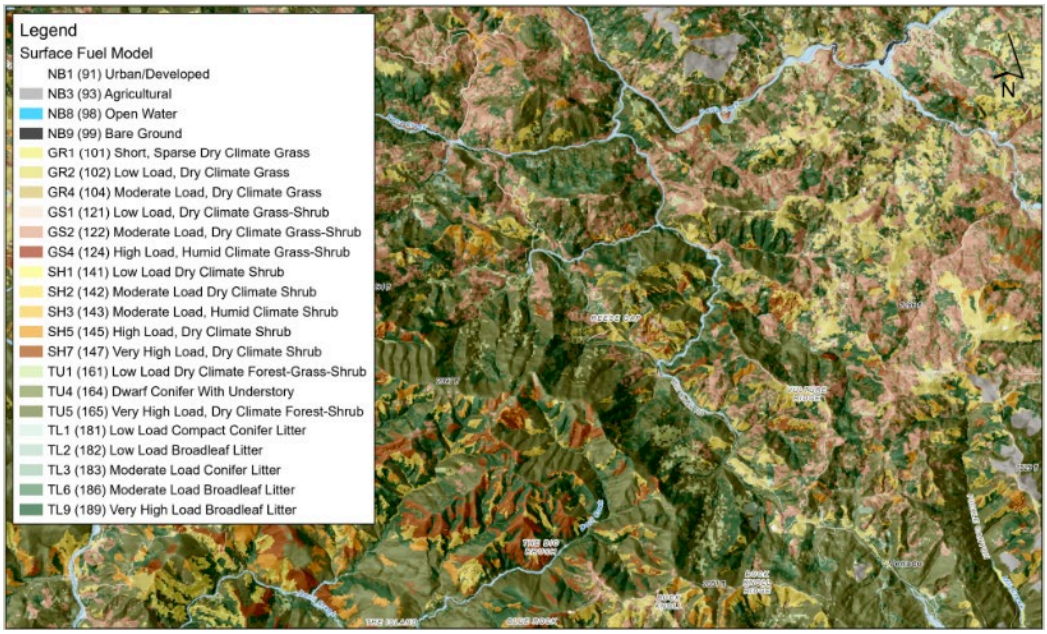

Figure 3: The 5m Scott and Burgan surface fuel model map of Sonoma County, CA.

Logic model and wildfire risk to structures

Wildfire hazard and wildfire risk to structures: Logic model

The logic model for the Wildfire Hazard and Wildfire Risk to Structures map consists of inputs such as flame length, extreme fire weather potential, ember load, and suppression difficulty, among other layers. The 5m surface fuel model was used in a fire behavior model (FlamMap) to predict flame length, which is the most highly weighted input in determining wildfire hazard.

Below, a graphic shows the logic model inputs from their weights.

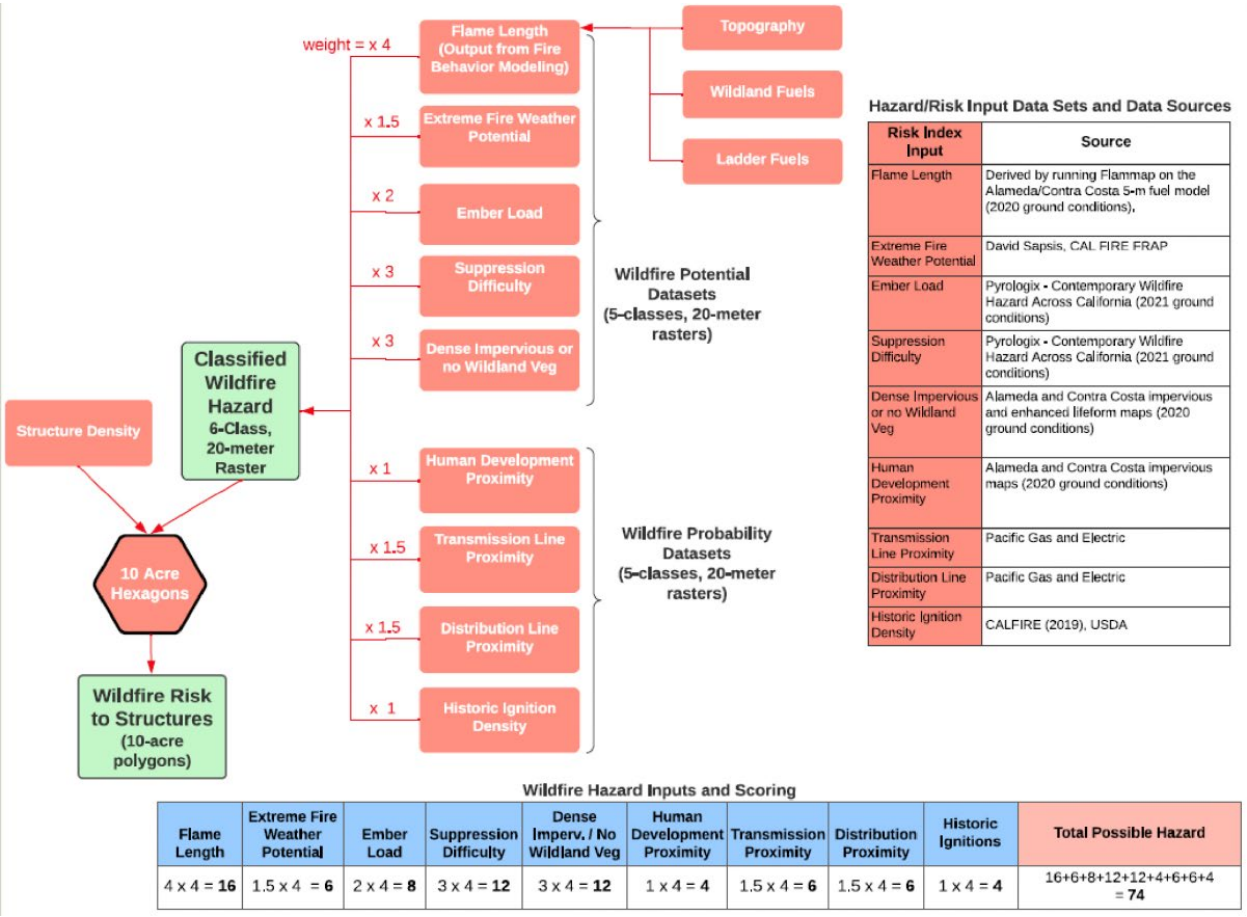

Hazard/Risk Input Data Sets and Data Sources

Risk Index Input	Source
Flame Length	Derived by running Flammap on the Alameda/Contra Costa 5-m fuel model (2020 ground conditions).
Extreme Fire Weather Potential	David Sapsis, CAL FIRE FRAP
Ember Load	Pyrologix - Contemporary Wildfire Hazard Across California (2021 ground conditions)
Suppression Difficulty	Pyrologix - Contemporary Wildfire Hazard Across California (2021 ground conditions)
Dense Impervious or no Wildland Veg	Alameda and Contra Costa impervious and enhanced lifeform maps (2020 ground conditions)
Human Development Proximity	Alameda and Contra Costa impervious maps (2020 ground conditions)
Transmission Line Proximity	Pacific Gas and Electric
Distribution Line Proximity	Pacific Gas and Electric
Historic Ignition Density	CALFIRE (2019), USDA

Wildfire Hazard Inputs and Scoring

Flame Length	Extreme Fire Weather Potential	Ember Load	Suppression Difficulty	Dense Imperv. / No Wildland Veg	Human Development Proximity	Transmission Proximity	Distribution Proximity	Historic Ignitions	Total Possible Hazard
4 x 4 = **16**	1.5 x 4 = **6**	2 x 4 = **8**	3 x 4 = **12**	3 x 4 = **12**	1 x 4 = 4	1.5 x 4 = **6**	1.5 x 4 = **6**	1 x 4 = **4**	16+6+8+12+12+4+6+6+4 = **74**

Figure 4: Logic model for the Wildfire Hazard and Wildfire Risk to Structures.

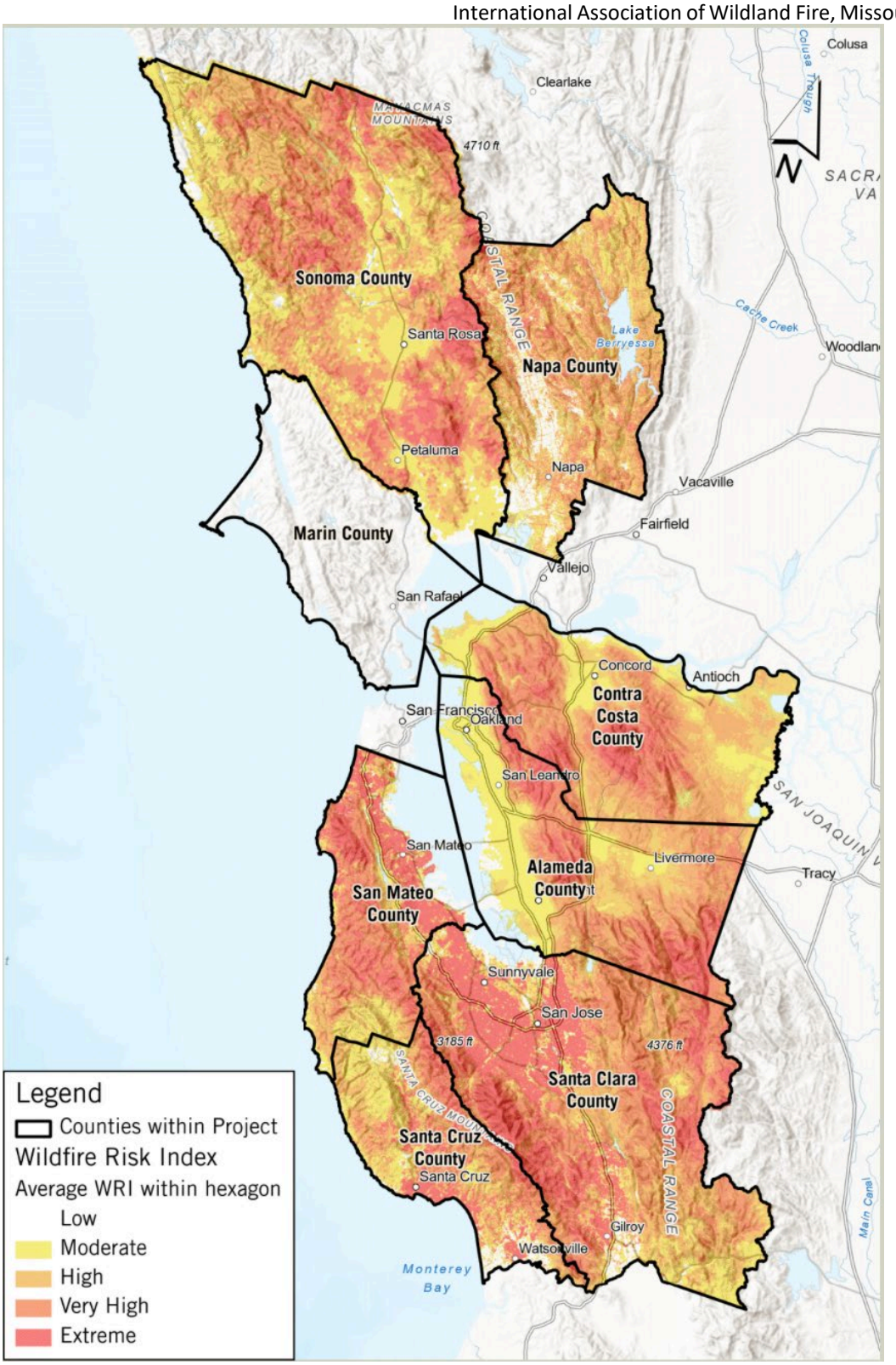

Figure 5: Map of Wildfire Risk to Structures.

Each of the nine input spatial data sets related to hazard is scaled from 0-5 (very short flame length receives a 0 whereas very long flame length receives a 5). To synthesize

these nine hazard spatial data sets, the variable's class (0-5) for a given pixel is multiplied by that variable's weight to produce a raw score for each variable. After computing raw hazard, pixels are "binned" into six hazard classes with 1 representing areas of lowest relative hazard, 6 representing the highest. The Wildfire Hazard dataset, a 20m-resolution raster dataset with pixel values ranging from 1 (lowest relative wildfire hazard) to 6 (highest relative wildfire hazard), is shown in Figure 3.

This hazard layer, coupled with the presence of structures on the landscape determined the Wildfire Risk to Structures layer.

All data and methodology documentation are available at pacficivegmap.org.

Proceedings for the 7th International Fire Behavior and Fuels Conference April 15-19, 2024, Boise, Idaho, USA – Tralee, Ireland – Canberra, Australia Published by the International Association of Wildland Fire, Missoula, Montana, USA

Estimating Ladder Fuel Contributions to Crown Fire Initiation

Daniel D. B. Perrakis*,
Natural Resources Canada-Canadian Forest Service, 506 West Burnside Road, Victoria, British Columbia, Canada, V8Z 1M5, Daniel.Perrakis@nrcan-rncan.gc.ca

Dan K. Thompson,
Natural Resources Canada-Canadian Forest Service, Sault Ste. Marie, Ontario, Canada, Dan.Thompson@nrcan-rncan.gc.ca

**Corresponding Author*

Introduction

Crown fires in boreal and sub-boreal conifer forests represent a significant safety hazard for fire managers and nearby communities. Crown fires typically involve high rates of spread and energy release, and have been associated with catastrophic community losses.

For predicting the onset of crowning, Van Wagner (1977) described a model (VW77) that remains in wide use today, based on empirical data and physical convection theory. His model was based on the surface fire intensity needed for flames to bridge the gap between surface fuels and the base of a continuous canopy layer, the live canopy base height (LCBH). Small-diameter fuel elements that occupy an intermediate position between the surface and canopy fuels are termed ladder fuels (LF); they are believed to be disproportionately important in facilitating crown fire initiation, but the effect has been difficult to quantify.

Here we show how the VW77 model can be rearranged to present a solution for estimating the effects of ladder fuels in crown fire occurrence, a simple but nuanced solution to a longstanding problem.

Rearranging the VW77 model

The VW77 model was originally formulated to solve for critical surface intensity (I_0) in a single-storied conifer stand, as follows:

$$I_0 = (chz)^{1.5}$$

[1], where h is heat of ignition, z is live crown base height (LCBH), and c is an empirical constant. This model has been implemented in full or in part in several popular modelling systems, notably in Canada (Forestry Canada Fire Danger Group (FCFDG) 1992) and the USA (Scott and Reinhardt 2001).

The structure of the VW77 model permits a vertical rescaling that relies on an implied proportionality between surface fuel consumption (SFC) and *z* (LCBH). When we replace

I_0 (eq. 1) with Byram's (1959) fireline intensity, as noted above, we get the following well-known equation:

$$H \cdot SFC \cdot ROS = (ch)^{1.5} z^{1.5}$$

[2], where H is the heat of combustion, SFC is surface fuel consumption, and ROS is rate of forward spread.

This relationship has often been evaluated in terms of identifying critical ROS for crown fire initiation (e.g. FCFDG 1992). However, we will presently solve eq. 2 for a critical SFC (*SFC₀*), assuming surface fire conditions near the crown fire initiation threshold:

$$SFC_0 = \frac{(ch)^{1.5} z^{1.5}}{h \cdot ROS}$$

[3]. This relationship places the emphasis on the mass of available surface fuel as the fire intensity engine that drives crowning.

Algebraically, it is apparent that *SFC₀* can also be compared between LCBH levels. If we consider z_1 and z_2 to be different vertical distances between surface and canopy fuels, then the following ratio is evident:

$$\frac{SFC_2}{SFC_1} = \frac{\left[\frac{(ch)^{1.5} z_2^{1.5}}{h \cdot ROS}\right]}{\left[\frac{(ch)^{1.5} z_1^{1.5}}{h \cdot ROS}\right]}$$

[4], where SFC_1 and SFC_2 represent critical SFC values at the two *z* levels. This also assumes no change in surface ROS or *h* when varying LCBH, a reasonable assumption in closed conifer stands. Finally, holding terms constant, we can simplify this to yield a basic general relationship between SFC and LCBH (*z*):

$$SFC_2 = \left(\frac{z_2}{z_1}\right)^{1.5} \cdot SFC_1$$

[5].

This equation can be used as a transformation function for comparing the influence of fuel elements at different heights.

A practical example helps illustrate the logic of comparing SFC_0 at two different z values (eq. 5). Using Van Wagner's empirical heat of ignition function (Van Wagner 1977), at 90% foliar moisture content (FMC) and LCBH=2 m, eq. 1 suggests I_0 of about 417 kW/m, the intensity of a low to moderate intensity surface fire. At some moderate surface ROS value, e.g. 2 m min^{-1}, eq. 3 predicts SFC_0 of 0.695 kg m^{-2}. If LCBH were increased from 2 to 5 m, SFC_0 would then increase (eq. 5) to 2.75 kg m^{-2}. Thus, a 2.5 times increase in LCBH results in a nearly fourfold increase ($(5/2)^{1.5} = 3.95$) in the critical SFC for crowning. For fuel elements affecting crown fire initiation, it is important to recognize that the key property is the vertical distance between a burning fuel element and the LCBH, not necessarily the height above ground. To avoid confusion, we restate eq. 5 in terms of ladder fuel structure measures. We define consumption of a LF layer as FC_L and the

centroid height of a ladder fuel layer or element as C_L (e.g., the midpoint of small diameter branchwood in a dead sapling layer beneath a conifer canopy; Figure 1). The surface-equivalent ladder fuel consumption value (FC_{SE}) can then be calculated and added to actual SFC. In this case, z remains the LCBH and ($z - C_L$) represents the fuel strata gap (Cruz et al. 2004; Perrakis et al. 2023) between ladder fuel elements and the LCBH:

$$FC_{SE} = \left(\frac{z}{z - C_L}\right)^{1.5} \cdot FC_L \ , \qquad z > C_L$$

[6]. This equation finally permits the estimation of the LF influence in the right scale for comparison with expected SFC to predict crown fire.

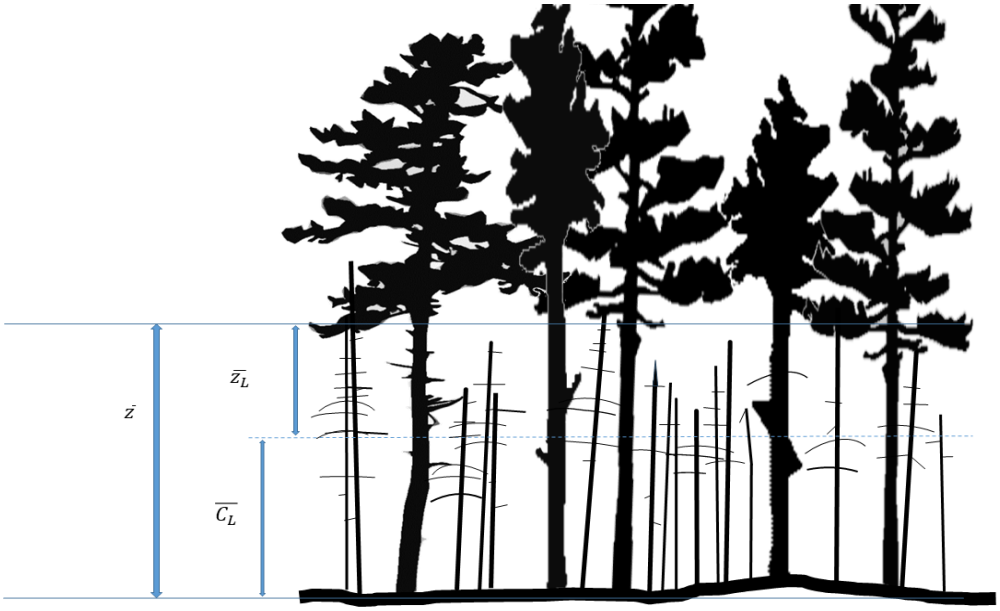

Figure 1. Simple conifer forests Diagram (not to scale) showing approximate estimation of live crown base height (z), dead ladder fuel centroid (C_L), and fuel strata gap (z_L) in a simple single-story stand, such as a developing jack pine stand.

Challenges and limitations

While logically consistent, at least three limitations are immediately apparent with eq. 6. First, the theoretical relationship between fuel elements does not account for the obvious structural differences between the surface and crown fuel complexes. Surface fuelbeds are much more compact (higher bulk density and packing ratio) than crown fuel complexes, with a much more aeration-limited combustion environment (Rothermel 1972; Schwilk 2015). The FBP System approach to SFC, where all consumed surface and ground fuels are assumed to contribute to I_0 (Van Wagner 1977; FCFDG 1992), likely overemphasizes coarse fuels (duff and coarse woody debris) that burn in post-frontal combustion, ignoring the notion of flame front residence time (Nelson and Adkins 1988;

Wotton et al. 2012). In contrast, fine textured canopy and LF strata are likely to be consumed completely in the flame front. Thus, scaling FC_L to generate FC_{SE} may be

insufficient to reconcile the scales of these consumption classes. This difference is not addressed here and will have to be reconciled via theoretical or empirical means.

Second, while eq. 6 specifies that the LF height cannot exceed the LCBH, it is apparent that as the difference between them ($z - C_L$) diminishes, FC_{SE} can grow to extreme levels, eventually producing a division by zero problem at $z = C_L$. Consider, for example, FC_L = 0.1 kg m^{-2} , 1 m below a 5 m tall canopy base (z = 5; $z - C_L$ = 1); eq. 6 scales this to FC_{SE} of 1.12 kg m^{-2}. But if C_L is raised closer to z (e.g., $z - C_L$ = 0.2 m), the same FC_L generates FC_{SE} = 12.5 kg m^{-2}. This is logically consistent – burning fuels are much more likely to ignite canopy fuels if they are located immediately beneath the canopy base, and a 0.2 m gap is almost negligible at the tree or stand scale. However, this suggests that caution is needed with eq. 6 to avoid inflating the LF effect to nonsensical levels.

Finally, there is the challenge of characterizing LF in three-dimensional space in terms of one or more discrete layers comparable to surface fuel loading. Although the example here (fig. 1) considered a dead sapling cohort as a single LF layer continuous with the ground, that assumption fails for discontinuous LF elements such as bark flakes or arboreal lichens. Estimating total LF effects precisely may demand techniques such laser scanning methods (e.g., Qi et al. 2022) and summing the contributions of individual vertical tranches of combustible fuel (e.g. Alexander et al. 2004).

Conclusion

In sum, a simple theoretical model for calculating LF influence in crown fire initiation was identified and described based on the well-known VW77 model. Where LF consumption and position can be reasonably estimated, the new equation provides a solution for scaled consumption values that can be added to actual SFC. This will be useful for quantifying the effects of proposed hazard reduction treatments as well as for overall fire behaviour prediction in conifer stands.

References

Alexander ME, CN Stefner, JA Mason, BJ Stocks, GR Hartley, ME Maffey, BM Wotton, SW Taylor, N Lavoie, GN Dalrymple (2004) ‘Characterizing the jack pine-black spruce fuel complex of the International Crown Fire Modelling Experiment (ICFME).’ Natural Resources Canada - Canadian Forest Service, Northern Forestry Centre (Edmonton, AB, Canada).

Byram GM (1959) Combustion of Forest Fuels. In “Forest Fire, Control and Use”. (Ed. KP Davis), Pp. 61–89 (McGraw-Hill: New York).

Cruz MG, ME Alexander, RH Wakimoto (2004) Modeling the Likelihood of Crown Fire Occurrence in Conifer Forest Stands. *Forest Science* 50 (5): 640–58.

Forestry Canada Fire Danger Group [FCFDG] (1992) ‘Development and Structure of the Canadian Forest Fire Behavior Prediction System.’ Information Report ST-X-3, Forestry Canada, Science and Sustainable Development Directorate (Ottawa, ON, Canada).

Nelson RM Jr, CW Adkins (1988) A Dimensionless Correlation for the Spread of Wind-Driven Fires. *Canadian Journal of Forest Research* 18 (4): 391–97.

Perrakis DDB, MG Cruz, ME Alexander, CC Hanes, DK Thompson, SW Taylor, BJ Stocks (2023) Improved Logistic Models of Crown Fire Probability in Canadian Conifer Forests. *International Journal of Wildland Fire* 32 (10): 1455–73. https://doi.org/10.1071/WF23074.

Qi Y, NC Coops, LD Daniels, CR Butson (2022) Comparing tree attributes derived from quantitative structure models based on drone and mobile laser scanning point clouds across varying canopy cover conditions. *ISPRS Journal of Photogrammetry and Remote Sensing*. 192:49–65.

Rothermel RC (1972) 'A Mathematical Model for Predicting Fire Spread in Wildland Fuels.' Research Paper RP-INT-115, USDA Forest Service Intermountain Forest and Range Experiment Station (Ogden, UT).

Schwilk DW (2015) Dimensions of Plant Flammability. *New Phytologist* 206 (2): 486–88.

Scott JH, ED Reinhardt (2001) 'Assessing Crown Fire Potential by Linking Models of Surface and Crown Fire Behavior.' Research Paper RMRS-RP-29, USDA Forest Service Rocky Mountain Research Station (Fort Collins, CO).

Van Wagner CE (1977) Conditions for the Start and Spread of Crown Fire. *Canadian Journal of Forest Research* 7: 23–34.

Wotton BM, JS Gould, WL McCaw, NP Cheney, SW Taylor (2012) Flame Temperature and Residence Time of Fires in Dry Eucalypt Forest. *International Journal of Wildland Fire* 21 (3): 270–81.

Evaluating the effect of experimental summer burning on litterfall biomass in Mediterranean pine forest ecosystems

*Juncal Espinosa
Sustainable Forest Management Research Institute (University of Valladolid), Avenida de Madrid, 52, 34004 Palencia, Spain, juncal.espinosa@uva.es

Óscar Rodríguez de Rivera
Department of Mathematics and Statistics, Faculty of Environment, Science and Economy, University of Exeter, Harrison Building, Room 201, EX4 4PY, Exeter, UK, o.m.rodriguez-de-rivera-ortega@exeter.ac.uk

Ana Carmen de La Cruz
Grupo de Incendios Forestales, Instituto de Ciencias Forestales (ICIFOR-INIA), CSIC, Carretera de La Coruña, km 7.5, 28040 Madrid, Spain, calleja@inia.csic.es

Javier Madrigal
Grupo de Incendios Forestales, Instituto de Ciencias Forestales (ICIFOR-INIA), CSIC, Carretera de La Coruña, km 7.5, 28040 Madrid, Spain, and ETSI Montes, Forestal y del Medio Natural, Universidad Politécnica de Madrid (UPM), Ramiro de Maeztu s/n, 28040 Madrid, Spain, incendio@inia.csic.es

Carmen Hernando
Grupo de Incendios Forestales, Instituto de Ciencias Forestales (ICIFOR-INIA), CSIC, Carretera de La Coruña, km 7.5, 28040 Madrid, Spain, lara@inia.csic.es

Cristina Carrillo
Grupo de Incendios Forestales, Instituto de Ciencias Forestales (ICIFOR-INIA), CSIC, Carretera de La Coruña, km 7.5, 28040 Madrid, Spain, and ETSI Montes, Forestal y del Medio Natural, Universidad Politécnica de Madrid (UPM), Ramiro de Maeztu s/n, 28040 Madrid, Spain, cristina.carrillo@inia.csic.es

Pablo Martín-Pinto
Sustainable Forest Management Research Institute (University of Valladolid), Avenida de Madrid, 52, 34004 Palencia, Spain, pmpintp@uva.es

Mercedes Guijarro
Grupo de Incendios Forestales, Instituto de Ciencias Forestales (ICIFOR-INIA), CSIC, Carretera de La Coruña, km 7.5, 28040 Madrid, Spain, guijarro@inia.csic.es

**Corresponding Author*

Introduction

Moderate-intensity spring and autumn prescribed burning carried out in *Pinus nigra* Arn. subsp. *salzmannii* stands of the Cuenca Mountains (Iberian Mountain Range) have shown a limited short-term effect on litterfall biomass, partly due to the of the multiple fire adaptations of this stands to typical recurrent low-intensity fires (Espinosa *et al.* 2018; 2020). However, the current fire regime has exceeded the historical patterns of intensity, extent, severity, seasonality and frequency (Sayedi *et al.* 2024). Fires in late spring can potentially increase litter consumption (Fernandes *et al.* 2022), which could decrease fire risk, but also cause irreversible changes in ecosystems processes such as litterfall. Litterfall is a good indicator of overall forest functions in forest ecosystems (Wang *et al.* 2021). Litter dynamics form an essential part of nutrient cycling and energy transfer in forest stands (Lado-Monserrat *et al.* 2016). It plays a crucial role in the global carbon cycle (Geng *et al.* 2022). In addition, litterfall biomass may provide an insight into the effects of climate change on forests (Hansen *et al.* 2009). Overall, the fall of leaves is considered to be an essential survival strategy of trees when the conditions get unfavorable for net primary production. Thus, the effect of disturbance caused by experimental summer burning on litterfall has been studied in the same experimental design used after spring and autumn prescribed burning carried out in the Cuenca Mountains.

Material and Methods

Monthly data of litterfall were collected from two locations in the Cuenca Mountains, Iberian Mountain Range, Central Spain. Beteta covered by *Pinus nigra* Arn. subsp. *salzmannii*, and El Pozuelo, a mixed forest of *P. nigra* (87±12%) and *P. pinaster* Ait. (13±12%). Experimental summer burnings were carried out in June 2019. Litterfall was collected monthly until December 2022, following the recommendations and parameters outlined in the manual published by the United Nations Economic Commission for Europe (UNECE) (Ukonmaanaho *et al*. 2016). A total of two treatments per experimental site (non-burned plots and summer-burned plots) with three replicates per treatment were established. Data were collected in six plots (30 x 30 m) per experimental site.

Experimental summer burnings were conducted in June 2019 by the Cuenca Forest Services by applying the strip head fire technique. The simulated wildfires were intended to reflect the typical early summer conditions in the area. The main parameters were recorded in Madrigal *et al.* (2023).

For the statistical analysis of the litterfall results, total litterfall and different fractions in were selected as target variables. A linear mixed model of repeated measurements analysis of variance with one between-subject factors was chosen: burning treatment (two levels: summer experimental fires and non-burned plots) and their interactions. One within-subjects factor (repeated measurements) was selected (levels

corresponding to months in temporal periods). A first-order autoregressive variance structure was considered for the errors in the linear mixed model.

Results

The mean annual amount of litterfall in burning plots of Beteta (pure stand) and El Pozuelo (mixed stand) was 3434±1524 kg ha^{-1} $year^{-1}$ and 3554±2898 kg ha^{-1} $year^{-1}$, respectively. In both stands, litterfall reached maximum levels mainly during August. The lowest amount of litterfall was collected during winter months (December, January and February). A slight increase in the litterfall was observed two months after summer fires in both stands, although the differences were not significant.

Needles comprised the largest litterfall fraction in both stands, accounting for 66±8% in Beteta and 65±11% in El Pozuelo. Bark and branch fractions showed high intra- and inter-variability.

Discussion and Managment Implications

Litterfall biomass could substitute, or at least complement, commonly used crown damage descriptors, particularly after fire management actions.

The mean annual litterfall in burning plots was similar to those reported by by ICP Forests (3337±841 kg ha^{-1} $year^{-1}$) after an 11-year-long study (2005-2014) of a *Pinus nigra* stand in Mora de Rubielos (Teruel), in which the altitude and latitude were similar to those the study area. Thus, the study findings suggest that summer fires had a limited influence on litterfall.

The fire altered litterfall patterns either. This often show a seasonal distribution. In the present study, the maximum levels of litterfall in summer months (June-August) are consistent with the results obtained by other authors in Mediterranean ecosystems (e.g., Blanco *et al.* 2006; Bueis *et al.* 2018).

The findings indicated a short-term effect (two months) on litterfall biomass, with an initial increase in the amount of litterfall collected in the burned plots. The effect of the treatment decreased gradually over time, as shown in a previous study with the same experimental design (Espinosa *et al.* 2018; 2020). Given the legal restrictions in some areas to carry out this type of treatment, these results may help managers to include it in the prevention plan treatments, particularly in fire adapted stands.

The amount of needles fraction was closer to the values observed in a similar ecosystem (e.g., Martínez-Alonso *et al.* 2007). The trend for needles is similar to that observed for total litterfall biomass. Intra- and inter-annual variability were observed in branch and bark fraction.

Acknowledgements
This research was funded by ENFIRES (Enhancing fire resilience of mediterranean forest systems, PID2020-116494RRC41/AEI/10.13039/501100011033). This study was also financed by European Social Fund "NextGenerationEU" through a grant "Margarita Salas" awarded to Juncal Espinosa within the project GFIRE (Gestión Forestal para la adaptación a los incendios forestales en el marco del cambio climático en el área mediterránea; UVa-2022-MS-TEZ02).

References

Blanco JA, Imbert JB, Castillo FJ (2006) Influence of site characteristics and thinning intensity on litterfall production in two *Pinus sylvestris* L. forests in the western Pyrenees. *Forest Ecology and Management*, **237**(1-3), 342-352.

Bueis T, Bravo F, Pando V, Turrión MB (2018). Local basal area affects needle litterfall, nutrient concentration, and nutrient release during decomposition in *Pinus halepensis* Mill. plantations in Spain. *Annals of Forest Science*, **75**(1), 1-12.

Espinosa J, Madrigal J, De La Cruz AC, Guijarro M, Jiménez E, Hernando C (2018) Short-term effects of prescribed burning on litterfall biomass in mixed stands of *Pinus nigra* and *Pinus pinaster* and pure stands of *Pinus nigra* in the Cuenca Mountains (Central-Eastern Spain). *Science of the Total Environment*, **618**, 941-951.

Espinosa J, Madrigal J, Pando V, De la Cruz AC, Guijarro M, Hernando C (2020) The effect of low-intensity prescribed burns in two seasons on litterfall biomass and nutrient content. *International Journal of Wildland Fire*, **29**(11), 1029-1041.

Fernandes PM, Rossa CG, Madrigal J, Rigolot E, Ascoli D, Hernando C, ..., Guijarro M (2022) Prescribed burning in the European Mediterranean Basin. Global Application of Prescribed Fire, 1st ed.; CRC Press: Boca Raton, FL, USA, 230-248.

Geng A, Tu Q, Chen J, Wang W, Yang H (2022) Improving litterfall production prediction in China under variable environmental conditions using machine learning algorithms. *Journal of Environmental Management*, **306**, 114515.

Hansen K, Vesterdal L, Schmidt IK, Gundersen P, Sevel L, Bastrup-Birk A, *et al.* (2009) Litterfall and nutrient return in five tree species in a common garden experiment. *Forest Ecology and Management*, **257**(10), 2133-2144.

Lado-Monserrat L, Lidón A, Bautista I (2016) Erratum to: Litterfall, litter decomposition and associated nutrient fluxes in *Pinus halepensis*: influence of tree removal intensity in a Mediterranean forest. *European Journal of Forest Research*, **135**(1), 203-214.

Madrigal J, Rodríguez de Rivera Ó, Carrillo C, Guijarro M, Hernando C, Vega JA, ..., Espinosa J (2023) Empirical modelling of stem cambium heating caused by prescribed burning in mediterranean pine forest. *Fire*, **6**(11), 430.

Martínez-Alonso C, Valladares F, Camarero JJ, Arias ML, Serrano M (2007) The uncoupling of secondary growth, cone and litter production by intradecadal climatic variability in a Mediterranean Scots pine forest. *Forest Ecology and Management*, **253**(1-3), 19-29.

Sayedi SS, Abbott BW, Vannière B, Leys B, Colombaroli D, Romera GG, ..., Daniau AL (2024) Assessing changes in global fire regimes. *Fire Ecology*, **20**(1), 1-22.

Ukonmaanaho L, Pitman R, Bastrup-Birk A, Breda N, Rautio P (2016) Part XIII: Sampling and analysis of litterfall. In 'Manual on methods and criteria for harmonized sampling, assessment, monitoring and analysis of the effects of air pollution on forests'. (Ed. UNECE ICP Forests Programme Co-ordinating Centre) 14 pp. (Thünen Institute of Forest Ecosystems: Eberswalde, Germany) Available at https://www.icp-forests. org/pdf/manual/2016/ICP_Manual_2016_01_part13.pdf [verified 23 July 2020].

Wang CG, Zheng XB, Wang AZ, Dai GH, Zhu BK, Zhao YM, ..., Li MH (2021) Temperature and precipitation diversely control seasonal and annual dynamics of litterfall in a temperate mixed mature forest, revealed by long-term data analysis. *Journal of Geophysical Research: Biogeosciences*, **126**(7), e2020JG006204.

Proceedings for the 7th International Fire Behavior and Fuels Conference April 15-19, 2024, Boise, Idaho, USA – Tralee, Ireland – Canberra, Australia Published by the International Association of Wildland Fire, Missoula, Montana, USA

Expert Scholar/Practitioner Perceptions of Wildfire Science: A Pilot Study

*Margaret V. du Bray
University of Northern Colorado, 501 20th St, Greeley, Colorado, USA, meg.dubray@unco.edu

Eric B. Kennedy
York University, 4700 Keele St., Toronto, Ontario, Canada, ebk@yorku.ca

Sarah Cowan
York University, 4700 Keele St., Toronto, Ontario, Canada, sarcowan@yorku.ca

Liza C. Kurtz
Arizona State University, 1151 S. Forest Ave., Tempe, Arizona, USA, liza.kurtz@asu.edu

Eric Toman
Colorado State University, Fort Collins, Colorado, USA, eric.toman@colostate.edu

**Corresponding Author*

Introduction

Among other factors, climate change and the desirability of living in the wildland-urban interface are increasing the risk of wildland fire in North America. Risks associated with wildland fire include increased financial costs for mitigating and responding to fires and rebuilding in the aftermath; increased displacement; and impacts on human health and well-being. In spite of a growing body of research, much of the expert knowledge remains siloed by discipline and country (Cowan and Kennedy 2023).

In an effort to align the field, the Blueprint for Wildland Fire Science in Canada (2019-2029) proposed a 10-year science strategy to understand the role of fire in a changing world (Sankey 2018). Members of our team subsequently proposed a collaborative North American Blueprint for Wildland Fire Science (Pérez Salicrup et al. 2020). Our collaboration focuses on collecting qualitative and quantitative data from stakeholders (emergency managers, scholars, wildland firefighters, etc) to a) improve international cooperation for wildland fire science; b) diversify fire science; c) align wildland fire research with current and future needs, and d) share results for decision-making.

The data presented here are the results of preliminary interviews with fire researchers from across Europe. These interviews were designed to test and adapt our interview protocol in advance of interviews with North American stakeholders.

Materials and methods

Sample selection

Interview data were primarily collected at the 2023 PyroLife Conference in Barcelona, Spain. PyroLife is an initiative that funds “a new, global initiative in wildfire research” (Who we are, n.d.). This initiative supports PhD students internationally with the goal of increasing interdisciplinarity in wildfire research. The PyroLife conference provided the opportunity for researchers funded under the initiative, along with other fire researchers, to convene and share results and experience on fire management.

This conference and its attendees were selected as our sample because they represent a heterogeneous mix of researchers and practitioners, including early stage researchers, policymakers, and practitioners with different life experiences. This heterogeneity meant that the respondents pushed productively on underlying assumptions in our preliminary interview protocol and improve its efficacy. Further, because our long-term target sample for the North American Blueprint for Wildland Fire Science is composed of North American researchers, policymakers, and practitioners, testing the protocol on primarily European stakeholders prevented us from potentially contaminating our final sample.

Data collection

One of the Principal Investigators (PI) conducted in-person interviews with 13 respondents during the conference. An additional 3 interviews were conducted over Zoom after the conference. All 16 interviews were recorded, transcribed, and de-identified to protect the participants.

Participants were asked open-ended questions about their role in wildland fire science, their perceptions of barriers to making fire science more useful and accepted, and perceptions of wildland fire. Questions were not static between interviews; participants were asked to elaborate on certain aspects and often covered themes without being asked.

Data analysis

Data were first analyzed using the six themes from the Blueprint for Wildland Fire Science in Canada (understanding fire in a changing world; recognizing Indigenous knowledge; building resilient communities and infrastructure; managing ecosystems; delivering innovative fire management solutions; and reducing the effects of wildland fire on Canada).

The data were subsequently read multiple times for emergent themes (communication, living with fire, and collaboration). These emergent themes informed the final iteration of the North American interview protocol.

Results

Findings from the European PyroLife interviews revealed two themes from the Blueprint for Wildland Fire Science in Canada, and three emergent themes. Interestingly, four of the six themes identified in the Blueprint for Wildland Fire Science in Canada were not regularly discussed. The exception to this was the recognition of Indigenous knowledge and the need to build resilient communities and infrastructure. The emergent themes occurred commonly across participants and included: communication, learning to live with fire, and building collaborations. The content of these themes will be discussed below.

Discussion

Emergent themes

Respondents who attended the PyroLife conference identified communication as a significant issue when it comes to wildland fire research. The participants noted that communication challenges can occur in multiple ways; there is a paucity of risk communication with community stakeholders, and communication between researchers and practitioners is often insufficient. As one person explains, “We need to speak in plain language; fire science knows a lot, and you [should] try to explain that to someone who’s not related to the topic. I’m always saying, tell your grandma and see what she thinks of it.” While the respondents at the PyroLife conference are largely engaged in academic-style research, they clearly identified that communication barriers are a significant challenge to engaging with community members and practitioners, and that scientific jargon can exclude multiple ways of understanding wildland fire and its risks.

Learning to live with fire was another emergent theme from the PyroLife interviews. Respondents indicated that, while we have long lived with fire suppression as our status quo, increasingly, we will need to adapt to and with fire regimes and allow fire to become re-naturalized (using traditional and/or local ecological knowledge), while also minimizing risk. While the perspective from participants at the PyroLife conference is very specific, particularly regarding the re-naturalization of fire (i.e., a view not shared across stakeholder groups), they note the importance of keeping risk in mind: “How can we have room, have space for that [fire] as an essential part of our ecosystems, while minimizing risk to life and property?” The goal of including fire on the landscape again, while addressing the fears of stakeholders, is a significant challenge, but one the PyroLife participants discussed eagerly.

Building collaborations was the last emergent theme. Interview participants noted that the PyroLife community is unique because it is transdisciplinary and collaborative, and they indicated that developing new collaborations were necessary to support fire science. These collaborations, they indicated, should not be exclusive to scholars or scientists, but should include community members, government officials, and emergency managers – in sum, these collaborations needed to include local communities to better embody a holistic understanding of wildland fire and its impacts. This particular point also relates to the lack of engagement with stakeholders; while research has historically extracted from communities, these scholar interviews pointed to the importance of bringing information and resources back to the communities they work with.

In sum, these data point to needed interventions in the field of wildland fire science. During the interviews, respondents helpfully pushed back on assumptions embedded in our draft interview protocol, and indicated that we needed to consider themes beyond what emerged in the Blueprint for Wildland Fire Science in Canada. Based on the feedback we received from participants at the PyroLife conference, we altered our interview protocol, which has now been used across North America. Our next steps include implementing a survey to capture more perspectives across the continent.

In addition to contributing to refining our interview protocol, these data demonstrate needs across wildland fire science. The PyroLife respondents regularly indicated the importance

of increased holism and reflexivity for those working with wildland fire to produce a more beneficial future for all who live and work with fire.

Acknowledgements
This work was supported by Natural Resources Canada.

References

Cowan, S., & Kennedy, E. B. (2023). Determinants of residential wildfire mitigation uptake: a scoping review, 2013–2022. *Fire safety journal*, 103851.

Pérez Salicrup, D., Sankey, S., Jolly, M., Boucher, J., Toman, E., Arseneau, C., & Norton, M. (2020). North American Blueprint for Wildland Fire Science Collaboration. *International Association of Wildland Fire Wildfire Magazine*, Oct-Dec.

Sankey, S. (2018). Blueprint for Wildland Fire Science in Canada (2019-2029). Northern Forestry Centre, Canadian Forest Service. (Edmonton, AB).

Who we are. PyroLife. (n.d.). https://pyrolife.lessonsonfire.eu/who-we-are/.

Proceedings for the 7th International Fire Behavior and Fuels Conference April 15-19, 2024, Boise, Idaho, USA – Tralee, Ireland – Canberra, Australia Published by the International Association of Wildland Fire, Missoula, Montana, USA

Framework for Rapid Economic Damage Assessment of Forest Fires Using Open-Access Data

Bushra Sanira Asif*
University of Genova, Genova, Liguria, Italy
bushra.sanira.asif@edu.unige.it

Introduction

Forest fires are a growing global concern, aggravated by climate change and increasing human activities. These fires result in significant economic losses, environmental degradation, and adverse health effects. Conventional methods for assessing the economic damage caused by forest fires are often slow and labor-intensive, delaying timely response and recovery efforts. This project proposes a framework that utilizes open-access data including satellite data to rapidly assess economic damages from forest fires, focusing initially on the loss of carbon storage.

The importance of carbon storage cannot be overplayed, as forests play a crucial role in mitigating climate change by absorbing and storing carbon dioxide. Accurate and rapid assessment of carbon storage loss due to forest fires is essential for understanding the broader economic impacts and developing effective mitigation strategies. The use of satellite data in environmental assessment has been well-documented. Chuvieco and Congalton (1989) demonstrated the application of remote sensing for forest fire hazard mapping, highlighting its potential to provide real-time data. Similarly, Loboda and Csiszar (2007) assessed fire ignition risk in the Russian Far East using a modeling framework that integrates satellite data, showcasing its effectiveness in fire threat assessment.

In economic impact assessment, Burke et al. (2015) explored the influence of climatic conditions on fire weather, emphasizing the importance of accurate data in understanding fire behavior and economic implications. Gill and Bradstock (2003) discussed fire regimes and their impact on biodiversity, underlining the necessity of comprehensive assessment tools for both economic and ecological damages. Meier et al. (2023) work on the economic impact of forest fires in Europe provides valuable insights into integrating climatological data with economic analysis. Her methodologies offer a robust foundation for developing frameworks that can swiftly and accurately estimate fire-induced economic losses.

The primary objective of the research is to develop an adaptable framework that utilizes satellite data to assess economic damages resulting from forest fires. The framework's initial focus is on evaluating damages to carbon storage, a critical ecosystem service provided by forests by absorbing and storing carbon dioxide.

Methodology

The framework begins with the collection of high-resolution satellite data and other openly accessible data, which provides real-time information on the extent and intensity of forest fires. This data is crucial for mapping the impacted regions and assessing the

immediate damage. Satellite data sources include MODIS, Landsat, and Sentinel satellites, which offer high spatial and temporal resolution, allowing for detailed analysis of fire-affected areas.

To ensure a comprehensive assessment, forest assets are categorized into direct assets such as timber resources, non-timber products, and recreational assets; indirect assets including water resources and wildlife habitats; environmental assets like carbon storage and biodiversity; and cultural assets such as heritage sites and archaeological structures. This categorization framework draws on previous studies that highlight the diverse impacts of forest fires on different asset types (Chuvieco and Congalton, 1989; Gill and Bradstock, 2003).

Economic damages are then classified into direct damages, such as the loss of forest cover and timber value; indirect damages, including job and business losses and infrastructure impacts; and environmental damages, focusing on the loss of carbon storage and biodiversity. This classification follows established methodologies for economic impact assessment of natural disasters (Burke et al., 2015; Meier, 2021).

The rapid assessment technique uses satellite data to provide quick and accurate estimates of economic damages. The next step is to process satellite imagery to detect active fires in near real-time, enabling immediate identification of affected areas. Spatial analysis using GIS tools maps the extent of fire-affected regions, integrating satellite data with geographic information to delineate the impacted zones. The integration of satellite data with databases containing information on forest assets facilitates the identification of assets within the affected areas. Economic models are then applied to estimate the monetary value of damages to these assets, using market prices, replacement costs, and other economic indicators.

Combining data from multiple satellite sources and other open-access data sources enhances the accuracy and reliability of the assessment. Cross-referencing data from MODIS, Landsat, and Sentinel satellites ensures comprehensive coverage and detailed analysis. The framework's ability to integrate various types of economic damages, including direct, indirect, and environmental impacts, allows for a more accurate and holistic assessment of the economic consequences of forest fires.

Anticipated Results

The proposed framework is expected to offer several significant benefits. The use of satellite data allows for rapid assessment of fire damages, enabling timely decision-making and resource allocation. High-resolution satellite imagery provides detailed and precise information on fire-affected areas, improving the accuracy of damage estimates. The comprehensive approach ensures that all valuable resources impacted by forest fires are accounted for, providing a clearer picture of the economic stakes involved.

One of the key advantages of this framework is its adaptability, allowing for future expansions to include additional types of economic and environmental damages. This adaptability ensures that the framework remains relevant and valuable as our

understanding of forest fires and their economic impacts expands. The framework's potential for application in different geographical contexts and fire regimes makes it a valuable tool for global fire management. The ability to tailor the models and methodologies to specific regional needs and conditions enhances the framework's relevance and effectiveness.

The validation of the framework through expert opinions and additional data sources enhances its reliability and accuracy. Ground-based observations and expert assessments can be used to validate the satellite data and economic estimates, ensuring the credibility of the rapid assessment. Future expansions of the framework can focus on improving the accuracy and reliability of the models and enhancing the integration of satellite data with ground-based observations.

Conclusion

The developing framework discussed will represent significant progress in the efficient and rapid assessment of forest fire economic damages, focusing initially on carbon storage values. Through the intelligent use of satellite data and adaptable modeling techniques, it promises to be an essential tool for various stakeholders during increasing forest fire incidents globally. The framework's comprehensive approach and adaptability ensure its relevance and value in understanding and mitigating the economic impacts of forest fires.

The future development of this framework will focus on expanding its scope to include additional types of economic and environmental damages, improving the accuracy and reliability of the models, and enhancing the integration of satellite data with ground-based observations. These advancements will further solidify the framework's position as a leading tool for forest fire damage assessment and management.

References

Chuvieco E, & Congalton R.G. (1989) Application of remote sensing and geographic information systems to forest fire hazard mapping. *Remote Sensing of Environment* 29(2), 147-159.

Burke M, Hsiang SM, Miguel, E. (2015) Global non-linear effect of temperature on economic production. *Nature*, 527, 235-239.

Meier S, Elliott R, Strobl, E (2023) The regional economic impact of wildfires: Evidence from Southern Europe'. Journal of Environmental Economics and Management vol. 118, 102787.

Loboda, TV, Csiszar IA (2007) Assessing the risk of ignition in the Russian Far East within a modeling framework of fire threat. *Ecological Applications* 17(3), 791-805.

Proceedings for the 7th International Fire Behavior and Fuels Conference April 15-19, 2024, Boise, Idaho, USA – Tralee, Ireland – Canberra, Australia Published by the International Association of Wildland Fire, Missoula, Montana, USA

Fuel Modification by Broadleaved Tree Inclusion in the European Boreal Forest

*Frida Vermina Plathner
Department of Fire Technology, Research Institutes of Sweden, Box 857, 501 15 Borås, Sweden, frida.vermina.plathner@ri.se

Johan Sjöström
Department of Fire Technology, Research Institutes of Sweden, Box 857, 501 15 Borås, Sweden, johan.sjostrom@ri.se

Anders Granström
Department of Forest Ecology and Management, Swedish University of Agricultural Sciences, 901 83 Umeå, Sweden, anders.granstrom@slu.se

**Corresponding Author*

Introduction

The European boreal region is dominated by two conifer tree species, Scots pine (*Pinus sylvestris*) and Norway spruce (*Picea abies*), often with an admixture of broadleaved species, primarily birch (*Betula* spp.) and aspen (*Populus tremula*). Both birch and aspen establish naturally on land disturbed by e.g. wildfire or clear-felling, especially on mesic soils (Lidman et al., 2024), although the proportion of deciduous trees decrease over time due to a progressively slower growth rate with age, compared to conifers (Holmström et al., 2021). More importantly, aggressive pre-commercial thinning of deciduous trees is usually done at stand heights of 3-5 m to favor conifers on managed forest lands.

Under evergreen coniferous boreal stands, the primary surface fuel consists of mosses and/or lichens with an admixture of litter, primarily needles. These moss- and lichen species (e.g. *Pleurozium schreberi*, *Hylocomium splendens* or *Cladonia* spp.) form a loose, aerated fuel bed (Schimmel & Granström, 1997). In contrast, the ground under deciduous trees is instead mainly covered by leaf litter, forming a structurally more compact fuel bed with reduced flammability (Vermina Plathner et al., 2022). The direct mechanisms whereby leaf litter excludes mosses has not been conclusively demonstrated, but experiments show that even 3-year-deposition of birch leaf litter severely reduces the growth of mosses (Jean et al., 2020). Thus, with an increasing number of broadleaved trees within conifer forests, the fuel bed is expected to gradually become less flammable. The porosity and depth of the surface layer are principal structural fuel characteristics that affect fire behavior (Andrews, 2018). However, the extent to which leaf litter alters the fuel bed and potential fire behavior in mixed stands has not yet been quantified. In this study we sampled structure and dry mass of surface fuels under a range of tree stand configurations with conifers and birch in Sweden to assess the potential fire behavior in this region.

Methods

The impact of leaf litter on fuel bed depth was evaluated in three settings: (A) adjoining pure stands of birch vs. spruce and birch vs. pine, (B) singular birch trees within conifer forests, and (C) mixed-species stands with varying degree of birch tree admixture, Fig. 1.

Figure 20. Three test series in which fuel bed depth was evaluated: (A) Adjoining stands, (B) Singular birch trees within conifer forests, and (C) Mixed-species stands.

For (A) we utilized 7-decade-old stands within the Siljansfors experimental forest, originally established to compare growth potential of different tree species. For (B) and (C) we sampled ordinary commercial forests with mixed conifer-birch composition, located across Sweden to capture stand variations.

The depth of the surface fuel bed, approximating the organic L and F layers (Soil Classification Working Group, 1998), was assessed with a penetrometer, with which a 15 N force was applied to the fuel bed through an L-shaped aluminum bar with 20 mm sides and 2 mm material thickness. A 15 x 1.5 cm lattice was first placed on the fuel bed as a reference for the pre-compression surface of the fuel bed. The penetration depth was read against this lattice on the engraved scale of the aluminum bar.

Fuel bed depth was sampled along transects, with two parallel sampling points each 0.5 m, separated orthogonally by 1 m. For series A, the transects started 10 m inside each birch stand and ended 20 m inside the adjoining coniferous stand. Two and one such transects were measured across the spruce-birch and pine-birch stands, respectively. For the B-series, transects began at the base of a birch trunk, then extended to 10-12 m from the tree. The sampled birch trees were well separated from other birches, in otherwise coniferous stands. We obtained 13 such transects in six stands. For the C-series, fuel bed depth measurements were collected in 153 stands. Here fuel bed dry mass was also destructively sampled. Two 0.25 m^2 plots (example in figure 1c) were randomly positioned and the entire fuel bed including field-layer vegetation was collected. The thickness of the humus layer was measured with a ruler but was not harvested. Later, the fuels were sorted into live/dead components and size classes in the lab (as per Fosberg (1971)), dried in 105ºC and weighed.

Results and discussion

The measured fuel bed depth within the pure stands in series A were ≈3 cm for birch, ≈6 cm for spruce and ≈6 cm for pine, which confer approximately to the average depths obtained in a nation-wide field inventory of homogenous stands (2, 5, and 8 cm for birch, spruce and pine respectively (Vermina Plathner et al., 2022)). This suggests that the test site was representative of mature homogenous forests in Sweden. Pure deciduous stands reduced the fuel bed depth about 10 m into the adjacent pure coniferous stands, indicating the degree of lateral spread of the leaves, Fig 2. Conifers, on the other hand, did not affect fuel bed depth in adjacent birch stands.

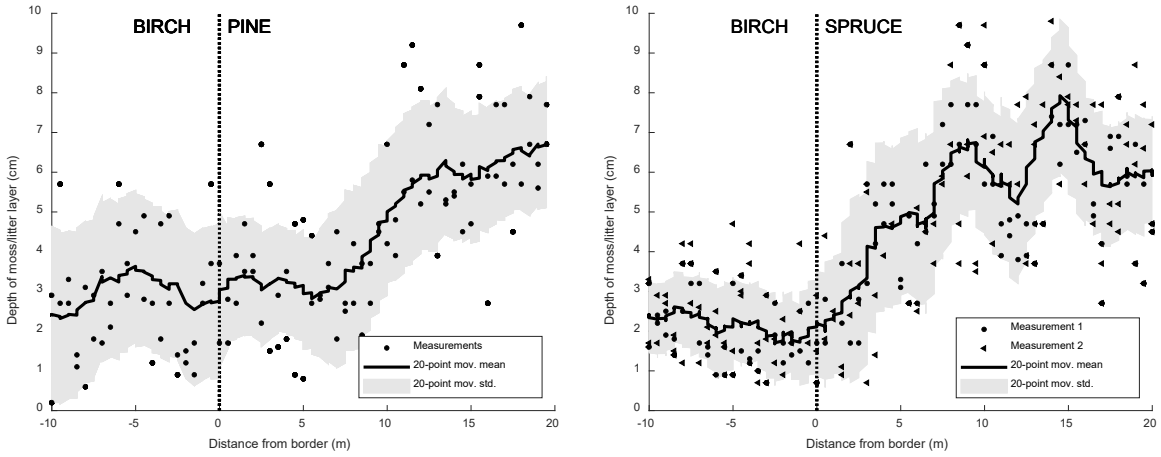

Figure 21. Fuel bed depth in pure-species tree stands in relation to distance from the stand border. Left hand panel: adjoining stands of pure birch and pine. Right-hand panel: adjoining stands of pure birch and spruce.

The lateral spread of birch litter from individual trees was further illustrated by experimental series B. On average, the effect of single birch trees decreased with distance from the tree stems but was still noticeable out to a distance of ≈6 m (varying between 4-8 m for different sites). This suggests that single large birch trees affect the fuel bed over an area of 50-200 m^2, Fig. 3.

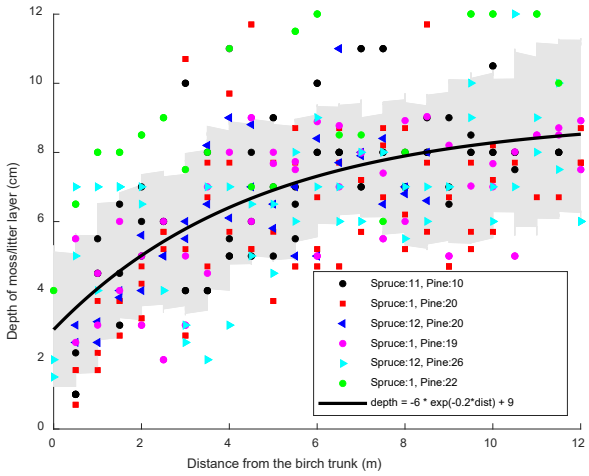

Figure 22. Surface fuel bed depth (excl. field layer) in relation to distance from single birch trees in mature coniferous forest. Basal area in the stands ranged 21-39 m^2/ha (specified in the legend). The solid line is an exponential fit applied to the full dataset.

With increasing amount of birch in coniferous stands, there was a progressive reduction in the depth of the upper part of the surface fuel bed. In addition, fuel bed mass decreased. This suggests that the leaf litter smothers the moss layer that is prevalent under conifers and renders the fuel bed more compact, with effects on the potential fire intensity and spread rate. The depth of the litter layer was reduced by 45 % already at a basal area of deciduous trees of 3-4 m^2ha^{-1}, corresponding to ≈10-20 % of the mature trees in the stand, Fig. 4. With increasing inclusion of deciduous trees, the surface fuel bed becomes fully 'deciduous-dominated' long before birch outnumber the conifers.

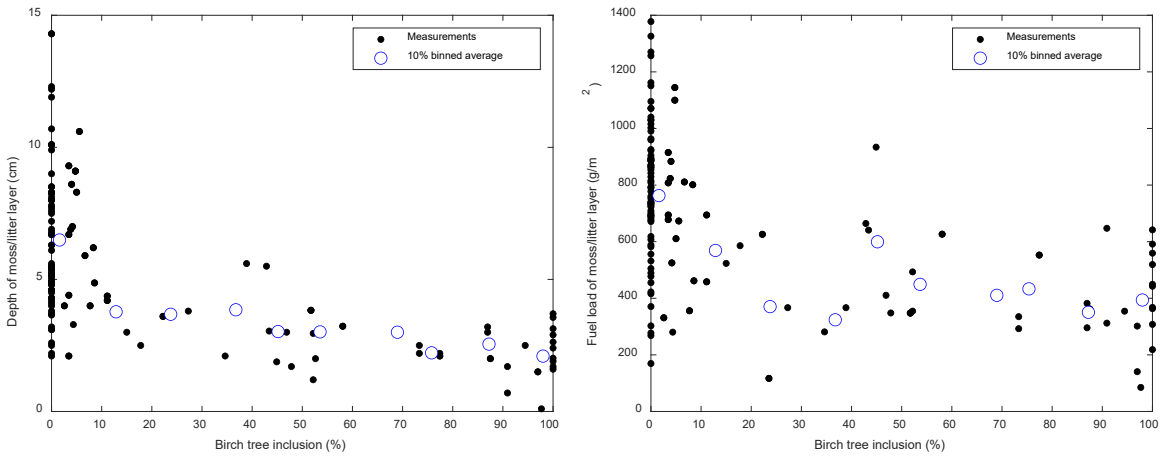

Figure 23. Fuel bed structure in relation to proportion of birch in 153 Swedish forest stands. Left: Fuel bed depth. Right: Fuel bed mass. The blue circles denote binned averages for every 10 % span.

Conclusions

Our results show a profound impact on the fuel bed structure through birch inclusion, suggesting that surface fire rate of spread and intensity will decrease significantly with only a moderate inclusion of birch in coniferous stands. This opens the possibility for reducing the flammability of the entire forest landscape through modified forest management in early succession, allowing a higher percentage of birch in the developing stands.

Acknowledgements

This study was funded by FORMAS (2021-02396) and MSB (2021-14648).

References

Andrews PL (2018) 'The Rothermel surface fire spread model and associated developments: A comprehensive explanation.' USDA Forest Service, Rocky Mountain Research Station General Technical Report RMRS-GTR-371. (Fort Collins, CO)

Fosberg MA, Deeming JE (1971) 'Derivation of the 1-and 10-hour timelag fuel moisture calculations for fire-danger rating'. USDA Forest Service, Rocky Mountain Research Station Research Note RM-RN-207. (Fort Collins, CO)

Holmström E, Carlström T, Goude M, Lidman FD, Felton A (2021) Keeping mixtures of Norway spruce and birch in production forests: insights from survey data. *Scandinavian Journal of Forest Research* **36**(2), 155–163.

Jean M, Melvin AM, Mack MC, Johnstone JF (2020) Broadleaf litter controls feather moss growth in black spruce and birch forests of interior Alaska. *Ecosystems* **23**(1), 18-33.

Lidman FD, Karlsson M, Lundmark T, Sängstuvall L, Holmström E (2024) Birch establishes anywhere! So, what is there to know about natural regeneration and direct seeding of birch? *New Forests* **55**(1), 157–171.

Schimmel J, Granström A (1997) Fuel succession and fire behavior in the Swedish boreal forest. *Canadian Journal of Forest Research* **27**(8), 1207-1216.

Soil Classification Working Group (1998) 'The Canadian system of soil classification' Agriculture and Agri-Food Canada Publication 1646. (NRC Research Press: Ottawa, ON).

Vermina Plathner F, Sjöström J, Granström A (2022) Influence of tree species on surface fuel structure in Swedish forests. In 'Advances in Forest Fire Research 2022' (Eds. DX Viegas, LM Ribeiro) pp. 1157-1166. (University of Coimbra Press: Coimbra, Portugal).

Proceedings for the 7th International Fire Behavior and Fuels Conference April 15-19, 2024, Boise, Idaho, USA – Tralee, Ireland – Canberra, Australia Published by the International Association of Wildland Fire, Missoula, Montana, USA

Fuel Treatment Impacts on Forest Carbon in Southeastern British Columbia

*Rachel S. Pekelney
University of British Columbia, Faculty of Forestry, 2424 Main Mall, Vancouver, British Columbia, Canada,
pekelney@student.ubc.ca

Bianca N.I. Eskelson
University of British Columbia, Faculty of Forestry, 2424 Main Mall, Vancouver, British Columbia, Canada,
bianca.eskelson@ubc.ca

Kea H. Rutherford
University of British Columbia, Faculty of Forestry, 2424 Main Mall, Vancouver, British Columbia, Canada,
kea@student.ubc.ca

Lori D. Daniels
University of British Columbia, Faculty of Forestry, 2424 Main Mall, Vancouver, British Columbia, Canada,
lori.daniels@ubc.ca

Corresponding Author

Background

Wildfires produce substantial carbon emissions and are increasingly causing forests to transition from carbon sinks to net carbon sources (Smyth et al., 2023; Pan et al., 2011). Strategies to mitigate climate change by maximizing carbon storage in dense forests conflict with strategies to mitigate wildfire risk by reducing tree density and fuel loads (Hurteau et al., 2019). Fuel reduction treatments are implemented with a primary goal of reducing wildfire risk in the wildland-urban interface. Treatments release carbon in the short-term, but long-term carbon dynamics have not been well-characterized (Hessburg et al., 2021). We partnered with five community forests in southeastern British Columbia to assess five types of mechanical fuel reduction treatments: combinations of thinning, pruning, and residue fuel management (Table 1).

Objectives

The objective of this work is to assess the short- and long-term carbon impacts of mechanical fuel reduction treatments in community forests to better understand the role of carbon wildfire mitigation efforts. By quantifying and comparing the carbon stored on-site before and after treatment, we aim to improve understanding of how carbon storage varies across treatment levels and the potential for carbon emissions from future wildfires.

Table 1: Mechanical Treatment Combinations

Treatment Type	Tree Removal	Pruning	Residue Fuel
1	Merchantable	No	Pile burn
2	Merchantable	Yes	Pile burn
3	Non-merchantable	No	Pile burn
4	Non-merchantable	Yes	Pile burn
5	Non-merchantable	Yes	Chipping

Methods

Study Sites

The study sites are located in five community forests in seasonally dry inland rainforests of southeastern British Columbia: Creston Community Forest, Harrop-Procter Community Forest, Kaslo and District Community Forest, Nakusp and Area Community Forest, and Slocan Integral Forestry Cooperative. Field data were collected in the summers of 2021 and 2022 to quantify fuels pre- and post-treatment. The climate consists of cool, wet winters and warm, dry summers. The pre-colonial, historical fire regime was dominated by frequent, low-to-moderate severity wildfires ignited by lightning or burning by Indigenous peoples.

Biomass Estimation

To calculate tree biomass, we used species- and region-specific allometric equations from the U.S. Forest Service's Forest Inventory and Analysis equation set that predict stem and bark biomass from diameter and height (Westfall et al., 2023; U.S. Dept. of Agriculture 2014a, 2014b). To estimate branch and foliage biomass while accounting for the effect of pruning, we used equations from Affleck (2019) and Brown (1978) for the Idaho Panhandle and western Montana that use crown length as a predictor. We used FIA wood density reduction factors and remaining bark and branch proportions to account for snag decay (Westfall et al., 2023). For shrubs, species-specific allometric equations were used to estimate biomass from either percent cover, crown volume, or height (Olson & Martin, 1981; McGinnis et al., 2010; Means et al., 1994). If there was no available species-specific equation, we grouped shrubs by structural characteristics and selected an equation that best approximated the grouping. We summarized surface and ground fuel loads by size class using methods described in Woodall and Monleon (2008; Figure 1).

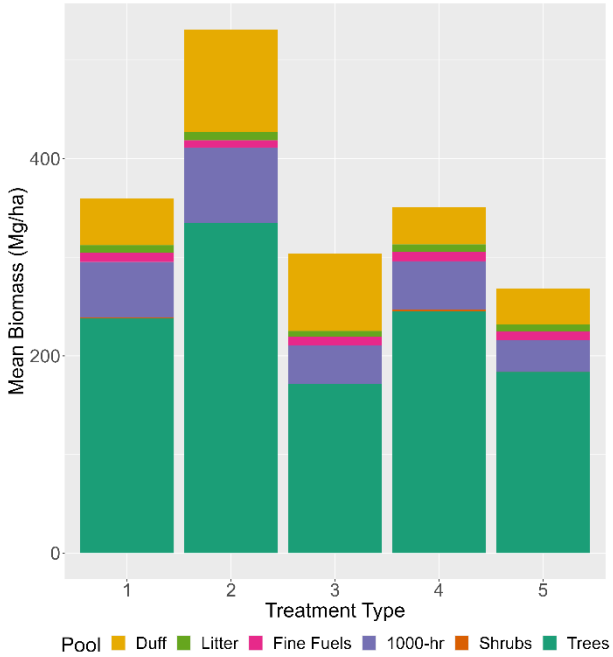

Figure 1: Mean Biomass by Pool and Treatment Type. Pre-treatment (2021) biomass (Mg/ha) only. Fine fuels are 1-100-hr fuels.

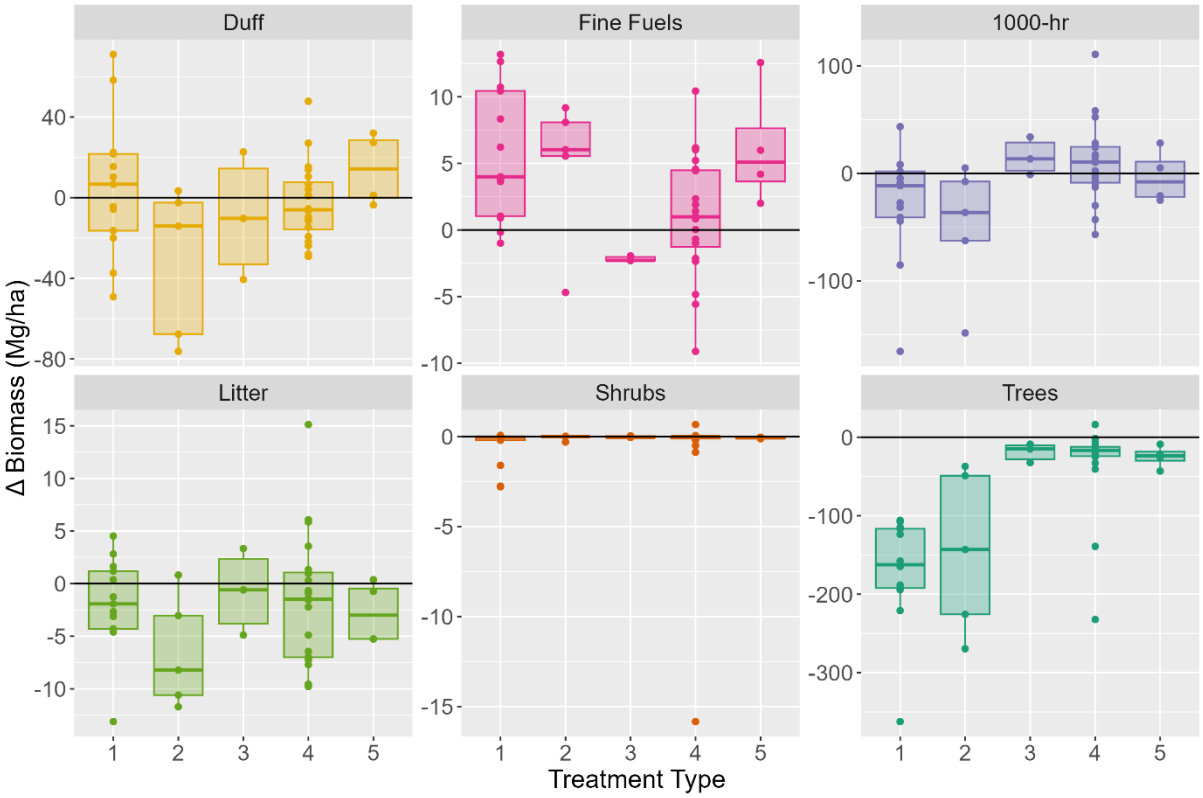

Figure 2: Difference in Biomass by Pool and Treatment Type. Delta Biomass (Mg/ha) = Post- (2022) minus Pre- (2021) treatment. Each dot represents a plot. Negative values represent a decrease in biomass after treatment.

Figure 3: Before and after treatment photo examples.

Preliminary Results: Short-term Carbon Impacts

Overall biomass stored on-site was lower after treatment for all treatment types, with the greatest decreases in biomass observed in the high-intensity thinning treatments (1 & 2). Fine fuels (1-100hr) increased after treatment, whereas all other pools decreased. Differences in duff after treatment are variable, likely because of mixing with soil after mechanical treatment (Figure 2).

Next Steps: Long-term Carbon Impacts

Methods

We plan to use the First Order Fire Effects Model (FOFEM) to predict potential carbon emissions under different wildfire scenarios in both treated and untreated stands. We will account for the carbon footprint of treatments by determining the fate of removed biomass: merchantable timber, pulp, firewood, chips, or fence posts.

Anticipated Results

We expect that modeled wildfires in untreated areas will release more carbon than modeled wildfires in treated areas because there is more available fuel to burn, which increases the likelihood of tree mortality. We also anticipate that management activities emit less carbon than modeled wildfires in the absence of treatment because of increased survivorship of large, long-lived trees that store the most carbon and are more resilient to disturbances.

Acknowledgements

Our research in the Kootenays was conducted on the traditional and unceded territory of the Ktunaxa, Secwépemc, Syilx, and Sinixt people. At the University of British Columbia, we work on the traditional and unceded territory of the Musqueam people.
This work was funded by BC Wildfire Service and the NSERC-Canada Wildfire Strategic Network. Thank you to Kea Rutherford and the field technicians who collected data in 2021 and 2022, and to our community forest collaborators.

References

Affleck, D.L.R. (2019). Aboveground biomass equations for the predominant conifer species of the Inland Northwest USA. *Forest Ecology and Management, 432*, 179–188. https://doi.org/10.1016/j.foreco.2018.09.009.

Brown, J.K. (1978). Weight and Density of Crowns of Rocky Mountain Conifers. U.S. Department of Agriculture Forest Service, Research Paper INT-197, 1–56. Intermountain Forest and Range Experiment Station, Ogden, Utah.

Hessburg, P. F., Prichard, S. J., Hagmann, R. K., Povak, N. A., & Lake, F. K. (2021). Wildfire and climate change adaptation of western North American forests: a case for intentional management. *Ecological Applications* 31(8):e02432. DOI:10.1002/eap.2432.

Hurteau, M.D., North, M.P., Koch, G.W., & Hungate, B.A. (2019). Opinion: Managing for disturbance stabilizes forest carbon. *Proceedings of the National Academy of Sciences, USA,* 116(21):10193-10195. doi: 10.1073/pnas.1905146116.

McGinnis, T. W., Shook, C. D., & Keeley, J. E. (2010). Estimating aboveground biomass for broadleaf woody plants and young conifers in Sierra Nevada, California, forests. *Western Journal of Applied Forestry*, *25*(4), 203–209. https://doi.org/10.1093/wjaf/25.4.203.

Means, J. E., Hansen, H. A., Koerper, G. J., Alaback, P. B., & Klopsch, M. W. (1994). Software for computing plant biomass - BIOPAK users' guide. *General Technical Report - US Department of Agriculture, Forest Service*, *PNW-GTR-340*.

Olson, C. M., & Martin, R. E. (1981). *Estimating Biomass of Shrubs and Forbs in Central Washington Douglas-Fir Stands*. U.S. Department of Agriculture Forest Service, Pacific Northwest Forest and Range Experiment Station. Research Note PNW-380. https://doi.org/10.5962/bhl.title.70631.

Pan, Y., Birdsey, R. A., Fang, J., Houghton, R., Kauppi, P. E., Kurz, W. A., Phillips, O. L., Shvidenko, A., Lewis, S. L., Canadell, J. G., Ciais, P., Jackson, R. B., Pacala, S. W., McGuire, A. D., Piao, S., Rautiainen, A., Sitch, S., & Hayes, D. (2011). A large and persistent carbon sink in the world's forests. *Science*, *333*(6045), 988–993. https://doi.org/10.1126/science.1201609.

Smyth, C., Xie, S.H., Zaborniak, T., Fellows, M., Phillips, C., & Kurz, W.A. (2023). Development of a prototype modeling system to estimate the GHG mitigation potential of forest and wildfire management. *MethodsX*, 10(1):101985. https://doi.org/10.1016/j.mex.2022.101985.

U.S. Department of Agriculture Forest Service. (2014a). *FIA Volume Equation documentation: Volume estimation for PNW-Databases*. Updated September 19, 2014. Retrieved March 12, 2024, from https://ww2.arb.ca.gov/sites/default/files/cap-and-trade/protocols/usforest/2014/volume_equations.pdf.

U.S. Department of Agriculture Forest Service. (2014b). *Regional Biomass Equations Used by FIA to Estimate Bole, Bark, and Branches*. Updated September 19, 2014. Retrieved March 12, 2024, from https://ww2.arb.ca.gov/sites/default/files/cap-and-trade/protocols/usforest/2014/biomass_equations.pdf.

Westfall, J.A., Coulston, J.W., Gray, A.N., Shaw, J.D., Radtke, P.J., Walker, D.M., Weiskittel, A.R., MacFarlane, D.W., Affleck, D.L.R., Zhao, D., Temesgen, H., Poudel, K.P., Frank, J.M., Prisley, S.P., Wang, Y., Sánchez, M., Andrew, J., Auty, D., Domke, G.M. (2023). A national-scale tree volume, biomass, and carbon modeling system for the United States [In press]. General Technical Report WO-104. Washington, DC: U.S. Department of Agriculture Forest Service. 60 p. https://doi.org/10.2737/WO-GTR-104.

Woodall, C.W., & Monleon, V.J. (2008). Sampling Protocol, Estimation, and Analysis Procedures for the Down Woody Materials Indicator of the FIA Program. General Technical Report NRS-22. U.S. Department of Agriculture Forest Service, Northern Research Station. https://www.fs.usda.gov/research/treesearch/13615.

Proceedings for the 7th International Fire Behavior and Fuels Conference April 15-19, 2024, Boise, Idaho, USA – Tralee, Ireland – Canberra, Australia Published by the International Association of Wildland Fire, Missoula, Montana, USA

How smoky was California before Euroamerican settlement?

*Andrea Duane
University of California, Davis, 3125 Wickson Hall, Davis, 95616, California, USA, anduane@ucdavis.edu

Rebecca Wayman
University of California, Davis, 3125 Wickson Hall, Davis, 95616, California, USA, rbwayman@ucdavis.edu

Hugh Safford
University of California, Davis, 3125 Wickson Hall, Davis, 95616, California, USA, hdsafford@ucdavis.edu

**Corresponding Author*

Introduction

California (USA) is increasingly threatened by high-severity fires, which have significant negative ecological and socioeconomic impacts. In response, the state has committed to using fire more extensively as a management tool, acknowledging that smoke will be an inevitable consequence, including over 40,000 hectares of prescribed fire annually. It is crucial that the use of fire as a management tool is supported by robust evidence of its benefits, while also considering the trade-offs of some undesirable impacts.

Among these concerns, smoke and carbon emissions are increasingly significant due to their effects on human populations and California's greenhouse gas balance. While reducing the negative impacts of smoke is important, we must ask whether a zero-tolerance policy for smoke is possible, reasonable, or even desirable.

A key step in addressing this question is to determine the pre-Euroamerican settlement (pre-1850) baseline. Baselines should not be viewed as static endpoints, but rather they can help us understand the temporal dynamics of ecosystem processes and patterns and recognize the nature and impact of human interactions with ecosystems (Safford et al., 2012).

Assessing pre-EAS emissions baselines can provide crucial context for regulatory responses, helping to appropriately balance short-term versus long-term and local versus regional considerations in ecosystem management planning. In this work, we aim to estimate historical annual emission baselines in California based on the latest scientific evidence.

Materials and methods

The present work reviews and updates the historical burned area and emissions estimates for California initially presented by Stephens et al. (2007) with science published in the last 18 years. Specifically, we addressed three main questions:

1. What type of vegetation covered California?

   To determine this, we used the Landfire Biophysical Settings (BpS) map (LANDFIRE, 2024) as our base map. This product represents potential vegetation layers through a complex modeling setup. BpS types were grouped into fire regime types using crosswalks. Notably, this product is biased towards late seral stages of vegetation, often misrepresenting grass-type vegetation. To update the surface of grasslands, we used three additional sources of information:

   - Phytolith data: Phytoliths are microscopic silica structures formed in and between plant cells produced by vegetation that remain in the soil for millennia. Grasses are prolific phytolith producers, and the density of these structures in the soil is a good indicator of grassland presence. We used the outputs from Fick et al. (2018) to map grasslands wherever the phytolith density was above 0.3%.

   - Native American village locations: Indigenous peoples had an intense cultural burning pattern for management, which, according to historical reports and Spanish diaries, created a grass-chaparral mosaic. Some studies suggest a half-day walk (around 4 km) buffer around each village was intensively managed (Keeley 2002). Using the atlas and handbooks information (Scherer, 1978), we mapped village locations and applied a 4 km buffer around each, designating the BpS-chaparral areas as grass vegetation.

   - Historical and hydrological maps: Certain regions in California have historical vegetation maps created from reconstructions of photographs, reports, etc. We used the California State University Chico Map (California State University, 2003), which represents vegetation before the year 1900 for the Central Valley.

2. How often did this vegetation burn?

   We used Fire Rotation Period (FRP) estimates for all California fire regime types, including commonly misrepresented groups such as grasses, deserts, and riparian vegetation. Fire Rotation Periods represent the number of years required to burn an area equal to the extent of the vegetation in question. We divided the total area of each fire regime type by its fire rotation period to estimate the

   average annual area burned (hectares per year per vegetation type). FRP data were retrieved from the literature, where they were calculated using various techniques

such as fire scar dendrochronology, archaeological site evidence, lake and ocean sediment cores, and written and oral histories.

3. What are the associated emissions?

   Once we estimated the annual burned area per vegetation type, we applied the modern FOFEM (First Order Fire Effects Model) simulation model v6.7. FOFEM estimates fuel consumption and smoke emissions caused by prescribed fires or wildfires. We applied a "light fuels" configuration to our fire regime types, assuming that forests had fewer fuels due to more frequent burns. Although moisture conditions are critical and mostly unknown for past burning conditions, we applied a mix of "dry" and "very dry" moisture regimes as proposed by Stephens et al. (2007).

Results

The current work does not yet define a burning regime for the entire state of California (due to ongoing calculations for the historical vegetation distribution map). Instead, it presents an application for the Central Valley.

The Central Valley BpS map shows a vegetation distribution with scarce grasslands but extensive oak woodland and chaparral (Figure 1-left). Using this map, we applied fire rotation burn area calculations and emissions simulations. The results estimated an annual burned area of 214,366 hectares, 2,134 Gg of carbon emissions, and 18.24 Gg of fine particulate PM2.5 emissions.

However, when we applied the same methodology using the California State University Chico Map, which represents much more extensive grasslands and marsh ecosystems, the annual burned area nearly doubled to 413,607 hectares (Figure 1-right). Despite the larger burned area, emissions were lower, with 1,595 Gg of carbon emissions and 11.12 Gg of fine particulate PM2.5 emissions.

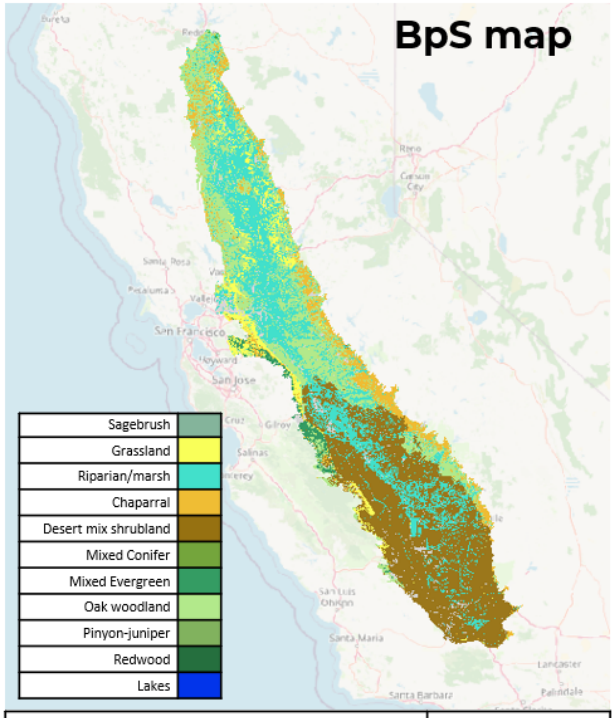

Burned area annually (ha)	214366
CO_2 emissions (Gg)	2134.00
PM2.5 emissions (Gg)	18.24

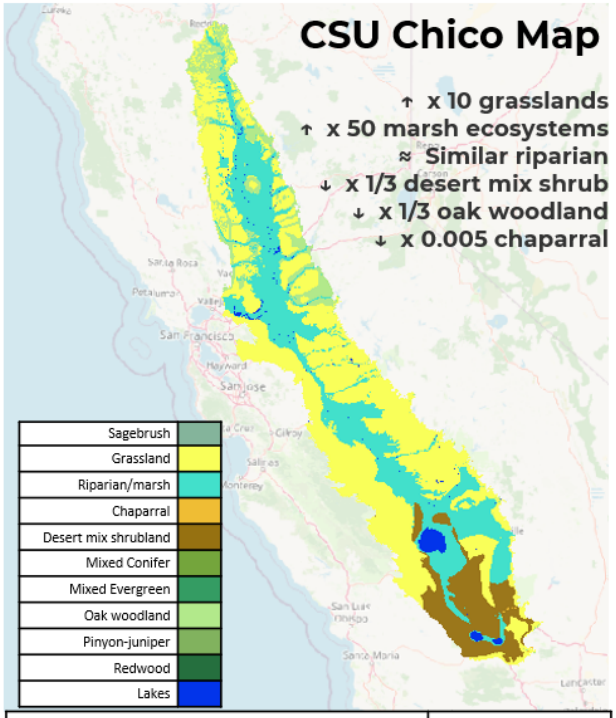

Burned area annually (ha)	413607
CO_2 emissions (Gg)	1595.00
PM2.5 emissions (Gg)	11.12

Figure 1. Comparison of the pre Euro-American fire regime in the Central Valley in California according to two different map sources: the Biophysical settings on the left, and the California State University Chico Map on the right.

Discussion

This work represents a first step towards a more accurate and updated estimation of pre-Euroamerican fire regimes in California. Our methodology includes the development of a revised and improved map of California's pre-European settlement vegetation, utilizing diverse and reliable sources of information. We also incorporate indigenous cultural burning practices into our estimates of vegetation type distribution and fire frequencies.

The provisional results for the Central Valley reveal contrasting and insightful findings: while an increase in grassland-type cover, when using the CSU Chico map, leads to a higher total burned area compared to using the BpS map, it results in lower total carbon and smoke emissions. The choice of the baseline map is critical for estimating historical burned area and emissions, especially when considering changes in highly burnable vegetation covers such as grasslands. The BpS map, although a valuable product for representing potential vegetation at a national scale, needs to be carefully evaluated in historically managed lands when assessing pre-Euroamerican features. Updating the baseline with other sources of information is essential to eventually achieve a reliable product.

California is clearly - and has been for many millennia - a smoky place. While mechanical fuel management and firefighting can protect human lives and infrastructure, they are unlikely to significantly curb the increasing trend of severe wildfires. Restoring fire as a management tool is critical to avoid the high emissions associated with high-fuel-load, high-intensity fires. Transparent and honest discussions are needed to decide whether to use controlled burning as a management tool under partially controlled and less emissive conditions or to allow California's forested lands to experience large, uncontrolled wildfires that exceed historical baseline emissions.

Acknowledgments
We want to thank the valuable contributions of Scott Stephens, Don Hankins, Frank Lake, Jon Keeley, Frank Davis, Carla d'Antonio, Robert Cuthrell and Kent Lightfoot for the realization of this work.

References

California State University (2003). THE CENTRAL VALLEY HISTORIC MAPPING PROJECT. (California State University, Chico Department of Geography and Planning and Geographic Information Center)

Fick, SE, & Evett, RR (2018). Distribution modelling of pre-Columbian California grasslands with soil phytoliths: New insights for prehistoric grassland ecology and restoration. *PLoS ONE*, *13*(4).

Forest Climate Action Team (2018) California Forest Carbon Plan: Managing Our Forest Landscapes in a Changing Climate. Sacramento, CA. 178p

Forest Management Task Force (2021). California's Wildfire and Forest Resilience Action Plan. California Department of Water Resources, Public Affairs Office, Creative Services Branch. Sacramento, CA. 84p

Keeley, JE (2002). Native American impacts on fire regimes of the California coastal ranges. *Journal of Biogeography*, 29, 303–320

LANDFIRE, (2024). *Biophysical Settings Layer.* (U.S. Department of the Interior, G. S. and U. S. D. of Agriculture). http://www.landfire/viewer.

Safford, HD, Hayward, GD, Heller, NE & Wiens, JA (2012). Historical ecology, climate change, and resource management: can the past still inform the future? In Historical environmental variation in conservation and natural resource management. Editors: John Wiens, Gregory Hayward, Hugh Safford and Catherine Giffen. (Wiley-Blackwell).

Scherer, JC (Ed.) (1978). Handbook of North American Indians, Vol. 8, California. (Smithsonian Institution).

Stephens, S., Martin, RE, & Clinton, NE (2007). Prehistoric fire area and emissions from California's forests, woodlands, shrublands, and grasslands. *Forest Ecology and Management*, 251(3), 205–216.

Proceedings for the 7th International Fire Behavior and Fuels Conference April 15-19, 2024, Boise, Idaho, USA – Tralee, Ireland – Canberra, Australia Published by the International Association of Wildland Fire, Missoula, Montana, USA

Hybrid Machine Learning and Physics-based Tool for Simulating Wildfire Spread in Urban Area: Application to Risk Management

*Mehdi Karzar Jeddi
Aon Impact Forecasting, 200 E Randolph St, Chicago, Illinois, USA,
medhi.karzar.jeddi@aon.com

**Corresponding Author*

Introduction

Wildfire spread into urban areas poses a significant risk to properties and businesses, making it a major concern for the insurance industry in the United States. Accurate quantification of this risk can help insurers mitigate the risks they are underwriting and enable citizens to be aware of potential financial losses and prepare accordingly. A key tool for the property and casualty insurance industry is natural catastrophe modeling, which involves creating thousands of years of probabilistic realizations to estimate loss projections for upcoming peril seasons. By using a stochastic sample of events, insurers can calculate the average annual loss estimate, events return period, and the probabilistic maximum loss for any given insurance portfolio. These parameters are essential for pricing the risk being transferred between stakeholders in the insurance industry (Mitchell-Wallace *et al*. 2017). The lack of a reliable probabilistic model for wildfire spread into wildland-urban interfaces has been an ongoing challenge for the insurance industry. In this work, we propose a machine learning model combined with a quasi-physics-based model for simulating wildfires that spread into urban areas.

Simulation of wildfires

The Rothermel equation, developed at FireLab, has been a major tool for simulating surface wildfire spread (Rothermel 1972). Over the past few decades, many models have been developed by combining Rothermel's surface fuel model with crown fire models for physics-based simulation of wildfires in wildland areas, such as (Finney 1998, Lautenberger 2013, Tymstra *et al.* 2010). Finney et al. developed a probabilistic model for wildfire occurrence and spread in the continental United States (Finney *et al.* 2011). These computational models use the standard fuel model of Scott and Burgan, combined with terrain and crown properties mapped by the USGS (www.landfire.gov). While Landfire provides essential information for simulating fire spread and intensity in wildland areas, it considers urban areas unburnable. Consequently, simulators stop the spread of wildfires when they reach the border of urban areas.

Recent efforts have aimed to accurately estimate fire spread in urban areas and the survivability of structures during wildfires. Researchers have used graph theory to model interactions between structures and their environment, considering each building as a node and connections representing factors such as proximity to vegetation, other buildings, and fire breaks (Chulahwat *et al.* 2022). A quasi-empirical model has also

been developed to consider radiation and fire spotting as major fire spread modes into urban interfaces (Masoudvaziri 2021). Additionally, CFD models have shown the capability to produce realistic fire behavior simulations (Ganteaume 2023). While these models provide valuable insights into fire spread in scenario-based simulations, their application for catastrophe modeling of wildfires—requiring continental-scale simulations with thousands of stochastic realizations of fire seasons—is not yet feasible with current computational resources.

In a recent work, we proposed an equivalent fuel model for Rothermel-based simulation of wildland fires spreading into urban areas. This model is based on the different fuel sizes and fuel loads of a single house, as well as the structure density of buildings in the urban area (Jeddi 2022). While this model is useful for calculating the spread and intensity of fires in urban areas, it does not account for the circumstances that can affect the probability of conflagration in urban areas.

Machine learning tool

The circumstances under which wildfires occur can significantly influence their spread into urban areas. A comparison of the footprints of Lightning Complex Fire (2008) and Camp Fire (2018) illustrates this point as shown Figure 1. On the left of the figure are the footprints of the Lightning Complex Fire (2008) and the Camp Fire (2018), both of which started near Paradise, California. Although both wildfires ignited at points very close to each other east of Paradise, the spread of the Lightning Complex Fire was controlled before it could reach Paradise. In contrast, the circumstances and rate of spread of the Camp Fire caused it to rapidly move westward into the city, resulting in catastrophic loss of lives and extensive structural damage (Maranghides et al. 2023).

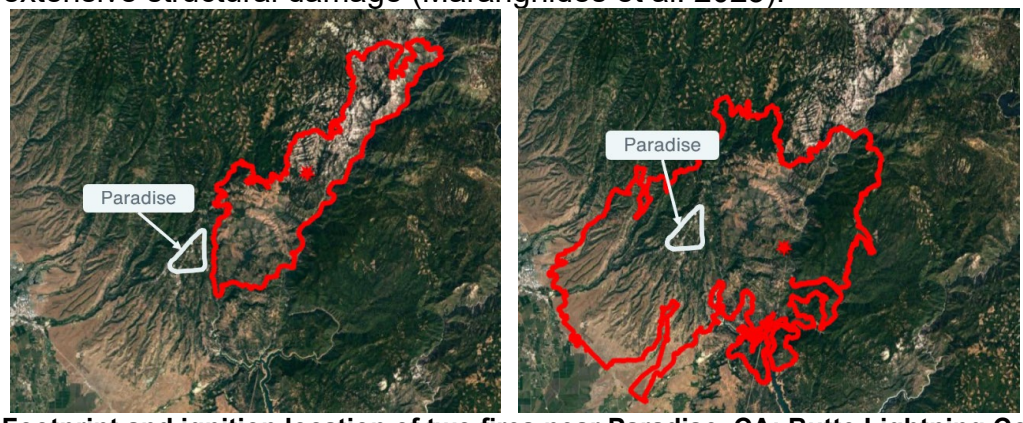

Figure 24: Footprint and ignition location of two fires near Paradise, CA: Butte Lightning Complex (2008) on the left and Camp Fire (2018) on right.

To account for the circumstances under which fires ignite and spread, we developed a two-step machine learning model. This model uses data on historical fire footprints, urbanization at the time of the fire, vegetation cover around the ignition area, wind conditions, and meteorological conditions both at the time of and prior to the fire. The machine-learning model first classifies whether wildfires could spread into urban areas.

If the model predicts that a wildfire could spread to an urban area, it then estimates how much of the urban area this wildfire will burn.

Before starting the simulation of wildfire spread, the ML model predicts whether the wildfire will spread into the urban area and, if so, how much of the urban area it will burn. For each time step the simulation is performed using a quasi-physics-based fire simulator. At the end of each time step of the fire spread simulation, the ML model checks how much of the urban area has been burned by the wildfire. When the wildfire burns as much of the projected urban area as predicted by the ML model, the model stops the fire from spreading further into the urban area. The simulation of wildfire spread in wildland continues until the fire reaches its assigned area.

Figure 2 shows sample simulations of wildfire spreads predicted to burn urban areas. In these simulations, the wildfire starts at the ignition location, jumps over the river, spreads into the urban area, and burns as much of the urban area as assigned by the ML model. It then stops burning more of the urban area and continues to burn only wildland until it reaches the final assigned footprint of the wildfire.

Using this model, we are developing the new edition of Aon's Impact Forecasting wildfire catastrophe model, in which we generate 10 years of realizations of wildfire seasons.

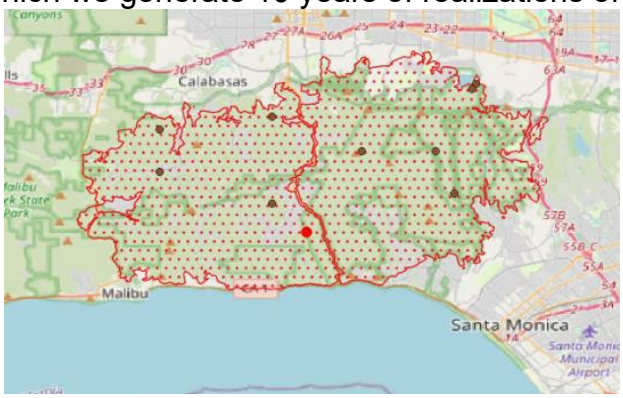

Figure 25: Footprint of a simulated stochastic fire originating northwest of Los Angeles, CA. The fire crosses State Route 27, affecting urban areas from Tarzana, CA and northwest of Los Angeles, CA.

References

Chulahwat A, Mahmoud H, Monedero S, Diez Vizcaíno FJ, Ramirez J, Buckley D, Forradellas AC (2022) Integrated graph measures reveal survival likelihood for buildings in wildfire events. *Scientific reports*, **12**(1), 15954, 1-12.

Finney MA (1998) *FARSITE, Fire Area Simulator-model development and evaluation* (No. 4). US Department of Agriculture, Forest Service, Rocky Mountain Research Station.

Finney MA, McHugh CW, Grenfell IC, Riley KL, Short KC (2011) A simulation of probabilistic wildfire risk components for the continental United States. *Stochastic Environmental Research and Risk Assessment*, **25**, 973-1000.

Ganteaume A, Guillaume B, Girardin B, Guerra, F (2023) CFD modelling of WUI fire behaviour in historical fire cases according to different fuel management scenarios. *International journal of wildland fire*, **32**(3), 363-379.

Jeddi M.K. (2022) An equivalent fuel model for wildland urban interface–Application to risk management. In 'Advances in Forest Fire Research', (Eds Viegas DX, Ribeiro LM), pp 509-5011. (Coimbra University Press, Coimbra).

Lautenberger C (2013) Wildland fire modeling with an Eulerian level set method and automated calibration. *Fire Safety Journal*, **62**, 289-298.

Maranghides A, Link E, Mell W, Hawks S, Brown C, Walton W (2023) A Case Study of the Camp Fire—Notification, Evacuation, Traffic, and Temporary Refuge Areas. (National Institute of Standards and Technology, Gaithersburg, MD), NIST Technical Note (TN) 2252.

Mitchell-Wallace K, Jones M, Hillier J, Foote M (2017) Natural catastrophe risk management and modelling: A practitioner's guide. John Wiley & Sons.

Masoudvaziri N, Bardales FS, Keskin OK, Sarreshtehdari A, Sun K, Elhami-Khorasani N (2021) Streamlined wildland-urban interface fire tracing (SWUIFT): modeling wildfire spread in communities. *Environmental Modelling & Software*, **143**, 105097, 1-15.

Rothermel RC (1972) *A mathematical model for predicting fire spread in wildland fuels* (Vol. 115). Intermountain Forest & Range Experiment Station, Forest Service, US Department of Agriculture.

Tymstra C, Bryce RW, Wotton BM, Taylor SW, Armitage OB (2010) Development and structure of Prometheus: the Canadian wildland fire growth simulation model. *Natural Resources Canada, Canadian Forest Service, Northern Forestry Centre, Information Report NOR-X-417.(Edmonton, AB)*.

Integrating fire management and heritage protection to create fire-resilient landscapes through remote sensing technologies and simulation software

Ana Solares-Canal
Escola de Enxeñaría Forestal, Universidade de Vigo, 36005 Pontevedra, Spain, ana.solares@uvigo.es

Thais Rincón
Escola de Enxeñaría Forestal, Universidade de Vigo, 36005 Pontevedra, Spain, thaisvirginia.rincon@uvigo.es

Laura Alonso
Escola de Enxeñaría Forestal, Universidade de Vigo, 36005 Pontevedra, Spain, laura.alonso.martinez@uvigo.es

Juan Picos
Escola de Enxeñaría Forestal, Universidade de Vigo, 36005 Pontevedra, Spain, jpicos@uvigo.es

*Julia Armesto
Escola de Enxeñaría Forestal, Universidade de Vigo, 36005 Pontevedra, Spain, julia@uvigo.es

**Corresponding Author*

Introduction

In the new era of large, high-intensity wildfire events, new fire prevention and extinction strategies based in the implementation of fire-resilient landscapes are needed (Ortega et al. 2024). For that end, it is important to find critical zones that can be considered as strategical management areas (SMA) for wildfires management (Madrigal et al. 2019, Krsnik et al. 2024), where fuel reduction can entail a different fire behavior or reduce fire risk.

Different strategies must be established according to the characteristics that define the identity of each territory. It has been observed that archaeological assets, that are defining elements, are placed in favorable topographic locations. Besides they are usually covered or surrounded by vegetation (Dimitropoulos et al. 2010). In addition, wildfires have been considered one of the main threats to heritage since the World Heritage Convention of 1972. Considering that vegetation is a key factor in wildfire spread, the management of archaeological sites could improve assets conservation and it would reduce the threat to visitors, considering that the periods of high risk coincide with the peak tourist season (Markham et al. 2016).

In this study a whole workflow process to identify those assets of interest and the necessary fuel treatments has been developed. This proposed workflow is based on the use of remote sensing and wildfire simulation software.

Materials

Study area

This study was conducted in a pilot area located in the region of Galicia, Spain (Figure 1). The pilot area has a total area of 365.19 km2.

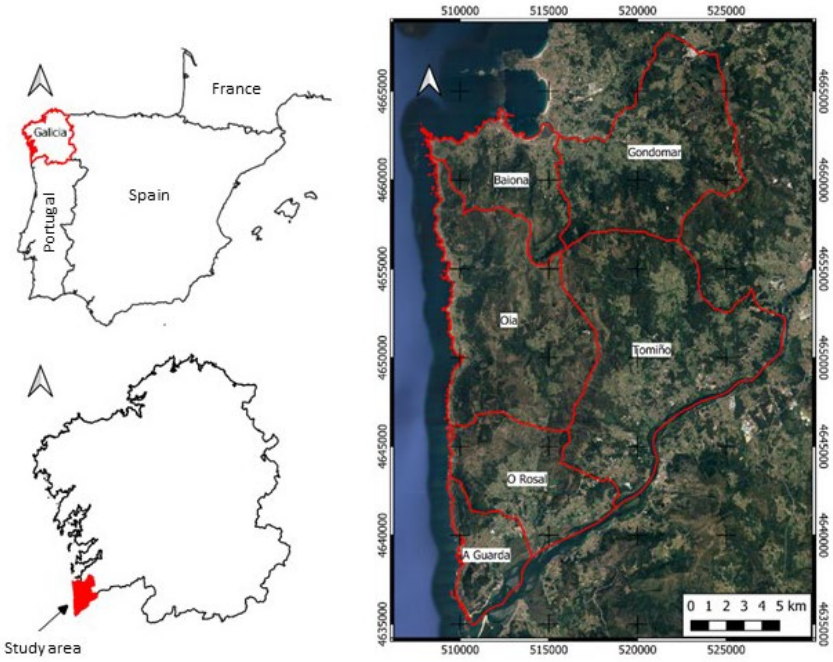

Figure 26: Study area

Main materials

The main materials are described in Table 1.

Table 1: Main materials.

PRODUCT	DATA	SOURCE
Georeferenced Galician heritage database	-	Xunta de Galicia
Sentinel-2 images	2019	European Space Agency (ESA)
LiDAR aerial data	2019	Instituto de Estudos do territorio (IET)

Methodology

Archaeological sites selection and paleointerface characterization

The location of the archaeological sites in the study area was accomplished through the official data base of heritage. Their influence areas (paleointerface areas) were created

by generating a buffer of 100 m around the elements. The overlapped areas were dissolved obtaining groups that could be used to define SMA. Their physical and topographical environment was characterized according to the type of land cover, the topographical situation (TPI index) and the area. The groups of interest were selected considering the values included in Table 2.

Table 2: Criteria to define potential groups of elements to be used as SMA.

SELECTION CRITERIA	VALUES
Land cover	Eucalyptus, conifers, broadleaves, shrubs, rocky areas
Area	5-20 ha
TPI	Upper slopes, hilltops

Forest fuel mapping

A methodology was followed to obtain updated fuel maps based on LiDAR data and multispectral satellite images (Solares-Canal et al., 2023). The multispectral images were used to obtain a land cover map, and the LiDAR data to characterize vegetation height and structure. Rothermel fuels models were mapped, since they are globally extended. The land cover map and the structural information were combined following the cited methodology. As a result, a map with the geospatial distribution of forest fuels in the study area was obtained.

Wildfire simulation in current conditions

The third task was to simulate wildfires with the obtained fuel model map following the methodology described in Rincón et al. 2024. A grid of 1kmx1km was defined to stablish starting points through a systematic criterion. Two conditions of meteorological values were defined: the typical conditions, using averaged values of a ten-years series (2012-2021), and the atypical conditions, using historical maximums. Each condition considers four different scenarios. A total of 2840 simulations were carried out.

Each simulation results in a vector polygon that represents the size that the fire reaches after the propagation time. Also, two raster layers are generated: one corresponds to the rate of spread (ROS) in kilometers per hour and the other to the front intensity (FLI) in kilowatts per meter. The main and secondary fire paths of each simulation are also obtained as a raster layer.

Wildfire simulation in modified conditions

The obtained fire paths were integrated according to their weather condition, and they were used to select the groups of archaeological elements that could be used to define

SMA. For that, they were intersected with the groups of interest selected in the first step of this methodology. Thus, the potential SMA are defined, considering the most endangered areas and the most visited elements. Finally, the fuel models were modified in those SMA using the fuel model map. In this case, the proposed modification is to change model 4 to 5 and 7 and 10 to 9. The previous cited methodology to simulate wildfires was applied using the modified map.

Results and discussion

Archaeological sites selection and paleointerface characterization

In the in the study area 755 heritages sites were archaeological sites, being 91.7% of them placed in forest areas. They were transformed in 319 groups, 39 of them were then considered candidates to be used as SMA.

Wildfire simulation in current conditions

Figure 2 graphically shows the main integrated results obtained from the simulations performed in typical conditions and in atypical conditions.

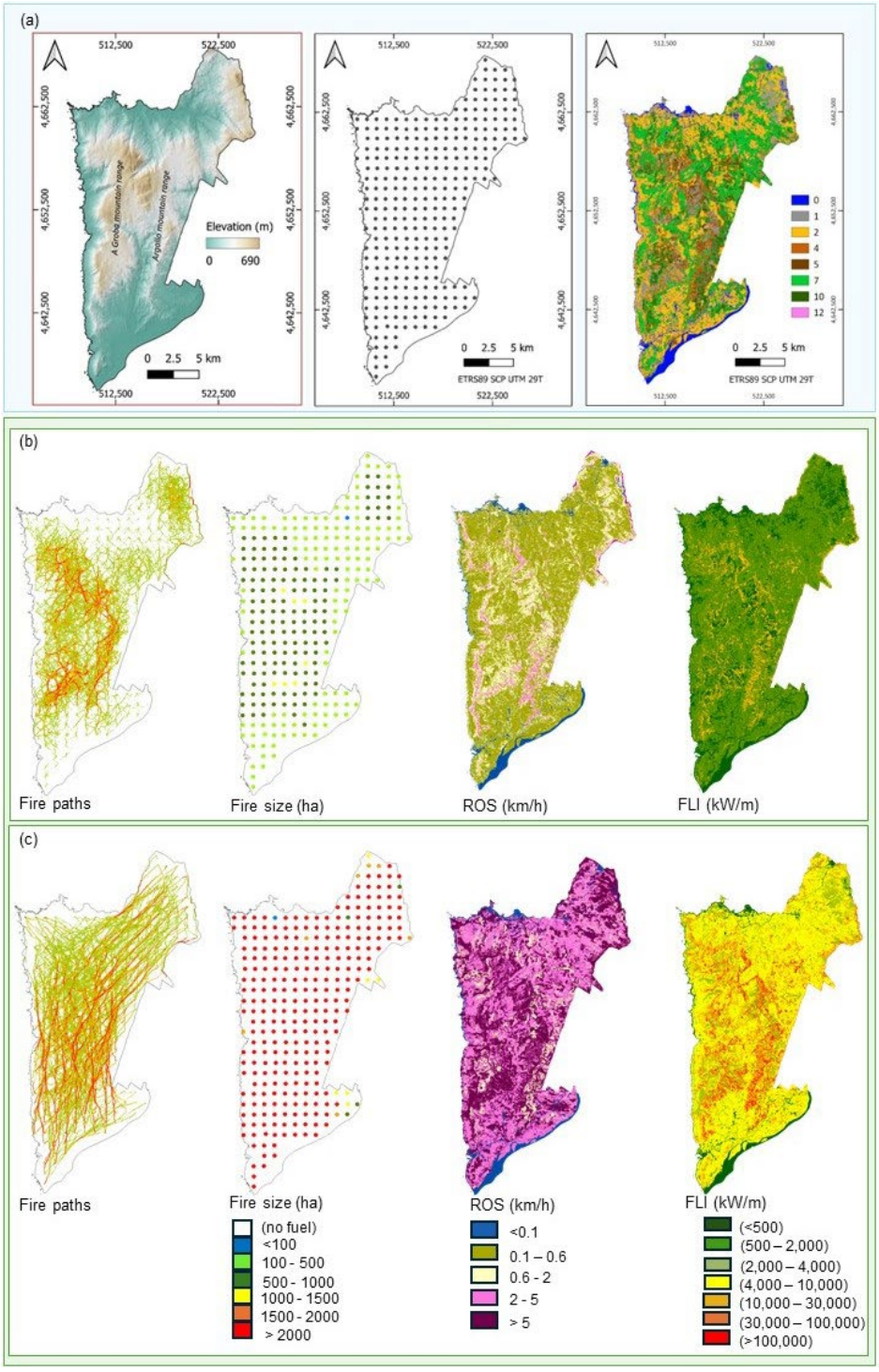

Figure 2: (a) Main inputs of the performed simulations. From left to right: DTM (digital terrain model); starting points; fuel model map. (b) Integrated results obtained from the typical weather scenarios. (c) Integrated results from the atypical weather scenarios.

Wildfire simulation in modified conditions

After intersecting fire paths and the 39 groups, 4 SMA were proposed. Examples of how the rate of spread and the intensity changes with the proposed modifications in one of the proposed SMA, can be observed in Figures 3 and 4.

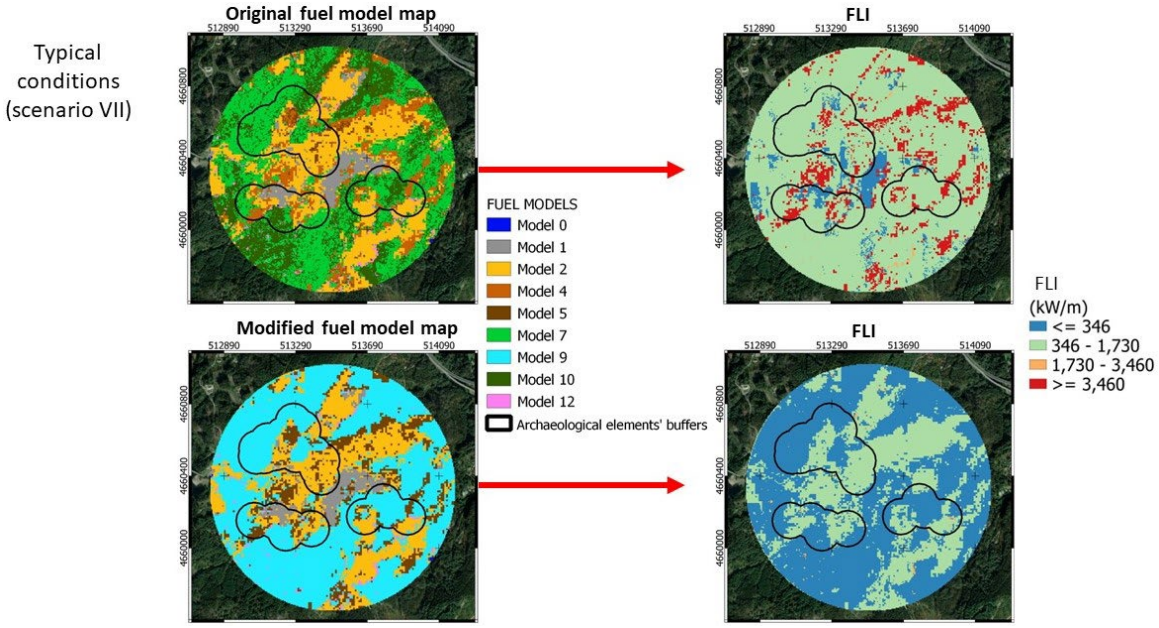

Figure 3: Comparison of the fire intensity obtained from wildfire simulations with the original fuel model map.

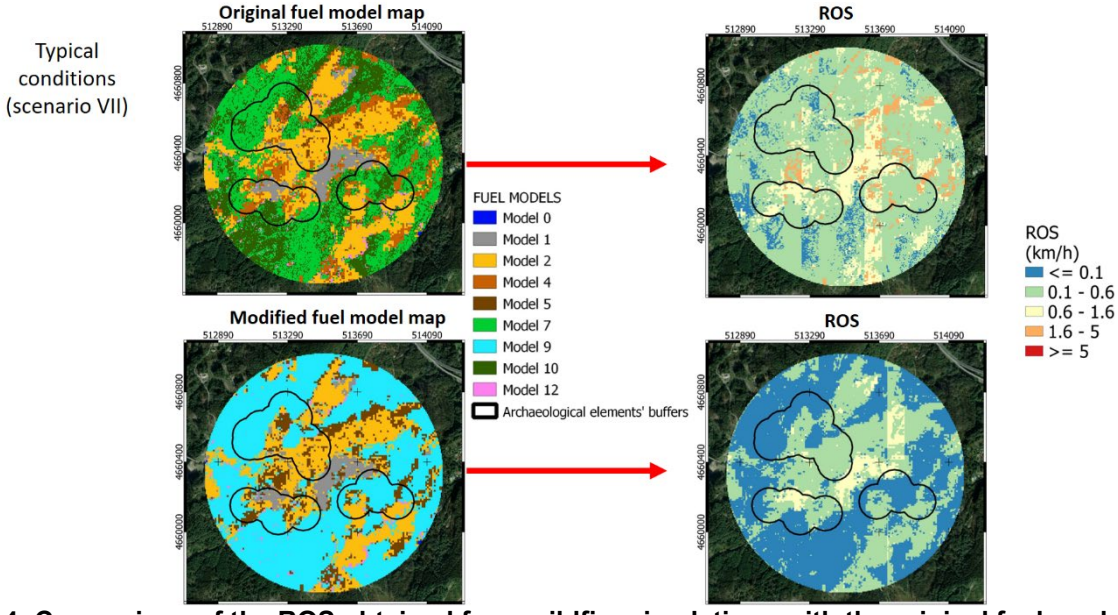

Figure 4: Comparison of the ROS obtained from wildfire simulations with the original fuel model map.

The examples with current fuels show that 11% of the area would develop very high intensity wildfires. The proposed modifications involve that most of the area (the 63%) develops very low intensity. Further, with the original fuel model map, the 5% of the area develops a very high ROS, whereas by modifying the fuels, this class of ROS becomes insignificant. With the original map, only the 9% of the area has a ROS under 0.1 km/h and with the modified map this percentage increases to 54%.

Conclusion

In this work, 39 groups of archaeological sites were established as potential strategic areas of management and defense against wildfires. Also, an operational and updated fuel model map was obtained for an Atlantic landscape was obtained. Finally, results obtained from the simulations allowed prioritizing the archaeological assets and the most adequate fuel treatments that lead to a fire-resilient landscape. This whole process will help to address in an integrated way fire management and archaeological heritage protection.

Acknowledgements

This research is part of the project “Prevention and management of the landscape exposed to large forest fires in cross-border rural areas between Spain and Portugal”, Program EP-INTERREG V, grant FIREPOCTEP+, and the project “Paleointerface: Strategic element for the prevention of forest fires. Development of multispectral and 3d analysis methodologies for integrated management” project, funded by MICIU/AEI/10.13039/501100011033, Spanish Ministry of Sciences and Innovation, Grant code PID2019-111581RB-I00.

References

Dimitropoulos K, Köse K, Grammalidis N, Cetin, E (2010) Fire detection and 3d fire propagation estimation for the Protection of cultural heritage areas. International Archives of the Photogrammetry, Remote Sensing and Spatial Information Sciences, 38(8), 2010, pp. 620-625.

Krsnik G, Olivé EB, Nicolau MP, Larrañaga A, Terés JÁ, Garcia-Gonzalo J, Olabarria JRG (2024). Spatial multi-criteria analysis for prioritising forest management zones to prevent large forest fires in Catalonia (NE Spain). *Environmental Challenges*, 15, 100959.

Madrigal J, Romero-Vivó M, Rodríguez y Silva F (2019) ‘Definición y Recomendaciones Técnicas en el Diseño de Puntos Estratégicos de Gestión’ Generalitat Valenciana; Conselleria d’Agricultura, Medi Ambient, Canvi Climatic i Desenvolupament Rural: Valencia, Spain. ISBN 978-84-941695-4-0

Markham A, Osipova E, Lafrenz Samuels K, Caldas A (2016). World Heritage and Tourism in a Changing Climate. United Nations Environment Programme, Nairobi, Kenya and United Nations Educational, Scientific and Cultural Organization, Paris, France. UNESCO publishing. ISBN: 978-92-3-100152-9

Ortega M, Silva FR, Molina JR (2024) Modeling fuel break effectiveness in southern Spain wildfires. *Fire Ecology* 20, 40.

Rincón T, Alonso L, Picos J, Molina-Terrén DM, Armesto J (2024) A Systematic Approach to Map and Evaluate the Wildfire Behavior at a Territorial Scale in the Northwestern Iberian Peninsula. *Fire* 7(7), 249.

Solares-Canal A, Alonso L, Rincón T, Picos J, Molina-Terrén DM, Becerra C, Armesto J (2023) Operational fuel model map for Atlantic landscapes using ALS and Sentinel-2 images. *Fire Ecology* 19, 61.

Proceedings for the 7th International Fire Behavior and Fuels Conference April 15-19, 2024, Boise, Idaho, USA – Tralee, Ireland – Canberra, Australia Published by the International Association of Wildland Fire, Missoula, Montana, USA

Intelligent Wildfire Surveillance and Management System

*Damir Krstinić, Ljiljana Šerić, Marin Bugarić, Darko Stipaničev
University of Split, Faculty of Electrical Engineering, Mechanical Engineering and Naval Architecture, Croatia, damir.krstinic@fesb.hr

**Corresponding Author*

Introduction

Environmental protection is one of humanity's most important tasks, with wildfires representing one of the greatest threats to the ecosystems, as well as for the infrastructure and human lives. Early detection of a forest fire, followed by a quick and effective response, is essential to reduce damage while minimizing the risk to people, both firefighters and civilians. Modern information and communication technologies can provide tools to help mitigate the risk of wildfires to all actors and services involved in the forests management and fire protection.

We present Intelligent Wildfire Surveillance and Management System based on integration of multiple data sources. The system is primarily designed to monitor large and inaccessible areas based on cameras in visible spectrum, trying to find early visual signs of fire. It is tightly coupled with the GIS and other sources of information, like meteorological information gathered in real-time from meteorological service. Augmented reality model of the terrain is developed and overlapped with the real world scene, integrating all of the collected and produced information to provide an operator a decision support system in all phases of wildfire management.

Croatian Experiences

Croatia belongs to countries with an increased risk of large forest fires. Traditionally, coastal areas and islands are the most threatened. However, due to climate change, forest fires are becoming more frequent in other parts of Croatia as well. The specificity of the Croatian coast is the indentation of the relief with villages and towns surrounded by dense pine forests which often enters settlements. There are also separate tourist settlements, such as auto camps, apartment complexes or isolated individual houses, and other places of increased human activity, such as places popular for adventure activity, hiking areas, etc. Furthermore, during the main fire season, which coincides with the peak of the tourist season, there is a significant population growth by the order of magnitude or even more. Two facts emerge from these considerations:

- The entire coastal area is practically Wildland Urban Interface (WUI)
- There is a high probability that someone will spot the fire very early

After the devastating fire in 2003 on the island of Hvar, the development of a system for early detection and monitoring of forest fires was initiated. From the very beginning the system was developed in cooperation with the firefighters. Based on the

aforementioned considerations, the following requirements for system functionalities were defined:

- Early detection, if possible only few minutes from the ignition
- Quick and accurate incident confirmation with the possibility of determining the exact location of the incident as precisely as possible
- Video presence with the aim of efficient and safer intervention management
- Decision support providing all the available information, including maps, fire spread prediction, meteorological data etc.
- Storage of all information collected in real time for later analysis or conducting investigations by competent services

STRIBOR – OIV FireDetect AI

Wildfire Surveillance and Management System, developed under the working name Stribor (Slavic god of wind and forest) at the Faculty of Electrical Engineering, Mechanical Engineering and Naval Architecture (FESB) of the University of Split was tested for the first time in 2007 and has been constantly improved with new functionalities based on suggestions of the end users (Stipaničev et al., 2007)(Stipaničev et al.,2009)(Štula et al., 2012)(Jakovčević et al. 2013). Since 2018, the system has been commercialized in cooperation with OIV Digital Signals and networks under the commercial name OIV FireDetectAI (OiV Fire Detect AI, 2024). The system integrates available sensory information and provides decision-making and management support in all phases of firefighting. The system is cloud-based and the user only needs a web browser and the appropriate credentials to access the system.

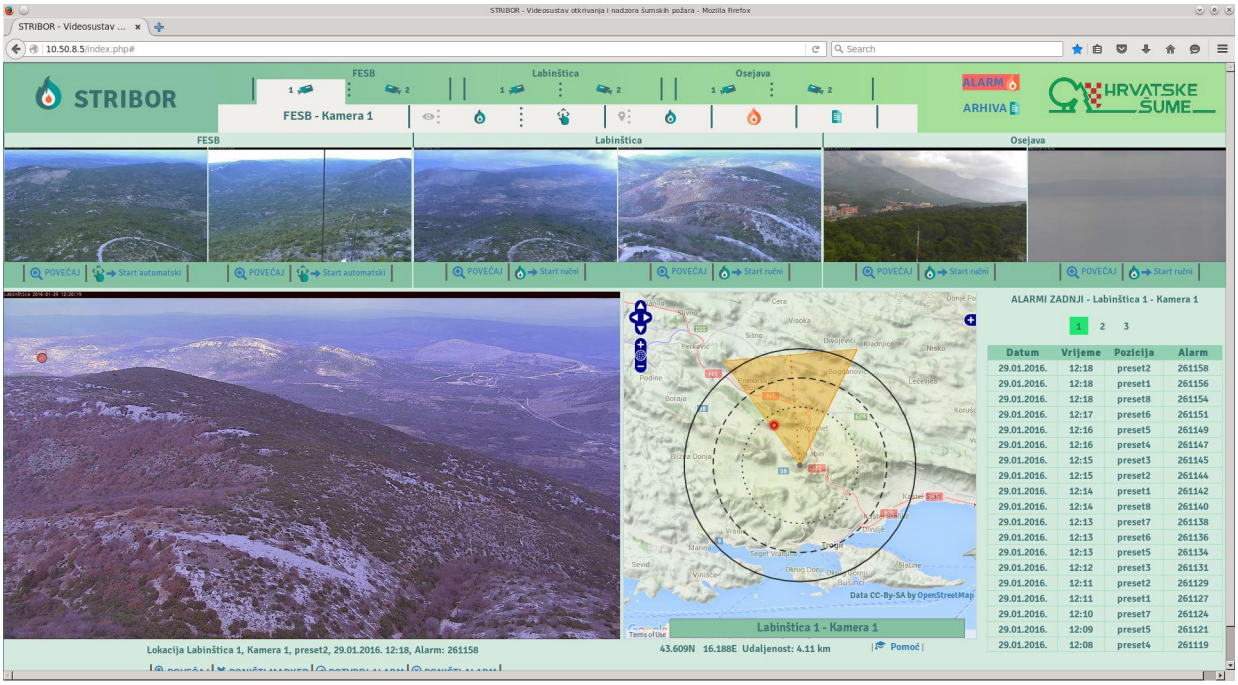

Figure 27: Wildfire surveillance system interface with an example of fire detection

Automatic early wildfire detection based on cameras in visible spectra

According to the previously defined system functionality requirements, the detection of early signs of a forest fire should be realized within 5 minutes from the moment of the fire outbreak, with the expected detection distance up to ten kilometers. Under these conditions, the smoke occupies only very small area of the image and is often hardly visible due to degradations like dust in the air, dirt on the lenses, sunlight effects etc. The system interface with an example of smoke detection is shown in Figure 1.

Figure 28: Automatic detection and incident confirmation using camera in manual mode

After incident notification, regardless of whether it is an automatic detection or a reported alarm, the operator has the option of switching to manual control mode. By using optical zoom up to 32 times, the operator rejects or confirms the alarm and initiates the intervention, as shown in Figure 2. Video presence is also useful for rapid hazard assessment and intervention management.

GIS integration

The system is tightly coupled with the GIS and other sources of information, like meteorological information gathered in real-time from meteorological service. Augmented reality model of the terrain is developed and overlapped with the real world scene, integrating all of the collected and produced information to provide an operator a decision support. Based on this model, the operator can precisely locate the point of fire outbreak by simply clicking on the image from the camera on which the smoke is visible. Coordinates from the image space are transferred based on augmented reality into geographic coordinates and are displayed on the map. Magnified map with the fire outbreak location of the incident in Figure 1 is shown in Figure 3.

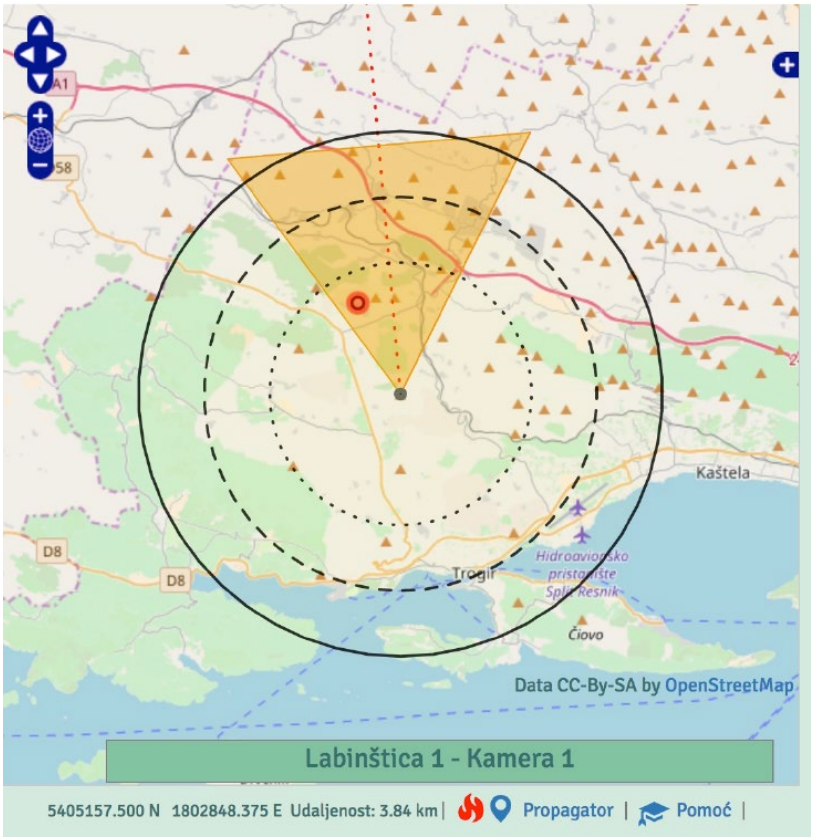

Figure 29: Locating the point of fire outbreak based on an augmented reality model

Fire spread simulation

Knowing the exact location of the fire outbreak, propagation simulation, which is also integrated into the system, can be started. The propagator collects the current meteorological situation and short-term forecast from the meteorological service and computes fire spread simulation. Input video streams and fire spread prediction produced by the system is shown on the map to provide a fire commander support in decision making, as shown in Figure 4.

Figure 30: Fire spread simulation based on real-time meteo data

Operator can also set meteorological data manually and start fire spread simulation using this data. This functionality is often used by fire commanders for training, preparation and risk assessment.

Based on the described functionalities of the system, common procedure includes the following steps:

1. Automatic detection (or fire reported by other means)
2. Confirmation by zooming in on the location of the fire
3. Pinpointing the location by clicking on the image from the camera
4. Running a fire spread simulation based on the current weather conditions
5. Intervention management using video presence based on one ore more cameras that have a developing fire in their field of vision, GIS suport, additional map layers ...

What next?

Intelligent Wildfire Surveillance and Management System is at the moment deployed at 76 locations in Croatia. At this moment, 38 new locations are being installed, which will be integrated into the system already this fire season.

In addition to the continuous development of the system according to the needs and requirements of all services and actors involved in fire fighting activities, additional value is represented by the data collected from the system. Video sequences are collected from cameras included in the system, together with other available information created at the time of recording the sequence, which will be used to improve system operation and develop new functionalities. In addition, we expect that the collected data can be valuable source of information for future research and a deeper understanding of the physics and mechanics of the wildfire.

References

(OiV Fire Detect AI, 2024) OiV Fire Detect AI (2024) Inteligent Solution for Early Fire

Detection, https://oiv.hr/en/services-and-platforms/oiv-fire-detect-ai/
(Stipaničev et al., 2007) Stipaničev, D, Hrastnik, B., Vujčić, R., Holistic Approach to Forest Fire Protection in Split and Dalmatia County of Croatia, Wildfire 2007 Int.Conference, Sevilla, Spain, May 2007.

(Stipaničev et al., 2009) Stipaničev, D., Štula, M., Krstinić, D., Šerić, Lj., Agent based Intelligent Forest Fire Monitoring System, Proc. of 32. Int. Conference MIPRO 2009, Opatija, May 2009. pp.258-263

(Štula et al., 2012) Štula, M., Krstinić, D., Šerić, Lj. (2012) Intelligent forest fire monitoring system, Information System Frontiers 14, 725–739 (2012). https://doi.org/10.1007/s10796-011-9299-8

(Jakovčević et al., 2013) Jakovčević, T., Stipaničev, D., Krstinić, D. Visual spatial-context based wildfire smoke sensor. Machine Vision and Applications 24, 707–719 (2013). https://doi.org/10.1007/s00138-012-0481-x

(Stipaničev et al.,2015) Stipaničev, D.; Šerić, Lj.; Krstinić, D.; Bugarić, M.; Wildfire video observers network with physical and virtual sensors, Proceeding of 10th EARSeL Forest Fire Special Interest Group Workshop - Sensors, Multi-Sensor Integration, large Volumes: New opportunities and Challanges in Forest Fire Research (CD ROM) / Limassol, Cyprus, 2-5.11.2015

Proceedings for the 7th International Fire Behavior and Fuels Conference April 15-19, 2024, Boise, Idaho, USA – Tralee, Ireland – Canberra, Australia Published by the International Association of Wildland Fire, Missoula, Montana, USA

LadderFuelsR: A new automated tool for vertical fuel continuity analysis and canopy base height detection using LiDAR

*Olga Viedma
Department of Environmental Science. University of Castilla-La Mancha (UCLM), Avda. Carlos III s/n, 45071 Toledo, Spain, olga.viedma@uclm.es

Carlos A. Silva
Forest Biometrics, Remote Sensing and Artificial Intelligence Laboratory (Silva Lab), School of Forest, Fisheries, and Geomatics Sciences, University of Florida, Gainesville, FL 32611, USA, c.silva@ufl.edu

Jose M. Moreno
Spanish Royal Academy of Sciences
Calle Valverde, nº 22 & 24 Madrid, Spain, josem.moreno@uclm.es

Andrew T. Hudak
USDA Forest Service, Rocky Mountain Research Station, Moscow, USA, andrew.hudak@usda.gov

**Corresponding Author*

Introduction

The widespread surface fuel accumulation in fire-adapted forested ecosystems has increased the threat of high-severity wildland fires, especially where fires have been excluded for much longer than was the historical norm. Dense ladder fuels can make fire suppression more difficult, increasing canopy damage (Mitsopoulos and Dimitrakopoulos 2014). Accordingly, vertical forest structure (arrangement of ladder fuels beneath the canopy) and forest canopy structure metrics such as crown base height (CBH), crown dimensions, and crown bulk density, are crucial factors for effective wildfire risk prevention and mitigation (Fernandes 2013; Alcasena et al. 2019; Popescu and Zhao 2008).

Despite advancements, challenges persist in accurately quantifying CBH and ladder fuels. Traditional field-based methods are known to yield reliable CBH measurements, but they are time-consuming and labour-intensive (Cruz et al. 2003). In addition, accurate estimation of CBH is challenging due to the absence of a standardized method for defining CBH thresholds and its difficulties in measurement due to the presence of multiple fuel layers (Cruz et al. 2003). The ability of LiDAR technology to penetrate forest canopies and assess sub-canopy structures makes LiDAR a powerful tool for advancing wildfire modelling and management (Popescu and Zhao 2008; Erdody and Moskal 2010; Zhao et al. 2011). The main objective of this study is to develop a direct wave-based method, built on the differences in LAD percentiles between height bins, to characterize

quantitatively fuel layers and gaps beneath trees and, to estimate the tree CBH according to different criteria.

Materials and methods

Package design

LadderFuelsR is an open-source R package for the analysis of vertical fuel continuity using Leaf Area Density (LAD) profiles from segmented trees. It quantifies ladder fuels properties (base height, depth, LAD percentage and vertical distances), and proposes different methods to identify tree CBH (maximum LAD, and maximum and last distance). The version 0.0.4 of the LadderFuelsR package comprises several functions for ladder fuels analysis and CBH detection and for plotting (Fig. 1).

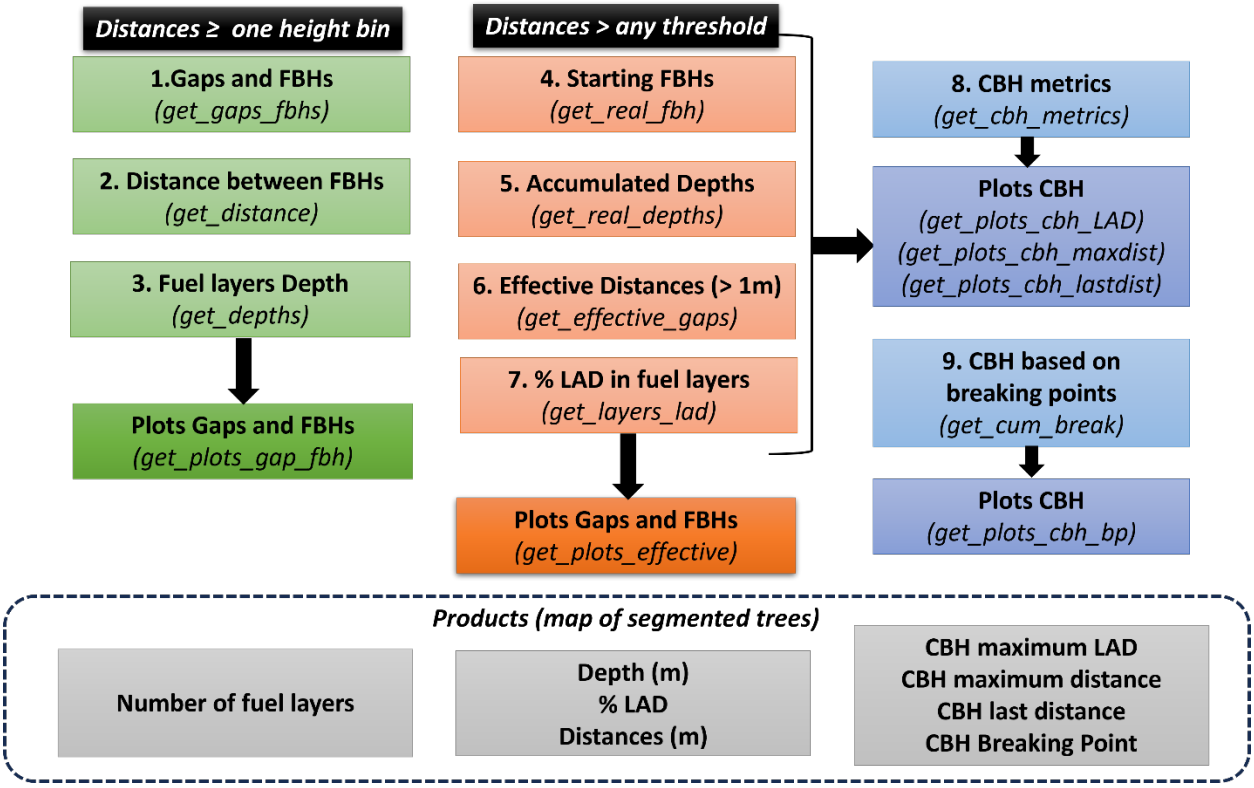

Figure 1. Flowchart to yield the products included in the LadderFuelsR package.

Gaps and Fuel Base Heights (FBHs) for each Vertical Height profile (VHP)

Function *calculate_gaps_perc*() applies the quantile function to the LAD values at each height bin to calculate the 5th, 25th, 50th, 75th, 90th, 95th, and 99th percentiles; and

classifies the LAD values into different groups based on which percentile range they fall into (Fig. 2).

Function *get_gaps_fbhs*() identifies groups of consecutive height bins with negative differences in LAD percentile; and subsets each group with the minimum LAD (< P25th). In addition, when there were no consecutive negative differences, it subsets consecutive height bins with LAD values less than P25th, taking only the first and last values of each group. For obtaining Fuel layer base heights (FBHs), it identifies consecutive height bins with positive differences in LAD percentile, and subsets each group with the minimum LAD (> P5th). For non-consecutive positive differences, it filters consecutive height bins with LAD values > P5th taking only the first and last values of each group (Fig. 2).

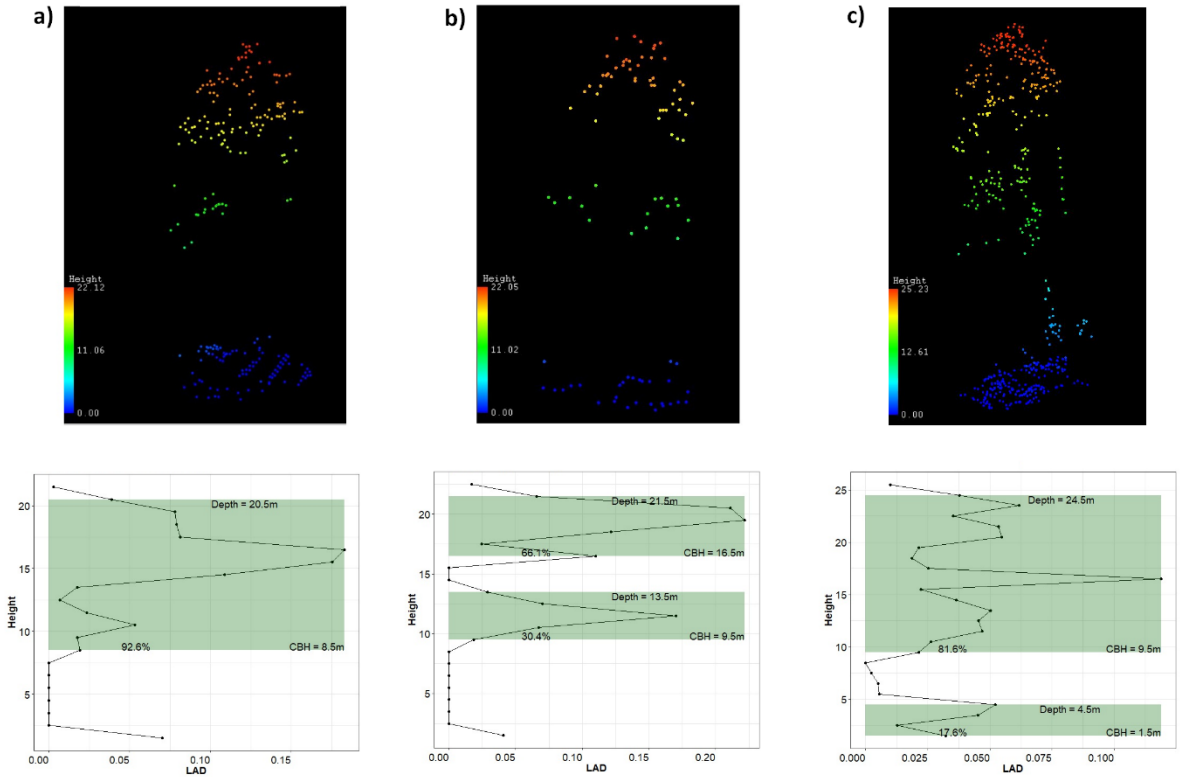

Figure 2. Plots of segmented trees and their LAD profiles with fuel layers in green. In text, the base height (CBH), the depth and the percentage of LAD in each fuel layer identified (outputs of LadderFuelsR).

Distance between Fuel Layers

Function *get_distance*() calculates the distance between fuel layers as the height difference between each pair of consecutive gaps and FBHs (Fig. 3a). In addition, when there are consecutive gaps, the distance is calculated as the difference between the minimum consecutive gap and the next FBH encountered (Fig. 3b).

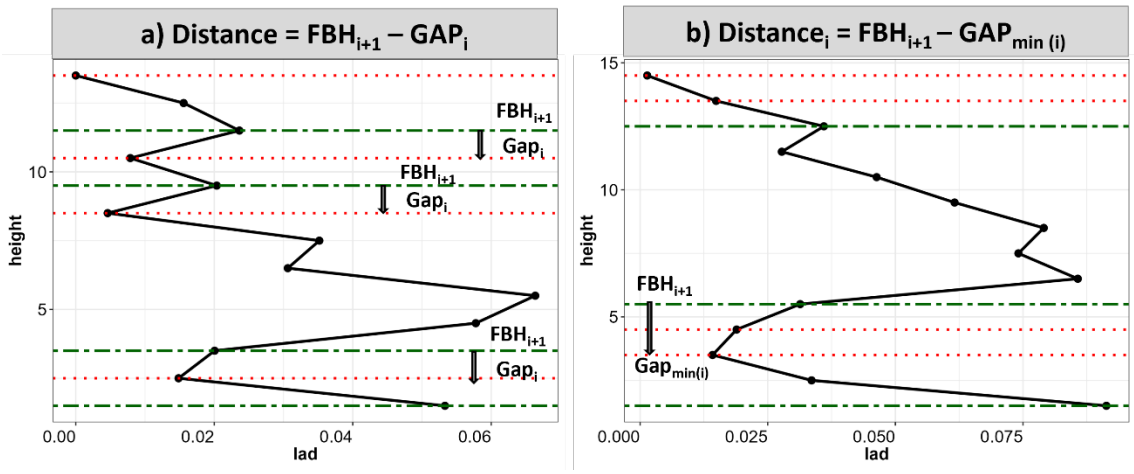

Figure 3. Plots of LAD profiles with fuel base heights (FBHs) in green, and gaps in red, showing how to calculate the distance between fuel layers when: a) there was a unique gap; and b) there are consecutive gaps.

Fuel layer Depth

Function *get_depths*() calculates the depth of each layer fuel as the difference between the gaps interleaved between FBHs (Fig. 4).

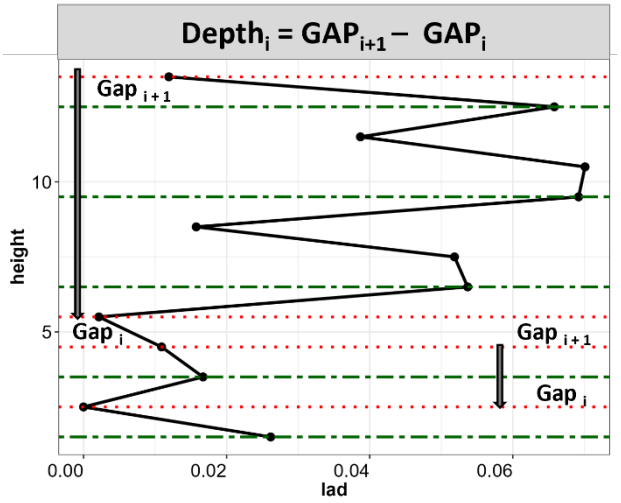

Figure 4. Plot of a LAD profile with fuel base heights (FBHs) in green, and gaps in red, showing how to calculate the depth of any fuel layers interleaved by gaps.

Real height of the Fuel Base Heights (FBHs) and the depth of fuel layers after removing distances equal to one height bin step

Function *get_real_fbh*() identifies the first FBH from consecutive FBHs or the first FBH from those ones separated by a distance = 1 (one height bin step). For each distance value, it locates the next FBH value. If the distance = 1, the height of that FBH is propagated forward. If the distance value is greater than one height bin step, the height

of the identified FBH is kept. The users can change the number of height bins considered for merging or separating fuel layers (Fig. 5).
Function *get_real_depths*() sums all consecutive distances and corresponding depth values when distance is = 1 (Fig. 5).

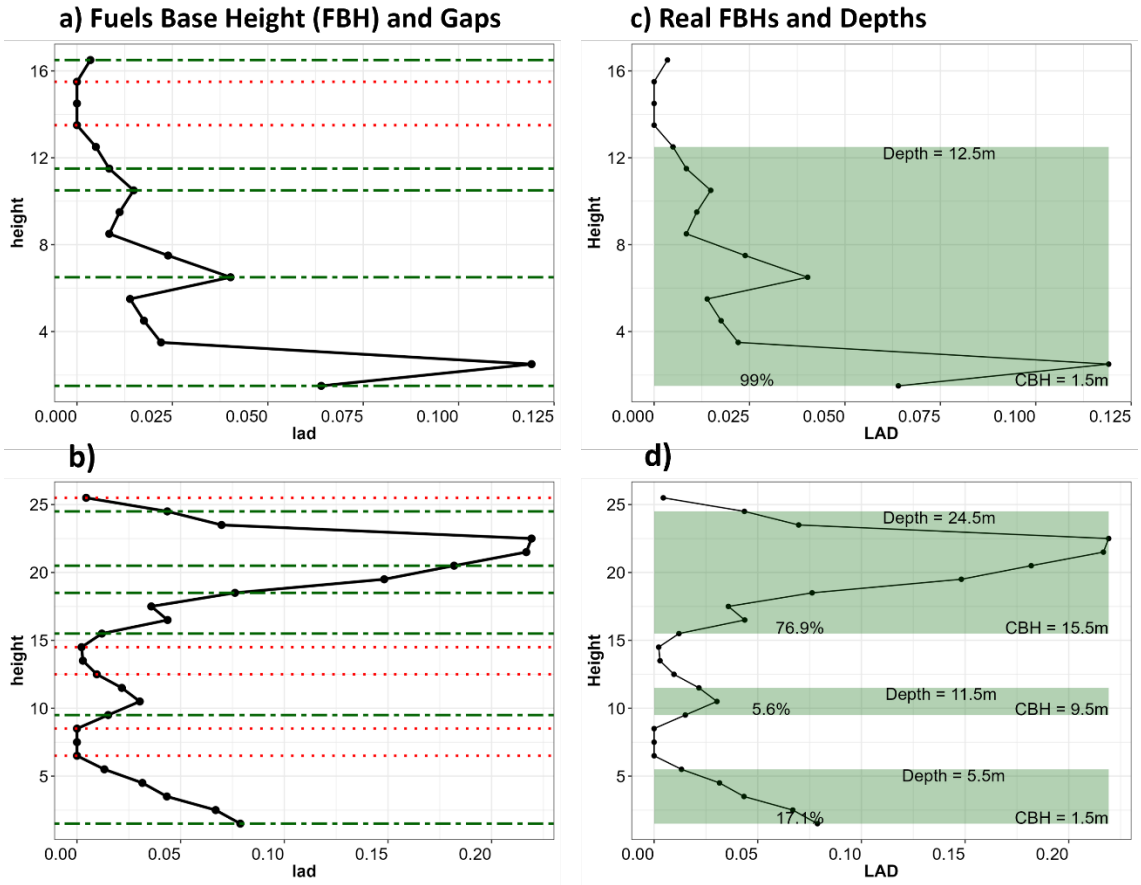

Figure 5. Plots of LAD profiles with: a-b) fuel base heights (FBHs) in green, and gaps in red [output of get_plots_gap_fbh()]; and c-d) real FBHs and depths (LAD % > 10 %) [output of get_plots_effective ()].

Effective distances between fuel layers (distances > one height bin step)

Function *get_effective_gap*() calculates the 'effective distance' (> any distance) between FBHs. It loops over all the FBHs, and at each iteration, it checks if the current value and the next value in FBHs are not equal. If they are not equal, it keeps the corresponding distance value, else it removes it (Fig. 6).

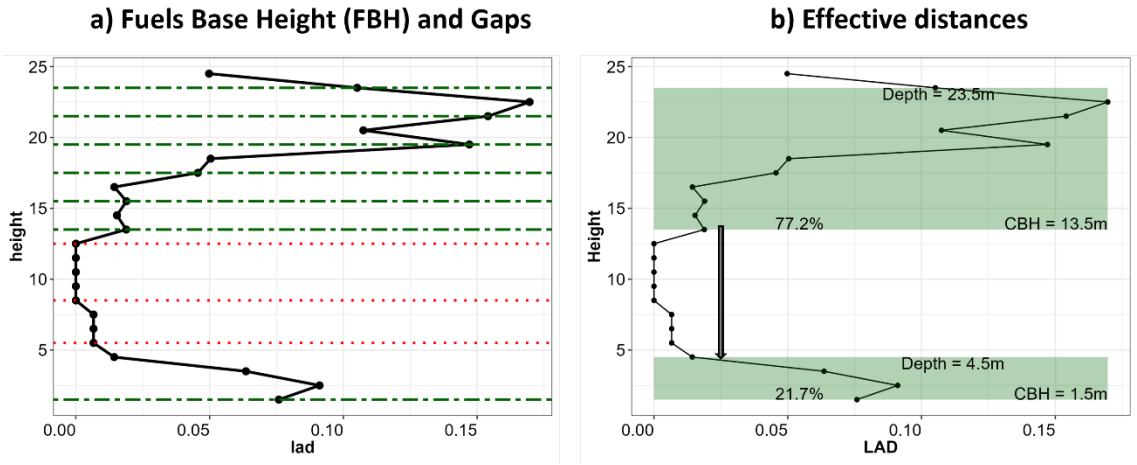

Figure 6. Plots of LAD profiles with: a) fuel base heights (FBHs) in green, and gaps in red [output of get_plots_gap_fbh()]; and b) effective distances (> one height bin step) [output of get_plots_effective ()].

Effective fuel layers based on the comprised percentage of total LAD

Function *get_layers_lad*() calculates the percentage of LAD within each fuel layer; and those that had a percentage less than a specified threshold (default is 25 %) were appended to the distances between or among them, recalculating the distances.

Canopy Base Height of a segmented tree based on different criteria

Function *get_cbh_dist*() applies three criteria to define the CBH in a segmented tree. Firstly, this function identifies the CBH of a tree as the fuel layer containing the maximum LAD percentage (Fig.7a). Later, it identifies the CBH selecting the fuel layer separated by the highest distance between fuel layers (Fig.7b); and finally, it identifies the CBH selecting the fuel layer separated by the last effective distance between fuel layers (Fig.7c).
Function *get_cum_break*() identifies a possible CBH, when the VHP has only one fuel layer, performing a segmented linear regression with an automatic breakpoint (BP) estimation. In addition, this function calculates the percentage of leaf area density (LAD) below and above a breakpoint. If the % LAD values above BP is greater than certain threshold (default = 75 %); the CBH value is set to the BP; if % LAD below the BP > threshold, the CBH = minimum height value. Finally, for trees with % LAD < threshold in both sides of the BP, the CBH value is get from the fuel layer with maximum LAD percentage (Fig.7d).

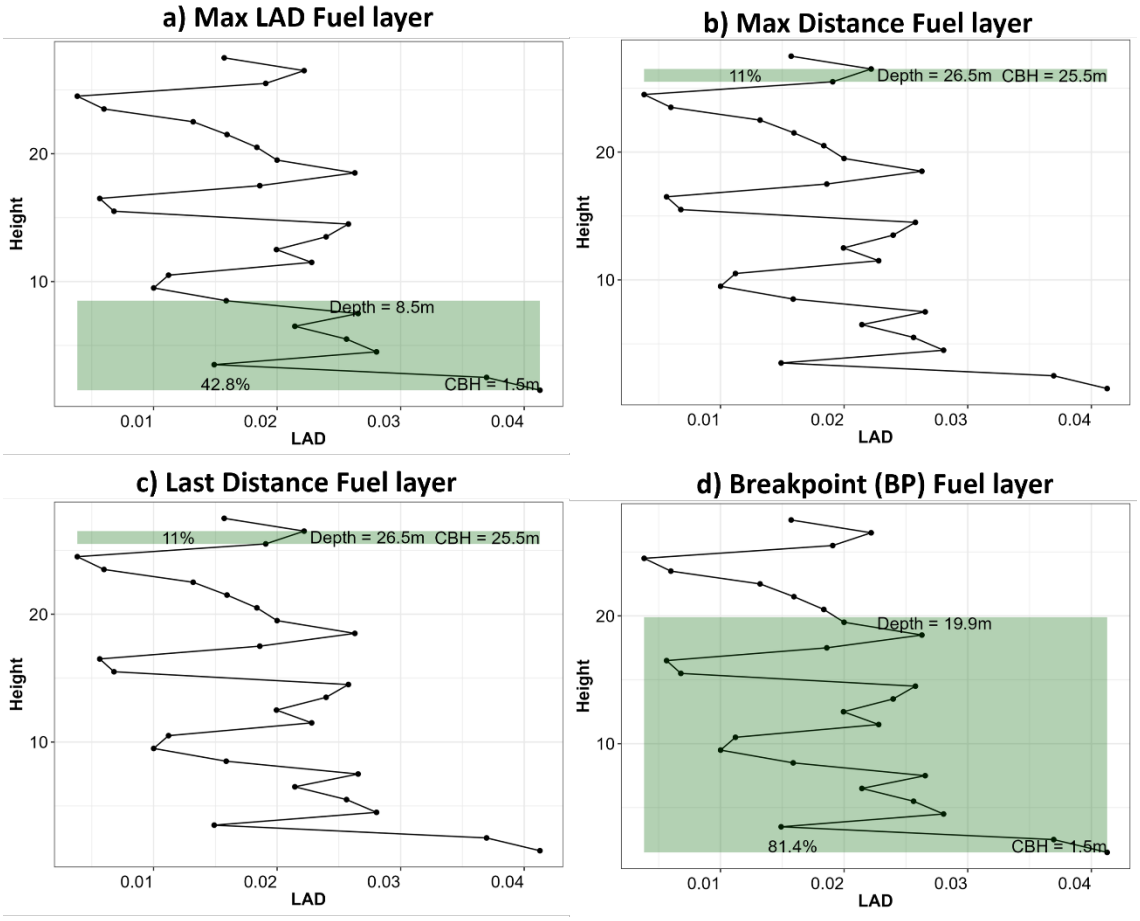

Figure 7. Plots of LAD profiles with the fuel layer identified as the tree Canopy Base height (CBH) following different criteria: a) maxLAD-CBH; b) Max. distance CBH; c) Last distance and d) breakpoint CBH.

Discussion

Our method represents an improvement with respect to indirect regression-based methods that use frequency-based and density metrics (Olszewski and Bailey 2022; Chamberlain et al. 2023), mainly because it allows explicitly capturing the spatial arrangement of vegetation and facilitates its interpretation in relation to the physical structure of the trees. Unlike other wave-based method that set the tree CBH to certain pre-established thresholds and conditions (Chamberlain et al. 2021), our approach permits setting CBH after identifying, with less strict thresholds, all possible gaps and FBHs at effective distances (defined by users). Accordingly, tree CBH can be estimated with greater flexibility using different criteria. Our approach is characterized by its simplicity and does not require adjusting any complex mathematical function to get the main gaps and FBHs (Popescu & Zhao, 2008; Zhou & Li, 2023). However, our methodology faces the same challenges of other wave-based methods in dense forests, due to weak laser pulse penetration and/or the low point density.

Acknowledgements
This research is part of the **project INFORICAM (PID2020-119402RB-I00),** funded by the Spanish government MCIN/AEI/ 10.13039/501100011033 and by the "European Union NextGenerationEU/PRTR".

References

Alcasena FJ, Ager AA, Bailey JD, Pineda N, Vega-García C (2019) Towards a comprehensive wildfire management strategy for Mediterranean areas: Framework development and implementation in Catalonia, Spain. *Journal of Environmental Management* **231**, 303–320. doi:10.1016/j.jenvman.2018.10.027.

Chamberlain CP, Cova GR, Kane VR, Cansler CA, Kane JT, Bartl-Geller BN, van Wagtendonk L, Jeronimo SMA, Stine P, North MP (2023) Sierra Nevada reference conditions: A dataset of contemporary reference sites and corresponding remote sensing-derived forest structure metrics for yellow pine and mixed-conifer forests. *Data in Brief* **51**, doi:10.1016/j.dib.2023.109807.

Chamberlain CP, Sánchez Meador AJ, Thode AE (2021) Airborne lidar provides reliable estimates of canopy base height and canopy bulk density in southwestern ponderosa pine forests. *Forest Ecology and Management* **481**. doi:10.1016/j.foreco.2020.118695.

Cruz MG, Alexander ME, Wakimoto RH (2003) Assessing canopy fuel stratum characteristics in crown fire prone fuel types of western North America. In 'Int J Wildland Fire', 39–50. (International Association of Wildland Fire) doi:10.1071/WF02024.

Erdody TL, Moskal LM (2010) Fusion of LiDAR and imagery for estimating forest canopy fuels. *Remote Sensing of Environment* **114**, 725–737. doi:10.1016/j.rse.2009.11.002.

Fernandes PM (2013) Fire-smart management of forest landscapes in the Mediterranean basin under global change. *Landsc Urban Plan* **110**, 175–182. doi:10.1016/j.landurbplan.2012.10.014.

Mitsopoulos ID, Dimitrakopoulos AP (2014) Estimation of canopy fuel characteristics of Aleppo pine (Pinus halepensis Mill.) forests in Greece based on common stand parameters. *European Journal of Forest Research* **133**, 73–79. doi:10.1007/s10342-013-0740-z.

Olszewski JH, Bailey JD (2022) LiDAR as a Tool for Assessing Change in Vertical Fuel Continuity Following Restoration. *Forests* **13**. doi:10.3390/f13040503.

Popescu SC, Zhao K (2008) A voxel-based lidar method for estimating crown base height for deciduous and pine trees. *Remote Sensing of Environment* **112**, 767–781. doi:10.1016/j.rse.2007.06.011.

Zhao K, Popescu S, Meng X, Pang Y, Agca M (2011) Characterizing forest canopy structure with lidar composite metrics and machine learning. *Remote Sensing of Environment* **115**, 1978–1996. doi:10.1016/j.rse.2011.04.001.

Proceedings for the 7th International Fire Behavior and Fuels Conference April 15-19, 2024, Boise, Idaho, USA – Tralee, Ireland – Canberra, Australia Published by the International Association of Wildland Fire, Missoula, Montana, USA

Land Tender: A collaborative, cloud-based decision support system for wildfire risk mitigation and ecosystem restoration

Hugh Safford[A,B,*], Tyler Hoecker[A,C], Danielle Perrot[A], Colton Miller[A], Katharyn Duffy[A,D], Mike Koontz[A], Sophie Gilbert[A,E], Joe Scott[A,F], and Scott Conway[A]

[A]Vibrant Planet, Truckee, CA, 96161, USA
[B]University of California, 1 Shields Avenue, Davis, CA 95616, USA
[C]University of Montana, 32 Campus Dr, Missoula, MT 59812, USA
[D]Northern Arizona University, 1295 Knoles Dr, Flagstaff, AZ 86011, USA
[E]University of Idaho, 875 Perimeter Drive, Moscow, ID 83844, USA
[F]Pyrologix, 111 N. Higgins Avenue, Suite 404, Missoula, MT 59802, USA

* *Corresponding Author*: hugh@vibrantplanet.net; hdsafford@ucdavis.edu

Introduction

Climate-change and human impacts to landscapes and ecological processes are jointly accelerating the scale and velocity of ecosystem degradation. This undermines human communities and economies, which depend on nature. Human-driven changes to ecological disturbance dynamics are a key driver of ecosystem degradation, and reducing the negative impacts of uncharacteristic disturbances – to humans as well as to ecosystems – has become a major component of global change adaptation around the world. In seasonally dry bioregions, fire is a keystone ecological disturbance, and anthropogenic changes to land use, fire frequencies, ecosystem structure, fuel loadings, and the climate are leading to progressively more severe impacts of fire on ecosystems and humans. Human responses to changing fire dynamics have been slow and reactive, with a primary focus on techniques and technologies to prevent ignitions and extinguish fires after they are ignited. This approach is having diminishing success, because suppressing fires in ecosystems adapted to frequent burning may be ecological degradation in itself; because an excessive number of years without fire in such ecosystems leads to uncharacteristically severe burning when fire returns; and because an unbalanced prioritization of resources toward fire response infrastructure and tactics is starving proactive and cost-efficient stewardship practices.

In 2022, UNEP published a report on the status of wildfire in the world and recommended a rebalancing of effort and funding across the five categories of actions that form the basis for Integrated Fire Management. Specifically, the report called for reducing the focus on fire suppression, and enhancing efforts in preparedness, risk reduction, and postfire restoration (UNEP 2022). However, the international wildfire problem presents major challenges to effective management due to the rate at which the problem is evolving, the geographic extent involved, and the multiscalar complexity of affected landscapes and human communities, which may span political boundaries, multiple watersheds, various management jurisdictions and plans, broad environmental

gradients, and users representing many different, often competing social strata and value systems. In this type of wicked problem (Rittel and Webber 1973), arriving at a management consensus can be a daunting task. Because the complexities of the wildfire wicked problem derive to a great extent from the people involved and their often idiosyncratic perceptions of the problem, it is fundamentally important to develop a "collaborative governance" framework, based on functional levels of trust; equal access to data and participation in the decision-making process; and transparency in process inputs, outputs, and recommendations, as well as in projected costs and benefits (USDA 1999, Scarlet and McKinney 2016) .

Land Tender™ is a collaborative, cloud-based, visual, scenario-building and decision support system constructed to support complex resource management planning at local, regional, and national scales. LT incorporates high-resolution imagery, climate data, disturbance simulations, optimization, and scenario comparisons to develop prioritized and sequenced management plans for large fire-prone landscapes. The tool efficiently incorporates user input and values through effective interfaces for hands-on and real-time engagement; turns decision-critical data into analytical outputs that can be interactively and iteratively generated, discussed, and manipulated by managers and partners alike; and cogently summarizes the benefits of potential ecosystem management actions.

Land Tender highlights include:

- LT workflow provides multiple windows for user engagement and ingestion of local/place-based knowledge and values
- LT is cloud-based and real-time, allowing rapid multi-objective management scenario iteration
- The easy-to-use platform democratizes access to outputs generated by underlying fire, forest growth, and optimization models that are not usable by the general public (e.g. F-Sim, WildEST, FVS, ForSys).
- Unlike other extant tools, LT explicitly identifies how, and by how much, alternative management scenarios might reduce risk
- LT not only evaluates wildfire risk reduction from management action, but also the potential for ecological benefits in the absence of disturbance
- LT estimates project costs, economic outputs (currently timber value and biomass), and impacts on ecosystem services (currently carbon, adding hydrology and biodiversity soon)
- LT deployment can cut months to years from the typical planning processes in collaborative landscape management, which may reduce overall cost

Methods and Results

Fig. 1 outlines the Land Tender analytical process. Boxes 1-5 in Fig. 1 develop the data template for deployment of the decision support system (DSS). Outputs from the DSS (Box 6) feed the development of a management plan proposal and the environmental analysis. Information collected from implementation and effects monitoring feeds back

into a refresh of the Base Data and SARA conditions, and the cycle begins again. We describe the general features of the Land Tender process below. For more detail see the Land Tender Product Guide (VP 2024).

Base data for LT include (Fig. 1, Boxes 1a-1c): Vegetation composition and structure, usually determined with a mix of lidar and high-resolution 2-dimensional imagery sources; landscape and jurisdictional data, including landform information and ownership and land designations; fire and fuels data, including various measures associated with fire and drought hazard; ecological departure, which includes

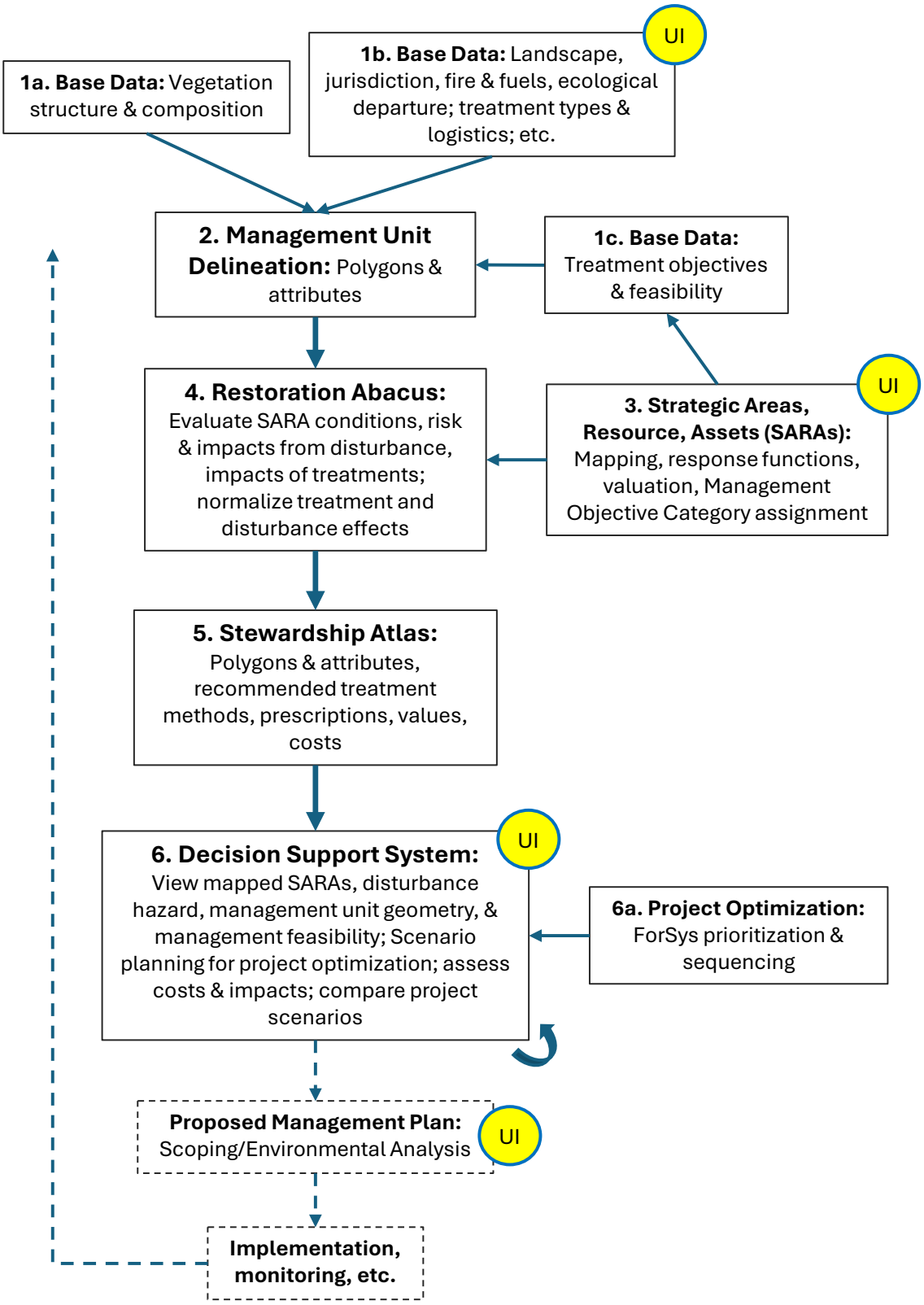

Figure 1. Land Tender workflow. Dashed lines and boxes indicate management steps subsequent to Land Tender deployment. Important user input indicated by yellow UI circles. See text and VP (2024) for details.

estimates of departures from desired structural and disturbance frequency conditions; treatment logistics, e.g. costs, and distances to roads, structures, and sawmills or biomass plants; and treatment types, which indicate which management interventions are permissible in different jurisdictions, land designations, and environmental conditions.

These base data are used to generate management units, beginning with vegetation structure, then adding topographic variables, fuels, and road and stream data (Fig. 1, Box 2). The resulting polygons are composed of areas with similar biophysical characteristics and administrative jurisdiction, across which a single treatment type could be applied. This comprehensive geospatial database summarizes pre-treatment landscape patterns and can be exported for use outside Land Tender.

Strategic Areas, Resources, and Assets (SARAs; Fig.1, Box 3) represent key values of interest in the project landscape and are distributed among eight Management Objective categories (Fig. 2). SARAs are determined in close consultation with users and may come from national or local datasets. SARAs must 1) be mappable, 2) have measurable socioecological value, 3) have sensitivity to the intensity levels of disturbances under consideration (Scott *et al.* 2013) and 4) have estimated effects to the potential treatments. SARA sensitivity to treatments and disturbance intensities is measured in semi-quantitative or quantitative “response functions”, determined through expert elicitation, literature review, or modeling.

In the next step (“Restoration Abacus”; Fig. 1, Box 4): (1) the delineated management units are assigned feasible treatment options based on their biophysical conditions and land designations; (2) information around cost, biomass removal, product benefit, and workforce estimates is attributed for each management unit and feasible treatment option; and (3) an algorithm assesses current SARA conditions and evaluates the relative ability of different treatment options to change those conditions. The total relative impact is compared – per management unit, per feasible treatment, and per Management Objective – by calculating the Restorative Return on Investment (RROI), which combines “Treatment Effects” (effects of potential treatments on SARA condition in a polygon in the absence of disturbance; this is a measure of the ecological restoration value of the treatment) and “Change in Disturbance Effects” (effects of potential treatments on SARA condition in the presence of disturbance and its modeled intensity; this is the classic avoided loss/risk reduction effect). Finally, the Restoration Abacus aggregates the individual SARAs to their respective Management Objective categories (see Fig. 2) and normalizes Treatment and Change-in-Disturbance Effects for all treatments and Management Objectives across management units.

The Land Tender DSS (Fig. 1, Box 6) provides users access to spatial data from the Stewardship Atlas, including the deployment landscape, SARA layers and their spatial RROI signatures, fire and drought hazard maps, and spatial limitations on feasibility of potential management actions. Most importantly, the DSS permits any user to easily develop management scenarios for the deployment landscape. Users generate a

management scenario by differentially weighting the eight Management Objectives along a scale from 0 to 5, which results in a map of the RROI impact score, where dark blue is high benefit and white is low benefit (Fig. 2, Boxes A and B). Negative impacts are not displayed visually in LT, but are used in project development (e.g. areas with a total weighted negative impact score are excluded from projects). Before optimizing a management plan for the scenario, users can exclude certain treatment types, balance the restoration and risk reduction priorities or focus mostly on one or the other (not shown). Users set constraints for the number of projects to model, maximum project budget and maximum project area.

In Fig. 2, Scenario 1 (Boxes A and A1) represents a management scenario focused on environmental protections, while Scenario 2 (Boxes B and B1) represents a scenario focused on fire safety and timber and biomass production. A third scenario was also run, which weighted all Management Objectives equally (not shown). In all three scenarios, clearcutting was not permitted, management priorities were balanced, 5 projects were modeled, maximum project area was 1000 ha, and maximum budget per project was $1,000,000 US. After optimization by the ForSys routine (which took 8-10 seconds per scenario in this case; Ager *et al.* 2012), Land Tender output five projects under each scenario that met the optimization constraints and maximized overall RROI in the landscape area (Fig. 2, Boxes A1, B1). Projects are listed in order of their RROI, providing a suggested sequence for management planning. Fig. 2 Box C displays some of the tools that are available to compare management scenarios, including percent of total available RROI that is accomplished by the three scenarios for each of the eight Management Objective categories; an overlay of the spatial locations of the project areas from all of the scenarios with consensus areas identified; and the RROI efficiency of each scenario (not shown), which is the ratio of percent of area treated versus percent RROI attainment.

Discussion

We conclude by discussing stakeholder participation in the Land Tender process, planning efficiencies, the complicated issue of decision support tool validation, and current and potential future LT deployments.

Collaborative participation occurs at a number of key stages in the LT workflow, and users can readily visualize tradeoffs, prioritizations, and sequencing of treatments among alternative management scenarios for a landscape. Collaborators can easily share and compare scenarios, thus arriving at agreement on management alternatives quickly and efficiently. We know of no other management planning application that provides such a high degree of access for the general public to such a high level of computing firepower. LT outputs include comprehensive spatial and
tabular comparisons of final management alternatives – including projected costs, economic outputs, and relative benefits of each alternative across all of Management Objective categories – that can be easily exported to environmental assessment processes that precede implementation. Combined, these features lead to notable efficiencies in the land and resource management planning process, which is typically very cumbersome and time- and money-intensive.

Like all complex models that predict future conditions, decision support tools are a challenge to validate (Finlay 1994). Based partly on Borenstein (1998), we are developing a comprehensive and automated validation and evaluation framework for Land Tender. Face

validation sensu Borenstein is continuous and has been underway for more than four years. Subsystem validation is based on validation and peer-reviewed publications supporting the fire and drought hazard, forest growth, and

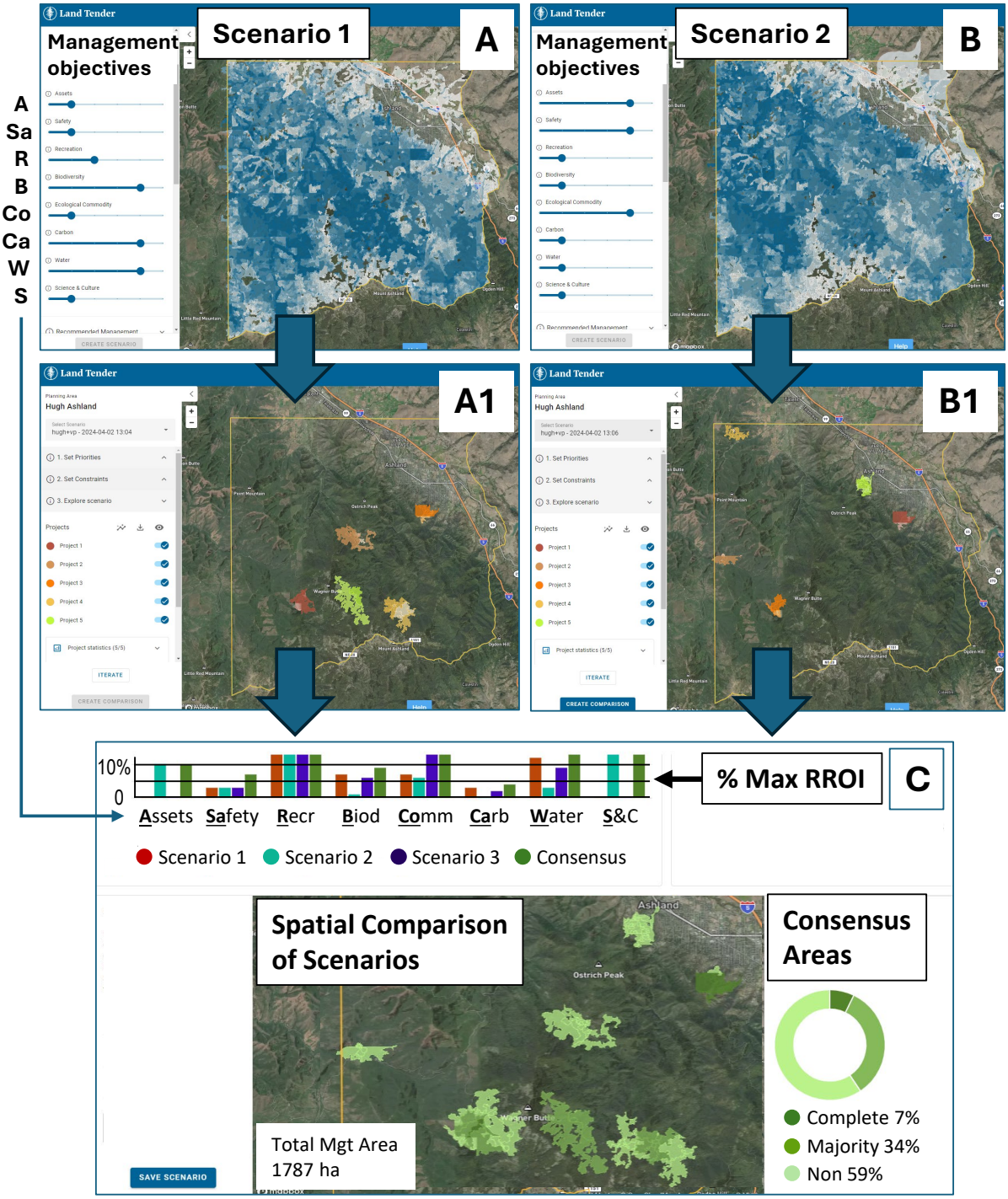

Figure 2. Land Tender processing of Stewardship Atlas data: Restorative Return on Investment (RROI) and management project optimization for a 35,000-ha test landscape. A: RROI for "Environmental" scenario, with highest weighting given to Biodiversity, Carbon, and Water

objectives, and intermediate to Recreation. B: RROI for "Fire Safety and Commodity" scenario, with highest weighting given to Asset Protection, Fire Safety, and Commodities. A1 and B1: For scenarios 1 and 2, respectively, prioritized and sequenced projects, optimized to maximize RROI under the given objective weightings and under a set of project constraints (see text). C: Comparison of scenarios 1, 2, and 3 (3 not shown) with respect to % of total RROI attained for each Management Objective category; and spatial distribution of the optimized projects under the three scenarios, with consensus areas identified. Under Management Objectives: A = Asset protection, Sa = Fire safety, R = Recreation, B = Biodiversity, Co = Commodities, Ca = Carbon, W = Water, S = Science and culture.

optimization submodules underlying the LT platform. In addition, the wildfire risk assessment framework (Scott *et al.* 2013) that forms the basis for LT has been widely used in the western US and validated on a number of landscapes (e.g., Thompson *et al.* 2015). Formal predictive validation (validating using test cases where the results are known) is difficult for decision support tools, but recently Ager (2024) conducted predictive validation of the ForSys optimization routine against known results from linear programming methods and demonstrated c. 95% concurrence and notable advantages in speed and transparency. We have also tested and calibrated our lidar-based vegetation structure modeling against stem-mapped forest stands from California. Early in LT development we conducted user validation exercises, but a more formal process for user validation is still in development. Field validation is carried out continuously through feedback from our project partners; field validation of our fire hazard modeling documents strong coincidence between modeled high hazard zones and subsequent severe burning, e.g. in the Lahaina Fire of 2023 and the Texas wildfires of early 2024; and finally, we are developing a plan for field checking of LT-derived management treatment prescriptions by a registered professional forester.

Today, Land Tender is being used as the decision support tool of choice by many land and resource management agencies and collaborative groups across more than 10 million hectares in the western US. For example, the US Forest Service and the National Forest Foundation have deployed Land Tender on many of the national "Wildfire Crisis Strategy" landscapes, including 500,000 to 2,000,000-ha deployments in Idaho, Colorado, New Mexico, and California; The Nature Conservancy and partners are using Land Tender as the principal planning tool for the Southern Oregon Forest Restoration Partnership; and CalFire recently contracted to Vibrant Planet for a Land Tender deployment on a 700,000-ha landscape in eastern California. Future work will focus on emulating the success of these deployments in the US to enable durable, collaborative management responses to the wildfire problem internationally– in both the developed and developing world. To that aim, we are actively pursuing deployments outside of the US. At the moment we are having had preliminary conversations with groups from Portugal, Turkey, Spain, Chile, and Australia, as well as the UN-Food and Agricultural Organization, which is seeking to develop a standard wildfire risk response platform for the developing world.

References

Ager A (2024) Improving the evaluation of spatial optimization models for prioritizing landscape restoration and wildfire risk reduction investments. *Journal of Environmental Management* **360**, 121001

Ager AA, Vaillant NM, Owens DE, Brittain S, Hamann J (2012) 'Overview and example application of the Landscape Treatment Designer.' PNW-GTR-859. USDA Forest Service. (Portland, OR).
Borenstein D (1998) Towards a practical method to validate decision support systems. *Decision Support Systems* **23(3)**: 227-239.
Finlay PN (1994) 'Introducing decision support systems.' (NCC Blackwell: Southampton, UK).
Rittel HWJ, Webber MM (1973) Dilemmas in a general theory of planning. *Policy Sciences* **4**. 155–169.
Scarlett L, McKinney M (2016) Connecting people and places: the emrging role of network governance in large landscape conservation. *Frontiers in Ecology and the Environment* **14**, 116-125.
Scott JH, Thompson MP, Calkin DE (2013) 'A wildfire risk assessment framework for land and resource management.' RMRS-GTR-315. USDA Forest Service. (Ft. Collins, CO).
Thompson MP, Haas JR, Gilbertson-Day JW, Scott JH, Langowski P, Bowne E, Calkin DE (2015) Development and application of a geospatial wildfire exposure and risk calculation tool. *Environmental Modelling & Software* **63**, 61-72.
UNEP (2022) 'Spreading like wildfire – The rising threat of extraordinary landscape fires.' UNEP Rapid Response Assessment. (United Nations Environment Program: Nairobi, Kenya).
USDA (1999). Challenges of collaborative planning. In 'Sustaining the people's lands. Committee of Scientists Report' pp. 121-144. (US Department of Agriculture, Forest Service: Washington, DC)
VP (2024) 'Land Tender Product Guide, February 2024.' Vibrant Planet, https://www.vibrantplanet.net/landtender

Leveraging Online Anti-Bot Technology To Boost Wildland Fire Detection And Prediction

*Guy Schumann
Research and Education Department, RSS-Hydro, L-3670 Kayl, Luxembourg
ImageCat Inc., Long Beach, CA 90802, USA
School of Geographical Sciences, University of Bristol, Bristol BS8 1SS, UK
gs@imagecatinc.com; gschumann@rss-hydro.lu

Marina Mendoza, Georgiana Esquivias, James Colannino, Ron Eguchi
ImageCat Inc., Long Beach, CA 90802, USA

Ajay Gupta, Paul Churchyard
Health Solutions Research LLC, Rockville, MD 20850, USA

Unmesh Kurup, Andrei Lapanik, Tomas Langer
Intuition Machines Inc., San Francisco, CA 94110, USA

Ron Hagensieker
osir.io, 10823 Berlin, Germany

Alice Pais de Castro, Chloe Campo
Research and Education Department, RSS-Hydro, L-3670 Kayl, Luxembourg

**Corresponding Author*

Introduction

Access to annotated data (i.e. labels) is crucial for various machine learning applications, including earth observation tasks like land use mapping. However, annotating technical image datasets is challenging, necessitating hard-to-source specific expertise for accurate interpretation (Yao, 2021).

Relying on the fact that everyday event images, often publicly collected through sources like cell phone photos, require minimal abstraction since their content, angles, and color channels are familiar even to untrained interpreters, we aim to harness the daily users of CAPTCHAs (Ahn et al., 2003) to crowdsource this task to an unprecedent scale.

This innovative way of leveraging existing anti-bot technology paves the way for a future where citizen science and artificial intelligence work in tandem to unlock the full potential of Earth observation (EO) data. By making image annotation accessible to everyone and continuously refining AI models, we can gain a deeper understanding of our planet and develop sustainable solutions for the challenges we face.

Here we present the first results obtained using wildland fires as a use case. Then we illustrate one way in which the online annotations obtained can be extracted and made available on a third party online platform. To conclude, we show a novel satellite Earth Observation (SatEO) application for monitoring wildland fires that can immensely benefit from real time online annotations as a means to instantly validate what we can detect from space.

The FireCapture Project: Using Online Antibot Technology to Annotate Satellite Images of Wildland Fires

There is a clear need for fully automated processing of big EO data. Many different models of machine learning algorithms are available but they generally require a huge amount of very high quality labels to train in order to yield the best possible inference, whether for prediction or monitoring.

This is particularly challenging when it comes to EO image data used for mapping wildfires or other disasters, where trusted data are needed in near real time in a format that can be easily ingested by stakeholders. Interpreting and labeling a multitude of different EO data types typically requires intensive effort from EO experts only able to provide a limited amount of labels, which substantially limits the performance of the ML models being trained on those labels.

The proposed service is based on crowdsourcing that makes use of CAPTCHAs (Ahn et al., 2003). It will be optimized for the EO context and extended by EO-specific, pre- and post-processing, which wrap around Intuition Machine's hCaptcha. The primary goal of the preprocessing module is to make EO imagery "Captcha user-ready". This readiness includes the technical readiness, e.g. image size, format, pre-processing for enhancing image features, etc. as required by hCaptcha, but also user readiness, meaning that the data is interpretable even by the general or non-expert public.

In the FireCapture project, users were presented with a series of images, and asked to 'label' the appropriate images as 'wildfires' (Figure 1 shows an example illustration). The innovation was the application of the hCaptcha technology specifically to enable wildland fire monitoring in real-time using multiple satellite sensor data, including the Landsat satellite series as well as the Sentinel-2 satellite. To this end, hCapture was adapted to collect many thousands of burned area labels.

It was successfully demonstrated that the Human Platform and hCaptcha technology can be used to generate thousands of labels for important wildfire parameters, such as active fire identification and burned area (see Figure 2 as an example). These labels can be used either directly by stakeholders to examine and take appropriate actions or to train ML models to allow detection and prediction of important wildfire parameters.

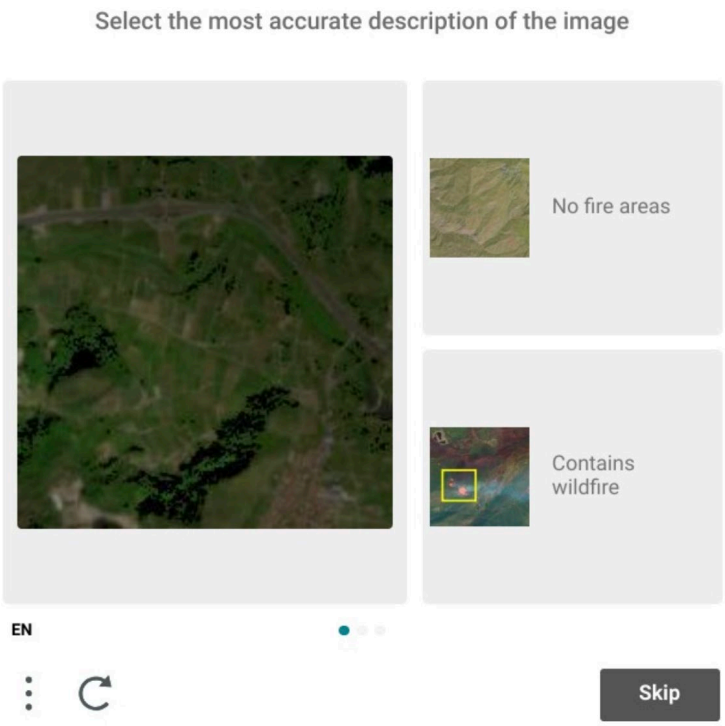

Figure 1. Illustration of a satellite image displayed for annotation using the well-known online antibot tool hCaptcha. Labeling was done by Intuition Machines Inc., in partnership with HUMAN

For the labeling performance assessment, the team used several wildland fire events with fire perimeter data collected in the field and available from the National Interagency Fire Center. Wildfires in different environments were included in the assessment: Colorado, Northern California, and Greece. It is important to note that significant work was required to geo-reference the images because CAPTCHAs do not (yet) support georeferenced imagery.

Figure 2 shows an example for wildfires in Colorado. In this kind of environment, it is worth noting that in general the online annotations received are correct (83%) but there are often mislabels when it comes to distinguishing burned areas from bare brown or dark-looking soils. This is typical of the landscape in Colorado, which results in false positives

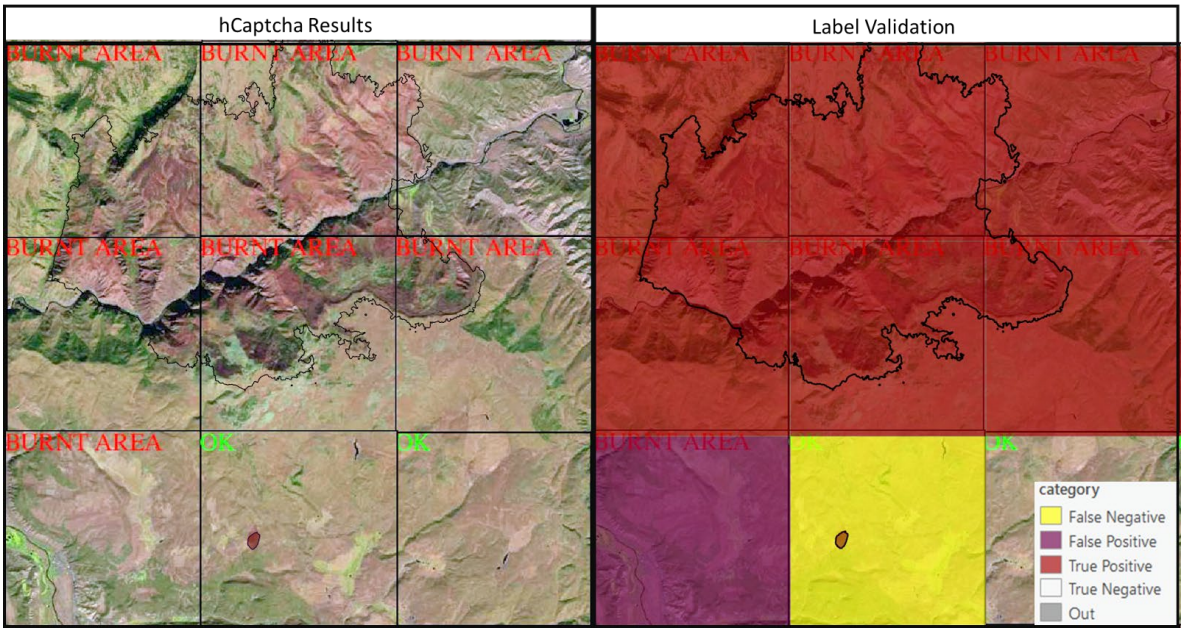

Figure 2. Grizzly Creek and Pine Gulch Fires (2020) in Colorado. Landsat-8, October 13, 2020

FireCapture successfully demonstrated that the Human Platform and online antibot hCaptcha technology can be used to generate thousands of labels for important wildfire parameters such as active fire identification and burned area; and it also identified stakeholders interested in their use for decision support. In a survey conducted during the project, out of 33 Firefighters, nearly 1/3 said they encountered medical emergencies, yet more than half (54%) did not receive information on the medical conditions of the disasters impacted individuals Stakeholders also indicated interest in maps of smoke plume extent that could be used by decision makers in hospitals and disaster response roles to aid in identifying those at greatest risk of adverse health outcomes, and provide guidance identifying evacuation and resource allocation priorities to meet the health and medical needs of those impacted by wildfires.

The Maptcha Project: Streamlining Online Annotations to Satellite Image Analysis Platforms

As a complementing parallel activity to the NASA-supported FireCapture project, the Maptcha project supported by the European Space Agency (ESA) aims to streamline the transfer of online annotations from satellite images to third party satellite image analysis platforms (Figure 3). It also facilitates the visualization and integration of these annotations with other geospatial datasets or analysis results.

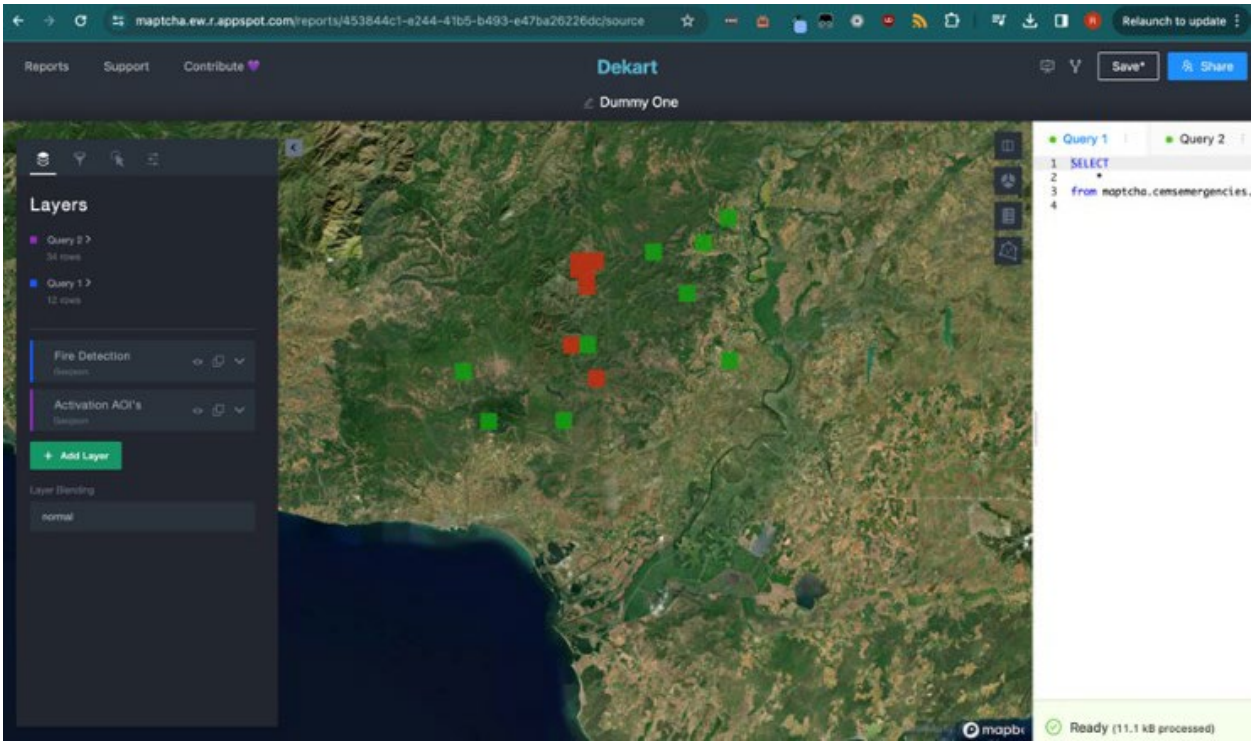

Figure 3. A live display example of online wildland fire annotations, based on kepler.gl and implemented through DEKART. in Google Cloud Platform (GCP)

Making massive volumes of online annotations rapidly available on other analysis platforms allows fast and valuable training for machine learning models. This has the potential to significantly improve the capabilities of AI-powered Earth observation applications, leading to advancements in environmental monitoring, resource management, and climate change analysis. Imagine near real-time tracking of deforestation or monitoring crop health across vast agricultural regions – these are just a few examples of the possibilities unlocked by the rich data environment fostered by Maptcha.

Real-world testing is crucial to validate the Maptcha concept. The project has identified potential users with specific needs in geospatial data marketplaces, emergency response, and disaster management. Engaging with these users throughout development ensures that the platform meets their specific requirements.

The next steps involve developing base layers for EO data, exploring integration with existing platforms, assessing the confidence of satellite image data, and conducting a first test distributing very high-resolution data via Maptcha. Successful completion of these steps will pave the way for a fully operational citizen science-led annotation pipeline, revolutionizing the way we extract information from satellite imagery for emergencies and beyond.

FireSENS: A Satellite Earth Observation Application for Real Time Monitoring of Wildland Fires

FireSENS is a SatEO app that tackles the critical issue of wildfire risk assessment. The streamlined methodology of FireSENS hinges on three key steps: data extraction, refinement, and classification (Campo et al., 2024).

Fire intensity information is extracted from the Sentinel-3 satellite's SLSTR Level 2 Fire Radiative Power dataset (Wooster and Xu, 2021). Here, the focus is on land-based wildfires, so the FRP_MWIR product is specifically chosen over its SWIR counterpart. Additionally, population data is obtained from relevant and mandated mapping or cadastral organizations, providing a snapshot of population distribution across regions or entire countries.

Next, the FireSENS method preprocesses the collected data to ensure coherency and consistency among datasets. Fire intensity values, along with their corresponding location data, are extracted and placed onto a grid system. This grid has a resolution of 1 square kilometer, aligning perfectly with the resolution of the fire intensity data itself. To eliminate any outliers or errors, the system filters out any suspicious FRP values. This guarantees that only reliable data is used for further analysis.

Finally, FireSENS leverages the prepared data to classify fire risk across regions. The fire intensity values within each administrative region are averaged. This process yields a general fire intensity rating, categorized as low (less than 50 MW), medium (between 50 MW and 100 MW), and high (greater than 100 MW). Similarly, the population data is transformed into a population density classification. Here, regions are categorized as having low (50-100 people per square kilometer), medium (100-500 people per square kilometer), or high (greater than 500 people per square kilometer) population densities.

By combining these two classifications – fire intensity and population density – FireSENS generates a final, comprehensive fire risk classification for each region in of any country. This final classification effectively pinpoints areas with a heightened risk of wildfires, allowing for targeted preventative measures and resource allocation. Indeed, the FireSENS application workflow is kept flexible to integrate any type of auxiliary information related to impact, such as GIS infrastructure layers, biomass, health risk indicators, or air pollution measurements; the latter being already implemented within FireSENS using daily measurements of atmospheric pollutants obtained from the TROPOMI instrument onboard Sentinel-5P.

Assessing the performance and detection accuracy of a real time monitoring tool such as FireSENS is vital to ensure robustness and consistency across multiple regions. Here, we suggest that real time validation of the FireSENS analysis output (Figure 4) could be done by live-streaming online annotations of active wildland fires using the previously described FireCapture-Maptcha pipeline. This would allow live annotations to

be displayed alongside the analysis output of FireSENS. Such a validation approach is currently being proposed.

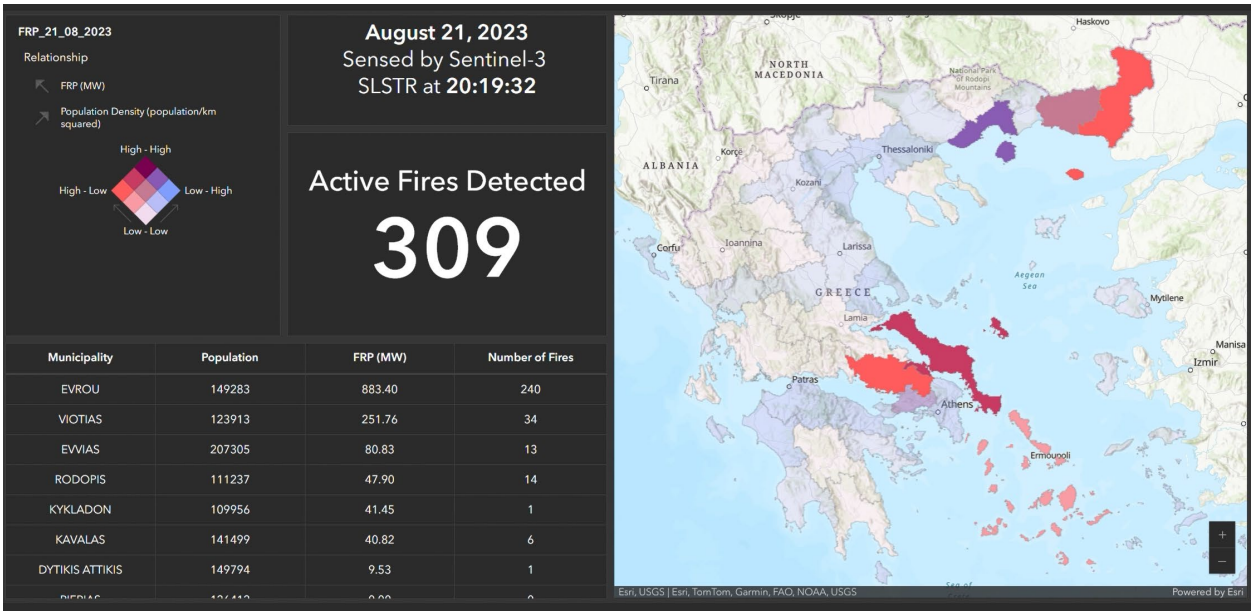

Figure 4. Example of the FireSENS analysis dashboard showing the risk associated with hundreds of individual wildland fires detected in August 2023 across Greece.

Conclusion

This paper highlights two novel projects with significant promise for improving wildfire monitoring and resource management. FireCapture demonstrates the effectiveness of crowdsourcing with CAPTCHAs to generate high-quality labels for satellite images, specifically focused on wildfire parameters. This approach has the potential to significantly enhance wildfire detection and ultimately improve decision-making for targeted interventions.

Complementing FireCapture, the Maptcha project tackles the challenge of integrating these crowdsourced labels with third-party satellite image analysis platforms. This streamlined workflow facilitates the use of these labels in training AI models, leading to further advancements in wildfire monitoring capabilities.

The paper also introduces the FireSENS application, a SatEO app that offers a real-time fire risk assessment solution by leveraging satellite data for regional classification. The potential for real-time validation of FireSENS using annotations from the FireCapture-Maptcha pipeline presents an exciting opportunity to strengthen the accuracy and robustness of fire risk monitoring on a global scale. By combining these innovative projects, we can move towards a future with more efficient wildfire response and mitigation strategies.

Acknowledgments
The FireCapture project has been led by ImageCat Inc. with support from the National Aeronautics and Space Administration (NASA) under grant number 80NSSC22K1844. The Maptcha project has been led by RSS-Hydro under a contract from the European Space Agency (ESA), number 4000142485.

References

Ahn, L. V., Blum, M., Hopper, N. J., & Langford, J. (2003). CAPTCHA: Using hard AI problems for security. In International conference on the theory and applications of cryptographic techniques (pp. 294-311). Springer, Berlin, Heidelberg.

Chloe Campo, C., Schumann, G., & Tamagnone P. (2024) Enhancing near real time wildfire health risk assessment with Earth observation, in Proceedings of IEEE IGARSS 2024, Athens, Greece, July 7-12, 2024.

Wooster, M.J. and Xu, W., “Sentinel-3 SLSTR Level 2 Active Fire Detection and FRP Product Algorithm.” King’s College London, Feb. 15, 2021.

Yao, F. (2021) Machine learning with limited data, arXiv 2101.11461, https://arxiv.org/abs/2101.11461

Monitoring wildfire emissions and smoke transport based on Earth Observation

*Mark Parrington, Enza di Tomaso, Johannes Flemming, Antje Inness, Joe McNorton, Francesca Di Giuseppe, Richard Engelen, Laurence Rouil
European Centre for Medium-Range Weather Forecasts, Robert-Schumann-Platz, Bonn, Germany / Shinfield Park, Reading, UK, mark.parrington@ecmwf.int

**Corresponding Author*

Introduction

Wildfires have received increasing levels of interest and widespread coverage in the global media in recent years following severe wildfire seasons, posing risk to life and environmental devastation, in the northern (e.g., California, Canada, eastern Russia, and the Arctic) and southern (e.g., Australia and Chile) hemispheres. The resulting smoke emissions and their impacts on air quality and human health are also critical aspects related to wildfires and biomass burning. While total burned areas, and estimated smoke emissions, have been decreasing over the past two decades at the global scale, related to changes in the use of fire for agriculture in the tropics (e.g., Andela et al, 2017), the frequency and scale of extreme fires at extra-tropical latitudes have been shown to be increasing (UNEP, 2022) with a recent study, based on satellite observations of fire radiative power (FRP), showing the boreal forest and taiga and temperate conifer forest biomes, and the northeastern Arctic region to have had the largest increase (Cunningham et al, 2024). Wildfire smoke emissions include a broad range of pollutants, including particulate matter, carbon gases and many other harmful chemicals which pose significant risks to human health through degraded air and water quality. Many of the pollutants constituting wildfire smoke have sufficiently long chemical lifetimes to be transported several thousand kilometres, including between continents, with further potential impacts on air quality and climate. Transport of smoke from wildfires in North America across the Atlantic to Europe and beyond is not uncommon and has been the main contributor to enhancements in atmospheric carbon monoxide measurements over Europe in the summer months (Petetin et al, 2018). In this short report we present a brief analysis of wildfire emissions from Canada during 2023 and the resulting smoke transport across the Atlantic in data products provided by the Copernicus Atmosphere Monitoring Service (CAMS, https://atmosphere.copernicus.eu), which is operated by the European Centre for Medium-Range Weather Forecasts (ECMWF) on behalf of the European Commission.

Materials and Methods

The analysis presented here is based on CAMS data of estimated wildfire carbon emissions and the global operational forecasts and reanalysis of aerosol optical depth (AOD):

- Wildfire emissions are provided by the Global Fire Assimilation System (GFAS) v1.2 (Kaiser et al, 2012) based on FRP observations from the MODIS instruments on the NASA Terra and Aqua satellites to provide daily global fire emissions estimates at a

- resolution of 0.1 degrees longitude by 0.1 degrees latitude from 1 January 2003 to the present day.
- Operational 5-day forecasts of global atmospheric composition at approximately 40 km spatial resolution are initialized at 00 UTC and 12 UTC each day, from 'analyses' which merge satellite observations of ozone, carbon monoxide, nitrogen dioxide, sulphur dioxide and AOD with the ECMWF Integrated Forecast System model (Benedetti et al, 2009).
- A reanalysis, which uses a combination of observations and numerical models to recreate historical conditions, of global atmospheric composition provides a self-consistent dataset from 2003 to present which can be used to evaluate decadal tendencies and interannual variability of key atmospheric pollutants (Inness et al, 2019).

All of these datasets are fully open access and available to download from https://ads.atmosphere.copernicus.eu/.

Results

Significant wildfires in Canada during 2023 began in early May with several large-scale fires in Alberta which were followed later in month, and early June, with fires in Quebec. Smoke from the Quebec fires was notable in global media due to the impacts on surface air quality across eastern Canada and the northeastern United States. The largest-scale Quebec fires burned until mid-July but fires in Alberta, along with those in other western Canadian provinces and territories, continued from late spring and through the summer until the end of September. In the Northwest Territories, fires developed over a few days in late May and early June but increased rapidly from early July to become the most affected Canadian territory, resulting in evacuations from many population centres and many days of widespread air quality degradation. Figure 1 shows the daily total cumulative wildfire carbon emissions for Canada between 1 January and 31 December 2023 and the almost continuous burning across the country from the beginning of May until the end of September. The annual total estimated emissions of 480 megatonnes of carbon were considerably higher than any of the other years for Canada in the GFASv1.2 dataset (shown as the grey dashed lines in Figure 1) and constituted ~22% of the annual global total fire emissions for 2023.

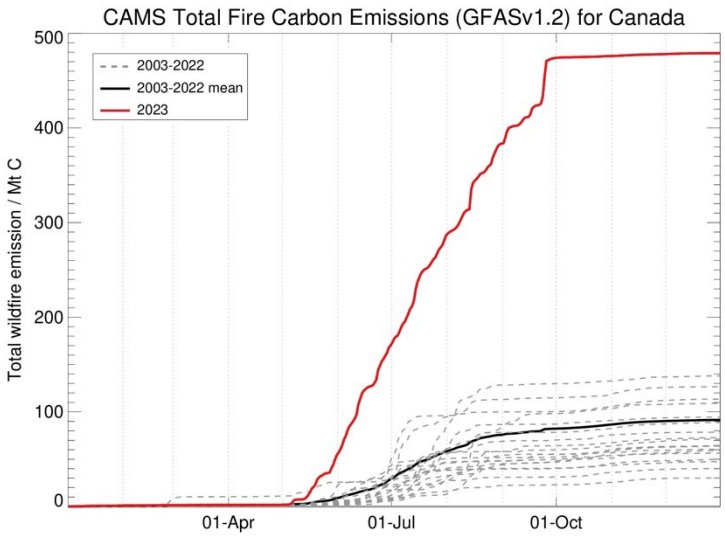

Figure 1: Daily total cumulative wildfire carbon emissions for Canada for 2023 (solid red line) compared to all years from 2003 to 2022 (grey dashed lines) and the mean of the 2003-2022 data (solid black line).

CAMS operational analyses and forecasts provided up-to-date information of the long-range transport of wildfire smoke throughout the duration of Canada's wildfires in 2023 around the northern hemisphere. Figure 2 illustrates an example of long-range smoke transport in AOD analyses valid for 00 UTC on 26 and 27 June. Very high AOD values (greater than 1) were forecast and observed to cross the North Atlantic and reach Europe on these days. The bottom two panels of Figure 2 show AOD enhancements on these days in the CAMS forecasts and independent NASA Aerosol Robotic Network (Aeronet, https://aeronet.gsfc.nasa.gov/) AOD observations made from sites at Graciosa, in the Azores, and Evora, Portugal.

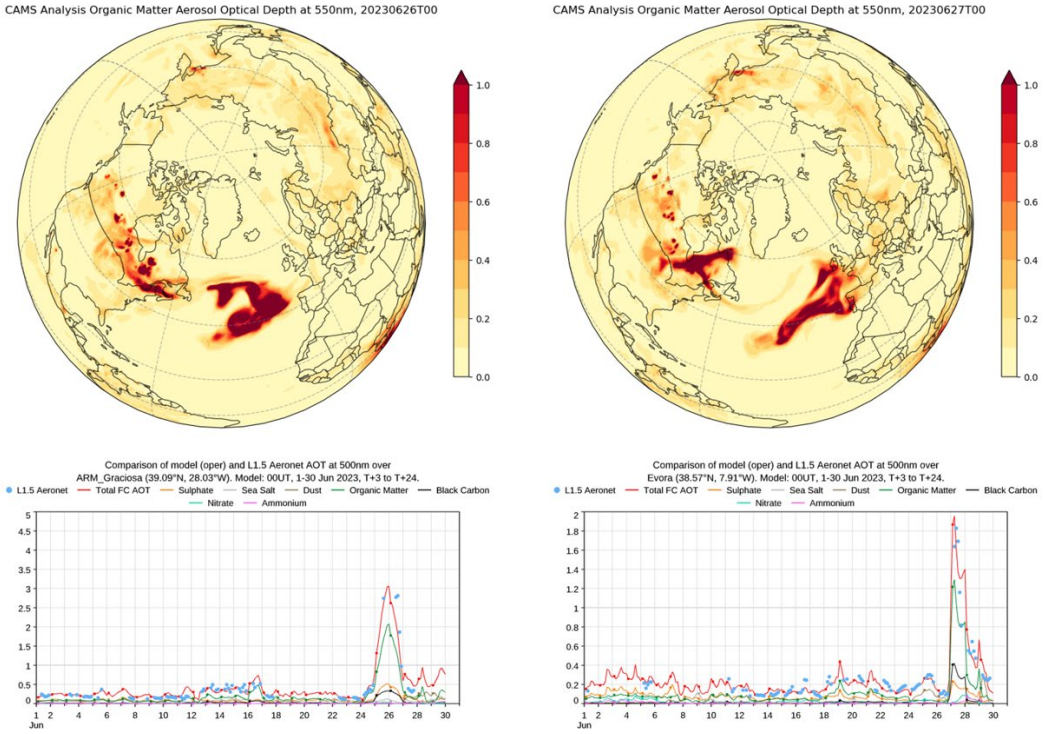

Figure 2: Global AOD analyses valid for 00 UTC on 26 and 27 June 2023 (top two panels) and evaluation of AOD forecasts against Aeronet observations from sites in Graciosa, the Azores and Evora, Portugal (bottom two panels; red and green lines correspond to total and organic matter AOD, respectively).

Monthly mean anomalies of atmospheric composition, relative to the climatology calculated as the mean of the data from 2003 to 2022, further illustrate the extreme impact of the 2023 Canada wildfire emissions. Figure 3 shows the monthly mean AOD anomaly for June 2023 covering a large area extending from western Canada across the northeastern US and the North Atlantic as far as Europe. Positive anomalies (red) where the AOD was above the climatological values by more than 0.3. It is also interesting to note the band of negative anomalies (blue) extending across the Atlantic further south indicating lower than average mineral dust transport from the Sahara over the ocean during June 2023. Other months in 2023 showed similar patterns in positive anomalies.

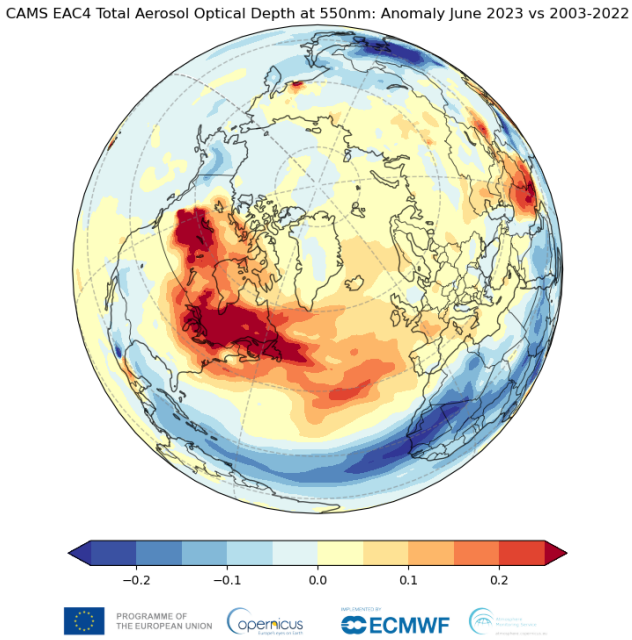

Figure 3: Anomaly in June monthly mean aerosol optical depth in 2023 relative to a climatology calculated from June monthly means from 2003 to 2022.

Discussion

Large-scale wildfires which can burn at high intensity for several weeks have been affecting many regions around the world in recent years. Wildfires at this scale result in vast amounts of smoke pollution which can severely degrade air quality close to the fires and be transported over much larger, inter-continental, distances. We presented the notably extreme Canadian wildfires of 2023 as an example to illustrate this. Wildfire emissions estimates based on satellite observations are available from a number of datasets which, while broadly showing consistent tendencies over the past two decades, are highly uncertain and can vary significantly in magnitude. Changes in the observing system also contribute to the quantifying and evaluating the long term evolution of global wildfires and their uncertainties. A new international activity on Biomass Burning Uncertainty: ReactioNs, Emissions and Dynamics (BBURNED, https://www2.acom.ucar.edu/bburned) aims to consolidate state-of-the-art science on fire ecology, fuel state and behaviour, and atmospheric chemistry to improve the emission estimation and resulting smoke impacts. Wildfire management activities under IAWF can play a key role in this activity through providing detailed local knowledge of fuels and wildfire behaviour. Recent and future developments in wildfire observations forecasting, in conjunction with machine learning and artificial intelligence, will further improve estimates of wildfire emissions and predicting smoke impacts on air quality.

References

- Andela, N et al (2017) A human-driven decline in global burned area. *Science*, 356, 1356-1362.
- Benedetti, A et al (2009) Aerosol analysis and forecast in the European Centre for Medium-Range Weather Forecasts Integrated Forecast System: 2. Data assimilation. *Journal of Geophysical Research*, 114, D13205.

- Cunningham, CX, Williamson GJ, Bowman DMJS (2024) Increasing frequency and intensity of the most extreme wildfires on Earth. *Nature Ecology and Evolution*.
- Inness, A et al (2019) The CAMS reanalysis of atmospheric composition, *Atmospheric Chemistry and Physics*, 19, 3515–3556.
- Kaiser, JW et al (2012). Biomass burning emissions estimated with a global fire assimilation system based on observed fire radiative power. *Biogeosciences*, 9, 527–554.
- Petetin, H et al (2018) The role of biomass burning as derived from the tropospheric CO vertical profiles measured by IAGOS aircraft in 2002–2017, *Atmospheric Chemistry and Physics*, 18, 17277–17306.
- United Nations Environment Programme, UNEP (2022). Spreading like Wildfire: The Rising Threat of Extraordinary Landscape Fires. A UNEP Rapid Response Assessment. (Nairobi, Kenya).

Proceedings for the 7th International Fire Behavior and Fuels Conference April 15-19, 2024, Boise, Idaho, USA – Tralee, Ireland – Canberra, Australia Published by the International Association of Wildland Fire, Missoula, Montana, USA

Picture Perfect Fuels: Applying In-Field Photoload Series In British Columbia

*Madison Hughes
Forsite Consultants Ltd, Thompson Rivers University, Kamloops, British Columbia, Canada, mhughes@forsite.ca

**Corresponding Author*

Introduction

With the current mega-fire regime seen on the landscape due to fuel loading, mitigation work is now essential across the landscape to prevent a worsening situation. Fuel management and risk reduction work needs to be conducted across the landscape in a timely, efficient, and non-costly manner as the current status quo is not working. Although large scale changes for fuel management on a provincial scale are needed for British Columbia, changing fuel sampling methods to be more efficient and cost effective can be the first step to addressing the problem within British Columbia.

The current standards for surface fuel data collection, outlined by the British Columbia Wildfire Service (BCWS), follow the line intercept fuel sampling method where dead and downed woody debris is tallied based on size along a transect to calculate fuel loading. Multiple transects must be completed per site to collect accurate information. This is a tedious costly method that makes conducting large landscape level fuel management prescriptions complicated to conduct. In addition to this, other fuel sources, such as vegetation, cannot be sampled with this method. To combat this, implementing a new method which quickly and accurately estimates surface fuel loadings should be used for these landscape fuel projects in British Columbia. This is the photoload sampling method (Keane and Dickinson 2007a, 2007b).

The photoload sampling method uses downward looking visual assessments of loading referenced pictures to depict estimated fuel loading for each fuel component. Photoload sampling allows efficient data collection of both woody debris and vegetative surface fuels for consistent fuel loadings at an accuracy required for fuel management prescriptions and treatment planning. This method is user friendly in the field and is faster and more efficient while having approximately the same biases as the line intercept method (Sikkink and Keane 2008).

This pilot study will adapt the previously developed photoload series methods so the first in-field photoload series can be created and applied to the biogeoclimatic (BEC) zone ecosystem classification of British Columbia.

Methods

Site Description

Data collection took place in the Thompson Very Dry Hot Interior Douglas-Fir (IDFxh2) BEC zone. This ecosystem is characterized by Interior Douglas-fir (*Pseudotsuga menziesii var glauca*) and Ponderosa Pine (*Pinus ponderosa*) trees and pinegrass (*Calamagrostis rubescens*) in the understory. The shrub layer is sparse, but contains common juniper (*Juniperus communis*), common snowberry (*Symphoricarpos albus*), and rose species (*Rosa spp.*). The Coastal Mountain rainshadow creates a very dry climate with hot summers. Although historic low frequency fires have maintained the open savannah like forests, neither of the sites have experienced fire in over 100 years. This fire exclusion has altered forest structure and dynamics, promoting a heavier fuel loading and accumulation of surface fuels.

Field Methods

Methods used to sample the sites for the photoload series followed the procedures presented by Stalling and Keane in their study on creating in-field photoload series (2020).

For fine woody debris (FWD), <7cm (0.07m) in diameter), and the vegetative fuels (grass, shrubs, and herbs), a 1 x 1 m square frame was used to define the boundaries of each plot. Plot locations were randomly chosen with the goal to sample a gradient of fuel loadings for each fuel type. Once the plot frame was laid on the ground, photos were taken directly over top the frame to capture the plot at a flat angle. Average height, species canopy cover and total canopy cover were collected for the vegetative fuels. All biomass for the specified surface fuel of that plot was collected from within the plot frame and above the litter layer. Samples were stored in labeled paper bags.

Since large diameter woody debris (LDWD), 7-19 cm (0.07-0.19m) diameter, and coarse woody debris (CWD), >20 cm (0.2m) diameter, fuels vary at a greater spatial scale then can be depicted by a 1 x 1 m photo, different sampling was conducted. This would allow fuel loading tables to be produced, instead of photoload series. These methods and results are not discussed further in this abstract.

Laboratory Methods

FWD samples for each plot were further separated into the BCWS FWD size classes to match fuel management prescription requirements. FWD and vegetative fuels were dried in a drying oven for a minimum of 48 hours at 90°C. After the drying process, the samples were removed and weighed for the dry weight. All weights were calculated in kg m^{-2}, then were associated with the plot photos to develop the photoload series.

The photoload series were formatted so photos are in order of lowest to highest fuel loadings to represent the entire gradient of fuels across the site. Any additional

measured attributes were also included with the photoload series. All photoload series were combined to develop the first photoload series book for the IDFxh2.

Results

In total, seven photoload series were constructed to represent FWD, grass, shrubs, and herbs across the IDFxh2 BEC zone. Each of the photoload series is composed of a total of nine images arranged in ascending order. Fuel loadings and any additional attributes are associated with the photograph. Two types of series were produced for each of the vegetative fuels, one sorted by fuel loading, and another sorted by canopy cover. The FWD photoload series is provided as an example (Figure 31).

Figure 31. Fine woody debris photoload series for Thompson Very Dry Hot Interior Douglas-fir (IDFxh2). Sorted ascending by fuel loading.

Discussion

The development of these photoload series will be beneficial for the use within the IDFxh2 during fuel management prescriptions in British Columbia. The design of the single page photoload series with only nine images allows for quick visual evaluations in the field. Rather than tallying each stick along a transect, quick snap decisions can be made on the fuel loading of the landscape. This technique is beneficial when time and money may be limited, while still having accurate estimates of fuel loadings (Sikkink and

Keane 2008). The FWD photoload series with all the combined size classes allows evaluators to determine total FWD fuel loading without previously determining the size class of each woody debris. This design of the FWD photoload series does compromise knowing the exact loadings of each individual size class that may be needed for an in-depth analysis of FWD. The development of the canopy cover photoload series for the vegetative fuels allows evaluators to estimate the canopy cover of the plot, then verify their estimate with the photoload series. These series also give an opportunity to quantify grasses, shrubs, and herbs fuel loadings that can affect fire behaviour and the need for fuel management. This was something that could not be conducted by using the line intercept fuel sampling method. The development of all the photoload series indicates the initial success of the pilot study.

Further research should be conducted to continually improve the photoload series for field application as subsequent series are developed. The introduction of the photoload series sampling technique to British Columbia is feasible, if further research goes into understanding the accuracy of the developed photoload series and continually improving upon the limitations. This study should contribute as the starting point for further photoload series development across the province of British Columbia.

Acknowledgments
I would like to extend deep gratitude and thanks to everyone who helped me throughout this project. First to my thesis committee, Dr. John Karakatsoulis, Dr. Wendy Gardner, and Jacqueline Sorensen for taking time to see this project to the end and provide academic support. To Andy Low, RPF and the team at Forsite for providing me with this project. Thanks to John and Andy as well for assisting me in the field on the 40°C days, and John for spending countless hours in the lab sorting sticks. Thank you to Laura Oldring who helped dry and weigh all the samples. Thank you to Robert Keane, Heather Heward, and the rest of the US Rocky Mountain Research Station Photoload team, who graciously provided feedback on the photoload series.

References

Keane RE, Dickinson LJ (2007a) ‘Development and Evaluation of the Photoload Sampling Technique’. USDA, Forest Service, Rocky Mountain Research Station Paper RMRS-RP-61CD. (Fort Collins, CO)

Keane RE, Dickinson LJ (2007b) ‘The Photoload Sampling Technique: Estimating Surface Fuel Loading from Downward Looking Photographs of Synthetic Fuelbeds’. USDA, Forest Service, Rocky Mountain Research Station General Technical Report No.: RMS-GTR-190. (Fort Collins, CO)

Sikkink PG, Keane RE (2008) A comparison of five sampling techniques to estimate surface fuel loading in montane forests. *International Journal of Wildland Fire* **17**, 363-379.

Stalling S, Keane RE (2020) 'Creating Photographic Loading Sequences in the Field for the Photoload Sampling Technique'. USDA, Forest Service, Rocky Mountain Research General Technical Report No.: RMRS-GTR-416. (Fort Collins, CO)

Proceedings for the 7th International Fire Behavior and Fuels Conference April 15-19, 2024, Boise, Idaho, USA – Tralee, Ireland – Canberra, Australia Published by the International Association of Wildland Fire, Missoula, Montana, USA

Prioritization of POD network fuel treatments using spatial data

*Joseph St. Peter
University of Montana, 32 Campus Drive, Missoula, Montana, USA, joseph.stpeter@mso.umt.edu

John Hogland
Rocky Mountain Research Station, USDA Forest Service, 800 E Beckwith Ave., Missoula, Montana, USA, john.s.hogland@usda.gov

**Corresponding Author*

Introduction

Potential Operational Delineations (PODs) have been used in the western United States in recent years to provide a spatial fire planning framework and help guide wildfire response using predefined strategic response zones (Thompson *et al.* 2022). POD spatial units are bound by potential control features on the landscape and can be used to summarize forest conditions, fire potential and risk. The process of developing, and updating PODs, is a risk based, easily documented, and scientifically sound framework for managing wildfire risk (O'Connor *et al*. 2017; Thompson *et al.* 2022). However, opportunities for using this framework to identify and prioritize fuels reduction, hardening or POD boundaries, or implementing other treatments to reduce wildfire risk, are underdeveloped. The project presented here uses spatial data and local knowledge in the Colorado Front Range to prioritize hazardous fuel treatments along POD boundary networks based on their relative cost. Prioritizing silvicultural prescriptions is meant to modify potential fire behavior so that the use of prescribed fire or unplanned ignitions within POD networks can be used to meet management objectives.

The landscape scale fuel treatment assessment workflow presented here quantifies the existing condition of fuels, the desired condition of fuels, and the cost to move the landscape from existing to desired condition building from the methods used in previous studies (Hogland *et al.* 2018; Hogland *et al.* 2021). The desired future condition is defined by local experts as the condition of the forest that reduces the severity of wildlife and the risk of transmission across POD boundaries. The total cost of modifying the landscape from current to desired condition includes the extraction costs of excess lumber as well as any potential transportation costs to mill locations and resulting revenue. The results of this workflow are relative treatment cost surfaces, and potential treatment units along and interior to POD networks. These results are designed to be used with risk assessments that our project partners are conducting, to provide cost and opportunity data to risk-based prioritization of fuel treatments. This assessment helps connect land and resource management objectives to fire management decisions spanning prescribed fire, managed wildfire, or full suppression.

Materials and Methods

Our workflow was developed using Python 3 (Van Rossum and Drake 2009) and incorporates the packages OSMnx (Boeing 2024) and Raster Tools (Hogland and Bunt 2024). The first step involves acquiring data for our area of interest, which in this project is the Arapaho-Roosevelt National Forest. We obtained the national forest boundary from OpenStreetMap (OpenStreetMap contributors 2024) using the OSMnx package, then buffered it by 0.03 degrees to define our study area. Within this area, we accessed streams, water bodies, and road layers from OpenStreetMap, as well as digital elevation models (DEM) from the 3DEP program (U.S. Geological Survey 2024) using the py3dep package (Chegini et al. 2021). We acquired the POD boundaries network for our study area from the National POD Network (National Interagency Fire Center 2024). To assess the existing forest condition, we used 2018 Treemap data (Riley et al. 2016) to extract basal area per acre, trees per acre, and above-ground biomass. The Treemap and DEM data were aggregated to a 30m horizontal spatial resolution. This baseline data is shown in Figure 1.

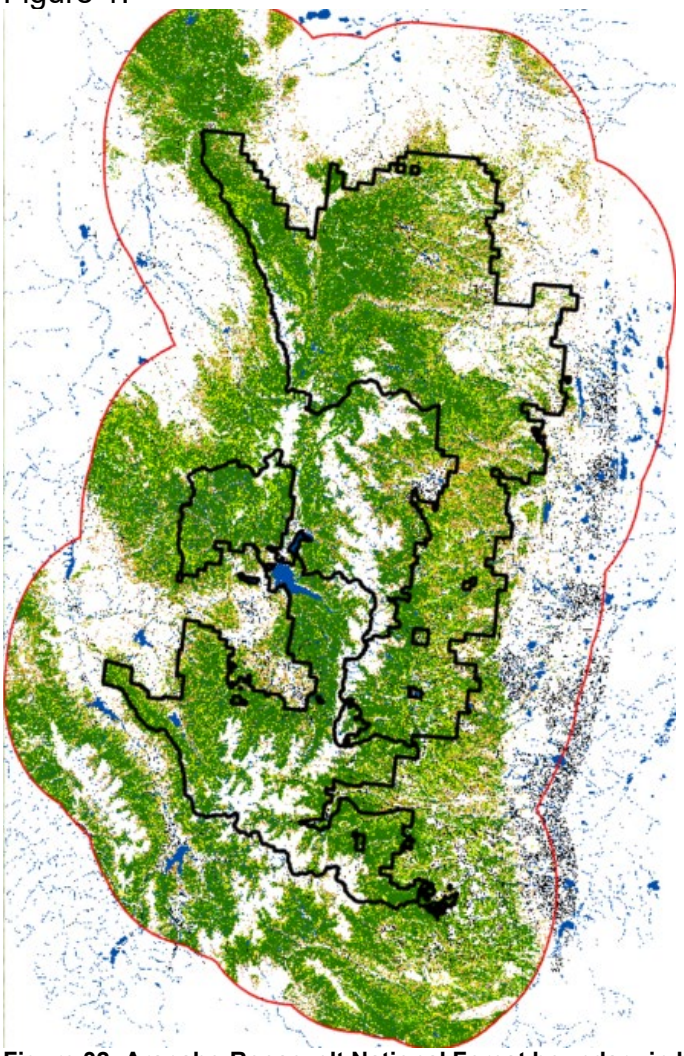

Figure 32: Arapaho-Roosevelt National Forest boundary in black with 0.03 degree buffer in red. Basal area per acre raster is shown along with waterbodies, streams and road network.

The next step is to define a desired future condition, which is a target forest metric aimed at reducing fire severity within and along POD network boundaries. For this area, we focused on basal area per acre (BAA). We set BAA targets for north-facing aspects (greater than 290 degrees and less than 70 degrees) to be less than or equal to 47 ft². For all other aspects, BAA was set to be less than or equal to 33 ft². Within 610 m of POD boundaries, BAA was set to be less than or equal to 24 ft². Additionally, a 30 m buffer was established around streams and on slopes greater than 50%, where no changes in BAA would be implemented due to legal or practical restrictions on fuel treatments. The resulting raster surface of desired future BAA was subtracted from the current BAA raster to create a raster surface indicating the BAA removal needed to reach the desired future condition.

The third step is adding costs to the fuel removals identified in the previous step. For this step we created a rate table that consists of the fuel treatment component, the system to be used, the cost and rate of travel, the payload and where these systems can be used, see table 1. These costs are applied to our study area to get a cost of extraction and delivery of fuel for every 30 m pixel.

Component	System	Cost	Rate of travel	Payload	Where it can occur
Offroad	Rubber tire skidder	$165/hr	1.5 MPH	1.25 CCF	Slopes <= 35% and Next to Roads (distance < 460 m from a road).
	Skyline	$400/hr	2.0 MPH	1.04 CCF	Slopes > 35% and within 305 m of a road.
	Helicopter	$8,000/hr	2.4 MPH	1.67 CCF	Areas not covered by the other two and distance < 915 m from landing area.
Felling	Feller buncher	$49.6/CCF	NA	NA	Slopes <= 35%
	Hand Felling	$56.4/CCF	NA	NA	Slopes > 35%
Processing	Delimbing, cutting to length, chipping, and loading	$60.90/hr	NA	NA	NA
On road	Log Truck	$160/hr	Road Dependent	12.25 CCF	NA
Additional Treatments	Hand Treatment	$3210/acre	NA	NA	Forested Areas
	Prescribed fire	$900/acre	NA	NA	Forested Areas

Table 33: Machine rate table for Arapaho-Roosevelt National Forest. CCF is hundred cubic feet

The final step in this process is to combine the treatment costs (and potential revenue if any) into treatment units. We defined this as continuous areas needed treatment of at least 1650 m^2. The cost for each treatment unit was calculated as the sum of the costs for all pixels contained within it.

Results

Across the study area the cost to treat the entire area was 10x higher than the cost to treat along the POD boundaries (see figure 2).

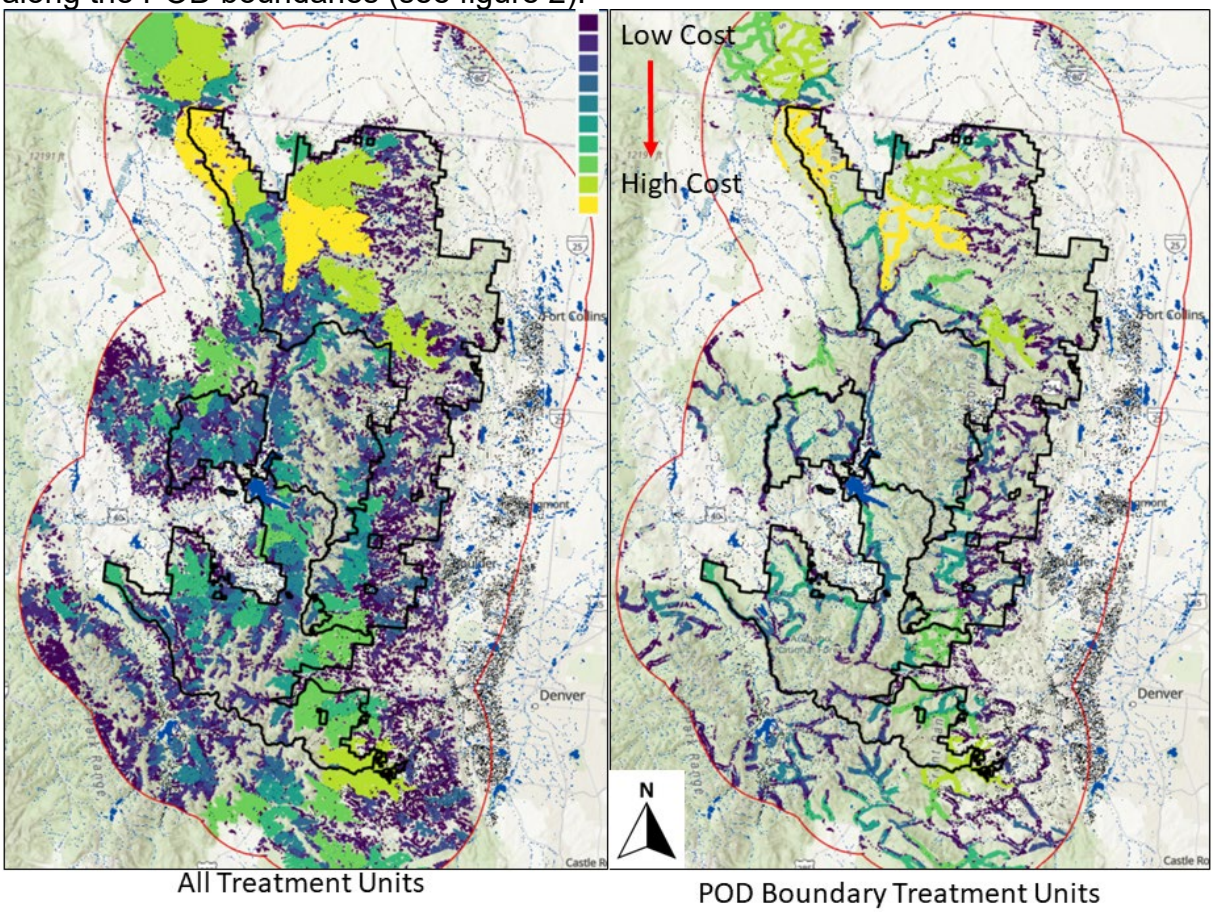

Figure 2: Resulting treatment units from entire study area (on left) and those along POD boundaries (on right).

Discussion

This example scenario demonstrates the usefulness of this scenario when properly parametrized. This process can be improved by using improved estimates of current condition information, possibly from modelling remotely sensed information or recent fire perimeters. Further improvements come from definable metrics for desired future condition and fuel treatment scenarios. We are currently interviewing land managers on their methods for defining these metrics. However this process is not meant to be run once, but to be packaged as a tool that can be run dynamically during planning and implementation phases to compare fuel treatment scenarios under different economic conditions. This project is ongoing and our results presented here are meant only as examples of the process. We also acknowledge that there are many factors beyond cost that go into deciding where fuel treatments occur on a landscape.

Acknowledgements
This research was supported by the U.S. Department of Agriculture, Forest Service with funding from the Infrastructure Investment and Jobs Act of 2021 and Inflation Reduction Act of 2022.

References

Boeing G (2024) "Modeling and Analyzing Urban Networks and Amenities with OSMnx." Working paper. URL: https://geoffboeing.com/publications/osmnx-paper/

Chegini T, Li H, Leung LR (2021) HyRiver: Hydroclimate Data Retriever. *Journal of Open Source Software* **66**(6), 1-3.

Hogland J, Anderson N, Chung W (2018) New Geospatial Approaches for Efficiently Mapping Forest Biomass Logistics at High Resolution over Large Areas. *ISPRS International Journal of Geo-Information* **7**(4),156.

Hogland J, Dunn CJ, James D. Johnston JD (2021) 21st Century Planning Techniques for Creating Fire-Resilient Forests in the American West. *Forests* **12**(8), 1084.

Hogland J, Bunt F (2024) Raster Tools, GitHub repository, https://github.com/UM-RMRS/raster_tools

National Interagency Fire Center (2024) National Potential Operational Delineations (PODs) Public. National Interagency Fire Center. https://data-nifc.opendata.arcgis.com/maps/cc50b6ca69734e4180d5399006058e58/about

O'Connor CD, Calkin DE, Thompson MP (2017) An empirical machine learning method for predicting potential fire control locations for pre-fire planning and operational fire management. *International Journal of Wildland Fire* **26**, 587-597.

OpenStreetMap contributors (2024) OpenStreetMap database, OpenStreetMap Foundation: Cambridge, UK. https://www.openstreetmap.org

Riley KL, Grenfell IC, Finney MA (2016) Mapping forest vegetation for the western United States using modified random forests imputation of FIA forest plots. *Ecosphere* **7**(10).

Thompson MP, O'Connor CD, Gannon BM, Caggiano MD, Dunn CJ, Schultz CA, Calkin DE, Pietruszka B, Greiner SM, Stratton R, Morisette JT (2022) Potential operational delineations: new horizons for proactive, risk-informed strategic land and fire management. *Fire Ecology* **18**, 17.

U.S. Geological Survey (2024) USGS 3D Elevation Program Digital Elevation Model, accessed February 7, 2024 at URL https://elevation.nationalmap.gov/arcgis/rest/services/3DEPElevation/ImageServer.

Van Rossum G, Drake FL. Python 3 Reference Manual. Scotts Valley, CA: CreateSpace; 2009

Proceedings for the 7th International Fire Behavior and Fuels Conference April 15-19, 2024, Boise, Idaho, USA – Tralee, Ireland – Canberra, Australia Published by the International Association of Wildland Fire, Missoula, Montana, USA

PROPAGATOR for Large Wildfires: Brazilian Case Study

Nicolò Perello*
Department of Informatics, Bioengineering, Robotics and Systems Engineering, University of Genoa, Via All'Opera Pia, 13, 16145 Genova, Italy
nicolo.perello@edu.unige.it

Ubirajara Oliveira
Universidade Federal de Minas Gerais, Centro de Sensoriamento Remoto, Instituto de Geociências. Av. Antônio Carlos, Pampulha, Belo Horizonte (MG), Brasil
ubiologia@yahoo.com.br

Mirko D'Andrea
CIMA Research Foundation, Via A. Magliotto, 2, 17100 Savona, Italy
mirko.dandrea@cimafoundation.org

Britaldo Silveira Soares-Filho
Universidade Federal de Minas Gerais, Centro de Sensoriamento Remoto, Instituto de Geociências. Av. Antônio Carlos, 6627, Pampulha, Belo Horizonte (MG), Brasil
britaldossf@gmail.com

Paolo Fiorucci
CIMA Research Foundation, Via A. Magliotto, 2, 17100 Savona, Italy
paolo.fiorucci@cimafoundation.org

**Corresponding Author*

Introduction

PROPAGATOR (*Trucchia et al. 2020, Perello et al. 2024*) is a wildfire propagation model developed in 2008 by CIMA Foundation. The objective of the model is to quickly provide a wildfire scenario to support decision-making during emergencies. Nowadays, the model is available in a user-friendly web application as an operational tool to the Italian Civil Protection Department.
Given the operational use purpose, the model must keep the computational time several orders of magnitude shorter than the actual wildfire propagation time. This has been possible so far thanks to the use of cellular automata, keeping computational time within a few minutes for typical Mediterranean wildfires (that is, on the order of hundreds or few thousands of hectares, see *Trucchia et al. 2024*).
Many authors argue that the effects of Climate Change, especially when coupled with socio-economic and land use changes (e.g., agricultural abandonment), can lead to an increase in particularly large and intense *extreme wildfires* also in the Mediterranean Basin (*Tedim et al. 2018*). For this reason, it has become necessary to evaluate the

capability of PROPAGATOR to simulate particularly large events and to find solutions to keep the computation time within a few minutes.

Material and Methods

PROPAGATOR is a semi-empirical stochastic cellular automata model. The domain is discretized into a square grid, where each cell can be *unburned*, already *burned* or is *burning*, and it is associated with static (fuel type, elevation) and dynamic (wind and fuel moisture) conditions given in input. It uses a custom fuel classification.
The fire propagation dynamics is a stochastic contamination process between *burning* and *unburned* cells, where spreading probability depends on cell conditions (both static and dynamic). Once it is ignited, the cell burning time depends on cell conditions. The contamination process is repeated many times (i.e., 100 times) producing a *simulation ensemble* within a Monte Carlo framework, used to compute the *fire probability map* based on the frequency of burning per each cell. See *Figure 1* for a model's schema.
In the last release, the model also provides rate of spread and fire-line intensity maps. Also, it is able to consider the spotting propagation process and firefighting actions.

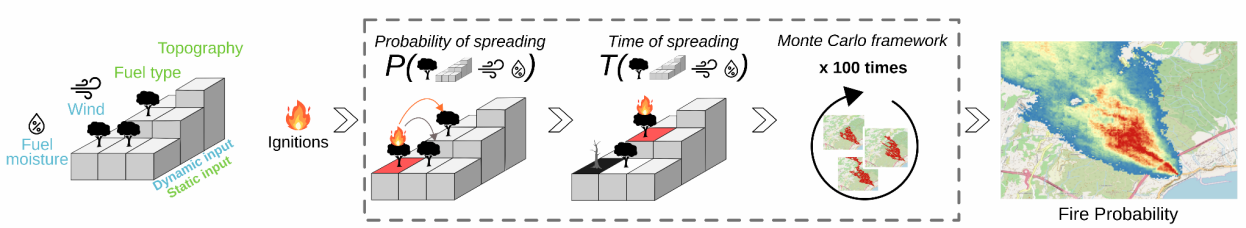

Figure 1: Graphical representation of PROPAGATOR model, highlighting inputs, outputs and main steps.

In the present work, the PROPAGATOR model has been implemented using Dinamica EGO (*Soares-Filho et al. 2013*), a freely available environmental modeling platform. It employs a dataflow language paradigm and presents a graphical interface to easily design a model. Thus it can be used to create user-friendly applications. Some key aspects of Dinamica EGO are the optimization of memory usage and the parallel computing. Also, it allows Python integration and specific algorithms for cellular automata. For these reasons, the software proved to be a useful tool for testing the reduction of computational time of PROPAGATOR.
Since PROPAGATOR is currently implemented in the Python language, its code was transported into Dinamica EGO. In *Figure 2* the schema of the final model is shown.

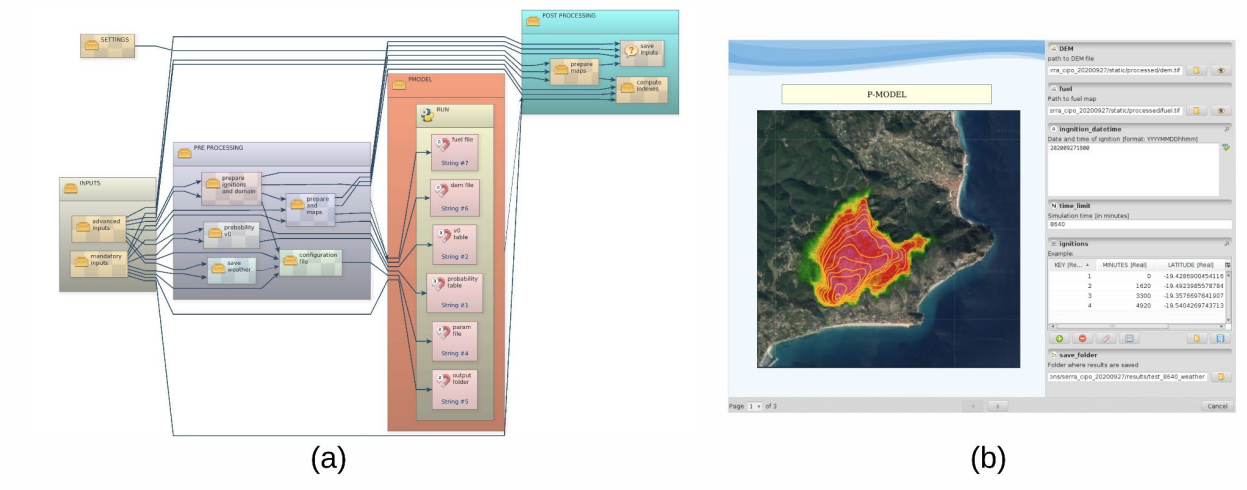

Figure 2: (a) Schema of PROPAGATOR implementation within Dinamica EGO; (b) user interface.

To test the performance for large wildfires, an event occurred in the Serra do Cipó National Park, Minas Gerais (BR) in September 2020 was selected. The area of the event is shown in *Figure 3*. A report[2] of the event is provided by the Centre for Remote Sensing (CSR) of the Federal University of Minas Gerais, in the context of the FIP-cerrado project[3] (*Oliveira et al. 2023*). The event started on 27th September, around 6:00 pm local time, and lasted for around 10 days burning almost 28 thousand ha. Four ignitions in total occurred, merging into a single event. A temporal schema of the ignitions is shown in *Figure 4*.
To simulate the event with PROPAGATOR, the 2019 land use map provided by FIP-Cerrado project has been converted into PROPAGATOR fuel classes (see *Table 1*), maintaining the conversion already adopted using the European CORINE land use map. Also, the DEM map provided within the project has been used.
The Global Forecast System (GFS) provided by CIMA Research Foundation has been used for the wind conditions, while the RISICO model (*Fiorucci et al. 2008*) running at global scale by CIMA Research Foundation was used for the fuel moisture (see *Figure 4).* Several simulations were performed by increasing the number of simulated days, up to 6 days. No fire-fighting actions were considered due to a lack of their precise spatial and temporal positioning.

[2]https://csr.ufmg.br/fipcerrado/wp-content/uploads/2020/10/RELEASE_PARQUE_ii_INCENDIO_28_setembro_de_2020.pdf (accessed: 20 June 2024).
[3]FIP-Cerrado. Projeto: "Desenvolvimento de sistemas de prevenção de incêndios florestais e monitoramento da cobertura vegetal no Cerrado brasileiro - Componente 2.2: Desenvolvimento de um sistema para prever o risco de espalhamentodo fogo no cerrado" (https://csr.ufmg.br/fipcerrado/, accessed: 20 June 2024).

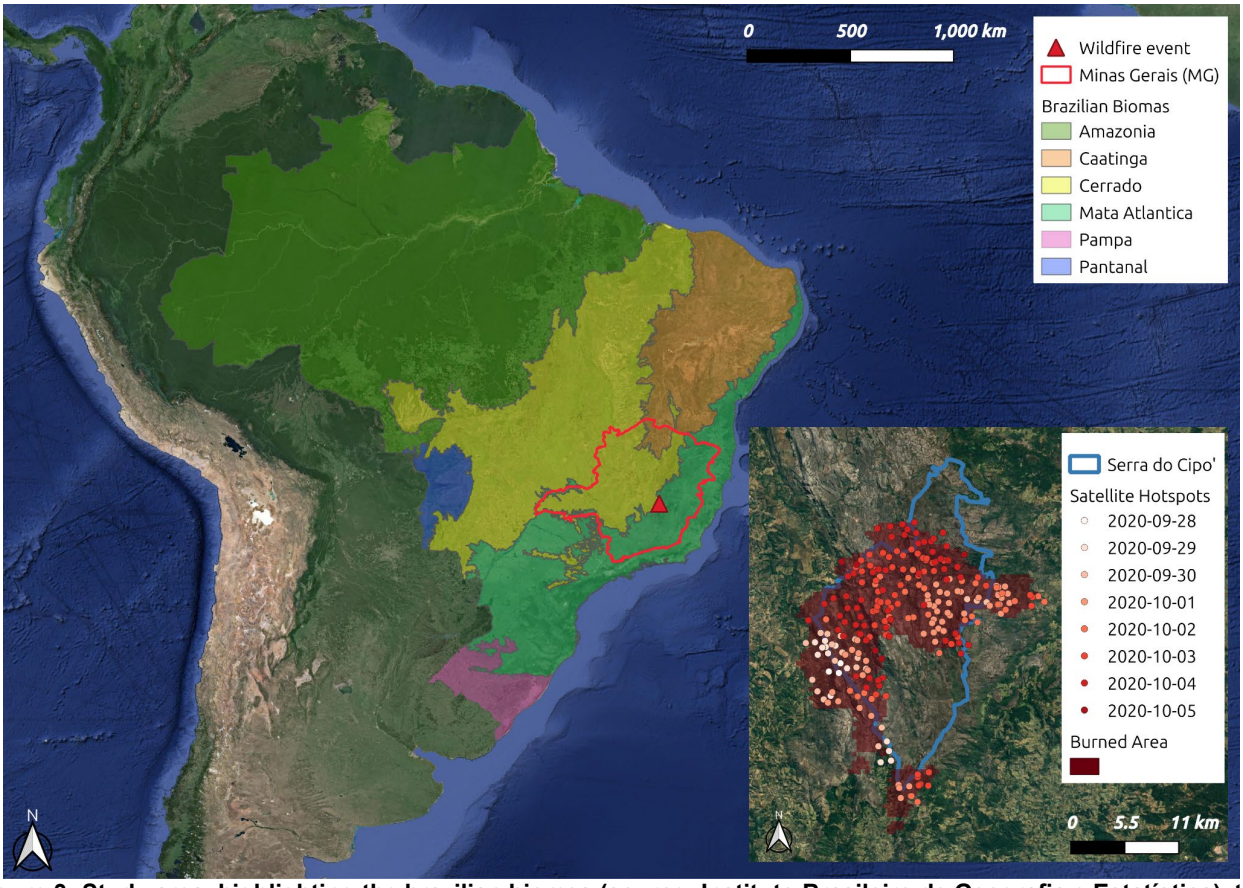

Figure 3: Study area, highlighting the brazilian biomes (source: Instituto Brasileiro de Geografia e Estatística), the satellite hotspots during the event (source: NASA's Fire Information for Resource Management System FIRMS), the Serra do Cipó National Park and the burned area (source: FIP-Cerrado).

Table 1: Conversion between land use categories and the PROPAGATOR fuel classes.

Land Use Category	PROPAGATOR Fuel Type
forest formation	broadleaves
savanna formation	shrubs
grassland pasture	grassland
other temporary crops forest plantation mosaic of uses	agro-forestry area
rocky outcrops urban area river, lake and ocean other non vegetated areas	non vegetated areas

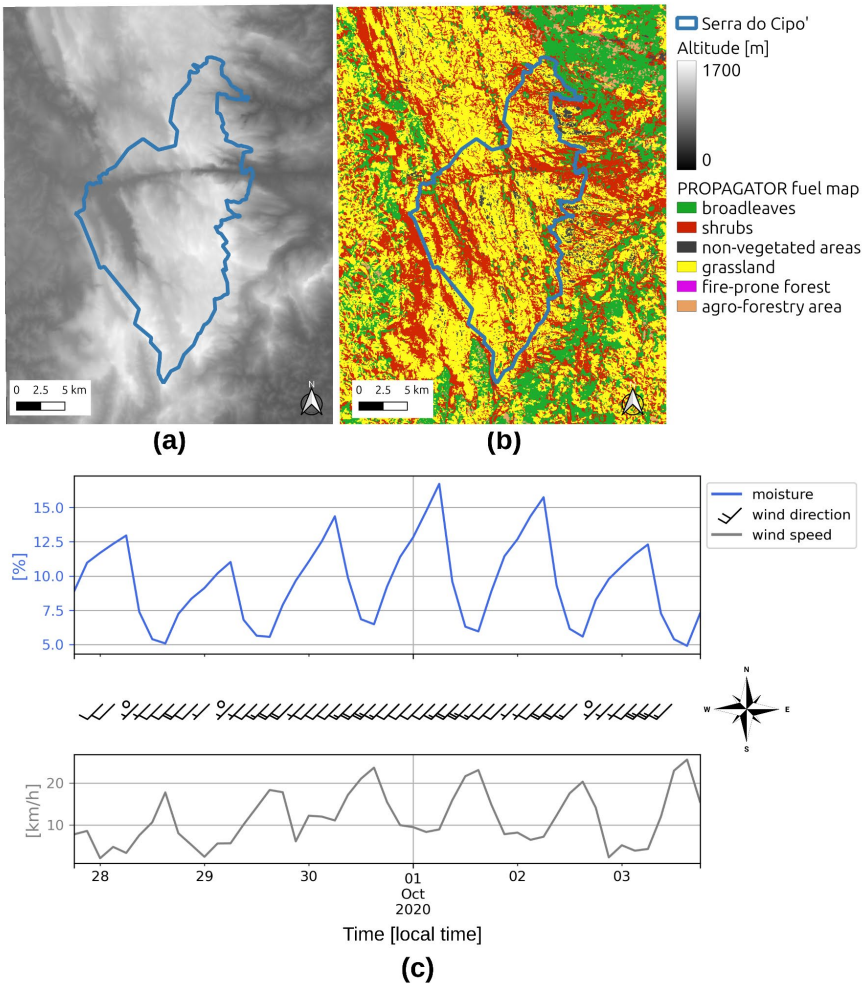

Figure 4: (a) DEM map; (b) PROPAGATOR fuel classes; (c) Fuel moisture and wind conditions.

Results and Discussion

In *Figure 5*, the results of the simulation are shown, while the comparison between the computational times of the operational implementation of PROPAGATOR and its implementation in Dinamica EGO are reported in *Table 2*.
The implementation of the model within Dinamica EGO allowed PROPAGATOR to leverage its optimized memory management and parallel computing capabilities, thereby reducing computation times.
This study has allowed us to identify possible technological choices to reduce the computational time of PROPAGATOR. They need to be further explored in the future to prepare the model for handling large wildfires.
However, the Python code of PROPAGATOR was implemented within Dinamica EGO without fully exploiting its potential for cellular automata models, thus paving the way for a full integration of PROPAGATOR within the software in the future.

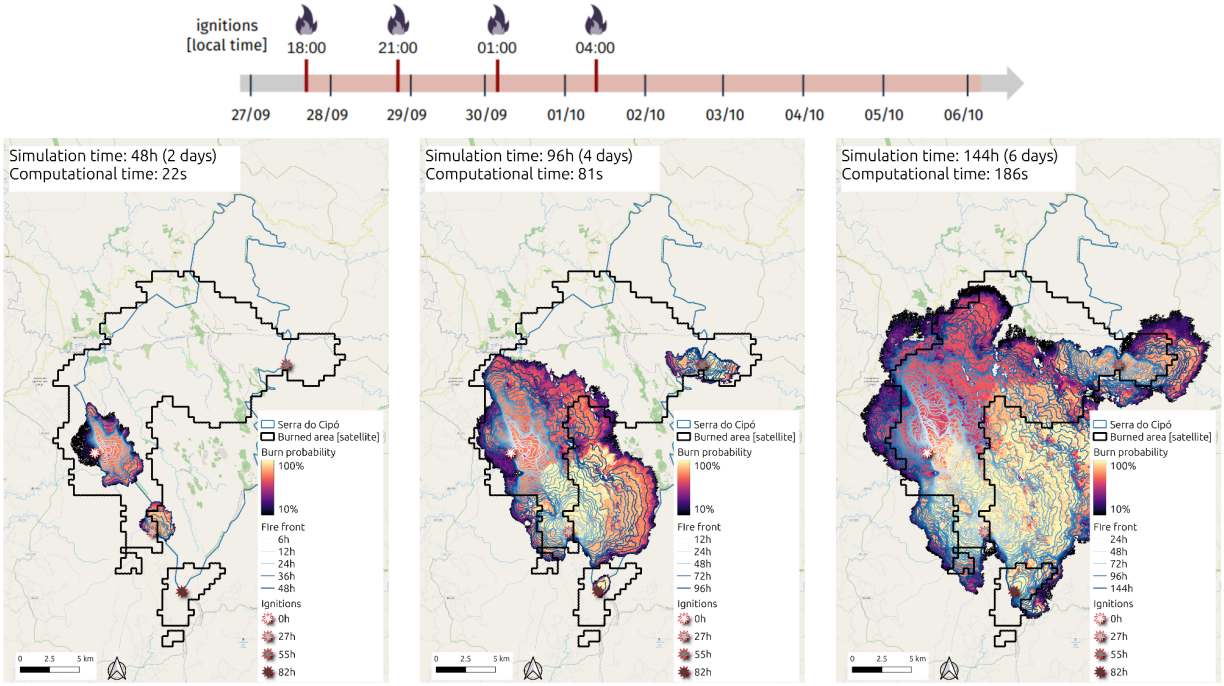

Figure 5: Simulation of the event - the simulation and computational time is highlighted. On top, the temporal schema of the event's ignitions.

Table 2: Comparison of the computational times for the operational implementation of PROPAGATOR and its implementation in Dinamica EGO.

Simulated time [days]	Computational time [s]	
	Operational implementation	Dinamica EGO implementation
1	38	11
2	78	22
3	109	40
4	195	81
5	267	135
6	353	186

References

Fiorucci P, Gaetani F, Minciardi R (2008) Development and application of a system for dynamic wildfire risk assessment in Italy. *Environmental Modelling and Software* **23**(6), 690–702.

Oliveira U, Soares-Filho BS, Rodrigues H, Figueira D, Gomes L, Leles W, Berlinck C, Morelli F, Bustamante M, Ometto J, Miranda H (2023) A near real-time web-system for predicting fire spread across the Cerrado biome. *Scientific Reports* **13**, 4829.

Perello N, Trucchia A, Baghino F, Asif BS, Palmieri L, Rebora N, Fiorucci P (2024) Cellular automata-based simulators for the design of prescribed fire plans: the case study of Liguria, Italy. *Fire Ecology* **20**, 7.

Soares-Filho B S, Rodrigues H, Follador M (2013) A hybrid analytical-heuristic method for calibrating land-use change models. *Environmental Modelling & Software* **43,** 80-87..

Tedim F, Leone V, Amraoui M, Bouillon C, Coughlan MR, Delogu GM, Fernandes PM, Ferreira C, McCaffrey S, McGee TK, Parente J, Paton D, Pereira MG, Ribeiro LM, Viegas DX, Xanthopoulos (2018) Defining Extreme Wildfire Events: Difficulties, Challenges, and Impacts. *Fire* **1**(1), 9.

Trucchia A, D'Andrea M, Baghino F, Fiorucci P, Ferraris L, Negro D, Gollini A, Severino M (2020) PROPAGATOR: An Operational Cellular-Automata Based Wildfire Simulator. *Fire* **3**(3), 26.

Trucchia A, D'Andrea M, Baghino F, Perello N, Rebora N, Fiorucci P (2024) Experiences and Lessons Learnt in Wildfire Management with PROPAGATOR, an Operational Cellular-Automata-Based Wildfire Simulator. In 'Responding to Extreme Weather Events'. (Eds D Sempere-Torres, C Rossi, P Quevauviller, A Karakostas) pp. 49-76. (John Wiley & Sons).

Acknowledgements

The authors acknowledge the Italian Civil Protection Department - Presidency of the Council of Ministers, who funded this research through the convention with the CIMA Research Foundation, for the development of knowledge, methodologies, technologies, and training, useful for the implementation of national wildfire systems of monitoring, prevention, and surveillance.
Soares-Filho is supported by the Brazilian National Council for Scientific and Technological Development (CNPq 304736/2023-6).

Rethinking the rocks: Exploring fire-induced rock spalling, landform evolution, and prospective research avenues

*Rowena Morris
Natural Hazards Research Australia, PO Box 116, Carlton South, VIC 3053 and University of Wollongong, Northfields Ave Wollongong NSW 2522 Australia, rowena.morris@naturalhazards.com.au

Solomon Buckman
University of Wollongong, Northfields Ave Wollongong NSW 2522 Australia, solomon@uow.edu.au

Shaun Hooper
Department of Climate Change, Energy the Environment and Water, 4 Parramatta Square, 12 Darcy Street, Parramatta NSW 2150 Australia, shaun.hooper@environment.nsw.gov.au

**Corresponding Author*

Fire-induced rock spalling is a geological weathering process where exposed rock surfaces flake off following intense, rapid heating or mechanical impact (Figure 1). Over the past century, this phenomenon has manifested in various forms, notably after the 2019/2020 wildfires in south-eastern Australia and the more recent 2021 California wildfires. While post-fire studies traditionally emphasise the impact on the environment, such as flora, fauna, soil, and water systems, there is a growing need to recognise the significance of fire-induced rock spalling in shaping landscapes. This includes understanding its role in sediment generation, erosion rates, and the preservation of indigenous rock art.

The immediate impacts of fire on rock features are clearly evident when the radiant heat directly impacts rock art causing exfoliation and damage to the paintings. Our field observations of fire spalling indicates that a rock's proximity to heat sources such as large tree trunks that burn long after the fire front has passed are more likely to cause fire spalling than rock surfaces exposed to fine fuels only. The sheets of fire-spalled rock are friable and easily crumble to form an apron of sediment that is easily eroded down slope by the action of flowing water. Generally post-fire studies focus on the loss of sediment from hillslopes and catchments rather than the source of sediment from rock faces on cliffs and large boulders in the headlands of the catchment.

Fire-induced rock spalling is an important mechanism of physical weathering in fire-prone landscapes and warrants inclusion into broader landscape evolution models. We present a new hypothesis (Buckman et.al. 2001) that identifies wildfire as a primary agent of flared slope (cave) development around the periphery of inselbergs such as Uluru and Wave Rock which also host important Indigenous rock art. The impact of fire spalling is particularly evident in semi-arid regions where lateral fire spalling dominates over fluvial and chemical weathering to create flared slopes and steep-sided inselbergs. Understanding

fire-induced rock spalling is required not only at a local scale, where it directly impacts rock art and hillslope processes, but also at a broader scale to comprehend its influence on landform evolution.

Figure 34: Examples of fire-induced rock spalling a) Left: 2019/2020 Bushfires, Cobargo, Australia b) Right: 2021 Wildfire, Lake Tahoe, USA

Future studies need to focus on differing rock types. We urge all fire ecologists to contribute to our research by sharing observations of fire-induced rock spalling through the hashtag #burntrocks on social media or via email to the authors of this abstract.

Reference

Buckman S, Morris RH, Bourman RP (2021) Fire-induced rock spalling as a mechanism of weathering responsible for flared slope and inselberg development. *Nat Communications* **12**, 2150.

Proceedings for the 7th International Fire Behavior and Fuels Conference April 15-19, 2024, Boise, Idaho, USA – Tralee, Ireland – Canberra, Australia Published by the International Association of Wildland Fire, Missoula, Montana, USA

Systematic exploration of the ignition of wildland ladder fuels

Yucheng He*
University of California, Riverside, 900 University Avenue, Riverside, California, USA
yucheng.he@email.ucr.edu

Sanika Ravindra Nishandar
University of California, Riverside, 900 University Avenue, Riverside, California, USA
sanika.nishandar@email.ucr.edu

Marko Princevac
University of California, Riverside, 900 University Avenue, Riverside, California, USA
marko@engr.ucr.edu

David R. Weise
USDA Forest Service, Pacific Southwest Research Station, 4955 Canyon Crest Dr, Riverside, California, USA
david.weise@usda.gov

**Corresponding Author*

Introduction

Prescribed burning is the planned application of fire under predefined meteorological conditions to produce desired fire behavior to accomplish various land management goals. The transition of fire from surface to elevated fuels is a significant factor in the increase in energy release and fire behavior in a wildland fire. This transition is defined as the process where a spreading surface fire moves vertically to ignite elevated fuels (Cobian-Iñiguez et al. 2022, Weise et al 2018), a phenomenon known as crowning (Van Wagner 1977). Some studies have explored factors influencing this vertical transition in shrub fuels (Lozano and Jesse Sandoval. 2011) and more studies have focused on coniferous forests (e.g., Cruz et al 2006a, b).

So-called ladder fuels are combustible materials that can act as a "ladder" for a surface fire to move vertically from the ground into a forest's canopy. Ladder fuels typically consist of smaller trees, shrubs, and the lower branches of larger trees. The current study explored the ignition characteristics of two types of ladder fuels using a dual layer setup: a ground layer with a surface fire source and an elevated layer to evaluate the ignition criteria of ladder fuels.

Tachajapong et al. conducted studies on dual layers to investigate the impact of crown fuel bulk density on the dynamics of crown fire initiation in shrublands (Tachajapong et al. 2008). Observations indicated that ignition occurred when the crown base was within the continuous flame region. Additionally, it was found that higher crown fuel bulk density leads to quicker crown fire ignition. Tachajapong et al. conducted a laboratory experiment to study the transition of surface fire to wet shrub crown fuels (Tachajapong et al. 2009). They observed that an increase in crown base height led to a decrease in the likelihood of crown fire initiation. Cobian-Iñiguez et al., have looked into

the transitions between a dual-layer system (Cobian-Iñiguez et al.2022). They found that the presence of wind enhanced fire spread behavior greatly in a laboratory setting. Such studies highlighted that the initiation of crown fires was primarily dependent on the rate of spread of the surface fire. The duration of heating was limited by the rate of spread in wind tunnel studies, and the ignition time on the upper fuel layer is less representative in such conditions.

In most, if not all, of the instances described above, evaluation of the effectiveness of fuel treatments to reduce crown fire potential has relied on a combination of modeling and empirical data related to fire behavior. Seldom, if ever, has a designed experiment (lab or field) manipulating the variables identified as important to the transition from a surface fire into ladder fuels resulting in a crown fire been performed. The objective of this study is to assess how ambient temperature, humidity, fire line intensity, heating duration, crown base height and fuel bulk density influence the ignition of ladder fuels through laboratory-scale fires. A technique involving the continuous movement of the fuel bed was utilized to sustain the flame in a consistent position.

Methods

The current experiment setup included a dual-layer system presented in figure 1. In order to isolate ignition requirements for elevated fuels, a sustained continuous flame source was employed in the current study (Fons et al. 1961, Jenkins et al 1993).

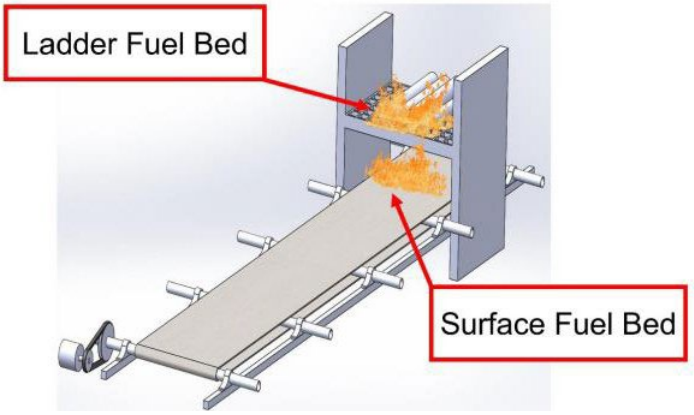

Figure 1. Experimental setup to provide constant heating source for elevated ladder fuels.

A mass of 1.2 kg of dry longleaf pine needles was evenly distributed over the 0.7 m x 1.7 m conveyor belt. A mass of 0.6 kg of ladder fuel (incense cedar or manzanita) was suspended in a 1 m x 1 m basket above the surface fuel bed. A load cell on top of the basket measured the mass loss rate of the ladder fuel bed. The vertical distance (crown base height - CBH) between the top of the surface fuel bed and the bottom of the ladder fuel bed was set to 75 cm, 85 cm, and 95 cm to vary the flame exposure of the ladder fuel bed. Type K thermocouples were mounted at different heights along the centerline of the fuel bed, capturing the gas temperature in the flame, within the ladder

fuel matrix (as in Tachajapong et al 2008) and in the plume. Visible and infrared video cameras recorded each experiment. The surface fuel bed was ignited at the end of the surface fuel bed closer to the ladder fuel bed and the conveyor belt quickly moved the surface flame below the center of the ladder fuel bed.

Results

Table 1. Number of ignitions and non-ignitions during the experiment

	Basket height	Manzanita ignited	Manzanita non-ignited	Incense cedar ignited	Incense cedar non-ignited
Summer	75	6	2	6	0
	85	4	5	6	0
	95	0	9	2	4
Winter	75	4	4	8	0
	85	0	8	7	1
	95	0	8	2	6

92 experiments were conducted to evaluate the impact of fuel characteristics, environmental variables, and heating duration on the vertical fire spread success for two different species of ladder fuel. Table 1 presents the number of ignitions and non-ignitions split by species, season and CBH.

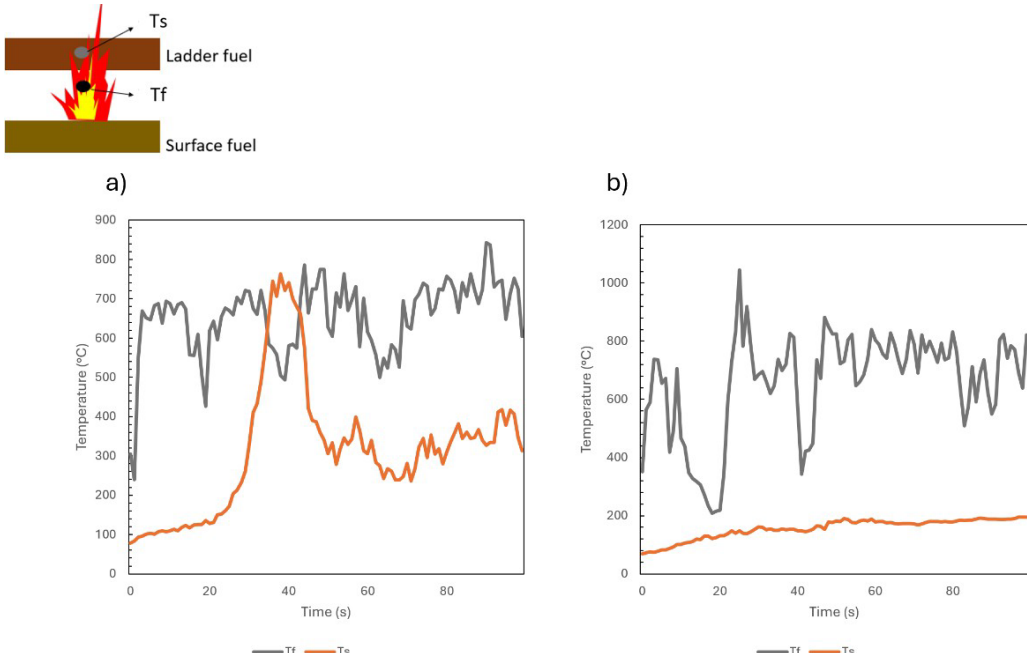

Figure 2. Temperature profiles associated with a) ignited case; b) non-ignited case

The preliminary temperature profile results are presented here. Figure 2 presents an example of the temporal temperature trend for ignited and non-ignited cases. Ts

indicates the temperature in the solid fuel bulk, while Tf indicates the temporal flame temperature. For this ignited case, the mean temperature for the flame is 654 °C; the solid fuel bulk temperature increases steadily during ignition, peaking around 762 °C at 40 seconds, then decreases gradually. For this non-ignited case, the mean temperature for the flame is 658 °C; the solid fuel bulk temperature gradually rises and stabilizes around 200°C, showing minor fluctuations. These results are being examined in detail statistically to identify differences and trends.

Summary

The repeatable laboratory-scale experiments provide a systematic framework for understanding the transition from surface to ladder fire. Well-designed laboratory experiments offer precise control over crucial variables. This control facilitates a detailed investigation of specific effects.

References

Cobian-Iñiguez, Jeanette, AmirHessam Aminfar, Joey Chong, Gloria Burke, Albertina Zuniga, David R. Weise, and Marko Princevac. 2017. “Wind Tunnel Experiments to Study Chaparral Crown Fires.” *Journal of Visualized Experiments*, no. 129 (November), 1–14. https://doi.org/10.3791/56591.

Cobian-Iñiguez, Jeanette, Amir Hessam Aminfar, Shusmita Saha, Kyle Awayan, David R. Weise, and Marko Princevac. 2022. “The Transition and Spread of a Chaparral Crown Fire: Insights from Laboratory Scale Wind Tunnel Experiments.” Edited by Benjamin Shaw. *Journal of Combustion* 2022 (July):5630594. https://doi.org/10.1155/2022/5630594.

Cruz, Miguel G., Bret W. Butler, Martin E. Alexander, Jason M. Forthofer, and Ronald H. Wakimoto. 2006. “Predicting the Ignition of Crown Fuels above a Spreading Surface Fire. Part I: Model Idealization.” *International Journal of Wildland Fire* 15 (1): 47–60. https://doi.org/10.1071/WF04061.

Fons, W.L., H.D. Bruce, and W.Y. Pong (1961) A Steady-State Technique for Studying the Properties of Free-Burning Wood Fires. The Use of Models in Fire Research 219–34.

Jenkins, Bryan M., Ian M. Kennedy, Scott Q. Turn, Robert B. Williams, Steven G. Hall, Stephen V. Teague, Daniel P. Y. Chang, and Otto G. Raabe. 1993. “Wind Tunnel Modeling of Atmospheric Emissions from Agricultural Burning: Influence of Operating Configuration on Flame Structure and Particle Emission Factor for a Spreading-Type Fire.” *Environmental Science & Technology* 27 (9): 1763–75. https://doi.org/10.1021/es00046a002.

Lozano, Jesse Sandoval (2011) ‘An Investigation of Surface and Crown Fire Dynamics in Shrub Fuels.’ Dissertation, Riverside, CA: University of California.

Lozano, Jesse, Watcharapong Tachajapong, David R. Weise, Shankar Mahalingam, and Marko Princevac. 2010. "Fluid Dynamic Structures in a Fire Environment Observed in Laboratory-Scale Experiments." *Combustion Science and Technology* 182 (7): 858–
78. https://doi.org/10.1080/00102200903401241.

Tachajapong, Watcharapong, Jesse Lozano, Shankar Mahalingam, and David R. Weise. 2014. "Experimental Modelling of Crown Fire Initiation in Open and Closed Shrubland Systems." *International Journal of Wildland Fire* 23 (4): 451–62. https://doi.org/10.1071/WF12118.

Tachajapong, Watcharapong, Jesse Lozano, Shankar Mahalingam, Xiangyang Zhou, and David R. Weise. 2008. "An Investigation of Crown Fuel Bulk Density Effects on the Dynamics of Crown Fire Initiation in Shrublands." *Combustion Science and Technology* 180 (4): 593–615. https://doi.org/10.1080/00102200701838800.

Tachajapong, Watcharapong, Jesse Lozano, Shankar Mahalingam, Xiangyang Zhou, and David R. Weise. 2009. "Experimental and Numerical Modeling of Shrub Crown Fire Initiation." *Combustion Science and Technology* 181 (4): 618–40. https://doi.org/10.1080/00102200802693617.

Van Wagner, C. E. 1977. "Conditions for the Start and Spread of Crown Fire." *Canadian Journal of Forest Research* 7 (1): 23–34. https://doi.org/10.1139/x77-004.

Weise, D.R., J. Cobian-Iñiguez, and M. Princevac. 2018. "Surface to Crown Transition." In *Encyclopedia of Wildfires and Wildland-Urban Interface (WUI) Fires*, edited by Samuel L. Manzello, 1–5. Cham: Springer International Publishing. https://doi.org/10.1007/978-3-319-51727-8_24-1.

Proceedings for the 7th International Fire Behavior and Fuels Conference
April 15-19, 2024, Boise, Idaho, USA – Tralee, Ireland – Canberra, Australia
Published by the International Association of Wildland Fire, Missoula, Montana, USA

Taking science to on-ground management – including on-off fire switches, fire-climate drivers and time-scales, into on-ground planning.

Diana Kuchinke
Federation University, Institute of Innovation, Science and Sustainability
PO Box 663, Ballarat, Victoria, 3353, Australia
d.kuchinke@federation.edu.au

Introduction

Wildfires that have burnt in recent years across California, Canada, Portugal, within the Amazon, across large tracts of Australia, and deep into the permafrost in the Sakha Republic of Russia in northern Siberia, are heralding an unprecedented level of megafires; fire events that are each more frequent, more intense, and of greater extent than the one preceding it. The 2019 to 2020 fire season in south-east Australia extended from July 2019 right through until March 2020, burning 19 million hectares and contributing to extensive population declines of at least 91 fauna taxa (Legge et al., 2022). While fire-spread is determined by the features of the landscape, fire-size is dictated mostly by climate variables (Brotons, 2013). In south-east Australia the four main climate drivers are the Southern Annular Mode (SAM), the Indian Ocean Dipole (IOD), El Niño Southern Oscillation (ENSO) and the Pacific Decadal Oscillation (PDO). As these vary with climate change, so too do fire parameters.

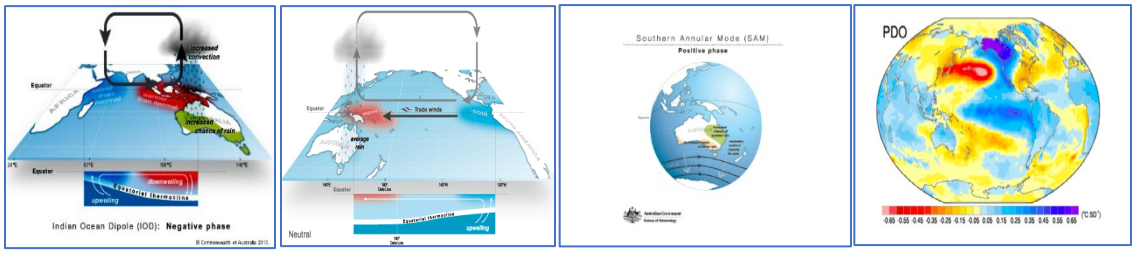

Fig 1. Four climate drivers of SE Aus. Source: Bureau of Meteorology

The beginnings of a simple theoretical framework are presented here; a plan outlining a framework of short-, medium- and long-term planning that includes the factors driving fire, underpinned by the climate drivers of the south-east Australia region. The objective is to begin to frame a pathway for improved information flow between science and the on-ground management of prescribed burns. The outcomes would be long-term strategies along with medium and short-term plans including the projections for the climate drivers that impact across different temporal scales, that could result in on-ground management plans more effectively preparing managed burns.

Recent changes in the fire regime

Increases in wildfire intensity, severity and frequency have long been predicted (Beer and Williams, 1995, Pitman et al., 2007, Cai et al., 2014), and fire regime drivers have been extensively studied (Bradstock, 2010). For decades the term 'unprecedented' was not used in the descriptions of wildfire in south-eastern Australia; Australians had witnessed no less than ten extensive wildfire seasons from 1851 to 2009, that each burnt more than 500,000 hectares across the temperate eucalypt forests. Worryingly, the inter-fire interval is now reducing.

Drivers of the fire regime are well understood. Drought is the ultimate hammer of climate change; fire is the manifestation of drought. Drought dries fuel for fire, making ground impenetrable to rain, creating flash floods. One of the main drivers of the fire regime is climate. Historically, adding complexity to research into the climate forces driving fire, are the infrequent disasters of high intensity and severity. These are not random, but rather, exist in a system of feedback loops channelling pulses of climate-related activity.

It has now become impossible to disentangle climate drivers that are predicted to occur within expected ranges, from extreme fire events. With fires now occurring at unprecedented scales of frequency, severity, intensity and extent, there is a clear mandate for greater cross-disciplinary processes, to enable greater protection of not only humans and assets, but also flora and fauna species.

What the increases in fire frequency means for our flora and fauna

Species persist within their 'realized niche' (Hutchinson, 1957); the total range of conditions under which a population survives. Intrinsic complexities arise from multiple spatial and temporal disturbances; a species will only continue to survive if its tolerable limits are not exceeded. So, in regions where temperatures are increasing, there are increasing stressors on species which alter the ranges within which species can survive; they must be able to thrive in altered habitats (BirdLife International, 2008).

In south-east Australia, climate scenarios consistently predict an increase in the number of hot days and declines in spring and autumn rainfall, that combined, will not only extend drought periods but also increase the frequency of high fire-danger days (Steffen et al., 2017). Already the changing fire regime is having profound impacts on Australia's flora and fauna (Woinarski and Recher, 1997, Recher et al., 2009, Bowman et al., 2012, Enright et al., 2012, Gill, 2012, Recher and Davis Jr, 2013, Lindenmayer et al., 2014).

In the forests and woodlands, the new climate is seeing unprecedented spread, intensity, and frequency of wildfire, yet the present management response to the complexities driving this state is merely to apply more prescribed fire to the landscape. A more nuanced approach is needed - on-ground management that is more proactive, rather than reactive.

A new framework: combining fire 'switches', time-scales, climate drivers and management processes.

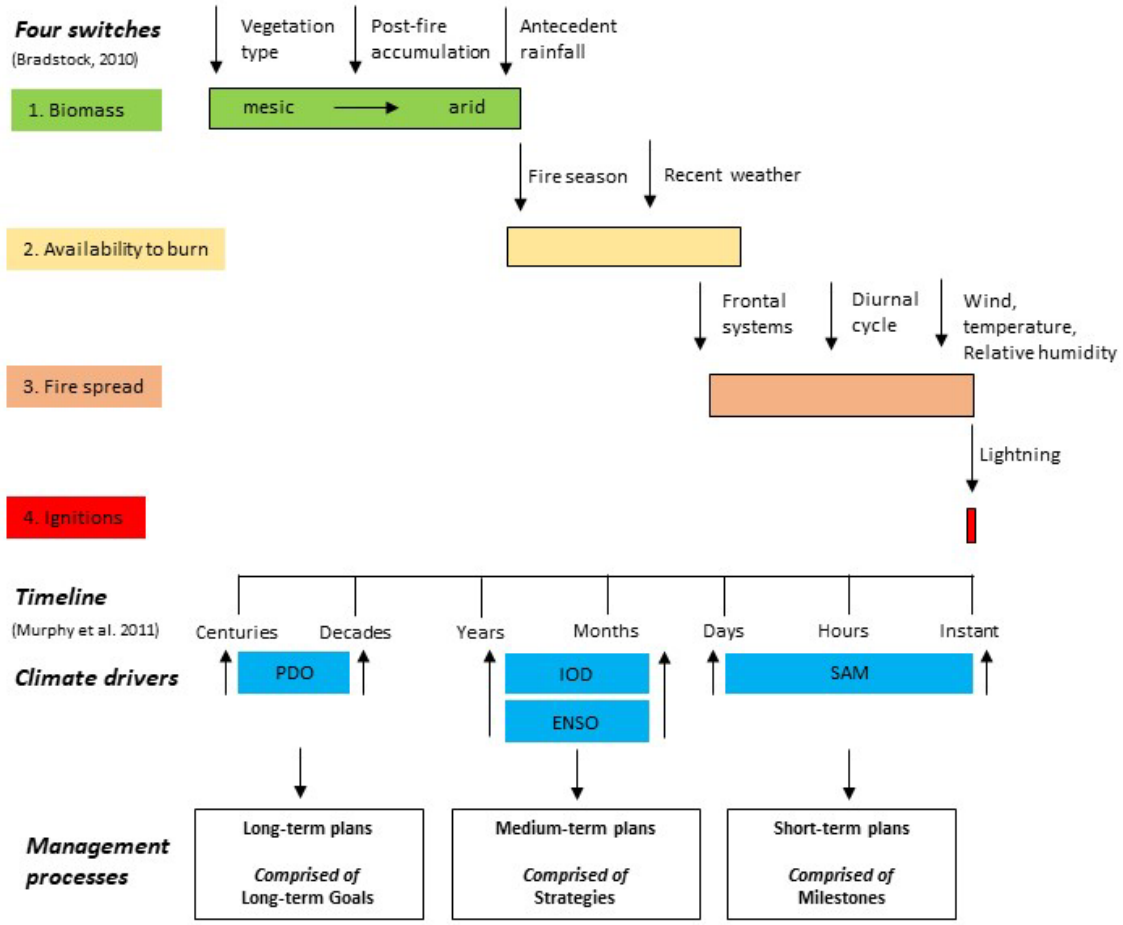

Fig 2. Conceptual framework defining processes that limit fire (Bradstock 2010); time-scales (Murphy et al. 2011); the climate drivers of south-eastern Australia, and management plans relevant to the timescale of the climate drivers. Acronyms: PDO Pacific Decadal Oscillation; IOD Indian Ocean Dipole; ENSO El Niño Southern Oscillation; SAM Southern Annular Mode.

Changes to the fire 'switches'

A conceptual framework was devised to define processes that limit fire, incorporating key drivers, as on/off switches. These comprise 1) biomass growth; 2) the availability of vegetation for burning; 3) ambient fire weather; and 4) ignition, from lightning and anthropogenic sources (Bradstock, 2010). Others supplemented this scheme by adding a range of time-scales over which the four switches will operate (Murphy et al., 2011, Williamson et al., 2016). As predictions of increased levels of wildfire are realised, frameworks such as Bradstock's need additional information.

The influences from the biogeographic factors affecting three of Bradstock's four switches have changed. If the 2019-20 season (in south-east Australia) heralds the new normal, then the fire season in Australia now extends to winter months (switch 2), temperature profiles have increased range and variability (switch 3) and dry lightning is now prevalent in locations where it has rarely been recorded (switch 4), (Fig 2). Patches of relict Gondwana vegetation in Tasmania, Australia burnt for the first time in millennia after the passage of a 24-hr storm produced approximately 3000 lightning strikes. Vegetation biomass, the fourth of Bradstock's switches (switch 1, Fig 2), has reduced in some areas of Australia, but disturbance in the remaining forest and woodland may result in increased flammability (Lindenmayer, 2016).

Adding timelines and climate drivers to the framework

In south-east Australia, the drivers of fire, are further moderated by the existence of the four key climate drivers: PDO, ENSO, IOD, and SAM (Figs 1, 2). Driven by winds and temperature variations, these four variants are the key climate elements to consider when forecasting future wildfire patterns across this region.

Research has highlighted that both positive IOD and negative SAM events precondition the landscape for wildfires (Cai et al., 2009, Mariani and Fletcher, 2016), exacerbating dry conditions. While there are clear trends in annual rainfall, and fire risk, predictions remain complex owing to the diversity of climate drivers that are impacted by tropical and temperate forces, both east and west of Australia.

An effort to contribute to on-ground managed burn planning

It can be argued that there is sometimes a disconnect between scientists and the on-ground managers. And yet, it is clear that a holistic approach is imperative. A two year data collection of bird responses to prescribed burn severity in south-east Australia showed a limited bird response, and yet, a before-after control-impact project design showed that some other factor was driving a reduction in bird numbers across the landscape (Kuchinke et al., 2020). The timing of the applied management burns coincided with a drying trend across the region. The solutions are complex and rely on not only extended research projects, but the existence of more clearly defined bridges between science and policy. Creating a collaboration between people from different disciplines, so that long-term strategies and the short-term plans that comprise medium-term goals, include the climate drivers that impact across different temporal scales (Fig 2), may result in on-ground management plans more effectively managing the landscape.

Fire patterns change over time and, as a result, policy changes and on-ground management must occur at a speed that keeps pace with these changes, otherwise policies that were intended to mitigate the impacts of severe fires may instead result in not only loss of human life and assets (Teague, 2010) but significant risks to the integrity of ecosystems (DellaSala et al., 2004).

Experts have issued dire warnings on the likelihood of species' extinctions within the next 20 years (Garnett et al., 2022). All the imperilled taxa noted in the Garnett (2022) journal exist wholly or partly in conservation reserves. As fire has no bounds, protection must extend to on-ground practice, rather than relying solely on conserving parts of the landscape.

References

Beer, T. & Williams, A. 1995. Estimating Australian forest fire danger under conditions of doubled carbon dioxide concentrations. *Climatic Change,* 29**,** 169-188.

BirdLife International 2008. State of the world´ s birds: Indicators for our changing world. *Birdlife International.*

Bowman, D. M. J. S., Murphy, B. P., Burrows, G. E. & Crisp, M. 2012. Fire regimes and the evolution of the Australian biota. *Flammable Australia.* CSIRO Publishing.

Bradstock, R. A. 2010. A biogeographic model of fire regimes in Australia: current and future implications: A biogeographic model of fire in Australia. *Global Ecology and Biogeography,* 19**,** 145-158.

Brotons, L., Aquilué, N., De Cáceres, M., Fortin, M.-J. & Fall, A. 2013. How fire history, fire suppression practices and climate change affect wildfire regimes in Mediterranean landscapes. *PLOS one,* 8**,** e62392.

Cai, W., Borlace, S., Lengaigne, M., Van Rensch, P., Collins, M., Vecchi, G., Timmermann, A., Santoso, A., McPhaden, M. J. & Wu, L. 2014. Increasing frequency of extreme El Niño events due to greenhouse warming. *Nature climate change,* 4**,** 111-116.

Cai, W., Cowan, T. & Raupach, M. 2009. Positive Indian Ocean Dipole events precondition southeast Australia bushfires. *Geophysical Research Letters,* 36.

DellaSala, D. A., Williams, J. E., Williams, C. D. & Franklin, J. F. 2004. Beyond smoke and mirrors: a synthesis of fire policy and science. *Conservation Biology,* 18**,** 976-986.

Enright, N., A. Keith, D., F. Clarke, M. & Miller, B. 2012. Fire regimes in Australian sclerophyllous shrubby ecosystems: heathlands, heathy woodlands and mallee woodlands.

Garnett, S., Hayward-Brown, B., Kopf, R., Woinarski, J., Cameron, K., Chapple, D., Copley, P., Fisher, A., Gillespie, G., Latch, P., Legge, S., Lintermans, M., Moorrees, A., Page, M., Renwick, J., Birrell, J., Kelly, D. & Geyle, H. 2022. Australia's most imperilled vertebrates. *Biological Conservation,* 270.

Gill, A. M. 2012. Bushfires and biodiversity in southern Australian forests. *Flammable Australia: fire regimes, biodiversity and ecosystems in a changing world'.(Eds RA Bradstock, RJ Williams, AM Gill) pp***,** 235-252.

Hutchinson, G. E. 1957. Cold spring harbor symposium on quantitative biology. *Concluding remarks,* 22**,** 415-427.

Kuchinke, D., Di Stefano, J., Sitters, H., Loyn, R., Gell, P. & Palmer, G. 2020. Prescribed burn severity has minimal effect on common bird species in a fire-prone forest ecosystem. *Forest Ecology and Management,* 475**,** 118437.

Legge, S., Rumpff, L., Woinarski, J. C. Z., Whiterod, N. S., Ward, M., Southwell, D. G., Scheele, B. C., Nimmo, D. G., Lintermans, M., Geyle, H. M., Garnett, S. T., Hayward-Brown, B., Ensbey, M., Ehmke, G., Ahyong, S. T., Blackmore, C. J., Bower, D. S., Brizuela-Torres, D., Burbidge, A. H., Burns, P. A., Butler, G., Catullo, R., Chapple, D. G., Dickman, C. R., Doyle, K. E., Ferris, J., Fisher, D., Gallagher, R., Gillespie, G. R., Greenlees, M. J., Hohnen, R., Hoskin, C. J., Hunter, D., Jolly, C., Kennard, M., King, A., Kuchinke, D., Law, B., Lawler, I., Lawler, S., Loyn, R., Lunney, D., Lyon, J., MacHunter, J., Mahony, M., Mahony, S., McCormack, R. B., Melville, J., Menkhorst, P., Michael, D., Mitchell, N., Mulder, E., Newell, D., Pearce, L., Raadik, T. A., Rowley, J. J. L., Sitters, H., Spencer, R., Valavi, R., West, M., Wilkinson, D. P. & Zukowski, S. 2022. The conservation impacts of ecological disturbance: Time-bound estimates of population loss and recovery for fauna affected by the 2019–2020 Australian megafires. *Global ecology and biogeography*.

Lindenmayer, D. 2016. Interactions between forest resource management and landscape structure. *Current Landscape Ecology Reports,* 1**,** 10-18.

Lindenmayer, D. B., Blanchard, W., McBurney, L., Blair, D., Banks, S. C., Driscoll, D. A., Smith, A. L. & Gill, A. M. 2014. Complex responses of birds to landscape- level fire extent, fire severity and environmental drivers. *Diversity and Distributions,* 20**,** 467-477.

Mariani, M. & Fletcher, M. S. 2016. The Southern Annular Mode determines interannual and centennial-scale fire activity in temperate southwest Tasmania, Australia. *Geophysical Research Letters,* 43**,** 1702-1709.

Murphy, B. P., Williamson, G. J. & Bowman, D. M. J. S. 2011. Fire regimes: moving from a fuzzy concept to geographic entity. *New Phytologist,* 192**,** 316-318.

Pitman, A., Narisma, G. & McAneney, J. 2007. The impact of climate change on the risk of forest and grassland fires in Australia. *Climatic Change,* 84**,** 383-401.

Recher, H. F. & Davis Jr, W. E. 2013. Response of birds to a wildfire in the Great Western Woodlands, Western Australia. *Pacific Conservation Biology,* 19**,** 188-203.

Recher, H. F., Lunney, D. & Matthews, A. 2009. Small mammal populations in a eucalypt forest affected by fire and drought. I. Long-term patterns in an era of climate change. *Wildlife Research,* 36**,** 143-158.

Steffen, W., Hughes, L., Alexander, D. & Rice, M. 2017. Cranking up the intensity. Climate change and extreme weather events.: Climate Council of Australia Ltd.

Teague, B. 2010. 2009 Victorian Bushfires Royal Commission. Victoria, Australia: State of Victoria.

Williamson, G. J., Prior, L. D., Jolly, W. M., Cochrane, M. A., Murphy, B. P. & Bowman, D. M. J. S. 2016. Measurement of inter- and intra-annual variability of landscape fire activity at a continental scale: the australian case. *Environmental Research Letters,* 11**,** 035003.

Woinarski, J. C. Z. & Recher, H. F. 1997. Impact and response: a review of the effects of fire on the Australian avifauna. *Pacific Conservation Biology,* 3**,** 183-205.

Proceedings for the 7th International Fire Behavior and Fuels Conference
April 15-19, 2024, Boise, Idaho, USA – Tralee, Ireland – Canberra, Australia
Published by the International Association of Wildland Fire, Missoula, Montana, USA

The "Grazing Paradox" Wildfire Resiliance In Germany

Juliane Baumann
Brandherde - Holistic Wildfire Prevention, Brandenburgische Str. 25, 12167 Berlin, Germany, julianebaumann@brandherde.info
www.brandherde.info

According to the nationwide forest fire statistics of Germany, which cover all 16 federal states, the state of Brandenburg is, on average, affected by the highest number of forest fires and has the largest burned forest area (BLE, 2024). The reason for the high susceptibility of Brandenburg's forests to wildfires is often referred to the high proportion of pine (*Pinus sylvestris* L.) monocultures planted on predominantly sandy soil sites and the continental climate. In addition, the control of wildfires on former armed conflict areas and military training sites is impeded by the contamination by unexploded ordnance (UXO), often resulting in larger areas burned (Goldammer et al., 2016).

The wildfire problem in Germany

Climate change is often used as an explanation for an increase of wildfire risk. However, the wildland-urban interface (WUI) is not evaluated as a risk factor or recognized as a key problem of vulbnerability and priority to be addressed. The extensive international knowledge on fire management is rarely included in the public discourse on solutions in wildfire risk reduction. On the other hand, there is an advanced knowledge and practice in nature conservation and landscape management, including targeted grazing and prescribed burning. Paradoxically, this knowledge is not applied to prevent forest fires – neither by prescribed burning nor by. Similarly, concepts of wood pasture, which could be used to targeted protection of settlements, are not practiced.

Fire Season 2018

Over the last five years, more wildfires occurred at the WUI. In 2018, evacuations of villages in Brandenburg State were necessary and an railway embankment fire, which burned into an urban area in Siegburg in the West of Germany, caused more than nine destroyed houses and 32 injured people.

Fire Season 2022

In 2022, several wildfires – some of them simultaneous – burned with high rate of spread and difficult to control. The same village that was evacuated in 2018 already in Brandenburg had to be evacuated again. In the town of Falkenberg, a wildfire affected 800 hectares with strong wind killed hundreds of pigs in a farm.

Especially in nature reserves, where forestry activities are reduced and more dead wood left for biodiversity conservation wildfires burned with very high severity and

fireline intensity and causing spot fires, e.g. in Gohrisch Heide or Elbsandstein on the border to Czech Republic.

UXO Sites
In case of known (mapped) or suspected sites contaminated by UXO, fire services are not allowed to directly fight the fire. According to regulations, personnel not protected by armoured equipment (vehicles, firefighting tanks) has to stay 500 meters (m) away from the fire, in highly dangerous UXO sites –1000 m (Goldammer et al., 2016). Such areas can be found in Brandenburg right up to village borders into the WUI. This causes a triple domino effect on the fire risk for the population:

1. Possible self-ignition of wildfire by phosphorus-containing ammunition
2. Explosion due to fire: direct risk for fire services and local residents
3. Escalation of wildfires due to lack of fast intervention of fire services because of theire regulation

Wildland-Urban Interface under Climate Change
One effect of climate change is the shift of vegetation zones to the higher latitudes – with consequences on changing regional / latitudinal fire regimes. In Germany, deciduous forests such as beech (*Fagus sylvatica* L.) stands, are becoming more vulnerable to fire as compared to previous decades (Goldammer, 2023). In 2023, the share of deciduous forests affected by wildfires was 69% vs, 31% coniferous stands (BLE, 2024). Furthermore, pests and diseases are damaging forest stands in large scale and as a consequence, dead wood in the forests increases, which in turn result in higher fire severities (Goldammer, 2022).

Fuel Management
Apart from that is the way how to react on climate change. Solutions in wildfire prevention has to be considered, which are independent of extreme weather conditions. That is the structure of the fuel and not just the tree species.

German Forestry departments are investing in converting pine monocultures to mixed deciduous forests (Goldammer, 2023a). This policy does not consider specific problems of the WUI and results in significantly more fuel in peripheral residential areas.

The other problem regarding wildfire risk is the development of nature conservation in Germany with specific theories of forest protection and human created wildness areas that are susceptible to fire. On the other hand, more important fire-resilient ecosystems like Central European lichen pine forests in these areas receive less public attention – e.g., in the Heidehof Golmberg reserve.

The biggest losses of biodiversity in Germany are noted in open land systems and not within the forests. When trees are protected by humans instead of being utilized, this kind of wilderness is overloaded with fuel like in Mediterranean regions – with implications on increased wildfire hazard.

The "Grazing Paradox"

Just as we have recognised the fire paradox in America – there is a "grazing paradox" in Europe.

Wood-Pasture Hhypothesis

For thousands of years there have been megaherbivores started with the dinosaurs that have thinned out the forests and created mosaic-like landscapes with more park structures in the forest. Wild herbivores such as the European bison, aurochs and elk as "creators of landscape" were long ago wiped out in Germany. The first wild European bison came back to Germany after one hundred years – crossing the Polish-German border in 2017.

The Megaherbivore Theory of Vera (2000) states that the absence of large herbivores was compensated by wood-pasture specially in central Europe.

Wood-pasture existed in Germany for centuries, it was the first human kind of agriculture long before arable farming. Oak trees in particular were selected as fodder trees with semi-open structures such as in *Hutewald* forests, which are relics from this period. They are still very rich in species, strictly protected and not typical fire prone due to the openness and reduced surface fuels.

Humans as a Part of Nature

Open forest structures with a high level of biodiversity are found on former military training areas as military exercises have shaped the open landscapes. Currently, some of these areas are being transformed into so-called wilderness areas that are neither managed nor touched by humans or grazing to conserve these habitats. These nature reserves are increasingly subjected to wildfires often in recent years, notably fire-sensitive moors and fire-adapted heathlands (*Calluna vulgaris* L.) (Goldammer et al., 2009).

Targeted Grazing

A number of former military training areas are bearing a rich biodiversity and are subjected to scientific monitoring research where no such heavy forest fires occur due to grazing and this well developed concept of "wild pastures" (Bunzel-Drüke et al., 2008), e.g. Oranienbaumer Heide and Döberitzer Heide. However, it is a paradox that wood pasture with such positive results in biodiversity conservation is rarely applied in Germany and grazing not officially recognized as a wildfire prevention concept.

With regard to forest fire resilient landscapes, Zev Naveh was one of the first to scientifically research the relationship between grazing and forest fires back in the 1970s (Naveh, 1990). In the 1980s, agro-silvopastoral wildfire protection corridors were published in a forest fire management handbook for Brazil (Goldammer, 1982, 1988).

Conclusions and recommendations

In Germany I realised that forest pasture as a means of fire management makes sense in four different ways (Baumann, 2019):

1. Wild pasture (Bunzel-Drüke et al., 2008) on former military sides with UXO to create open mosaic-like structures with low fire intensity and windows of opportunities to handle wildfires.
2. Ecological fire management below power lines to reduce fuel in an economic way.
3. Ecologic fuel reduction in classic fire breaks (Missbach, 1972) that was common in the former GDR in Germany and has to be maintained with machines when not threw grazing.
4. Buffer zones in the WUI to protect settlements.

The key players have to understand that fire management is mandatory for their own interests and that there is already a huge international and historic toolbox for designing the landscape towards wildfire resilience with an international consensus on how to protect settlements.

Forest pasture is not just a measure to prevent wildfire, it could be the key to a resilient landscape according to agriculture, nature conservation and forestry.

References

Baumann J (2019) Einsatz von Nutztieren zur Waldbrandprävention am Beispiel des Landes Brandenburg. MSc Thesis, Hochschule für Nachhaltige Entwicklung Eberswalde.

BLE (Bundesanstalt für Landwirtschaft und Ernährung). 2024. Forest fire statistics of Germany 1990-2024. https://www.bmel-statistik.de/forst-holz/waldbrandstatistik/

Bunzel-Drüke M, Böhm C, Finck P, Kämmer G, Luick R, Reisinger E, Riecken U, Riedl J, Scharf M, Zimball O (2008) Wilde Weiden – Praxisleitfaden für Ganzjahresbeweidung in Naturschutz und Landschaftsentwicklung. Arbeitsgemeinschaft Biologischer Umweltschutz, Bad-Sassendorf-Lohne.

Goldammer JG (1982) Incêndios florestais. Prevençào, controle e uso do fogo. Destaque especial para os reflorestamentos de Pinus spp. Colégio Florestal Irati, Brazil.

Goldammer JG (1988) Rural land-use and fires in the tropics. *Agroforestry Systems* 6, 235-252.

Goldammer JG (2023) G20 Study on Restoration of Forest Fire impacted Areas for Recovering the Natural Biodiversity: Country Profile – Germany. German Federal Ministry for the Environment, Nature Conservation, Nuclear Safety and Consumer Protection and Federal Ministry of Food and Agriculture

Goldammer JG (2022) Wie können die Wälder in Deutschland, Österreich und der Schweiz umgebaut werden, sodass sie resilienter gegenüber Waldbränden sind? Science Media Center, 27 Mai 2022

Goldammer JG, Brunn E, Hoffmann G, Keienburg T, Mause R, Page H, Prüter J, Remke E, Spielmann M (2009) Einsatz des Kontrollierten Feuers in Naturschutz, Landschaftspflege und Forstwirtschaft – Erfahrungen und Perspektiven für Deutschland. *Naturschutz und Biologische Vielfalt* 73, 137-164.

Goldammer JG, Brunn E, Hartig S, Schulz J, Meyer F (2016) Development of technologies and methods for the application of prescribed fire for the management of Calluna vulgaris heathlands contaminated by unexploded ordnance (UXO): Problems and first experiences gained in a research and development project in Germany. *Naturschutz und Biologische Vielfalt* 152, 87-122.

Missbach K (1972) Waldbrand. Verhütung und Bekämpfung (VEB Deutscher Landwirtschaftsverlag: Berlin)

Naveh Z (1990) Fire in the Mediterranean – A landscape ecological perspectve. In: Fire in ecosystem dynamics. Mediterranean and northern perspectives (Eds JG Goldammer, MJ Jenkins) pp 1-20 (SPB Academic Publishing: The Hague)

Vera FWM (2002) The dynamic European forest. Arboricultural Journal 26, 179–211.

Proceedings for the 7th International Fire Behavior and Fuels Conference
April 15-19, 2024, Boise, Idaho, USA – Tralee, Ireland – Canberra, Australia
Published by the International Association of Wildland Fire, Missoula, Montana, USA

The Role of Vorticity-Driven Lateral Spread in Firebrand Transport: Insights from FIRETEC Simulations over a Mountain Ridge

Mukesh Kumar| Katherine Smith| Alex Josephson| Rod Linn
Los Alamos National Laboratory, NM 87544, USA

Abstract

This study examines the role of vorticity-driven lateral spread (VLS) in the spread of firebrands, particularly in the presence of mountainous terrain. The FIRETEC model is used to simulate wildfire behavior, considering the complex interactions of fuel, weather, and topography. Our main objective is to analyze the effect of VLS on the travel distances of firebrands, comparing scenarios without VLS over flat terrain. When comparing scenarios with VLS and without VLS across flat terrain, it is found that the presence of the mountain increases firebrand travel distances. This shows that when fires occur in mountainous areas, VLS is an active process that contributes to the long-distance transport of firebrands. In addition, the trajectories of firebrands launched from the mountain demonstrate the VLS effect. The lateral spread caused by VLS alters firebrand trajectories, causing them to travel longer distances than in conditions without VLS. This observation provides evidence to the theory that VLS influences the behavior and spread of wildfires in mountainous terrains. These findings have important implications for fire management and mitigation strategies in mountainous regions. The increased travel distances of firebrands due to VLS pose challenges in terms of fire suppression efforts, evacuation planning, and infrastructure protection. Understanding and quantifying the role of VLS in these scenarios can contribute more effectively and accurately predict fire behavior and inform decision-making processes.

Proceedings for the 7th International Fire Behavior and Fuels Conference
April 15-19, 2024, Boise, Idaho, USA – Tralee, Ireland – Canberra, Australia
Published by the International Association of Wildland Fire, Missoula, Montana, USA

The Use of Machine Learning-informed Fuel Map in the Wildfire Propagation Model PROPAGATOR

Nicolò Perello*
Department of Informatics, Bioengineering, Robotics and Systems Engineering, University of Genoa, Via All'Opera Pia, 13, 16145 Genova, Italy
nicolo.perello@edu.unige.it

Andrea Trucchia
CIMA Research Foundation, Via A. Magliotto, 2, 17100 Savona, Italy
andrea.trucchia@cimafoundation.org

Giorgio Meschi
CIMA Research Foundation, Via A. Magliotto, 2, 17100 Savona, Italy
giorgio.meschi@cimafoundation.org

Farzad Ghasemiazma
Department of Informatics, Bioengineering, Robotics and Systems Engineering, University of Genoa, Via All'Opera Pia, 13, 16145 Genova, Italy
farzad.ghasemiazma@cimafoundation.org

Mirko D'Andrea
CIMA Research Foundation, Via A. Magliotto, 2, 17100 Savona, Italy
mirko.dandrea@cimafoundation.org

Silvia degli Esposti
CIMA Research Foundation, Via A. Magliotto, 2, 17100 Savona, Italy
silvia.degliesposti@cimafoundation.org

Paolo Fiorucci
CIMA Research Foundation, Via A. Magliotto, 2, 17100 Savona, Italy
paolo.fiorucci@cimafoundation.org

**Corresponding Author*

Introduction

In recent decades, changes in wildfire regimes and extreme events have challenged global Wildfire Risk Management systems (*Tedim et al. 2018*). The need for an innovative Integrated Fire Management paradigm has been highlighted by the wildfire community. Integrating diverse data sources, modeling tools, and AI technologies has shown promise in addressing future fire regimes driven by climate change. This can be particularly promising in the field of fuel mapping for wildfire risk management, which is still an open issue in the literature.

In the present work, a Machine Learning-informed fuel map has been defined and integrated into the PROPAGATOR wildfire propagation model, developed by CIMA Foundation as a decision-support tool during emergencies. This integration improves simulation accuracy and represents progress toward the definition of a fuel map that can be used in wildfire risk management for both planning and emergency support.

Materials and Methods

PROPAGATOR (*Trucchia et al. 2020)* is a semi-empirical, stochastic cellular automata model where each cell can *be unburned*, *already burned* or *is burning*. The fire propagation is a stochastic contamination process between burning and unburned cells, with the spreading probability depending on both static (fuel type, topography) and dynamic (wind, fuel moisture) cell conditions. This contamination process is repeated multiple times to compute a fire probability map based on the frequency of burning for each cell. PROPAGATOR uses 7 custom fuel classes: *grassland, broadleaves, shrubs, conifers*, *agroforestry areas, non-fire prone forest*. The fuel type is involved in both the propagation between cells, through a *transition matrix* between fuels, and in the *standard rate of spread* v_n. These parameters are then modified according to topography, wind and fuel moisture conditions (see *Trucchia et al. 2020* for more details).

Given the importance of fuel and its associated parameters in propagation, in this work Machine Learning techniques were used to obtain a custom fuel map for the PROPAGATOR model, in order to enhance its fire simulation capabilities. The ML-informed fuel map combines information on wildfire susceptibility with the vegetation classes.

The susceptibility map indicates the tendency of the territory to ignite and propagate fires, and it is representative of the current geo-environmental and climatic conditions (*Trucchia et al. 2023*). The predisposing factors used in the analysis are listed in *Table 1*. The EFFIS burned areas database in the period 2008-2022 was used to identify the wildfire pixels, dividing then the dataset into 75% training and 25% test datasets. A *Random Forest Classifier* with 750 decision trees and 15 nodes max depth was adopted. As result, a continuous susceptibility value in [0, 1] was obtained.

Table 1: Predisposing factors adopted for the pan-european susceptibility map.

Predisposing factor	
geo-environmental inputs	Elevation[4]
	Slope[1]
	North and South direction (aspect)[1]
	Vegetation type[5]
	Neighbor vegetation (percentage)[2]
	Tree cover density[6]
climatic inputs[7]	Annual average temperature (43-years mean)
	Annual average max daily temperature (43-years mean)
	Annual cumulative precipitation (43-years mean)
	Annual average wind speed (43-years mean)
	Annual maximum consecutive dry days (43-years mean)
	Annual maximum consecutive wet days
	Annual relative humidity (43-years mean)

The continuous susceptibility map was then classified into three susceptibility classes (*low, medium, high*) according to the quantiles of its values obtained within wildfires. In particular, the high susceptibility class was selected to include 80% of the wildfire pixels, while the low susceptibility class included only 1% of them. The susceptibility values of the classes are highlighted in *Figure 1*.

Then, the three susceptibility classes have been crossed with four vegetation classes that highlight the different main fire behavior expected, namely *grassland, broadleaves*, *shrubs* and *conifers*.
Doing so, each vegetation class is divided into three susceptibility classes, obtaining 12 fuel classes (see *Figure 1*). The pan-european fuel map was provided with 100 m spatial resolution.

[4] Source: DEM - Multi-Error-Removed Improver-Terrain (MERIT). Spatial resolution: 100 m.

[5] Source: Copernicus Global Land Cover. Unclassified forest types from global land cover have been masked with CORINE 2018. Portugal and Galicia (Spain) national land cover maps have been used to add Eucalyptus type (due to its high flammability). Spatial resolution: 100 m.

[6] Source: Copernicus tree cover density. Spatial resolution: 100 m.

[7] Source: Inter-Sectoral Impact Model Intercomparison Project (ISIMIP). Spatial resolution: 50 km..

	grassland (G)	broadleaves (B)	shrubs (S)	conifers (C)
	low intensity surface fire	medium intensity forest fire	high intensity bushfire	high intensity forest fire
low susceptibility s < 0.18	**G1**: low intensity surface fire, low likelihood	**B1**: medium intensity forest fire, low likelihood	**S1**: high intensity bushfire, low likelihood	**C1**: high intensity forest fire, low likelihood
medium susceptibility 0.18 < s < 0.45	**G2**: low intensity surface fires, medium likelihood	**B2**: medium intensity forest fire, medium likelihood	**S2**:high intensity bushfire, medium likelihood	**C2**: high intensity forest fire, medium likelihood
high susceptibility s > 0.45	**G3**: low intensity surface fire, high likelihood	**B3**: medium intensity forest fire, high likelihood	**S3**: high intensity bushfire, high likelihood	**C3**: high intensity forest fire, high likelihood

Figure 1: Description of the 12 fuel classes obtained with the ML-informed fuel map.

To integrate this map into PROPAGATOR, each fuel class must be associated with the fuel parameters identified before. To do so, it was decided to start from the original PROPAGATOR fuel classes corresponding to the four considered vegetation classes (see *Figure 2a*), perturbing their values according to the susceptibility class.

To limit the complexity, the transition matrix perturbation is defined by multiplication of perturbation parameters identified per each susceptibility class, differentiating between unburned and burning cells (respectively, parameters u_i and b_i, see *Figure 2b*). Instead, the perturbation of v_n is given by three parameters r_i .
The final transition matrix and standard rate of spread parameters are obtained by crossing this information - see *Figure 2c*.

Transition Matrix		Burning cell G	B	S	C
Unburned cell	G	0.475	0.45	0.475	0.475
	B	0.25	0.3	0.375	0.275
	S	0.35	0.375	0.375	0.4
	C	0.25	0.225	0.325	0.35
V_n [m/h]		120	100	140	200

(a)

Transition Matrix Perturbation $u_i \in (0, 1]$ $b_i \in (0, 1]$			Burning cell low susceptibility	medium susceptibility	high susceptibility
			b_1	b_2	b_3
Unburned cell	low susceptibility	u_1	$S_{11} = b_1 u_1$	$S_{21} = b_2 u_1$	$S_{31} = b_3 u_1$
	medium susceptibility	u_2	$S_{12} = b_1 u_2$	$S_{22} = b_2 u_2$	$S_{32} = b_3 u_2$
	high susceptibility	u_3	$S_{13} = b_1 u_3$	$S_{23} = b_2 u_3$	$S_{33} = b_3 u_3$
v_n perturbation			r_1	r_1	r_1

(b)

Transition Matrix		Burning cell G			B			S			C		
		G1	G2	G3	B1	B2	B3	S1	S2	S3	C1	C2	C3
Umbruned cell	G	G1											
		G2	x 0.475		x 0.45			x 0.475			x 0.475		
		G3											
	B	B1											
		B2	x 0.25		x 0.375			x 0.375			x 0.275		
		B3											
	S	S1											
		S2	x 0.35		x 0.375			x 0.375			x 0.4		
		S3											
	C	C1											
		C2	x 0.25		x 0.225			x 0.325			x 0.35		
		C3											
V_n [m/h]		x 120			x 100			x 140			x 200		

(c)

Figure 2: (a) original PROPAGATOR fuel classes parameters; (b) perturbation parameters; (c) the final fuel parameters are obtained by multiplying the different contributions.

A genetic algorithm was tested to identify the perturbation parameters in order to calibrate the map and better fit past wildfire events. In the present study, a test on the *La Torre de l'Espanyol* wildfire occurred in Catalunya (Spain) in 2019 was done. A detailed report of the event is provided by local authorities[8]. Wind data from the report was used in simulation, while the RISICO model (*Fiorucci et al. 2008*) was used to simulate fuel moisture (see *Figure 4*). 36 hours of the event were simulated.
Four tests were performed, by different assumptions on the perturbation parameters - see *Figure 4* for more details, and for the hyper-parameters used. The goodness-of-fit function proposed by *Fraga et al. 2022* was used as the objective function. To test the results, the Sorensen coefficient was adopted (*Trucchia et al. 2020*).

Results and Discussion

In *Figure 3* the pan-european fuel map is presented, together with the distribution of the 12 classes for the whole territory, and within the burned areas 2008-2022. As derived from the analysis, the map allows for identifying the areas most affected by fires. By combining this information with the potential fire behavior, the capabilities of PROPAGATOR to simulate fires can be improved.

The preliminary results of the parameters calibration are shown in *Figure 4*. The calibration process is promising, but a sufficiently large dataset of past wildfires is needed to properly calibrate the parameters and allow PROPAGATOR to leverage the information contained in the ML-informed fuel map.

[8] Source: Catalan wildfire database - https://interior.gencat.cat/ca/arees_dactuacio/bombers/foc-forestal/incendis_forestals/informes-dincendis-forestals/

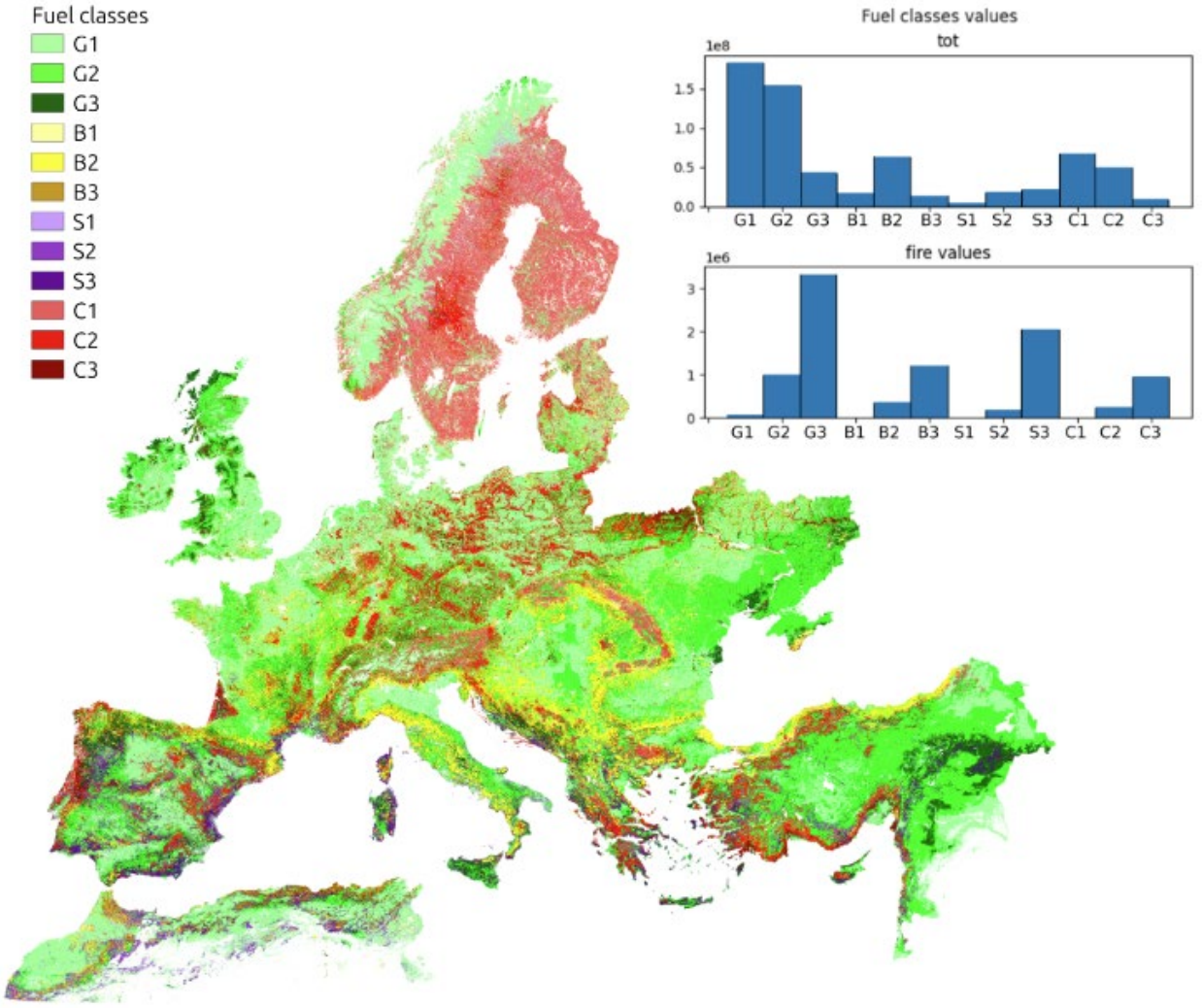

Figure 3: Pan-european fuel map. On top-right, the distribution of the 12 classes for the whole territory, and within the burned areas 2008-2022.

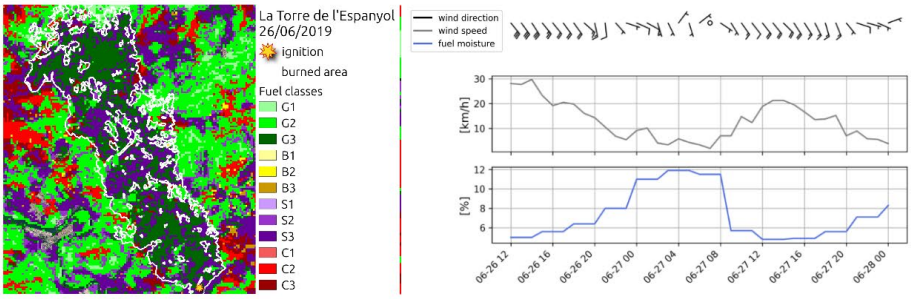

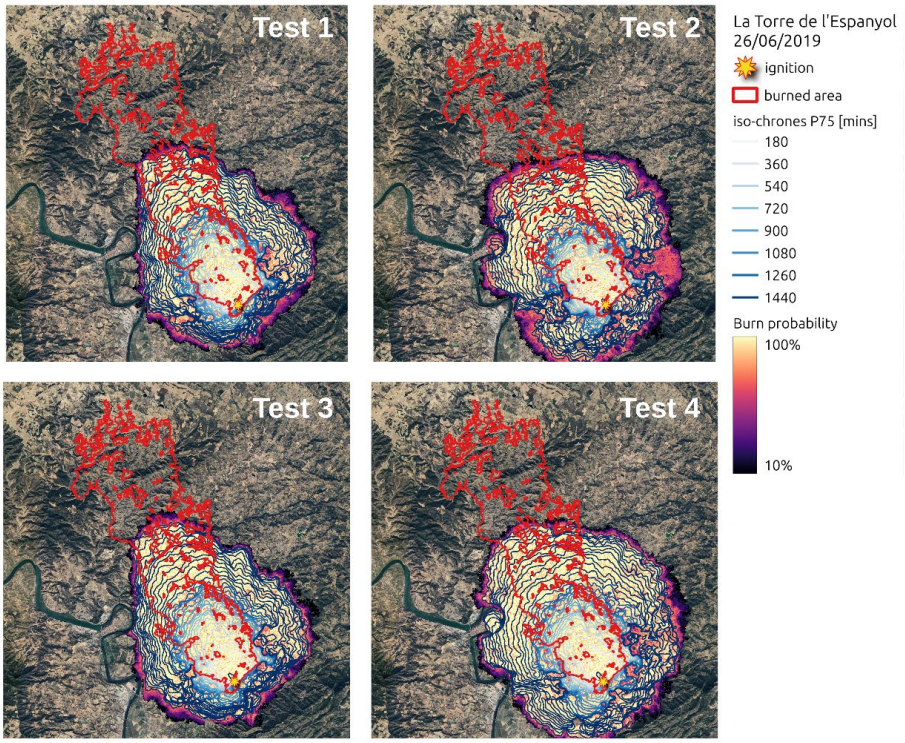

	Perturbation indices			GoF	Sorensen
	Unburned cell	Burning cell	v_n		
Test 1	u_1=0.908 u_2=0.985 u_3=0.995	$b_1=u_1$ $b_2=u_2$ $b_3=u_3$	r_1=0.5 r_2=1 r_3=2	0.73	0.46
Test 2	u_1=0.969 u_2=0.943 u_3=0.970	$b_1=u_1$ $b_2=u_2$ $b_3=u_3$	r_1=0.826 r_2=1.906 r_3=1.858	0.78	0.49
Test 3	u_1=0.968 u_2=0.979 u_3=1.000	b_1=1 b_2=1 b_3=1	r_1=0.5 r_2=1 r_3=2	0.72	0.46
Test 4	u_1=0.846 u_2=0.934 u_3=0.992	b_1=1 b_2=1 b_3=1	r_1=0.744 r_2=1.653 r_3=1.944	0.72	0.40

identified by the algorithm
constrained parameters
forced parameters

Hyper-parameters:
searching space:
u_i: [0.7, 1]
b_i: [0.7, 1]
k_i: [0.5, 2]
Population: 20
Generations: 10
Tournament parameter: 4
Crossover probability: 0.7
Mutation probability: 0.3
Elitism: 5%
Probability threshold (for wildfire shape): 75%

Figure 4: On top, sciatic and dynamic data used in the *La Torre de l'Espanyol* wildfire simulation. The parameters obtained in the tests with the genetic algorithm are shown in the table in the bottom of the figure. The simulation results are reported.

References

Fiorucci P, Gaetani F, Minciardi R (2008) Development and application of a system for dynamic wildfire risk assessment in Italy. *Environmental Modelling and Software* **23**(6), 690–702.

Fraga E, Cortes A, Margalef T, Hernandez P (2022) Efficient Cloud-Based Calibration of Input Data for Forest Fire Spread Prediction. *Proceedings - 2022 IEEE 18th International Conference on e-Science, EScience*, 128–136.

Tedim F, Leone V, Amraoui M, Bouillon C, Coughlan MR, Delogu GM, Fernandes PM, Ferreira C, McCaffrey S, McGee TK, Parente J, Paton D, Pereira MG, Ribeiro LM, Viegas DX, Xanthopoulos (2018) Defining Extreme Wildfire Events: Difficulties, Challenges, and Impacts. *Fire* **1**(1), 9.

Trucchia A, D'Andrea M, Baghino F, Fiorucci P, Ferraris L, Negro D, Gollini A, Severino M (2020) PROPAGATOR: An Operational Cellular-Automata Based Wildfire Simulator. *Fire* **3**(3), 26.

Trucchia A, Meschi G, Fiorucci P, Provenzale A, Tonini M, Pernice U (2023) Wildfire hazard mapping in the eastern mediterranean landscape. *International Journal of Wildland Fire*, **2**(3), 417–434.

Acknowledgements

The research activities described in this poster have been partially funded by the italian "Piano Nazionale di Ripresa e Resilienza – PNRR", Missione 4 Componente 2, Investimento 1.3 - D.D.1243 2/8/2022, project RETURN ‘‘Multi risk science for resilient communities under a changing climate’’ - Partenariato Esteso PE00000005- M.I.U.R Ministry of Education and Merit."

The authors acknowledge the Italian Civil Protection Department - Presidency of the Council of Ministers, who funded this research through the convention with the CIMA Research Foundation, for the development of knowledge, methodologies, technologies, and training, useful for the implementation of national wildfire systems of monitoring, prevention, and surveillance.

Proceedings for the 7th International Fire Behavior and Fuels Conference
April 15-19, 2024, Boise, Idaho, USA – Tralee, Ireland – Canberra, Australia
Published by the International Association of Wildland Fire, Missoula, Montana, USA

Understanding Community Vulnerability to Wildfire in the Robson Valley Canada

James Whitehead[1,2], Tristan Pearce[1,2]
1. Department of Geography, Earth, and Environmental Sciences, University of Northern British Columbia, Prince George, BC V2N 4Z9, Canada
2. Natural Resources and Environmental Studies Institute, University of Northern British Columbia, Prince George, BC V2N 4Z9, Canada

** Corresponding Author*

Introduction

The risk and impact of wildfires in British Columbia are rising due to factors including historic fire exclusion, climate change, and the wildland-urban interface (WUI) expansion. Recent major fire seasons have highlighted the inadequacy of suppression-focused models (Copes-Gerbitz et al., 2022), underscoring the need to understand community vulnerability and plan for wildfire as an inevitable part of the social-ecological system. Existing literature has often focused on the biophysical aspects of wildfire behavior and mitigation, with limited social science research examining the impacts on and resilience of communities. There has been less work with a focus on vulnerability in the Canadian context and specifically applying this approach to rural, non-Indigenous communities in the context of wildfire. As such, we have a limited understanding of how communities are at risk from wildfires, who and what are susceptible to harm, and what is the capacity to plan for, respond and recover. This work employs a community-based vulnerability approach to understand how the Robson Valley's rural communities are susceptible to wildfire risks.

Study Area

The Robson Valley (*figure 1*), a rural region in East-Central BC, spans over 230 km from Dome Creek to the Alberta border. It is situated on the traditional territory of the Lheidli T'enneh and Simpcw peoples. The study area (ranging from Tete Jaune Cache to Dome Creek) has a population of approximately 2100 and is represented politically by the Fraser-Fort George Regional District and the Village of McBride. The study specifically focused on

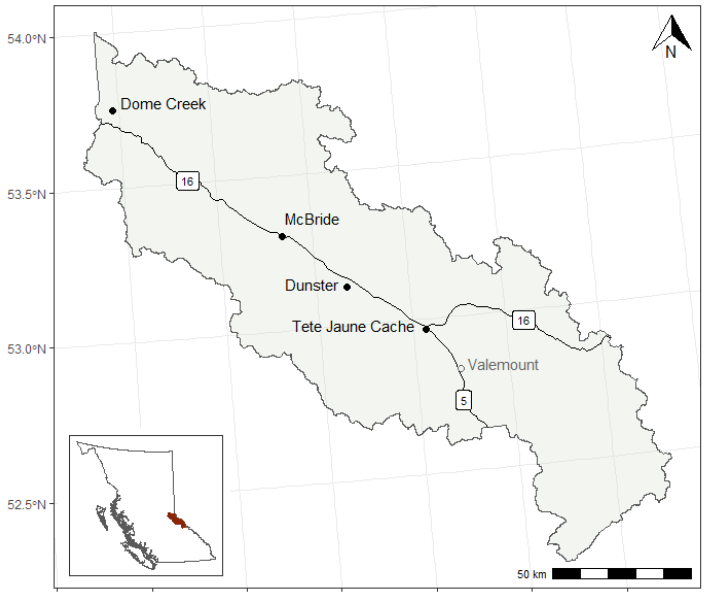

Figure 35 A map of the Robson Valley with study communities denoted in Black

the communities of Dome Creek, McBride, Dunster and Tete Jaune Cache. Notably, residents were impacted by wildfire in 2003, when power supply was lost for more than a week due to more than 200kms away from the region.

Methods

This research employed a vulnerability approach methodology, which describes vulnerability as a function of exposure to a hazard, sensitivity to the effects of the hazard and adaptive capacity or the ability of a system to address their exposure sensitivity. Data were collected through semi-structured interviews with key informants and three public meetings were held in communities without political representation. Supplementary data were gathered through participant observations and reflective diaries and all data were analyzed using latent content analysis to identify themes related to wildfire risk, vulnerability, resilience, adaptation, and barriers to adaptation.

Results

The study identifies several themes impacting community vulnerability and resilience. While these results are unique and specific to communities within the Western Robson Valley, there are likely significant parallels with other communities who share some of the social, geographical and economic traits of the Robson Valleys.

Community Isolation and Infrastructure Vulnerabilities

A key theme identified in this research is the isolation of the Robson Valley communities, which amplifies the sensitivity of the region to wildfire. The region's remoteness means that communities are reliant on exposed infrastructure including power lines and roads. A key compounding impact of the remoteness with the potential consequence of food loss due to power outages for a remote area, where many are reliant on hunting and agriculture. Additionally, the isolation of the region impacts the response times for emergency service organizations and impacts and presents significant connectivity and logistical challenges during emergency response.

Government Services and Jurisdictional Challenges

The centralization of government services, through the shuttering of the local Ministry of Forests office, the centralization of wildland firefighting and the decline in provincial representation was commonly identified as a key frustration by participants who expressed frustration with the top-down approach implying that it did not recognize the capacity within the region and does not leverage local knowledge or prioritize community-specific concerns. Additionally, jurisdictional challenges complicate mitigation initiatives due the complexity of aligning objectives and funding across private, municipal and public lands.

Economic Dependency and Demographic Shifts

The Robson Valley's economy has undergone significant transition over recent decades. As the economy has transitioned away from timber dependence and many forestry dependent families have left, the sensitivity, exposure and adaptive capacity to respond to fires has changed. Historically, with an economic dependence on local forests, there was a high exposure to local wildfires, a high economic sensitivity timber loss and a strong adaptive capacity through the role of forestry workers suppressing wildfires and reducing wildfire hazard. As this industry has declined, local vulnerability to fire has changed, with exposure, sensitivity and adaptive capacity all declining.

An increased focus on tourism has altered wildfire vulnerability and highlights the impact of economic transitions. While there is a significant potential impact of local wildfires impacting tourism operations, one of the most substantial potential exposures is that of smoke from elsewhere degrading air quality and impacting the safety and aesthetic appeal of outdoor recreation. Crucially, the tourism industry is less involved in fire suppression operations and is unlikely to be able to contribute in the event of a local fire. In comparison to the forest sector, tourism is potentially less sensitive to the impacts of a local fire; however, the range of potential exposure can span hundreds of kms when considering the impacts of smoke.

Local Adaptive Strategies and Community Resilience

Despite these challenges, Robson Valley communities exhibit resilience and have developed adaptive strategies to mitigate hazard. One notable initiative included investing in both diesel and hydro power generation to reduce reliance on vulnerable power lines and enhance energy security during wildfires and other outages. There have also been some efforts to lead community wildfire mitigation activities including recent fuel treatments conducted by the provincial government in the community of Tete Jaune Cache.

Furthermore, as a community that has long been isolated from larger centers, there is a strong culture of enhancing local resilience through local support and collaboration. Participants and residents commonly talked about supporting their neighbors and community members whenever needed and spoke of an expectation that others would do the same. Social networks such as these are crucial to building adaptive capacity as they have been shown to enable people to collaborate for a common purpose in good faith (Adger, 2003)

Barriers to Adaptation and Recommendations

Several barriers were identified by residents as hindering their ability to adapt to wildfires. These included financial constraints at both the personal and community levels, poor communication between governments and residents about available

resources and legislative barriers around fire suppression, which some felt prevented them from supporting their communities.

Building on these findings, this research proposed four recommendations:

1. **Policy Clarity:** Improved communications on rights, responsibilities and legislation to engage residents in prevention and response.
2. **Increased interactions:** Increased opportunities for relationship building between residents and local firefighters.
3. **Local Champions:** Build locally led initiatives by supporting the work of community leaders and local champions.
4. **Rural Programming:** Develop decentralized programming to better engage rural residents who may be deterred by centralized governance.

Discussion

Communities in the Robson Valley have seen significant social and economic change which has shaped and altered community vulnerability to wildfire. The region's isolation and dependency on exposed infrastructure highlight the need for robust local adaptations, while centralized government services have struggled to effectively engage and support local engagement in fire prevention and response. By better understanding the community specific vulnerabilities, along with the adaptive capacity present, local leaders can better prepare for wildfire and better support community led resilience efforts.

This work was novel for its application of a vulnerability approach to the context of a rural British Columbia and highlights the need for further vulnerability and resilience work in addressing the risk of wildfire. This research presented the novel finding that economic transitions impact a community’s vulnerability to wildfire in various ways. Overall, we suggest that enhancing community resilience requires a multifaceted approach and a strong understanding of locally specific vulnerabilities in advance of a wildfire. These insights contribute to the broader discourse on rural resilience, providing a framework for similar communities facing wildfire risks.

Conclusion

In conclusion, this case study provides a valuable lesson in community resilience and vulnerability. While the region faces significant challenges due to its isolation, economic dependencies, and lack of local engagement in fire prevention and response, the community's adaptive strategies and resilience efforts offer a potential avenue. This study highlights the critical need for a holistic, community-centered approach to wildfire management, which can be applied to other rural and remote communities globally facing similar threats.

References

Adger, W. N. (2003). Social Aspects of Adaptive Capacity. In *Climate Change, Adaptive Capacity and Development* (pp. 29–49). Imperial College Press.

Copes-Gerbitz, K., Hagerman, S. M., & Daniels, L. D. (2022). Transforming fire governance in British Columbia, Canada: An emerging vision for coexisting with fire. *Regional Environmental Change*, *22*(2), 48.

Proceedings for the 7th International Fire Behavior and Fuels Conference
April 15-19, 2024, Boise, Idaho, USA – Tralee, Ireland – Canberra, Australia
Published by the International Association of Wildland Fire, Missoula, Montana, USA

Using GEDI Spaceborne LiDAR to develop a height-varying Wind Reduction Factor model.

*Molly A. Harrison
The University of Melbourne, Melbourne, Victoria, Australia,
molly.harrison1@unimelb.edu.au

Thomas P. Keeble
The University of Melbourne, Melbourne, Victoria, Australia,
tom.keeble@unimelb.edu.au

Philip J. Noske
The University of Melbourne, Melbourne, Victoria, Australia, pnoske@unimelb.edu.au

Christopher S. Lyell
The University of Melbourne, Melbourne, Victoria, Australia, clyell@unimelb.edu.au

Darcy P. Prior
Department of Energy, Environment, and Climate Action, Victoria, Australia,
darcy.prior@dewlp.vic.gov.au

Patrick N.J. Lane
The University of Melbourne, Melbourne, Victoria, Australia, patrickl@unimelb.edu.au

Gary J. Sheridan
The University of Melbourne, Melbourne, Victoria, Australia, sheridan@unimelb.edu.au

**Corresponding Author*

Introduction

Local wind speed is a key factor in the propagation of bushfires and is a critical input variable in fire simulators,(Cruz et al., 2021; Massman et al., 2017; Pimont et al., 2022). Forest structural properties (i.e., height and density) are key parameters impacting sub-canopy wind speed, and therefore, in driving fire rate of spread (ROS) (Dupont et al., 2011; Massman et al., 2017; McGowan et al., 2021; Moon et al., 2019; Mueller et al., 2014). Accurately capturing these properties is essential for characterising the wind reduction effect beneath the canopy, which is represented by a wind reduction factor in fire modelling (WRF, dimensionless).

Vertical and lateral heterogeneity in vegetation properties result in significant variation in the wind reduction effect, across landscapes and within the vertical profile of a forest (Pimont et al., 2022). Landscape level classifications (e.g., ecological vegetation classes (EVCs) or fuel types, in Australia) are often used to represent changes in forest

structural characteristics, however, these do not adequately capture shifts in forest height and density at a sufficient scale. Further, previous work has highlighted the importance of representing vertical change in wind speed for fire spread (Massman et al., 2017; Moon et al., 2019). As fires develop and flame height changes, the wind experienced by the fire will also change, meaning the application of WRFs that do not vary with height may result in prediction error.

Despite this, single value WRFs are often applied across large parts of the landscape, and without regard for the height-varying nature of wind reduction within forests. The use of spaceborne LiDAR to parameterise WRF models may help to overcome these shortcomings. The Global Ecosystem Dynamics Investigation (GEDI) spaceborne LiDAR L2B product captures canopy height (m) and Plant Area Index (PAI, m2/m2) in 25m footprints, between 51.6˚N and 51.6˚S (Dubayah et al., 2020). This freely available data set provides relatively high-resolution structural data (canopy height and vertical change in PAI) across almost all the world's forests. Additionally, previous work has shown good agreement between GEDI's L2B product and airborne LiDAR outputs, indicating it is able to successfully capture the required forest attributes (Dhargay et al., 2022). This dataset could therefore not only improve the lateral characterisation of forest structure across the landscape, but also provide information on the vertical forest attributes key to modelling wind reduction. The continuation of GEDI until 2031 means that models parameterised by this dataset can be continually updated with up-to-date observations of forest structural metrics.

The aim of this research is to develop a three-dimensional forest windspeed reduction factor (WRF) model that can be easily parameterised in any forest globally using freely available spaceborne lidar (GEDI). We achieve this aim by;

1. Developing a modelling approach that uses GEDI generated forest stand-level structural properties of height and plant area index to predict the WRF
2. Measuring windspeed reduction factors laterally across a diverse range of forest structures
2. Measuring windspeed reduction factors vertically across a height gradient of forests
4. Testing the new 3-dimensional forest WRF model against field observations

Methods

Data inputs

We instrumented paired (open and forested) sites to observe the wind reduction effect across different forest types. Each was instrumented with a 10m guyed mast, along with five 3D sonic anemometers at 2m, 4m, 6m, 8m, and 10m. The masts were moved at each site for replication, and recorded observations for between one and two months at each replicate site.

Mast locations were selected in such a way that topographic influence and forest edge effects were accounted for. To assess the performance of this model across the entire vertical forest profile, we derived vertical wind profiles from the publicly available OzFlux network flux tower anemometers. We selected only flux towers that had wind speed measurements above the canopy, to be used as a proxy 'open' wind speed. This allowed for model testing across a range of forest types, from a tall wet forest to an Acacia woodland.

The Automatic Fuel Moisture Monitoring Network (AFMMN), which is a network of 28 weather stations throughout Victoria forests, was used to develop a dataset of 2m WRFs. To derive a WRF, we extracted an 'open' windspeed value from the reconstructed fire weather VicClim dataset. This dataset provides modelled hourly weather from 1970 to 2020, at a grid scale of 4kmx4km (Brown et al., 2016). The WRF was estimated from the daily 'open' windspeed and the daily averaged 2m observed windspeed values from the AFMMN monitoring stations.

GEDI spaceborne LiDAR was used as the sole spatial data input in this model's development. Square buffers were created around each site for both the AFMMN locations and the mast/flux sites, with a distance of 500m from the site. This resulted in buffers with a total edge distance of 1000m. Where the buffer intersected non-forested areas, they were amended to avoid them. We then extracted the footprints of GEDI L2B LiDAR that intersected these buffers and extracted height (m) and vertical PAI in 5m bins.

Model development

We combined these datasets to develop a laterally and vertically varying WRF model. The resulting model takes a stepwise linear form for each 5m PAI bin and assumes a monotonically declining function from the canopy down. It is bound by a 2m WRF value and a nominal canopy top WRF of 1.15. The difference in wind reduction between the canopy top and 2m above the ground is then distributed proportional to the distribution of PAI across the vertical profile of the forest.

The twenty-eight 2m WRFs derived from the AFFMN and VicClim datasets were used to train and test a sub-model for estimating the 2m WRF. This was achieved using a multivariate non-linear least squares (NLS) regression. The quantity of PAI in the 0-5m height bin was used to account for the distribution of PAI across the vertical profile.

Results

Model testing found good agreement between the observed vertical WRF profile and the predicted WRFs based on PAI and height. When provided with an observed 2m WRF, we found the model's capacity to predict the WRF as a function of height was very good (Figure 1). Future improvements will see the coupling of the 2m WRF model with this height-varying model, to allow the prediction of the WRF at any height using only GEDI spatial inputs.

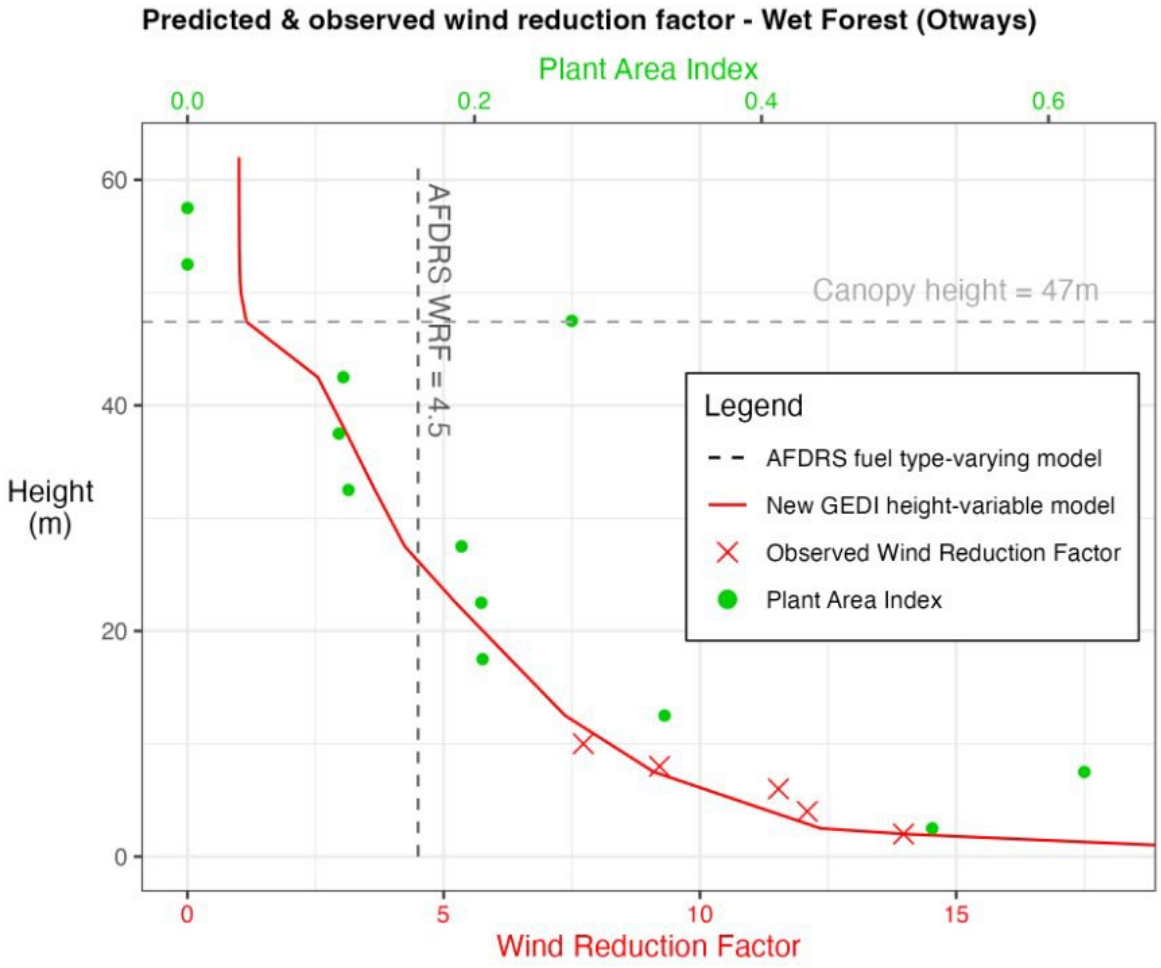

Figure 1. Red crosses depict observed WRF values at height within the canopy space. Red line is modelled WRF profile based on difference between 2m observed value, canopy WRF value, and distribution of GEDI derived PAI. Green dots are GEDI PAI distribution, and grey line is static Australian Fire Danger Rating System (AFDRS) WRF currently in use. Empirical value at 2m above ground used as model input.

Compared to the WRFs currently in operation in Australia, which do not vary with height and are applied across coarse resolution fuel type classifications, we found significant

improvement. Figure 2. compares the currently used AFDRS static WRFs and the output of our height-varying model with the observed values across our sites (model used empirical input for 2m value here).

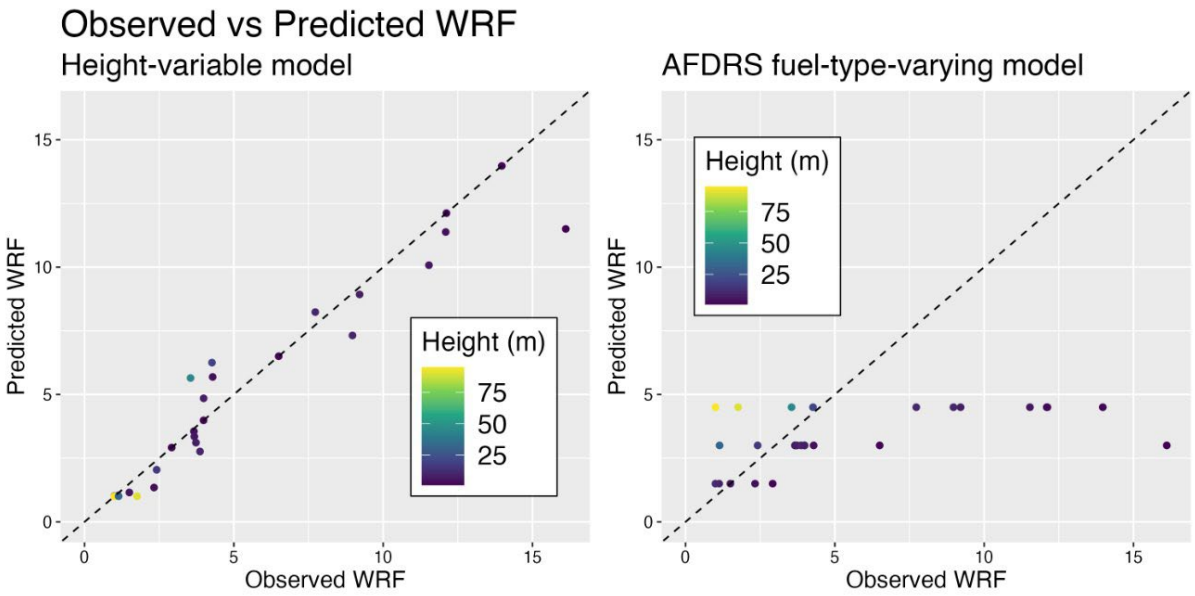

Figure 2. A) Observed Wind Reduction Factor at various heights throughout the vertical canopy space across mast and flux tower sites vs. predicted WRF from GEDI height-varying model. B) Observed WRF at various heights throughout the vertical canopy space across mast and flux tower sites vs. Static AFDRS WRFs currently used across all heights.

Discussion

The integration of a large-scale vertically varying spatial dataset with a height-varying model for the prediction of forest WRFs provides an opportunity to overcome some key limitations in the current use of WRFs in fire modelling. Namely, this model allows for the prediction of a WRF based on flame height, overcoming potentially critical modelling error that follows from the use of static WRFs. Furthermore, the use of GEDI allows for changes in key forest properties to be characterised on higher resolution spatial scales than landscape scale fuel type classifications.

Requiring only spatial inputs from the freely available GEDI L2B spaceborne LiDAR product, this model can be applied anywhere that there is GEDI coverage and can be updated as GEDI is. Further, the model maintains computational and analytical simplicity, while improving upon the prediction of WRFs.

Model testing was limited by the number of available sites that had full vertical wind profiles available. This model should be further tested on a wider range of forest types, particularly on non-eucalypt forests. While GEDI performs well in its characterisation of the vertical PAI profile in our test cases, this may not be the case in forests of different structures.

Overall, this work has contributed a successful proof-of-concept in the use of GEDI to develop and parameterise a WRF model.

References

Brown T, Mills G, Harris S, Podnar D, Reinbold H, Fearon M (2016). A bias corrected WRF mesoscale fire weather dataset for Victoria, Australia 1972-2012. *Journal of South. Hemisphere Earth Systems Science* **66**, 281–313.

Cruz M G, Cheney N P, Gould J S, McCaw W L, Kilinc M, Sullivan A L (2021). An empirical-based model for predicting the forward spread rate of wildfires in eucalypt forests. *International Journal of Wildland Fire* **31**, 81–95. https://doi.org/10.1071/WF21068

Dhargay S, Lyell C S, Brown T P, Inbar A, Sheridan G J, Lane P N J (2022). Performance of GEDI Space-Borne LiDAR for Quantifying Structural Variation in the Temperate Forests of South-Eastern Australia. *Remote Sensing* **14**, 3615. https://doi.org/10.3390/rs14153615

Dubayah R, Blair J B, Goetz S, Fatoyinbo L, Hansen M, Healey S, Hofton M, Hurtt G, Kellner J, Luthcke S, Armston J, Tang H, Duncanson L, Hancock S, Jantz P, Marselis S, Patterson P L, Qi W, Silva C (2020). The Global Ecosystem Dynamics Investigation: High-resolution laser ranging of the Earth's forests and topography. *Science of Remote Sensing* **1** https://doi.org/10.1016/j.srs.2020.100002

Dupont S, Bonnefond J-M, Irvine M R, Lamaud E, Brunet Y (2011). Long-distance edge effects in a pine forest with a deep and sparse trunk space: In situ and numerical experiments. *Agricultural and Forest Meteorology* **151**, 328–344. https://doi.org/10.1016/j.agrformet.2010.11.007

Massman W J, Forthofer J M, Finney M A (2017). An improved canopy wind model for predicting wind adjustment factors and wildland fire behavior. *Canadian Journal of Forest Research* **47**, 594–603. https://doi.org/10.1139/cjfr-2016-0354

McGowan H, Rosenthal K, Bott R, Myles J (2021) 'Wind speed Reduction Factors (WRFs): utilities for WRF assessment and communication.' Bushfire and Natural Hazards CRC.

Moon K, Duff T J, Tolhurst K G (2019). Sub-canopy forest winds: understanding wind profiles for fire behaviour simulation. *Fire Safety Journal* **105**, 320–329. https://doi.org/10.1016/j.firesaf.2016.02.005

Mueller E, Mell W, Simeoni A (2014). Large eddy simulation of forest canopy flow for wildland fire modeling. *Canadian Journal for Forest Research* **44**, 1534–1544. https://doi.org/10.1139/cjfr-2014-0184

Pimont F, Dupuy J-L, Linn R (2022) Wind and Canopies In ' Wildland Fire Dynamics'. (Eds Speer K and Goodrick S). pp. 183-208 (Cambridge University Press: Cambridge)

Proceedings for the 7th International Fire Behavior and Fuels Conference
April 15-19, 2024, Boise, Idaho, USA – Tralee, Ireland – Canberra, Australia
Published by the International Association of Wildland Fire, Missoula, Montana, USA

Using Simple fire-weather indices to illustrate differences between fire-danger ratings generated by the Australian Fire Danger Rating System and the McArthur-based system for Eucalypt forests

*Kevin Tory
Bureau of Meteorology, Australia, kevin.tory@bom.gov.au

Musa Kilinc
Country Fire Authority, Victoria Australia

**Corresponding Author*

Introduction

The procedures for assessing fire danger across the country underwent a major overhaul with the introduction of the Australian Fire Danger Ratings System in 2022 (AFDRS, e.g., Hollis et al. 2024). Substantial changes were introduced, incorporating a broader range of vegetation types, new and improved headfire-spread-rate functions, and a comprehensive treatment of fuels. For Eucalypt forests, there were changes in the fire-weather and fuel availability components, and the introduction of sophisticated fuel representation that were absent in the previous system. A change in fire-danger rating labelling also accompanied the AFDRS implementation to simplify and unify fire-danger messaging across the country. The compounding effect of all these changes for operational users was an unfamiliar system that, among other things, responded in an unfamiliar way to input variables. Becoming familiar with the new system has obvious challenges, such as the need to adjust or reconstruct decision-making matrices. These challenges are compounded by ongoing necessary system developments such as vegetation and fuel updates with non-trivial impacts on the system. In this paper we compare components of the old and new fire-danger ratings systems for Eucalypt forests (hereafter abbreviated to 'OLD' and 'NEW') to help elucidate their differences, and provide additional insight into the contribution to fire danger ratings from each input term.

OLD vs. NEW comparison

Due to document size limitations only a superficial overview can be provided in this short paper, with the reader referred to Noble et al. (1980) and AFDRS (2019) for relevant OLD and NEW equations respectively. The OLD and NEW for Eucalypt forests are depicted schematically in Fig. 1. The OLD is based on McArthur's Forest Fire Danger Index version 5 (FFDI), which includes Fuel Availability (fraction of fuel that will burn on a given day, yellow box) and a weather term (blue box) expressed as an exponential function of temperature (T), relative humidity (RH) and wind speed (V). The NEW includes a Fuel Load (amount of fuel present, green box), multiplied by a Fuel Availability (yellow box), which together yield the mass of fuel that will burn on any given day. Multiplying this fuel mass by a fire-spread-rate (three boxes inside the purple outline) gives a fuel consumption rate expressed as a fireline intensity that defines the

fire danger rating. The Vesta fire-spread-rate model, used for Eucalypt forests, is shown in Fig. 1 separated into a Fuel Hazard (a measure of fuel structure and distribution, green/brown box), Fuel Availability (FA, yellow boxes) and a weather term (blue box).

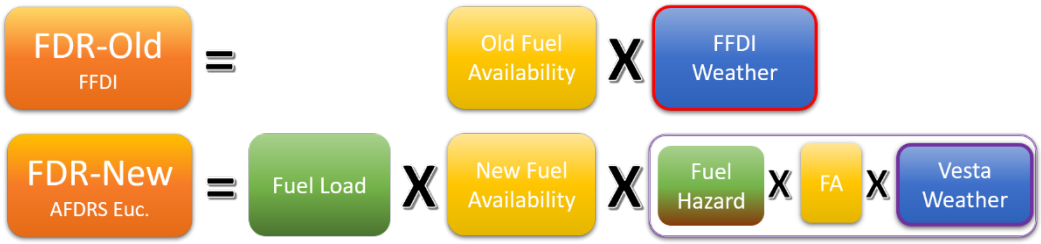

Figure 1: Schematic depiction of the OLD and NEW Eucalypt-forest fire danger rating models.

Weather function comparison

Figure 2 shows how the contribution from each weather input varies between the OLD (red) and NEW (purple) weather functions, after matching the functions at $V = 20\ km\ hr^{-1}, RH = 30\%$, and $T = 24℃$. The OLD weather function used exponential relationships for all terms (red curves) yielding steadily increasing values with windiness, dryness and temperature. In contrast, two of the NEW terms (purple) are almost linear: wind (left) and temperature (right). Consequently, the NEW sees lesser fire danger for light and very high windspeeds (< 20 and $> 80\ km\ hr^{-1}$), compared to the OLD and greater fire danger for inbetween wind speeds. The NEW relative humidity term (centre) sees greater fire danger for humid conditions ($RH > 30\%$) with little difference for $RH = 10 - 40\%$. The greatest difference between the OLD and the NEW weather functions is in the temperature term. The NEW term has very minimal temperature sensitivity, varying by only 26% across the $T = 0 - 50℃$ parameter space, compared with a more than four-fold increase for the OLD.

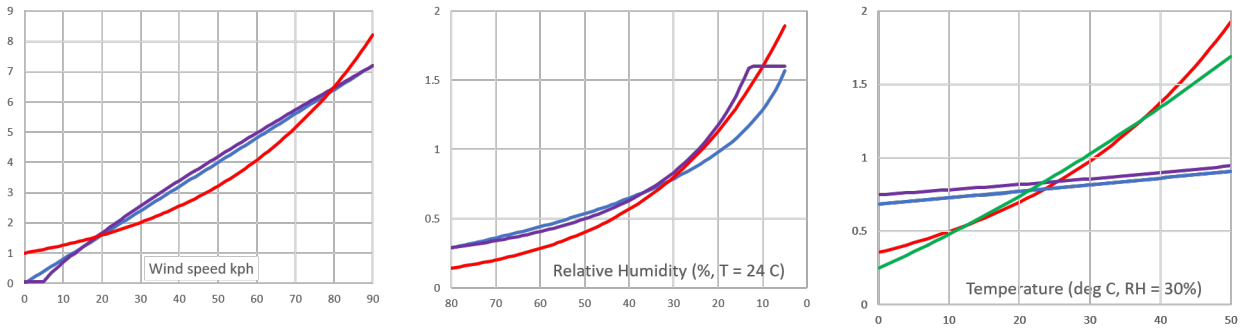

Figure 2: Wind (left), relative humidity (centre) and temperature (right) contributions to the OLD (red) and NEW (purple) weather functions. The equivalent DWI approximation to the NEW is shown in blue, and a simple temperature term (green) approximating the OLD is shown in green.

The Vesta fire-spread rate function for sunny, summer afternoons assuming default Fuel Hazard terms, is well approximated by a form of the Dry Windy Index DWI_V,

$$DWI_V = \frac{V}{500}(DPD + 5). \qquad 1.$$

Here DPD is dewpoint depression (the difference between the temperature and dewpoint temperature). DWI_V provides an excellent approximation to Vesta (Fig. 2, blue lines) for all terms except for $RH \sim 10-25\%$, where the DWI_V (blue) is less than both the OLD (red) and NEW (purple). However, our interpretation of a recent study assessing the role of fuel moisture on fire spread rates in Eucalypt forests (Cruz et al. 2022) suggests DWI_V might be more realistic.

All three models are similar when conditions are near to the matching values ($V = 20\ km\ hr^{-1}, RH = 30\%, T = 24$°C). They will also be similar where differences *compensate* one-another (e.g., cool-humid and calm, or warm and windy). Conversely, the OLD and NEW will differ most when their weather term differences *accumulate* (e.g., cool-humid and windy, or warm and calm). For example, the NEW will maintain a higher rating with the passage of a blustery cold front than the OLD, due to higher contributions from all terms. The stark difference between the OLD and NEW temperature term will dominate in hot or cold conditions. However, an extra temperature term, $(T + 12)/2$ (Fig. 2, green line) can be multiplied by DWI_V to create a simple approximation to the OLD.

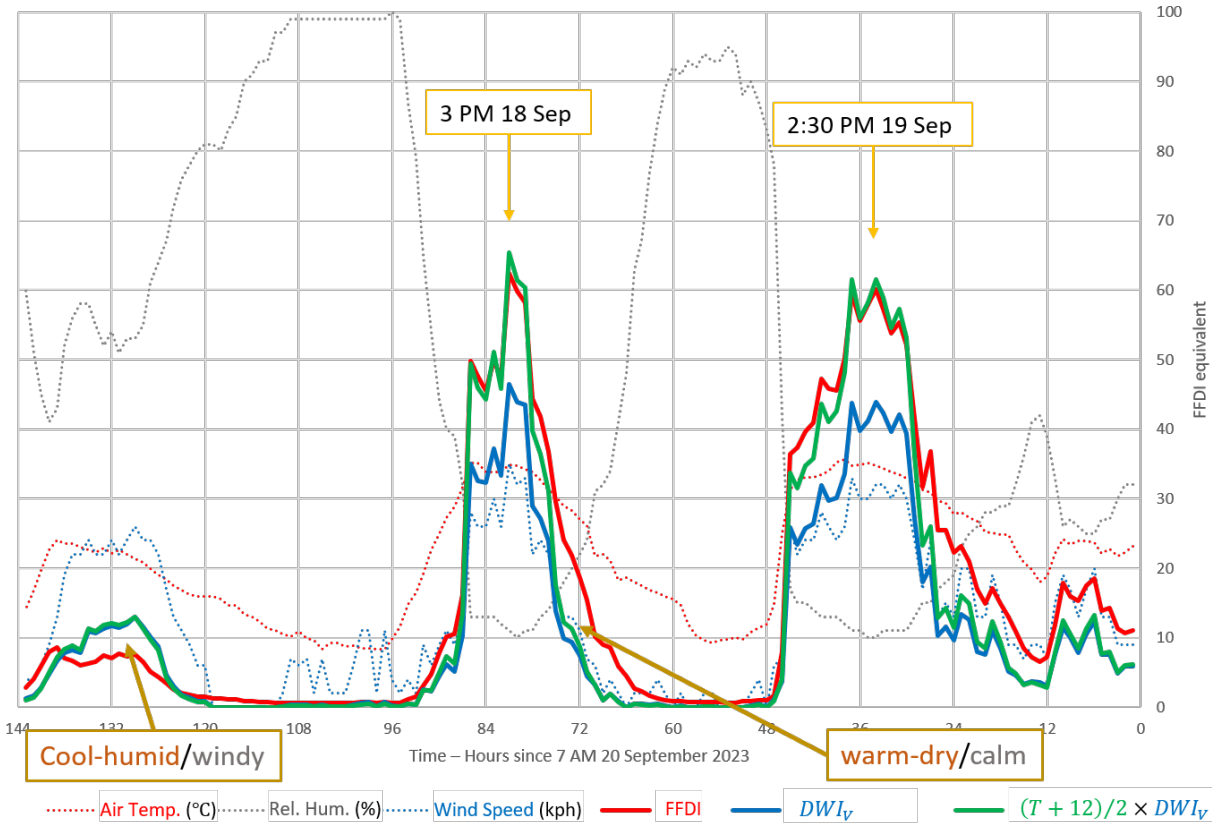

Figure 3: Time-series comparison of the OLD (red) and approximated OLD (green) and approximated NEW (blue) using weather data from the Bega Automatic Weather Station during the Bega fires of September 2023. Weather fields are also plotted (dotted lines, see legend).

A time-series of weather variables (dotted lines) and weather terms (solid lines) for the Bega fire (September 2023) is presented in Fig. 3, to highlight the differences between the OLD (red) and the two approximated functions (blue and green). A purple line corresponding to the NEW was not included as it was barely distinguishable from its approximated form (DWI_V, blue). Fig. 3 shows DWI_V (blue) underrepresents the OLD (red) during hot midday conditions ($T{\sim}35℃$), and demonstrates the value of the temperature term in approximating the OLD (green). Two examples of *accumulated* differences between the approximated functions (blue and green) and the OLD (red) are labelled in Fig. 3. The Cool-humid/windy example suggests greater fire danger in both approximated equations than the OLD (primarily due to $RH{\sim}55\%$), and vice versa for warm-dry/calm example (primarily due to $V < 12\ km\ hr^{-1}$). In both examples the temperature is not sufficiently cold or hot for the temperature term to establish a distinction between the two approximated functions.

Fuel terms

Shifting the focus to the fuel terms (Fuel Load, Fuel Hazard and Fuel Availability) we combine the green and yellow boxes in the Fig. 1 schematic, and the OLD and NEW weather functions are replaced by their approximate forms to take advantage of the DWI_V component they have in common. This is depicted schematically in Fig. 4. (The ratio of fuel hazard to the default fuel hazard appears in the fuel term, because DWI_V represents the Vesta weather function multiplied by the default fuel hazard.)

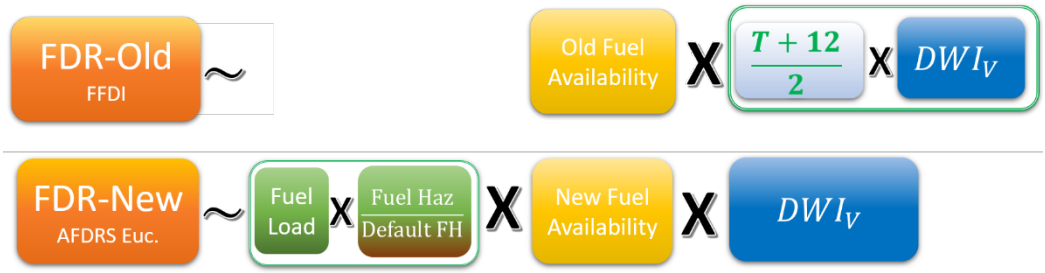

Figure 4: As in Fig. 1 but with the DWI_V approximations replacing the respective weather functions, and the fuel terms combined in NEW.

Fuel Availability

Figure 5 shows that the NEW fuel availability (Fig. 4, yellow boxes) can be substantially less than the OLD, depending on drought factor and forest type. In the OLD fuel availability varied linearly with drought factor from 0 to 1 (red line), but it is nonlinear in the NEW. (Both the OLD and NEW use the same drought factor.) These differences can be highlighted in Fig. 5 by considering the different drought factors (dashed lines) corresponding to a fuel availability of 0.5. For the OLD, NEW-dry and NEW-wet, these drought factors are 5, and about 7.7 and 9.3 respectively.

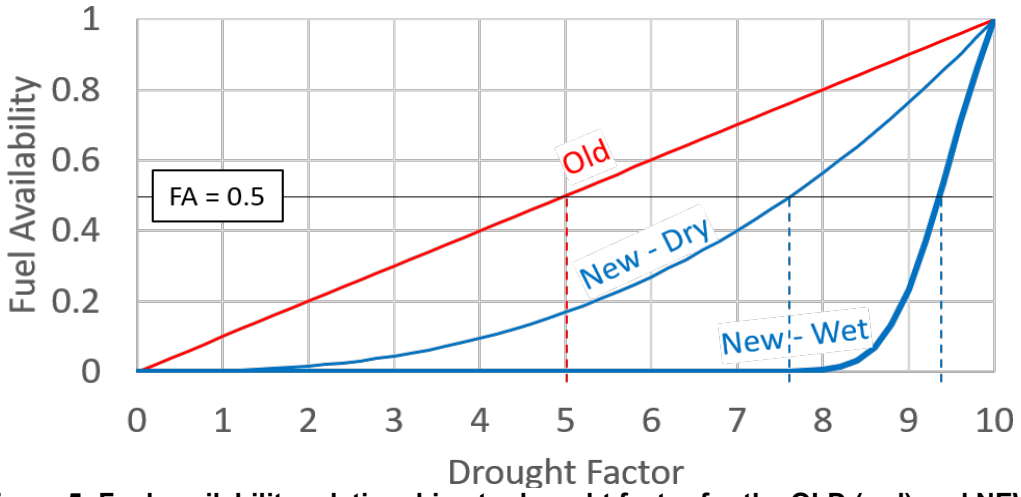

Figure 5: Fuel availability relationships to drought factor for the OLD (red) and NEW (blue) fire-danger ratings systems. Fuel availability relationships differ between wet and dry Eucalypt forests (as labeled). Dashed lines show the drought factor values that correspond to a fuel availability of 0.5.

Fuel Load

The combined fuel terms in NEW (Fig. 4, green box) can introduce an order of magnitude variation across the landscape, due to differences in vegetation characteristics and time since last burn. Since these factors were not explicitly incorporated in OLD, it would be useful to know the fuel term values in NEW that produce similar fire-danger ratings to OLD, to enable an assessment of the relative contributions from these terms. The fuel load contribution can be somewhat isolated by assuming a drought factor of 10 (OLD and NEW fuel availability = 1, Fig. 5) and default fuel hazard terms. Then the OLD and NEW reduce to just linear functions of DWI_V (Fig. 6a, b respectively). This allows NEW to be expressed as a function of OLD (Fig. 6c), and plotted as line graphs (Fig. 7).

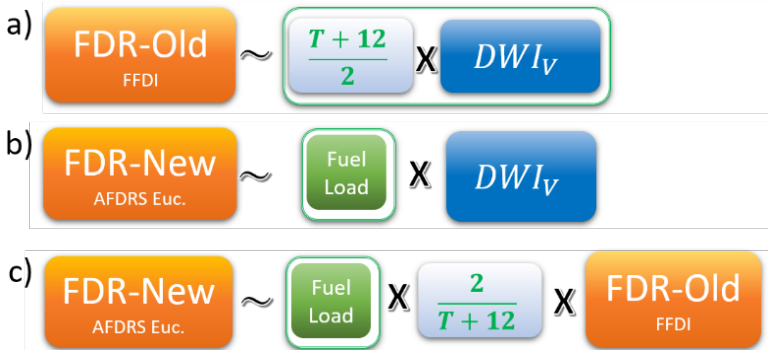

Figure 6: a) OLD, b) NEW with fuel availability and fuel hazard terms = 1. c) NEW expressed as a function of OLD.

For a given temperature and fuel load, all possible combinations of weather variables and their corresponding DWI_V values reside somewhere on a diagonal line emanating from the plot origin in Fig. 7. The line slope is determined by the temperature and fuel

load (Fig. 6c), with the slope increasing with higher fuel loads and lower temperatures. Lines representing specific fuel loads (units, tonnes/hectare) are marked on the plots for two representative temperatures, $24℃$ (left) and $40℃$ (right). The beginning of each fire danger rating regime (Moderate, High, Extreme, Catastrophic) is marked at the relevant point on the OLD and NEW scales. The stars at the intersections of these lines show where OLD and NEW are identical. It follows that wherever the diagonal lines are above the stars NEW diagnoses greater fire danger than OLD, and vice versa wherever the lines are below the stars. For $T = 24℃$ any fuel load above 10 t/ha results in NEW always diagnosing greater fire danger than OLD. Focusing on the High to Extreme fire-danger rating range (yellow—orange), NEW diagnoses greater fire danger for any fuel loads greater than about 6 t/ha. Since fuel loads are often greater than 6 t/ha (unless recently burnt or fuel reduced), NEW might generally predict greater fire danger than OLD for cooler temperatures. However, due to the higher temperature sensitivity of OLD, this bias is reduced at higher temperatures. For example, OLD and NEW are well matched in the High to Extreme range at $T = 40℃$ for fuel loads of about 10 t/ha.

For drought factors other than 10, the line slope can be adjusted to match the fractional difference between the NEW and OLD, which can be estimated from Fig. 5 (e.g., a drought factor of 6 would halve the line slopes for dry forests).

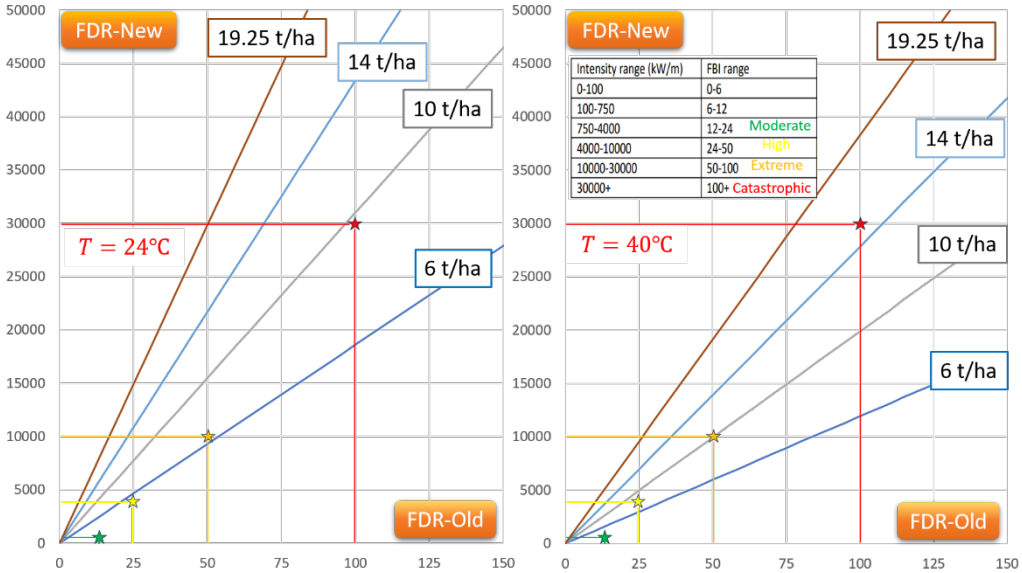

Figure 7: Fire danger rating comparisons for a selection of fuel loads at T = 24 C (left) and T = 40 C (right). The vertical axis is fireline intensity, and the horizontal axis is McArthur's FFDI. Stars mark the corresponding fire danger rating transition points (see inset) for OLD and NEW.

Summary

This paper provides insight into how the recently implemented Australian Fire Danger Ratings System (NEW) differs from its predecessor (OLD) for Eucalypt forests. Comparative studies such as this can assist the transition of critical decision-making matrices, that use fire-danger ratings as inputs, from OLD to NEW. Both OLD and NEW

incorporate the same weather inputs (wind, relative humidity, temperature) and same climate input (drought factor), however, their respective functions of these inputs differ substantially. Consequently, Fig. 2 shows, lighter winds see a reduction in fire-danger potential, while moderate to high winds and higher humidity see an increase in fire-danger potential between the OLD and NEW. Furthermore, strong temperature dependance in the OLD is almost completely absent in the NEW. Fig. 5 shows that for drought factors less than 10, the NEW Fuel Availability function imposes a greater moderating effect on fire-danger potential than the OLD, with the relative differences increasing with decreasing drought factor. Furthermore, the differences are extreme for wet Eucalypt forests, where fuel availability is virtually zero for drought factor less than eight. Finally, Fig. 7 offers insight into Fuel Load amounts that yield similar fire-danger rating outcomes between the OLD and NEW. These vary with temperature and drought factor.

Acknowledgements
This work benefitted from many discussions over the years with Stuart Matthews, Miguel Cruz, Lachie McCaw, Paul Gregory, and Meaghan Jenkins. Thanks also to internal reviews from Paul Gregory and Paul Fox-Hughes.

References
AFDRS (2019) Australian Fire Danger Ratings System – Research Prototype. Section 3.3.5 https://www.afac.com.au/docs/default-source/afdrs/afdrs_research_prototype_report_2019.pdf?sfvrsn=6

Cruz MG, Cheney NP, Gould JS, McCaw WL, Kilinc M, Sullivan AL (2022) An empirical-based model for predicting the forward spread rate of wildfires in eucalypt forests. *International Journal of Wildland Fire,* **31(1)**, 81—95, https://doi.org/10.1071/WF21068

Hollis JJ, Matthews S, Fox-Hughes P, Grootemaat S, Heemstra S, Kenny BJ, Sauvage S, (2024) Introduction to the Australian Fire Danger Rating System. *International Journal of Wildland Fire*, 33(3). https://www.publish.csiro.au/WF/justaccepted/WF23140

Noble IR, Bary GAV, Gill AM (1980) McArthur's fire-danger meters expressed as equations. *Australian Journal of Ecology*, **5**, 201–203. Doi:10.1111/j.1442-9993.1980.tb01243.x

Proceedings for the 7th International Fire Behavior and Fuels Conference
April 15-19, 2024, Boise, Idaho, USA – Tralee, Ireland – Canberra, Australia
Published by the International Association of Wildland Fire, Missoula, Montana, USA

Wildfire ignition probabilities by cause for the western and southeastern United States

*Christopher Moran
Pyrologix, LLC, 111 N Higgins Suite 202, Missoula, Montana, USA,
chris.moran@pyrologix.com

Joe H Scott
Pyrologix, LLC, 111 N Higgins Suite 202, Missoula, Montana, USA,
joe.scott@pyrologix.com

Matthew Thompson
Pyrologix, LLC, 111 N Higgins Suite 202, Missoula, Montana, USA,
matt.thompson@pyrologix.com

**Corresponding Author*

Introduction

Whether a situation calls for wildfire to be promoted, prevented, or mitigated, understanding and quantifying wildfire risk provides useful information for its management. Fundamental determinants of wildfire patterns are the initial ignition location and timing. The drivers of where and when depend on the cause, which can be broadly classified as natural (i.e. lightning) or human caused, and previous research has shown the spatial variation in ignition probability can be described (Catry et al. 2009, Syphard and Keeley 2015). Reducing human-caused ignitions is an immediate option for addressing the current wildfire crisis in the US because damaging fires are largely human-caused (Balch et al. 2017, Downing et al. 2022). The other mitigation options identified function broadly and cannot be nearly as direct (ON FIRE 2023).

Here, we produce wildfire ignition probability datasets for both human and natural ignition sources for the western and southeastern portions, the predominant wildfire regions of the continental US. These datasets describe modern ignition patterns in the form of annual ignition probability maps and inform resource allocation and other land management through improved fire modeling and fire risk assessments, among other useful applications.

Materials and Methods

We utilized observed ignition locations from the comprehensive US fire occurrence database (FOD; Short 2022) along with coincident variables known to influence ignition probability (Baker 2009), such as vegetation type, proximity to roads and urban areas, and topographic variables. Table 1 lists all the features and the data sources. We evaluated other feature data during model development, such as electrical transmission lines and topographic aspect, but these were found to not be useful in this approach.

Table 1. Description of candidate input features for ignition probability model development. See Table 2 for final model formulations.

Feature	Native Resolution	Data Source
Spatial Trend (ignitions km^{-2})	Vector Point Locations	Short et al. 2022
Biophysical Setting (BPS) Vegetation Type (majority class at both 120m and 4km)	30 m	LF 2.2.0
Slope (degrees)	30 m	LF 2.2.0
Elevation (m)	30 m	LF 2.2.0
Topographic Position Index (TPI)	120 m	LF 2.2.0
Distance to Roads (m)	30 m	LF 2.2.0
Road Cost Distance (m*slope)	30 m	LF 2.2.0
Distance to Urban (m)	30 m	LF 2.2.0
Urban Cost Distance (m*slope)	30 m	LF 2.2.0
Annual Precipitation (mm)	800 m	PRISM 2022
Solar Radiation (MJ m^{-2} day^{-1})	800 m	PRISM 2022
Maximum Vapor Pressure Deficit (VPDmax; hPa)	800 m	PRISM 2022

Data Processing and Model Development

All features were resampled to a consistent raster grid template of the analysis area at 120m resolution with an Albers Equal Area projection (EPSG: 5070). From the FOD, ignitions were split between human and natural causes and then summed to the raster grid. FOD data cleaning included removing ignitions with duplicated spatial coordinates and those below the fire size thresholds. Our intent was to focus on wildfire locations that had growth potential. Therefore, fires less than 100 ha in size for the western US and 8 ha for the southeastern US were removed.

The model response variable was binary, having an ignition within the 120m cell anytime during the data record. The negative samples vastly outnumbered the positives, which was mitigated with SMOTE sampling techniques (Chawla et al. 2002) to a 2:1 class balance for training.

The random forest (RF) algorithm was configured to produce probabilistic outputs that are comparable to logistic regression (Malley et al. 2012) and trained using the parameters listed in Table 2 with the ranger R package (Wright and Ziegler 2017).

Post-Prediction Processing

Probability predictions were scaled to the observed 2006-2020 ignition rate above the fire size threshold because the output probabilities were biased by the SMOTE sampling of the training data. Before scaling, nonburnable land area (water, snow, and ice) were removed from the area calculations for human ignitions with the additional removal of high intensity urban development for the natural ignition model.

Table 2. Final model input features by ignition cause and study region.

Region	**Southeastern US**
Human Ignitions	*P(Ign)* = BPS_Veg120m + BPS_Veg4km + Elevation + PPT + VPDmax + SolarRad + HumanSpatialTrend + UrbanDist + UrbanCostDist + RoadDist + RoadCostDist
Natural Ignitions	*P(Ign)* = BPS_Veg120m + BPS_Veg4km + Elevation + PPT + VPDmax + SolarRad + NaturalSpatialTrend
Region	**Western US**
Human Ignitions	*P(Ign)* = BPS_Veg120m + BPS_Veg4km + Elevation + Slope + TPI + PPT + VPDmax + SolarRad + HumanSpatialTrend + UrbanDist + UrbanCostDist + RoadDist + RoadCostDist
Natural Ignitions	*P(Ign)* = BPS_Veg120m + BPS_Veg4km + Elevation + Slope + TPI + PPT + VPDmax + SolarRad + NaturalSpatialTrend

Results

The resulting maps show that human- and natural-caused ignitions are spatially-separated with high densities of human ignitions visible in CA for the western US dataset. Natural ignitions are more homogenous across the western US but are focused on the state of FL in the southeastern US with human ignitions more evenly dispersed (Fig 3 and Fig 4).

Evaluating model performance, the Brier scores of 0.166 and 0.146 for the western US human and natural ignitions, respectively, and 0.149 and 0.127 for the southeastern US human and natural ignitions, respectively, derived from out-of-bag samples, indicate a useful probabilistic forecast.

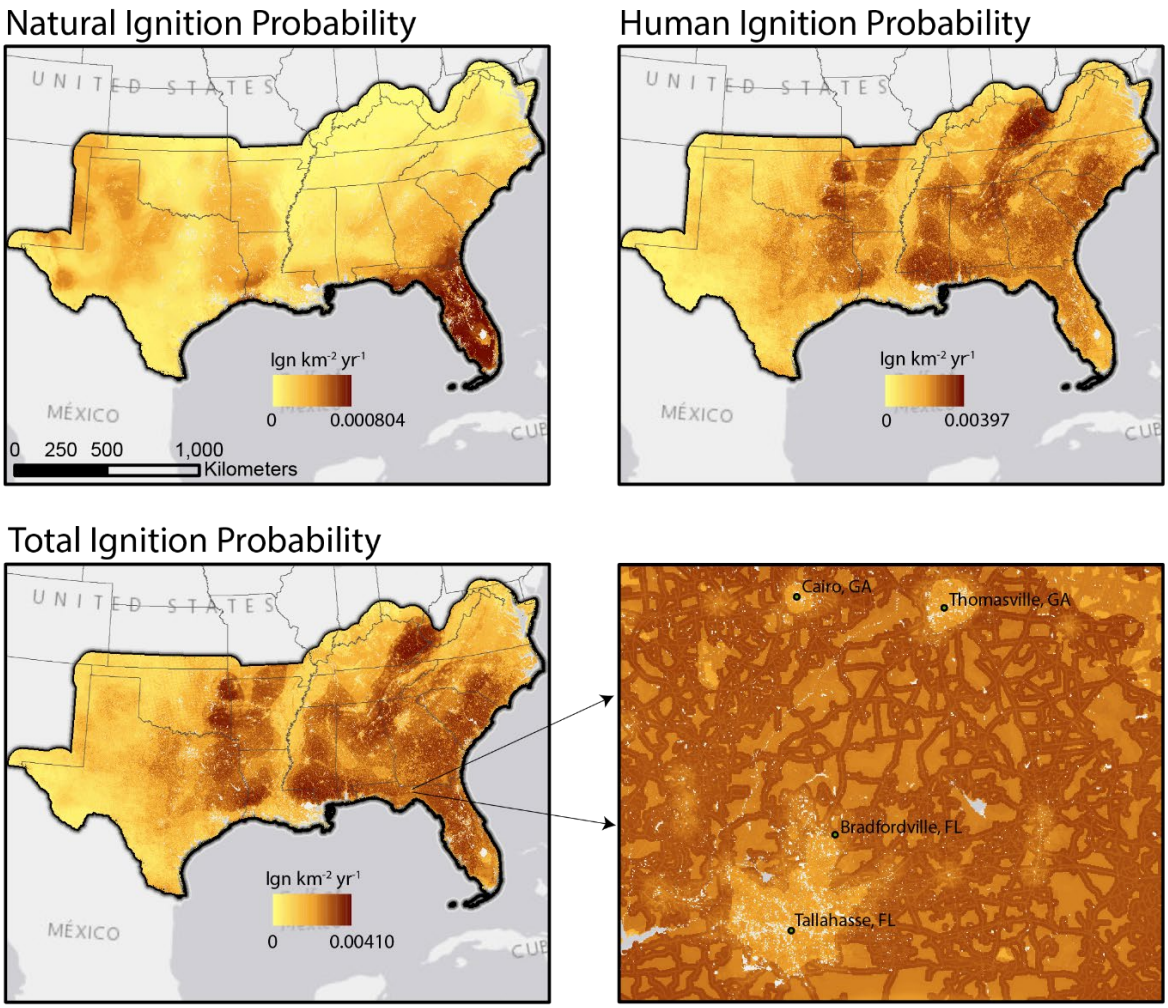

Figure 3. Maps of wildfire ignition probabilities for the southeastern (SE) US. Natural ignitions (top left) and human ignitions (top right) are derived from separate models and then summed to produce total ignition probabilities (bottom left). The inset (bottom right) shows the fine-scale variation from roads and urban areas around Tallahasse, FL.

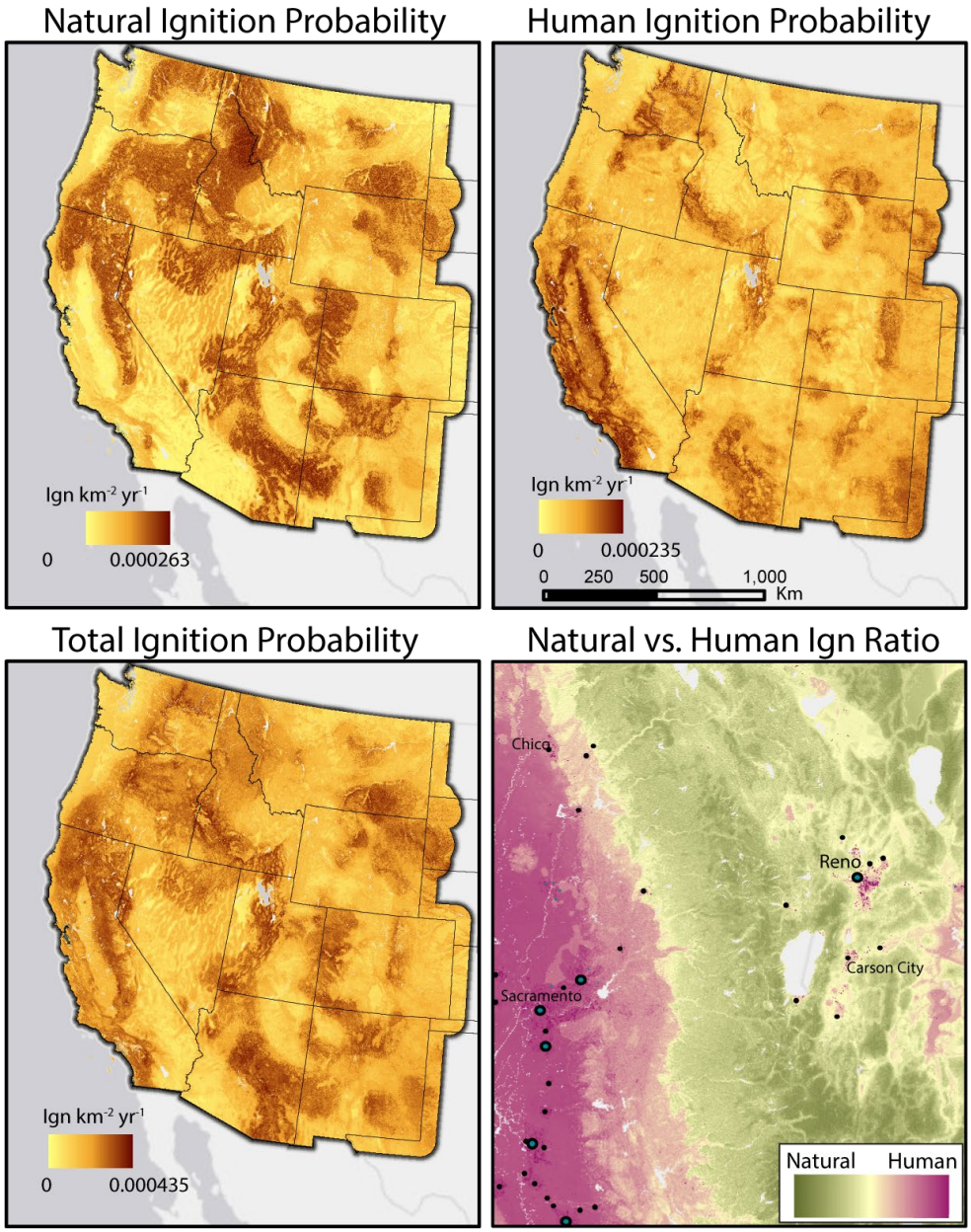

Figure 4. Wildfire ignition probabilities and ignition cause ratio for the western US. Natural ignitions (top left) and human ignitions (top right) are derived from separate models and then summed to produce total ignition probabilities (bottom left). The ignition ratio (bottom right) shows the Sacramento to Reno gradient of human to natural ignition causes.

Discussion

Here we generalize observed ignition patterns in the US by finding relevant spatial data, training a machine learning model, and predicting probability over broad areas. The primary added value over simply interpolating ignition location observations (the previous method for generating fire modeling inputs), is the identification of areas that

have similar conditions for ignitions leading to growth but have yet to experience them in the FOD record. Given the rapidly shifting climatic and environmental landscape, this generalization should prove advantageous for future-looking management. The use of the spatial trend input feature derived from observations balances this generalization however, while also characterizing other information not easily mapped, such as variable suppression strategies in the wilderness versus the wildland-urban interface.

These datasets are made available on the Vibrant Planet Data Commons (www.vpdatacommons.org/technical-details/ignition-probability-tech), whose mission is to provide data and meaning for increasing the pace and scale of forest restoration.

Acknowledgements
This work was funded in part by the USDA Forest Service, Fire and Aviation Management, Strategic Analytics Branch.

References

Baker, W.L. 2009. Fire ecology in Rocky Mountain landscapes. Island Press, Washington DC, USA.

Balch, J.K., B.A. Bradley, J.T. Abatzoglou, R.C. Nagy, E.J. Fusco, and A. Mahood. 2017. Human-started wildfires expand the fire niche across the United States. *PNAS* 114(11) 2946-2951.

Breiman, L. 2001. Random forests. *Machine Learning,* 45:532.

Catry, F. X., Rego, F. C., Bação, F. L., & Moreira, F. (2009). Modeling and mapping wildfire ignition risk in Portugal. *International Journal of Wildland Fire*, *18*(8), 921-931.

Chawla, N. V., Bowyer, K. W., Hall, L. O., and Kegelmeyer, W. P. (2002). Smote: Synthetic minority over-sampling technique. *Journal of Artificial Intelligence Research*, 16:321-357.

Downing, W.M., C.J. Dunn, M.P. Thompson, M.D. Caggiano, and K.C. Short. 2022. Human ignitions on private lands drive USFS cross-boundary wildfire transmission and community impacts in the western US. *Scientific Reports* 12: 2624.

LF 2.2.0: LANDFIRE Data products layers version 2.2.0. U.S. Department of Interior, Geological Survey, and U.S. Department of Agriculture. Available: http://landfire.cr.usgs.gov/viewer/

Malley, J.D., J. Kruppa, A. Dasgupta, K.G. Malley, and A. Ziegler. 2012. Probability machines: consistent probability estimation using nonparametric learning machines. *Methods Inf Med* 51: 74-81.

ON FIRE: The report of the Wildland Fire Mitigation and Management Commission. 2023. Available at https://www.usda.gov/sites/default/files/documents/wfmmc-final-report-09-2023.pdf
Accessed July 5 2024.

PRISM Climate Group, Oregon State University , https://prism.oregonstate.edu, data created December 2022, accessed 11/7/2023.

Short, Karen C.; Grenfell, Isaac C.; Riley, Karin L.; Vogler, Kevin C. 2020. Pyromes of the conterminous United States. Fort Collins, CO: Forest Service Research Data Archive.

Short, K.C., 2022. Spatial wildfire occurrence data for the United States, 1992-2020 [FPA_FOD_20221014]. 6th Edition. Fort Collins, CO: Forest Service Research Data Archive.

Syphard A. D. and J.E. Keeley (2015) Location, timing and extent of wildfire vary by cause of ignition. *International Journal of Wildland Fire* **24**, 37-47.

Wright MN, Ziegler A (2017). ranger: A Fast Implementation of Random Forests for High Dimensional Data in C++ and R. *Journal of Statistical Software*, **77**(1), 1–17.

Proceedings for the 7th International Fire Behavior and Fuels Conference
April 15-19, 2024, Boise, Idaho, USA – Tralee, Ireland – Canberra, Australia
Published by the International Association of Wildland Fire, Missoula, Montana, USA

Wildfire propagation potential for Split-Dalmatian County in Croatia

*Darko Stipaničev, Marin Bugarić, Dunja Božić Štulić, Ljiljana Šereić, Damir Krstinić
FESB - Faculty of El.Eng., Mech.Eng. and Naval Architecture, University of Split, Split, Croatia, darko.stipanicev@fesb.hr

**Corresponding Author*

Introduction

Wildfire propagation potential indicators are factors that affect the likelihood and intensity of wildfire spread. They are an important part of wildfire risk estimation, as proposed by the FirEUrisk project (FirEUrisk, 2021) in its integrated approach to wildfire risk assessment (Chuvieco et al., 2023).

Wildfire risk is connected with certain territories depending on three main factors:

- Wildfire danger
- Wildfire exposure
- Wildfire vulnerability

Wildfire danger is estimated from the probability of wildfire ignition and its propagation potential. Wildfire exposure includes population and assets exposure, as well as ecosystem exposure. It is estimated from two factors: fire metrics based on propagation potential indicators and atmospheric emission, and human assets and ecosystem services values at risk. The third factor, wildfire vulnerability, is determined by values of potential losses of ecosystem services, ecological values, and human assets, as well as resilience in terms of coping capacity and recovery time.

Wildfire propagation potential indicators directly influence wildfire danger (hazard) and wildfire exposure risk estimation. These indicators are usually variables directly connected with wildfire behavior, primarily wildfire fireline intensity (flame length) or wildfire rate of spread. These variables depend on weather conditions, topography, and fuel loading. Propagation potential indicators are usually calculated using statistically processed meteorological data of past wildfires in certain territories, giving an overall cumulative estimation, but they can also be calculated using real-time meteorological data. Simulating propagation potential leads to generating scenarios of intensity/severity maps, fuel consumption, including emissions and smoke plume maps for prevention and preparedness planning.

They are typically used by wildfire management agencies to assess the potential risk of a wildfire in a particular area.

In this paper, we present an estimation of wildfire propagation potential indicators for Split-Dalmatian County, a region in Croatia with quite high wildfire danger, chosen and used as one of the FirEUrisk Demonstration Areas (DAs).

Methodologies

In the FirEUrisk project, propagation potential was calculated using two different methodologies and resolutions. The first one (Methodology 1) was used for the European Territory (ET) in 1 km spatial resolution and the second one (Methodology 2) for selected Pilot Sites (PS) in 100 m spatial resolution. Demonstration Areas (DAs) are used to apply different methods locally in order to test them before application on either the European Territory (ET) or selected Pilot Sites (PS). Therefore, working on the propagation potential calculation methodology, we first applied it in our Demonstration Area – Split-Dalmatian County in Croatia in 100 m spatial resolution.

Both methodologies for propagation potential estimation are based on standard wildfire propagation models:

- Rothermel model for surface wildfire propagation (Andrews, 2018) and
- Standard crown wildfire propagation models (Scott & Reinhard, 2001).

Both models were custom implemented in Python for cell-based wildland landscape fire growth simulations. Figure 1 shows our procedure used for surface fire growth simulation on the European territory.

Input maps were:

- Fuel maps based on new FirEUrisk fuel models calculated for Split-Dalmatian County in 100 m spatial resolution (Bugarić et al., 2024)
- Terrain characteristics (slope and aspect)
- Meteorological data including temperature, relative humidity used for dead fuel moisture estimation, wind speed, and wind direction.

One of the most important meteorological variables for propagation potential simulation was fuel moisture, both live and dead. Considering dead fuel moisture content (DFMC), we analyzed five different DFMC models (Stipaničev et al., 2023) to determine which one is the most suitable for propagation potential calculation. Our analysis shows that the Fosberg and Deeming model, defined as standard Fire Behavior Analysis Tables (FBA Tables) adapted for the Mediterranean region by MeteoGrid, provides not only the smallest median value but also a narrow and symmetric box between the 1st and 3rd quartile (the 25th and 75th percentiles) as well as close and symmetric Upper and Lower Adjacent Values, making it the most suitable for DFMC estimation.

Live fuel moisture content (LFMC) was estimated using Scott-Burgan Fuel Moisture Scenarios (Scott & Burgan, 2005), additionally improved in (Pettinary & Chuiveco, 2017) by adding Live Crown Foliar Moisture Content.

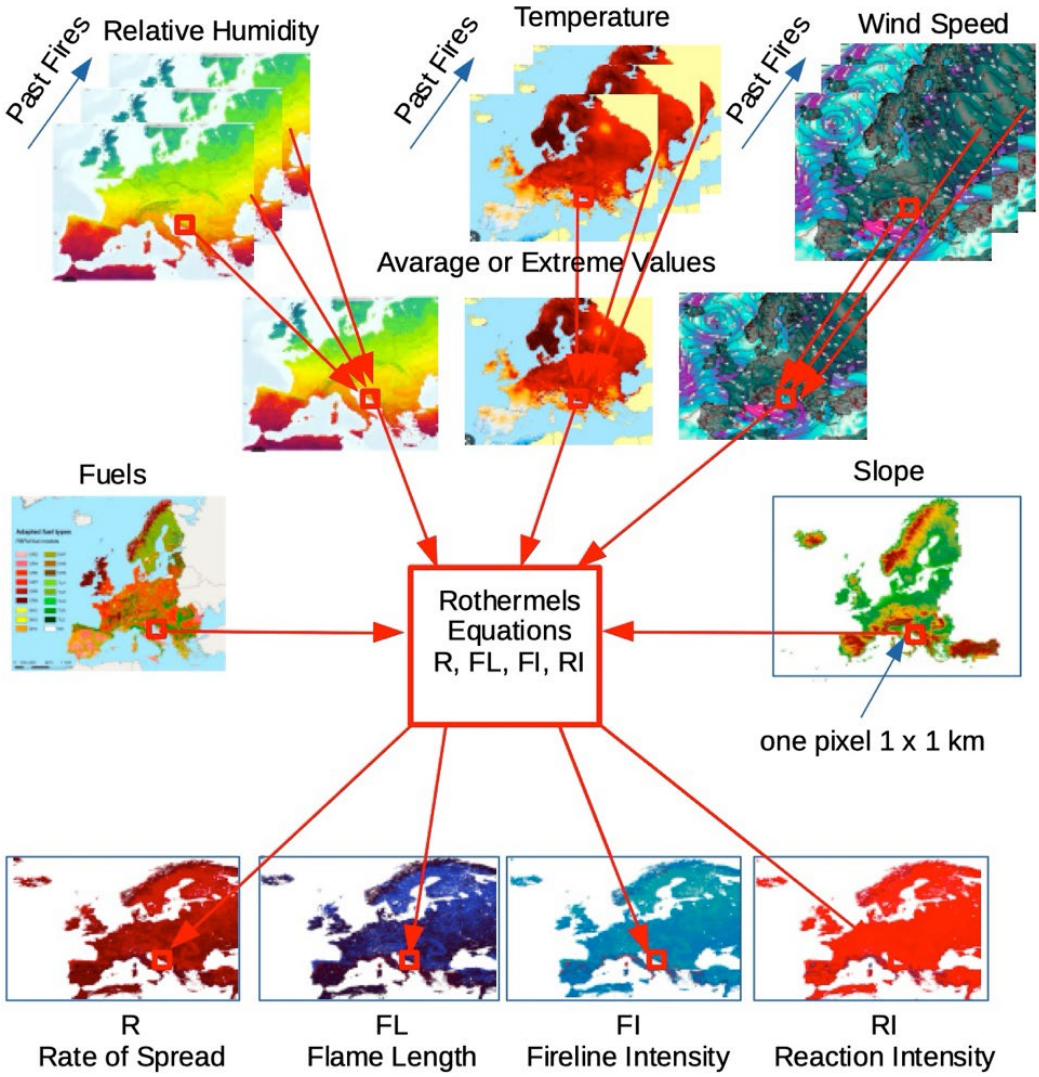

Figure 36: Cell-base wildland landscape surface fire grown simulation for European territory

The difference between the methodologies lies primarily in which meteorological data are used and how they were prepared for the simulations.

For **Methodology 1**, used for the European territory (ET) in the FirEUrisk project, past fires on ET from 2001 to 2019 larger than 2000 ha were selected. There were 403 such fires. For their dates, maps of meteorological parameters were extracted from ERA5 by MeteoGrid, and finally, two map sets for two weather scenarios were prepared:

- Average weather conditions (50th percentile) and
- Extreme weather conditions (5th percentile for fuel moisture and 95th percentile for wind speed).

For **Methodology 2**, used for selected Pilot Sites (PS) in the FirEUrisk project, historical fires in Split-Dalmatia County from 2008 to 2022 larger than 1 ha were collected with all

meteorological data. There were 117 fires (Figure 2). Eight weather scenarios were defined according to 8 wind directions (North, Northeast, East, Southeast, South, Southwest, West, Northwest).

For each scenario, propagation potential indicators were calculated, again using the 50th percentile scenario to represent average conditions and the 95th percentile scenario to represent extreme conditions..

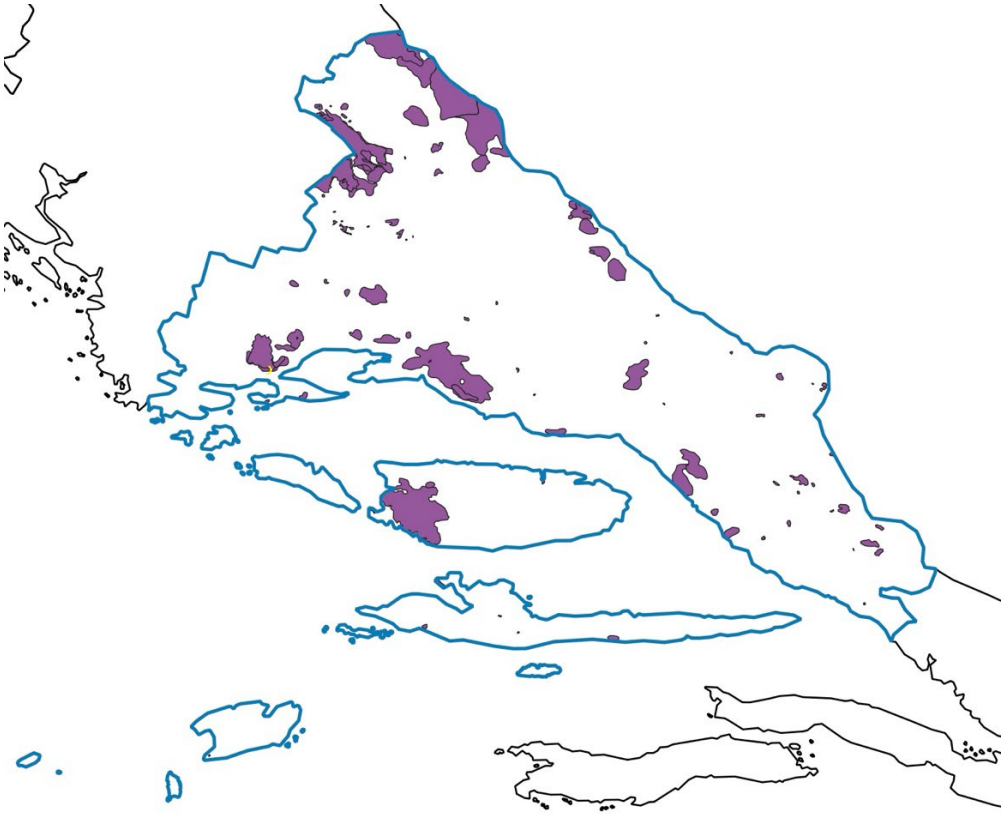

Figure 2: Historical fires in Split-Dalmatia County from 2008 – 2022 bigger than 1 ha

Results and conclusions

For both methodology output maps considering surface fire behavior included:

- Rate of Spread – R [m/s]
- Reaction Intensity – RI [kW/m2],
- Fireline Intensity – FI [kW/m] and
- Flame Length – FL [m]

and for crown fire behavior:

- Crown Factor Burned – CFB [fraction], Crown Fire Activity (CFA)
- Active and passive crown fire Rate of Spread – CR [m/s]
- Active and passive crown fire Reaction Intensity – CRI [kW/m2],
- Active and passive crown fire Fireline Intensity – CFI [kW/m]

- Active and passive crown fire Flame Length – CFL [m]

Figure 3 shows as an illustration comparison of calculated fireline intensity for both methodologies and extreme conditions.

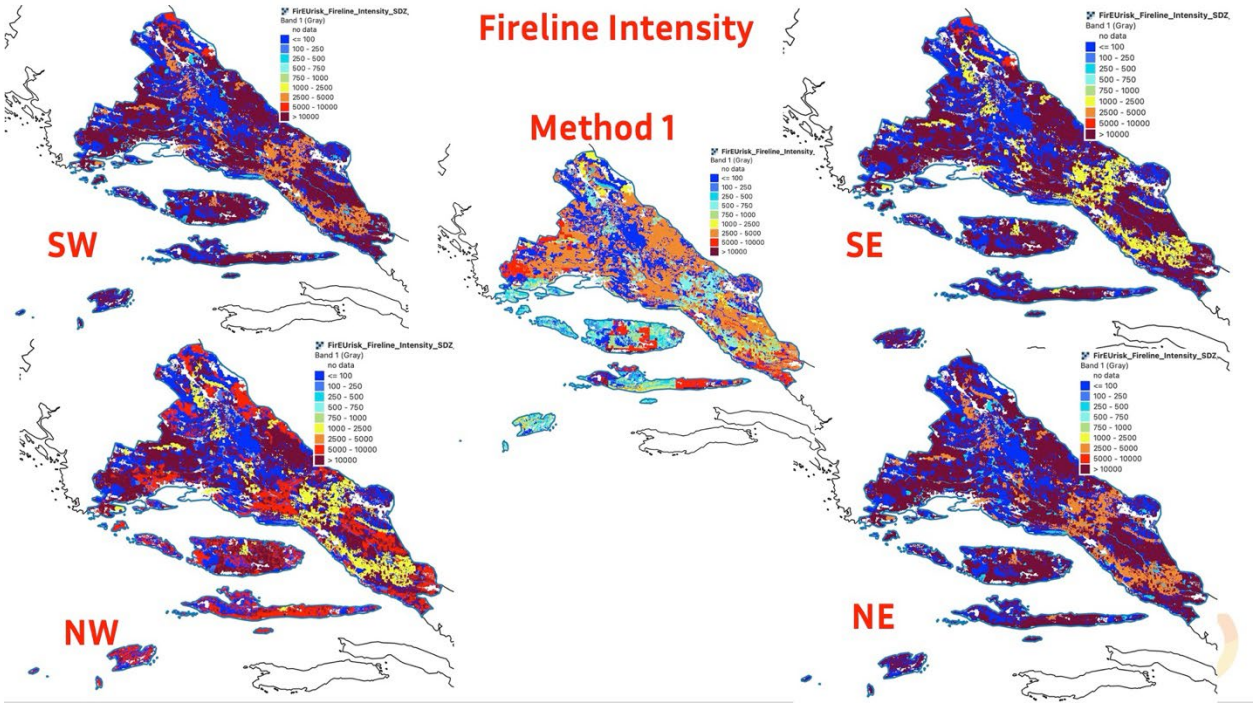

Figure 3: Comparison of fireline intensity calculation for both methodologies and extreme conditions

It is evident that Methodology 2 gives much higher results and, therefore, considering wildfire danger, as it is better to overestimate than underestimate, Methodology 2 is more suitable..

Final question: Why we doing all this?

Our intention is to further improve the Croatian wildfire intelligent monitoring and surveillance system (Krstinić, 2024) OiV Fire Detect AI (OiV Fire Detect AI, 2024). Future improvements of this system will partly be based on these results. Operators will have two options considering propagation potential danger (hazard) and other wildfire risk indicators:

1. The first will be based on these historical fires. For example, if a southwest wind is blowing, a firefighter operator could see which part has the most severe danger considering propagation potential indicators.
2. The second is even more important. Propagation potential danger indicators (besides other wildfire risk indicators) will also be calculated dynamically on a daily basis using daily meteorological data (in cooperation with the Croatian Hydrometeorological Service – DHMZ), so operators will have insight into (daily) real-time wildfire risk indicators.

We hope that this will further improve safety from wildfires in Croatia.

Acknowledgement
Research in this paper has received funding from the European Union's Horizon 2020 research and innovation programme under grant agreement No 101003890 – project firEUrisk.

References

(Andrews, 2018) Andrews, P. L. (2018) 'The Rothermel surface fire spread model and associated developments: A comprehensive explanation' USDA Forest Service, Rocky Mountain Research Station Research Paper RMRS-GTR-371.

(Bugarić et al. 2024) Bugarić M., Stipaničev D., Šerić Lj., Krstinić D. (2024) Calculation and validation new high resolution fuel map of Croatia**,** Proceedings for the 7th International Fire Behavior and Fuels Conference, April 15-19, 2024, Tralee, Ireland

(Chuvieco et al., 2023) Chuvieco, E., et al. (2023) Towards an Integrated Approach to Wildfire Risk Assessment: When, Where, What and How May the Landscapes Burn, *Fire* **6**, No. 5: 215

(FirEUrisk, 2021) FirEUrisk Project (2021) Developing a Holistic Risk-wise Strategy for Wildfire Management, 2021, https://fireurisk.eu

(Krstinić, 2024) Krstinić, D. (2024) Intelligent Wildfire Monitoring and Survaillance System, Proceedings for the 7th International Fire Behavior and Fuels Conference, April 15-19, 2024, Tralee, Ireland

(OiV Fire Detect AI, 2024) OiV Fire Detect AI (2024) Inteligent Solution for Early Fire Detection, https://oiv.hr/en/services-and-platforms/oiv-fire-detect-ai/

(Pettinary & Chuiveco, 2017) Pettinari, M. L. and Chuvieco, E. (2017) Fire Behavior Simulation from Global Fuel and Climatic Information, Forests 2017, 8, 179.

(Scott & Burgan, 2005) Scott, J. H.; Burgan, R. E. (2005) Standard fire behavior fuel models: a comprehensive set for use with Rothermel's surface fire spread model, *Gen. Tech. Rep. RMRS-GTR-153.* U.S. Department of Agriculture, 72 p.

(Scott & Reinhard, 2001) Scott, J. H., Reinhardt, E. D. (2001) 'Assessing crown fire potential by linking models of surface and crown fire behavior.' USDA Forest Service, Rocky Mountain Research Station Research Paper RMRS-RP-29.

(Stipaničev et al., 2023) Stipaničev, D., Bugarić, M. (2023) Dead Fuel Moisture Content in Wildfire Propagation Potential Estimation for Split-Dalmatia County, Proc. of 8th Int. Conference SpltTech 2023 - Wildfire Track. Bol, Croatia June 21-24, 2023